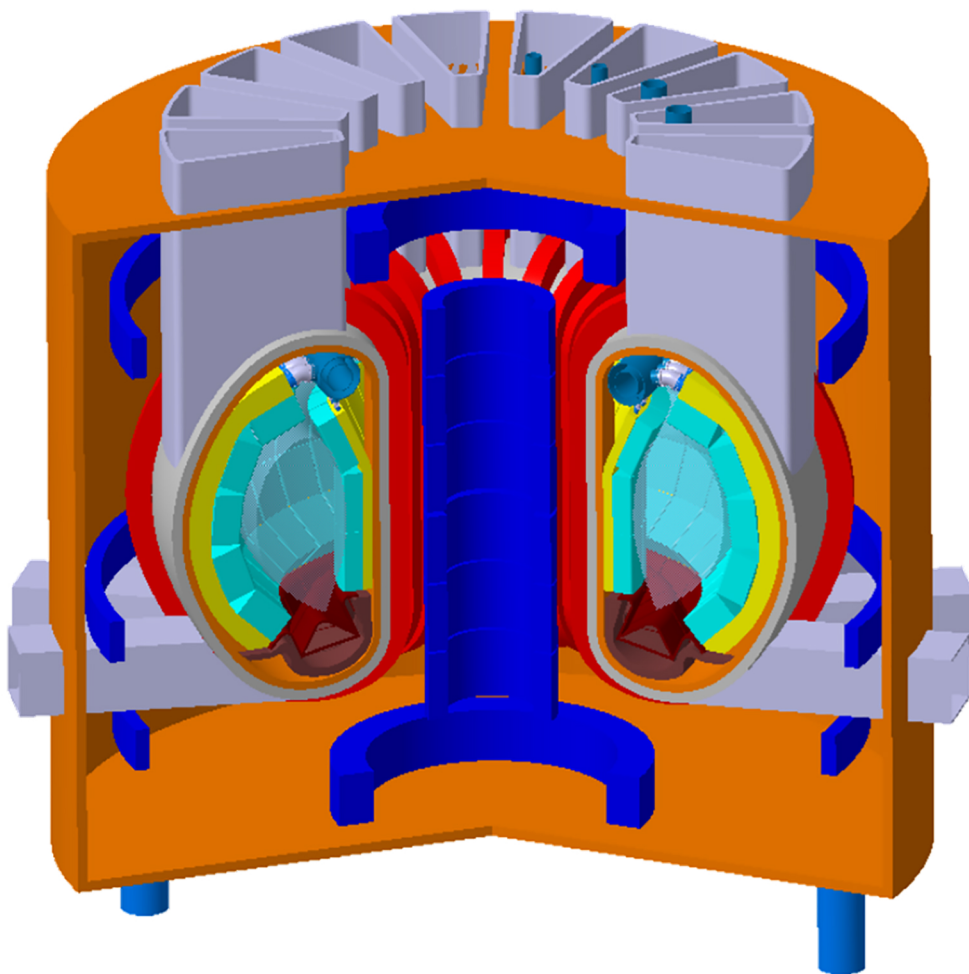


# FUNFI2

2<sup>ND</sup> INTERNATIONAL CONFERENCE ON FUSION-FISSION  
SUB-CRITICAL SYSTEMS FOR WASTE MANAGEMENT AND SAFETY

## BOOK OF PROCEEDINGS



# FUNFI2

2<sup>nd</sup> International Conference on Fusion-Fission  
sub-critical systems for waste management and safety

## Book of Proceedings

Following the first successful edition of FUNFI held in Varenna in yr 2011 ( Proceedings AIP Conference Nr 1442 , 2012, editors J Kallne, D Ryutov, G Gorini and C Sozzi) , we present the book of proceedings of the second edition of the conference. FUNFI2 is dedicated to the physics, technology and engineering of machines where fusion reactions drive a fission blanket. Such hybrid devices can be used for energy generation, fissile fuel production and nuclear waste transmutation. The concept of Fusion-Fission hybrid (FFH) systems was introduced in a famous paper by H.Bethe (Physics Today 1979) and recently reviewed by H. Rebut (Plasma Physics Controlled Fusion 2006). The Deuterium-Tritium fusion reactions produce 14MeV neutrons which are able to induce fission reactions in most of actinides including uranium 238 and thorium. The fission reactions deliver an energy 10 times that of the neutrons produced by fusion: so with one fission reaction per one fusion reaction there is an energy gain of 10. In this condition the fusion system producing neutrons can work at low minimum gain of  $Q_{\text{fusion}} \approx 3$  , for realizing a global energy gain of the integrated fusion-fission system  $Q_{\text{FFH}} \approx 30$ . The main aim of FUNFI2 conference is to identify the proposals/projects with a high degree of reliability to make the technology available, making the analysis of the level of readiness of the technology for a medium term (25yrs) realization of a FFH reactor. Contributions concerning the following arguments are inserted in the programme:

- 1) Mission and priorities of Demonstrators;
- 2) Device comparison: Tokamak or mirror based systems, stellarators and other configurations including accelerator based hybrid systems;
- 3) Level of readiness of the technologies and R&D essential programme.

The programme is divided into five sessions :

DAY 1 - session 1: introduction and tokamak

DAY 2 - session 2: open systems and ADS; session 3: open systems and fuel cycle

DAY 3 - session 4: diagnostics; session 5: discussions of level of readiness of fusion technologies and challenges of the integration of fusion and fission in a new hybrid device.

FUNFI2 is organized by ENEA (*Italian National Agency for New Technologies, Energy and Sustainable Economic Development*), INFN (*Italian National Institute for Nuclear Physics*), CNR (*National Research Council*) and CIRTEN (*Italian Interuniversity Consortium for Technological Nuclear Research*).

About 62 Scientists, representative of all the countries where the FFH studies are carried out, participated to FUNFI2, and 34 talks were given in a 2.5 days conference. The message from the participants in the lively discussion session is to organize the FUNFI conferences systematically (possibly every two years), since the interest on Fusion-Fission studies is increasing and FUNFI is the place where the worldwide results can be presented and discussed.

**Aldo Pizzuto**  
ENEA  
Chairman FUNFI2

**Francesco Paolo Orsitto**  
CREATE Consortium and ENEA  
Scientific Secretary FUNFI2

# FUNFI2

2<sup>ND</sup> INTERNATIONAL CONFERENCE ON FUSION-FISSION  
SUB-CRITICAL SYSTEMS FOR WASTE MANAGEMENT AND SAFETY

## ENEA

Italian national agency for new technologies,  
energy and sustainable economic development

# 26-28 OCTOBER 2016

**Frascati Research Center**  
Via Enrico Fermi, 45  
Frascati, Rome, Italy  
**Bruno Brunelli Room**

**FUNFI2** is the second edition of an international conference dedicated to the physics, technology and engineering of machines where fusion reactions drive a fission blanket. Such Hybrid devices are intended for energy generation, fissile fuel production and nuclear waste transmutation. FUNFI2 is organized by ENEA (Italian National Agency for New Technologies, Energy and Sustainable Economic Development), INFN (Italian National Institute for Nuclear Physics), CNR (National Research Council) and CIRTEN (Italian Interuniversity Consortium for Technological Nuclear Research).

### CHAIRMAN

A. Pizzuto (ENEA,I)

### CO-CHAIR

Y. Wu (CN)

M. Lontano (CNR,I)



The main aim of the conference is to identify the proposals/projects with a high degree of reliability to make the technology available.

Contributions concerning the following arguments are expected:

- 1) Mission and priorities of Demonstrators;
- 2) Device comparison: Tokamak or mirror based systems, stellarators and other configurations;
- 3) Level of readiness of the technologies and R&D essential programme.

### INTERNATIONAL ADVISORY BOARD

O. Agren (SE)  
A. Botrugno (IAEA)  
Z. Chen, J. Jiang, M. Wang, Y.Wu (CN)  
M. Gryaznevich (UK)  
A. Krasilnikov (RU)  
V. Moiseenko (UA)  
S. Radhakrishnan (IN)  
M. Ricotti, M. Ripani(I)  
M. Salvatores (USA)

### ORGANIZING COMMITTEE

F.P. Orsitto (CREATE,I)  
M. Angelone, M. Cimino, M. Ciotti, J. Manzano,  
G. Mazzitelli, F. Miglietta, S. Tosti (ENEA,I)  
C. Sozzi, M. Tardocchi (CNR,I)

### CONTACTS

Monica Cimino

email : [funfi2@enea.it](mailto:funfi2@enea.it)

phone : +39-06-9400-5754

[www.fusione.enea.it/FUNFI2](http://www.fusione.enea.it/FUNFI2)

### SCIENTIFIC SECRETARY

F.P. Orsitto (CREATE,I)  
G. Gorini (International Centre  
Piero Caldirola,I)

### IMPORTANT DATES

Submission of abstract until June 15, 2016

Notification to authors by Aug 15, 2016

Poster presentations until September 10, 2016

Deadline for registration: September 26, 2016



## Index

<b>N°</b>	<b>Title</b>	<b>Page</b>
1	- Fusion-Fission Hybrid Reactor Research in China	5
2	- Nuclear Waste Transmutation: the Potential Role of Hybrid Systems and Major Technical Requirements	13
3	- Feasibility of early fusion applications	14
4	- Development of tokamak based fusion neutron sources and fusion-fission hybrid systems	15
5	- The SABR TRU-Zr Fuel, Modular Sodium-Pool Transmutation Reactor Concept	22
6	- Plasma controls in FFH machines	31
7	- Development and Experiment of Fusion Neutron Driven Zero Power Subcritical Fast Reactor	32
8	- Development and Application of Super Monte Carlo Simulation Program for Fusion and Fission Nuclear Energy Systems	33
9	- Application of a new fast reactor for fission-fusion hybrid systems	34
10	- ST40 as a prototype of the fusion core for FFH: design and status of construction	40
11	- The Reversed Field Pinch as Neutron Source for Fusion-Fission Hybrid Systems: Strengths and Issues	47
12	- Analysis of safety problem in Fusion Reactors	48
13	- Safety assessment of critical and subcritical systems with fast neutron spectrum	49
14	- MYRRHA Project Status and New Implementation Plan.	50
15	- Stellarator-mirror fusion-fission hybrid systems	56
16	- Current status of R&D of Accelerator-Driven System for minor actinide transmutation in JAEA	64
17	- The SFLM Concept for Fusion Driven Energy Production by Incineration of Spent Nuclear Fuel	73
18	- Conceptual Design of Z-pinch Driven Fusion-Fission Hybrid Reactor	79
19	- A short overview of ITER-like pulsed MCF reactors application as hybrid nuclear systems for actinides transmutation	80
20	- The possible role of the Italian Universities consortium CIRTEN for the engineering study of a fission-fusion hybrid reactor	88
21	- First Wall Lifetime Extension with Flowing Liquid Zone for Fusion Reactors	94
22	- Thorium blanket driven by fusion neutron source: generation for fission reactors of a unique fuel characterized by super high fuel burn-up	97
23	- First preliminary conceptual experimental set up towards a hybrid reactor blanket	104
24	- Neutronic Analysis of Spent Fuel Recycling Option in a Hybrid System with DUPIC Fuel	110
25	- Neutron Flux Map from Fusion to Fusion-Fission System	115
26	- Neutron Production and Fast Particle Dynamics in Reversed-Field Pinch Plasmas in RFX-mod	120
27	- Development of liquid metal technologies for innovative nuclear systems	121
28	- DEMO-like minimum set of Diagnostics and controls for a pilot FFH Reactor	131
29	- Fusion Reactor Relevance of the ITER Diagnostics Developed in Russia	139
30	- Neutron diagnostics for fusion-fission hybrid: lessons learned from integration of neutron diagnostics on JET and ITER	147
31	- Gamma-ray diagnostics for fusion-fission hybrids	148
32	- Comments on neutron measurements on fusion, fission and hybrid reactors	149
33	- Nuclear Detectors for Hybrid reactors : Lesson learned from the EU Tritium Breeding Modules of ITER	155
34	- Level of readiness of technologies used in Fusion devices proposed for Fusion-Fission hybrid (FFH) reactors	161

# 1 - Fusion-Fission Hybrid Reactor Research in China

Yican Wu

Key Laboratory of Neutronics and Radiation Safety, Institute of Nuclear Energy Safety Technology, Chinese Academy of Sciences, Hefei, Anhui, 230031, China

## Abstract

Fusion-fission hybrid reactor is a potential solution to overcome difficulties in fission energy, with the functions of waste transmutation, fuel breeding and energy production. It is a feasible approach to early fusion energy application considering its low plasma parameters requirement. China has performed research on hybrid reactor for 30 years and has won a series of achievements in terms of conceptual designs and related R&D activities.

Keywords: Fusion-fission hybrid reactor, Nuclear technology, Nuclear material, Nuclear software.

## 1. Introduction

Nuclear energy is an economic and clean source of base load energy, which provides about 11% of the world's electricity today. Nuclear capacity will keep increasing to meet energy demand and climate change challenge as a competitive large scale alternative to fossil fuels, mainly spurred by deployment in China[1]. However, there are challenges to make nuclear energy as a sustainable technology, such as low efficiency utilization of uranium sources, growing inventory of nuclear waste, nuclear safety issues and so on. Generation IV reactors have more advances in sustainability, economics, reliability and proliferation-resistance than conventional reactors. And fusion energy may also provide a potential solution to meet increasing global energy demand, but still needs hard work before commercial applications.

Fusion-fission hybrid reactor is a highly promising approach as a bridge between fission and fusion energy development, by combining a fusion-powered core with a fission blanket shown in Fig.1. Meanwhile, hybrid reactor shares lots of vital technologies with fission and fusion reactors. For example, lead-based technology could be employed in both Generation IV fast reactor system and liquid PbLi blanket.

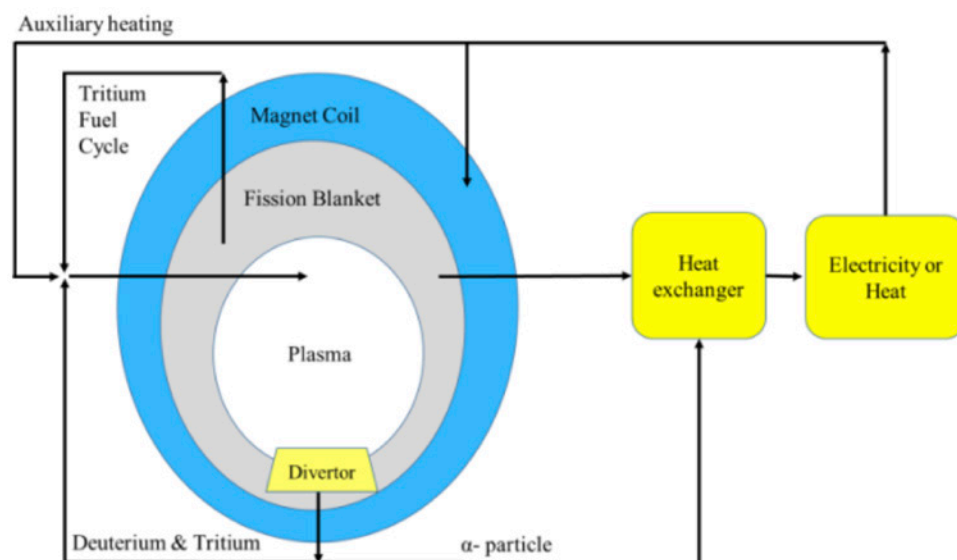


Fig.1. Schematic of fusion fission hybrid reactor

China has performed research on hybrid reactor for 30 years since the national Hi'Tech program ("863" program) started. The related research units includes Chinese Academy of Sciences (CAS), China Academy of Engineering Physics (CAEP), Southwestern Institute of Physics (SWIP), and some colleges, etc[2]. Multi-functional hybrid reactor concepts FDS-SFB and FDS-MFX were proposed as intermediate steps toward the final application of fusion energy. Except for conceptual designs, a series of R&D studies in blanket engineering and analysis software were performed, which included development of the China Low Activation Martensitic (CLAM) steel, the series liquid PbLi experimental loops (DRAGON), the High Intensity D-T Fusion Neutron Generator (HINEG), the Accelerator-based Fusion neutron source Driven sub-critical fission System (AFDS), the Super Monte Carlo Simulation Program for Nuclear and Radiation Process (SuperMC), etc. In this contribution, the progress of fusion fission hybrid reactor research has been summarized, and some suggestions for future development have been given.

## 2. Features of hybrid reactor

Hybrid reactor has many features, which can reduce the requirements of fusion devices and achieve the early application of fusion energy. It also could solve the problems of fission energy by using the excess neutrons to transmute long-lived radionuclides and breed fissile fuels. Compared with fusion reactor, hybrid reactor has the following advantages:

### Easy-achieved Plasma Parameters

The requirement of fusion plasma technology of hybrid reactor are much lower than fusion power reactor due to the higher energy multiplication factor of hybrid reactor, and the fusion plasma parameters of different devices are shown in Table 1. The fusion power requirement of hybrid reactor is only tens of MW and JET already achieved about a fusion power of 16 MW. The neutron wall loading requirement of hybrid reactor may be 0.5-1 MW/m<sup>2</sup>, which is far below fusion power reactor. The fusion energy gain (Q) requirement of hybrid reactor is around 1, which is close to the experimental achievements[3]. Fig.2 shows the fusion triple product of a series of experimental facilities and the requirement parameters of hybrid reactor. Fig.3 shows the neutron wall loading of a series of fusion reactors, fusion DEMO reactors and hybrid reactors.

Device	Fusion Power(MW)	Neutron Wall Loading(MW/m <sup>2</sup> )	Q
JET/JT-60U	16	0.2	~1
ITER	500	0.57	10
Fusion Power Reactor	2000~3500	4~7	10~30
Hybrid Reactor	10~100	0.5~1	~1

Table 1 Fusion plasma parameters of different devices

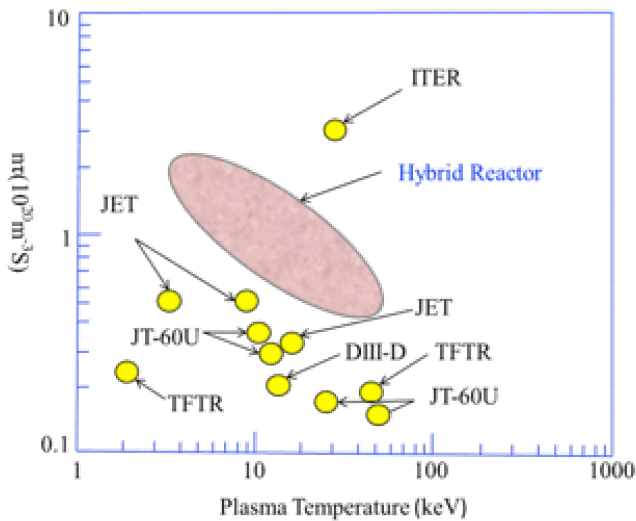


Fig.2. Fusion triple product of a series of experimental facilities and hybrid reactor

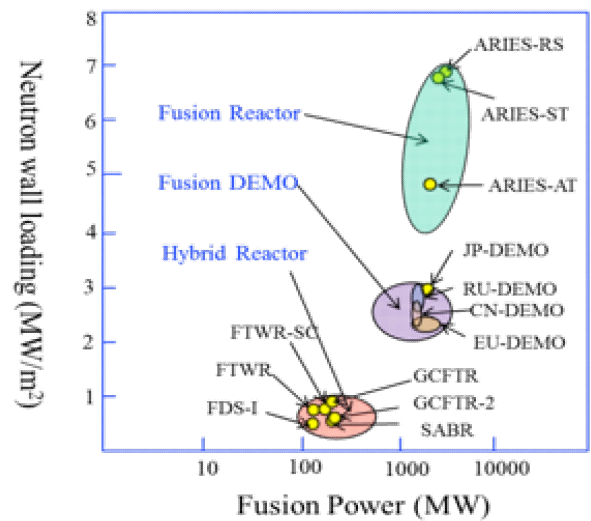


Fig.3. Neutron wall loading of a series of fusion and hybrid reactors

### Higher Tritium Breeding Ratio

The tritium self-sufficiency is one of the challenges of fusion reactors because of its low tritium breeding ratio (TBR) in blanket. The TBR of fusion reactor is about 1.1 and difficult to be improved[4], while the TBR of hybrid reactor can be much higher with the fission neutron multiplication materials in blanket[5]. Fig.4 shows the TBR of a series of fusion and hybrid reactors.

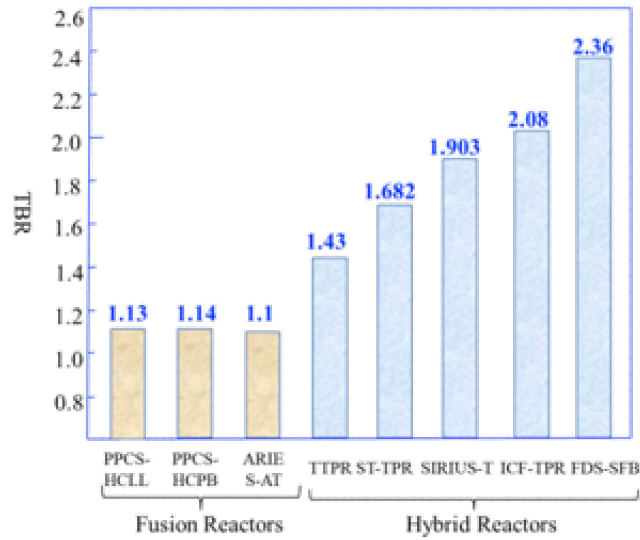


Fig.4. TBR of a series of fusion and hybrid reactors

Compared with current fission reactor, hybrid reactor has the following advantages:

### Better Sustainable Features

The excess high energy neutrons from the fusion reactions can be used to achieve outstanding waste transmutation and fuel breeding performances. Thus hybrid reactor has higher transmutation support ratio (TSR) and breeding ratio (BR) than current fission reactor. Table 2 shows the BR of liquid metal fast breeder reactor (LMFBR) and hybrid reactor[6,7]. Table 3 shows the TSR of different types of reactors[8-10].

Reactor Type	Initial Fuel	Fuel Cycle	BR
LMFBR	15-25% Pu	U/Pu	1.2-1.4
LMFBR	12-20% U-233	Th/U	1.03-1.15
Hybrid Reactor	Nat U	U/Pu	2.5-3

Table 2. BR of LMFBR and hybrid reactor[6,7]

Reactor Type	TSR of MA	TSR of LLFP
Thermal Reactor	1~3	>2
Fast Reactor	2~20	-
Hybrid Reactor	15~55	>10

Table 3. TSR of different reactors[8-10]

### More Flexible Fuel Loading

Some kinds of fuel loading need to be restrained in critical fission reactors. For example, the fraction of Pu in fuel should not exceed 13% in thermal reactor[11]. However, hybrid reactor could operate under subcritical condition, thus it has large safety margin and flexible fuel options. Hybrid reactor has a wide range of uranium enrichment options, not only natural or highly enriched uranium, but also depleted uranium. It could use more kinds of fission fuels, even 100% of TRUs could be loaded in the hybrid reactor.

### Deep Burnup

Excess reactivity is reserved for the loss from burnup and accumulated fission products when fresh fuel is loaded in critical reactor, and refueling is needed when excess reactivity is exhausted. Hybrid reactor could control the operation of blanket by external neutrons to acquire deep burnup and long reload cycle.

Except for those advantages, hybrid reactor also combine some difficulties of both fusion and fission reactors.

### 3. Research progress

Great progress on conceptual designs, nuclear technologies, materials and nuclear software have been achieved in China.

#### 3.1 Conceptual Designs

The FDS series hybrid reactor concepts including FDS-I/SFB, FDS-MFX, FDS-ST and FDS-GDT have been proposed and some new concepts are being developed such as AFDS (Accelerator-based Fusion neutron source Driven sub-critical fission System). Fig.5 gives the schematic view of the FDS series concepts and Table 4 gives the main parameters.

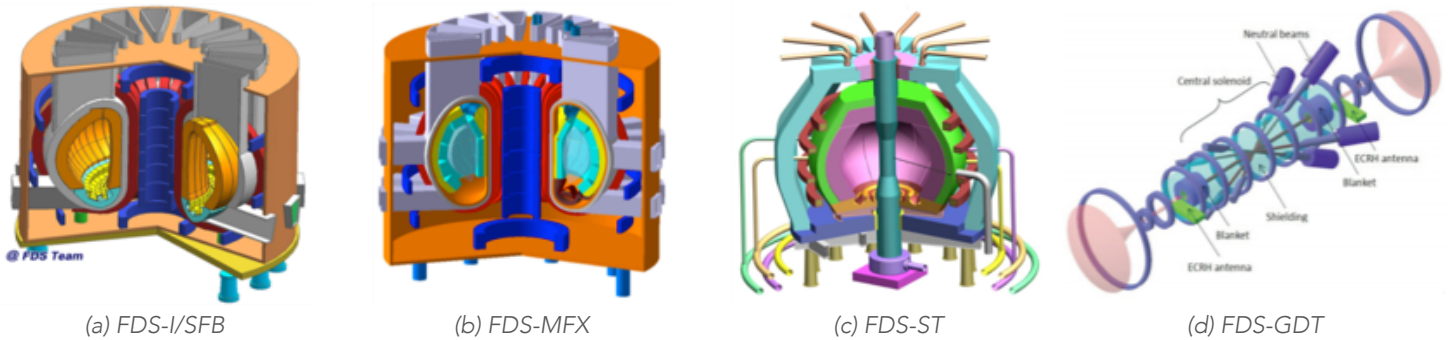


Fig.5. Schematic view of FDS series hybrid reactor concepts

Fusion-driven subcritical system (FDS-I) was presented as an intermediate step toward the final application of fusion energy, which use the regular tokamak as fusion neutron driver. Fusion Driven subcritical System for Spent Fuel Burning (FDS-SFB) is a hybrid reactor concept based on FDS-I and used for nuclear waste transmutation, fissile fuel breeding and energy production. The subcritical blanket was designed based on the well-developed technologies of fission reactor and makes use of spent nuclear fuel as fuel, liquid lead lithium as coolant and tritium breeder[12].

Fusion Driven subcritical Multi-Functional Experimental Reactor (FDS-MFX) was designed for testing and validating the construction and operation of fusion DEMO and fusion-fission hybrid DEMO. It provides an experimental platform to relevant techniques. Three-stage tests will be carried out by using three different blankets: the tritium breeding blanket, natural/enriched uranium-fueled blanket and spent-fuel-fueled blanket[13,14]. The Fusion Driven Subcritical reactor based on Spherical Tokamak (FDS-ST) was proposed for breeding fissile fuel and transmuting nuclear waste. This studies were undertaken to investigate the potential advantages of the low aspect ratio tokamaks FDS-ST was designed with high energy multiplication due to fission reaction for highly economical operation. This can compensate the large fraction of recirculating power in a Spherical Tokamak (ST), reduce the neutron wall loading and irradiation on the first wall (FW)[15, 16]. A fusion neutron source based on Gas Dynamic Trap (GDT) magnetic mirror was featured with inherent steady state operation, compact structure, easy construction and maintenance, relatively low tritium consumption, and flexible operation. FDS-GDT was proposed to explore the potential application of fusion neutron source based on GDT in hybrid system. It can be used to drive a hybrid reactor to produce energy or drive a transmutation reactor to burn the radioactive waste[17]. AFDS is a subcritical nuclear power system driven by an external high intensity fusion neutron source, it is an easy-achieved hybrid reactor concept, which avoid the technical difficulty of plasma controlling and have the potential for nuclear waste transmutation and nuclear fuel breeding. With the characteristics of self-sustained burning depleted uranium or nuclear waster, AFDS has the advantages of high resource utilaiton ratio, deep burn up, and minimum nuclear waste production. Due to the subcritical design, the system also has the feature of inherent safety without supercritical risk.

Parameters	FDS-SFB	FDS-MFX	FDS-ST	FDS-GDT
Fusion Power (MW)	150	50	100	15
Major Radius (m)	4	4	1.4	-
Minor Radius (m)	1	1	1.0	-
Neutron Wall Loading (MW/m <sup>2</sup> )	0.49	0.17	1.0	2.0
Fuel	Spent fuel	Depleted / Natural / Enriched Uranium	Spent fuel	Spent fuel
Coolant	PbLi & Helium	PbLi & Helium	PbLi & Helium	PbLi & Helium
Structure Material	CLAM	CLAM	CLAM	CLAM

Table 4. The main parameters of FDS series hybrid reactor concepts

### 3.2 Nuclear Technology and Material

To explore the features of fusion neutron in fusion and hybrid reactor, China has been developing the HINEG for testing of nuclear technology and safety. The HINEG will be achieved by three phases: HINEG-I, is designed to achieve the intensity of  $10^{12}$ - $10^{13}$  n/s, HINEG-II, aims to reach  $10^{15}$ - $10^{16}$  n/s. HINEG-III, which is a volumetric fusion neutron source with the neutron yield of more than  $10^{18}$  n/s. HINEG-I has already been constructed shown in Fig.6 and successfully produced a D-T fusion neutron yield of  $6.4 \times 10^{12}$  n/s, while the related research on the key technologies of HINEG-II and the design of HINEG-III are going on. HINEG can be used for the development of hybrid reactor technology and safety, including not only basic research on validation and measurement of nuclear data, neutronic method and software, radiation protection, etc., but also materials irradiation, neutronic performances, integration test of components nuclear performances and so on. Its applications could extend to nuclear medicine, radiotherapy, neutron radiography, and other nuclear technology applications [18].

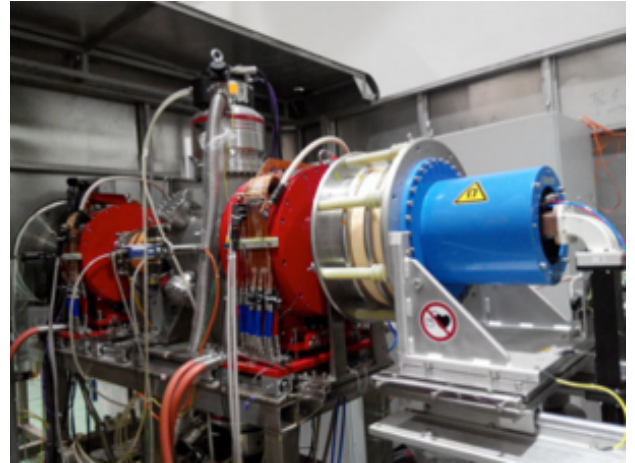


Fig.6. High intensity D-T fusion neutron generator (HINEG-I)

AFDS-0 has been built for nuclear physics validation of AFDS, as shown in Fig.7. AFDS-0 consists of HINEG and Lead-based Zero Power Sub-critical/Critical Reactor (CLEAR-0) [19]. CLEAR-0 is a multi-functional zero-power reactor for simulating neutronic process in various fast reactors and hybrid systems. The core of CLEAR-0 is designed to be flexible with sufficient safe considerations, which could load various fuel and coolant materials, such as lead or lead-based alloy. AFDS-0 is an experimental platform for the integrated validation of neutronics and control strategy of subcritical core in hybrid reactor. Meanwhile, it is taking advantages of the flexible core, robust safety control system and intensity fusion neutron.



Fig.7. Accelerator-based Fusion neutron Driven zero power sub-critical System (AFDS-0)

CLAM steel is one of the candidate structural materials for fusion and hybrid reactors. It has been chosen as the structural material in the PbLi blanket designs of the FDS series fusion and hybrid reactors because of its high strength, high thermal conductivity, high irradiation resistance and low activation features. It has been developed in the past decade, leading by the Institute of Nuclear Energy Safety Technology (INEST), CAS with the participation of more than thirty domestic and overseas research units [20,21].

Extensive physical and mechanical tests have been conducted on CLAM steel, as well as compatibility tests in liquid PbLi and neutron irradiation tests in reactors up to 3 dpa and in spallation neutron source up to 21 dpa. At present, CLAM steel has reached industrial mass production, and code qualification for application in ITER is undergoing. It is the primary candidate structure material for Chinese Helium Cooled Ceramic Breeder (HCCB) and Dual Function Lithium Lead (DFLL) Test Blanket Module (TBM) in China, whose updated design is ongoing and the 1/3 mockup of TBM modules are fabricated, as shown in Fig.8[22,23].



Fig.8. 1/3 scale DFLL TBM mockup

The liquid PbLi blanket is one of the most promising blanket concepts for hybrid reactor. Aiming at better development of PbLi blanket technology and engineering application, the key issues of PbLi blanket should be investigated such as materials corrosion, the magnetohydrodynamic (MHD) effect and so on. A series of PbLi experimental loops have been designed and built successfully such as DRAGON-I/II and DRAGON-IV. Some experiments were conducted to investigate the corrosion behaviors of CLAM steel in magnetic field, the purification technology of liquid PbLi and MHD effect. To support the engineering design validation of DEMO blanket with the parameters covering the requirements of ITER-TBM and China DEMO, a Dual Coolant Thermal Hydraulic Integrated Experimental Loop (DRAGON-V) was designed, which can also be used to develop the key techniques in-pile and the engineering design of hybrid reactor. It is composed of a lead-lithium loop and a helium loop. The maximum temperature in the test section is designed to be 1100 °C, the maximum flow rate of PbLi can reach 40 kg/s, and the magnetic field is up to 5 T. The maximum helium pressure is 10.5 MPa[24,25].

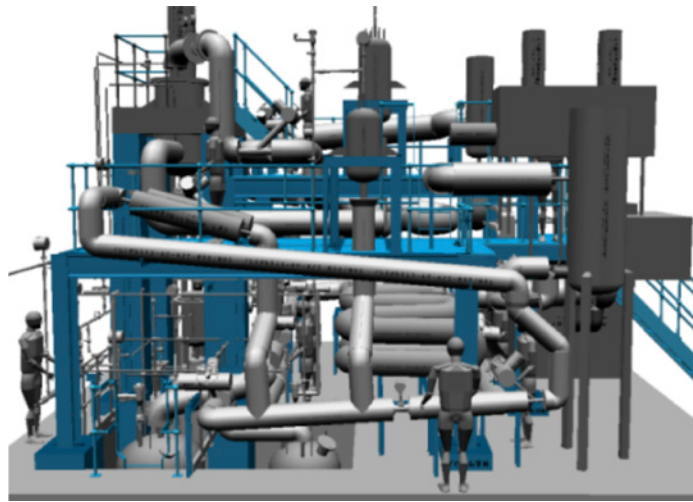


Fig.9. Dual Coolant Thermal Hydraulic Integrated Experimental Loop (DRAGON-V)

### 3.3 Nuclear Software

Based on advanced methodology, nuclear software was developed for reactor design, evaluation, phenomenon and feature prediction. The software is divided into three hierarchies including physics and engineering calculation, digital reactor, virtual nuclear power plant, taking SuperMC, VisualBUS, Virtual4DS as the representatives respectively.

SuperMC is a general, intelligent, accurate and precise simulation software system for the nuclear design and safety evaluation. It is designed to perform the comprehensive neutronics calculation, taking the radiation transport as the core and including the depletion, radiation source term/dose/biohazard, material activation and transmutation, etc. It supports the multi-physics coupling calculation including thermo-hydraulics, structural mechanics, biology, chemistry, etc. The latest version of SuperMC supports the comprehensive neutronics simulation including radiation transport, depletion of isotopes, activation and dose. Automatic modeling of geometry and physics, efficient radiation transport calculation, multi-D visualization analysis and cloud computing are the advanced capabilities.

Advanced capabilities and features of SuperMC were developed by FDS Team to solve the new problems of hybrid reactor, especially focusing on the following points. (1) The geometry of fusion and hybrid nuclear energy systems is extremely complicated. Tediousness, intensive labor and error-prone in geometry modeling process makes the accurate analysis unrealistic. The automatic CAD-based geometry modeling methods were developed with outstanding capabilities of decomposition and conversion of very complex geometry, void free geometry description, processing of high order surfaces, visual-based hierarchical structure modeling and etc. (2) Deep penetration of radiation shielding is another challenge situation. Series of novel methods were proposed to accelerate the convergence. Global weight window generator was proposed and speeded up the global flux calculation 635 times for the ITER (International Thermonuclear Experimental Reactor) C-Lite model. In this method, the expected contribution to a uniform particle distribution was considered at a very fine level and an efficient automatic iteration scheme was employed. The Optimal Spatial Subdivision method and Bounding Box method were proposed for geometry processing acceleration based on particle location anticipation. (3) Neutrons in fusion and hybrid nuclear energy systems are strongly anisotropic in large energy range with complex energy spectrum structure. The hybrid evaluation nuclear data libraries in SuperMC include fine-group, coarse-group, fine-group and point-wise nuclear data with selecting suitable energy structure and weight functions were developed. The physical effect was corrected including resonance self-shielding, thermal neutron up-scattering and temperature Doppler effect.

SuperMC has been verified by more than 2000 benchmark models and experiments. Now SuperMC has been applied in more than 30 major nuclear engineering projects. [26,27].

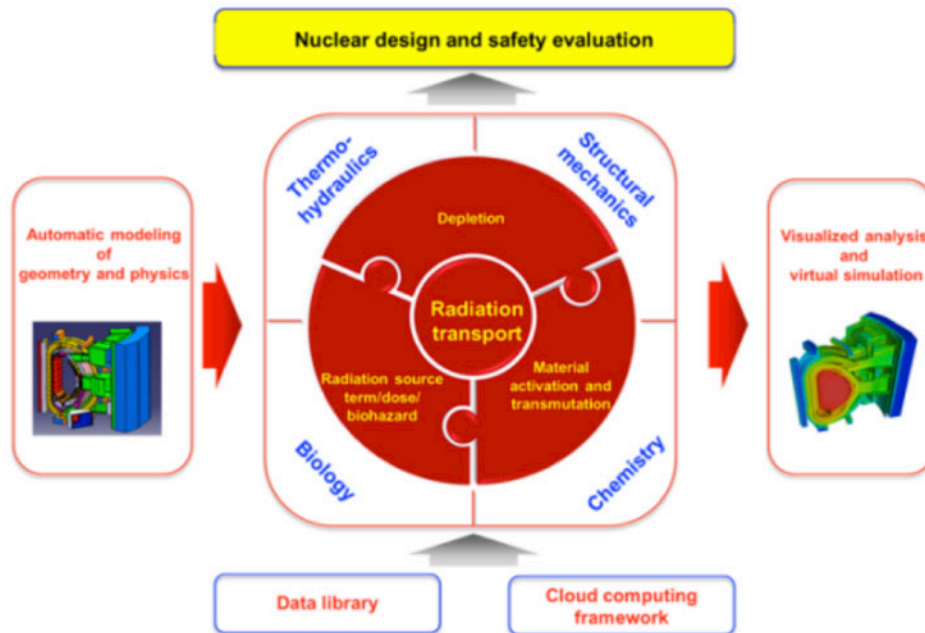


Fig.10. Architecture of SuperMC

The Digital reactor named VisualBUS takes SuperMC as the core. For fission application, it supports design optimization, performance assessment in normal operation condition and nuclear emergency simulation in accident operation condition. For fusion application, it supports the simulation and prediction of new phenomena based on multi-physics-coupling, safety design and evaluation in the whole space with high fidelity and collaborative research. The Virtual Nuclear Power Plant named Virtual4DS is full-scope and full-period simulation and emergency decision platform for operational safety in the digital environment. It supports social risk assessment based on nuclear big data, drill and intelligent decision of nuclear emergency, accident warning and process simulation, large-scale radionuclide diffusion and environment consequence prediction. [28-30].

#### 4. Summary

The fusion-fission hybrid reactor studies have been performed for nearly 30 years in China to seek for early applications of fusion energy, covering conceptual designs and R&D on relevant nuclear technology and material, advanced nuclear software and virtual reactor, etc. Although impressive progress has been made in the international community, there are still much work to be done with some suggestions given as below:

- (1) A consensus of hybrid reactor roadmaps should be reached. Many different concepts have been proposed with different goals and sub-systems, but unfortunately in the community none of them has been well recognized as the candidate which is likely to move to the engineering design phase.
- (2) Technical gaps and requirements need to be detailedly specified especially regarding the hybrid technology R&D, such as fission blanket technologies, safety technologies, system integration technologies, etc.
- (3) Tight international cooperation is suggested, such as establishing an international standing committee for hybrid reactor research, developing some projects for international/multi-/bi-lateral cooperation within the frames of IAEA Coordinated Research Project (CRP) and IEA Technology Collaboration Program (TCP).
- (4) Strengthen the training of youth talents would be an important task in the future. Educating and encouraging young people to join the hybrid reactor research activities with more workshops, seminars and training courses is necessary.

#### 5. Acknowledgments

This work was supported by National Magnetic Confinement Fusion Energy Development Research with grant No. 2013GB108005 and other many funding projects. Further thank the great help from other members of FDS Team in this research.

#### 6. References

- [1] [www.world-nuclear.org](http://www.world-nuclear.org)
- [2] Y. Wu. Progress in Fusion-Driven Hybrid System Studies in China[J]. Fusion Engineering and Design, 2002, 63-64: 73-80.

- [3] M. Kotschenreuther, S. Mahajan, P. Valanju. Fusion Drivers for Hybrids[R]. Report of the conference on hybrid fusion-fission systems. Washington, D.C., May 19-20, 2009.
- [4] U. Fischer, C. Bachmann, J. Jaboulay, et al. Neutronic performance issues of the breeding blanket options for the European DEMO fusion power plant[J]. *Fusion Engineering and Design*, 2016,109-111:1458-1463.
- [5] K. Ishibashi, S. Fujimoto, T. Matsumoto. An optimization study of structure materials, coolant and tritium breeding materials for nuclear fusion-fission hybrid reactor[J]. *Nuclear Science and Technology*,2014,4:130-133.
- [6] G. Kessler. Sustainable and safe nuclear fission energy: Technology and safety of fast and thermal nuclear reactors[M]. Springer Science & Business Media, 2012.
- [7] P. Fortescue. Comparative breeding characteristics of fusion and fast reactors[J]. *Science* 196.4296 (1977): 1326-1329.
- [8] B.Liu, K. Wang, J.Tu, et al. Transmutation of minor actinides in the pressurized water reactors[J]. *Annals of Nuclear Energy*, 2014, 64: 86-92.
- [9] W. You, S. Hong. A neutronic study on advanced sodium cooled fast reactor cores with thorium blankets for effective burning of transuranic nuclides[J]. *Nuclear Engineering and Design*, 2014, 278: 274-286.
- [10] B. Hong. Conceptual study of fusion-driven system for nuclear waste transmutation[J]. *Fusion Engineering and Design*, 2014, 89(9): 2493-2497.
- [11] T. Fujishiro, J. West, L. Heins, et al. Overview of safety analysis, licensing and experimental background of MOX fuels in LWRs[C]//MOX Fuel Cycle Technologies for Medium and Long Term Deployment (Proc. Int. Symp. Vienna, 17-21 May 1999), IAEA-SM-358. 1999.
- [12] Y. Wu , FDS Team. Conceptual design activities of FDS series fusion power plants in China[J]. *Fusion Engineering and Design*, 2006, 81(23): 2713-2718.
- [13] Y. Wu, S. Zheng, X. Zhu, et al., Conceptual Design of the Fusion-Driven Subcritical System FDS-I[J]. *Fusion Engineering and Design*, 2006, 81, Part B: 1305-1311.
- [14] Y. Wu, J. Jiang, M. Wang, et al. A Fusion-Driven Subcritical System Concept Based on Viable Technologies[J]. *Nuclear Fusion*, 2011, 51(10):103036.
- [15] L. Qiu, Y. Wu, B. Xiao, et al. A Low Aspect Ratio Tokamak Transmutation System[J]. *Nuclear Fusion*, 2000, 40: 629-633.
- [16] Y. Wu, L. Qiu, Y. Chen. Conceptual Study on Liquid Metal Center Conductor Post in Spherical Tokamak Reactors[J]. *Fusion Engineering and Design*, 2000, 51-52: 395-399.
- [17] H. Du, D. Chen, et al. Physics analysis and optimization studies for a fusion neutron source based on a gas dynamic trap[J]. *Plasma Science and Technology*,2014,16(12):1153-1157.
- [18] Y.Wu. Development of High Intensity D-T Fusion Neutron Generator HINEG[J]. *International Journal of Energy Research*.doi:10.1002/er.3572.
- [19] Y. Wu. Design and R&D Progress of China Lead-Based Reactor for ADS Research Facility[J]. *Engineering* 2016,2:124-131.
- [20] Q. Huang, C. Li, Y. Li, et al. Progress in Development of China Low Activation Martensitic Steel for Fusion Application[J]. *Journal of Nuclear Materials*, 2007, 367-370:142-146.
- [21] Q. Huang, FDS Team. Development status of CLAM steel for fusion application[J]. *Journal of Nuclear Materials*, 2014, 455(1): 649-654.
- [22] Y. Wu, X. Zhu, S. Zheng, et al. Neutronics Analysis of Dual-cooled Waste Transmutation Blanket for the FDS[J]. *Fusion Engineering and Design*, 2002, 63-64: 133-138.
- [23] Y. Wu, FDS Team. Conceptual Design and Testing Strategy of a Dual Functional Lithium-Lead Test Blanket Module in ITER and EAST[J]. *Nuclear Fusion*, 2007, 47(11):1533-1539.
- [24] Y. Wu, Q. Huang, Z. Zhu, et al. R&D of DRAGON series lithium-lead loops for material and blanket technology testing[J].*Fusion Science and Technology*, 2012,62(1):272-275.
- [25] Y. Wu, Q.Huang, Z. Zhu, et al. Progress in design and development of serious liquid lithium-lead experimental loops in china[J]. *Chinese Journal of Nuclear Science and Engineering*, 2009,29 (2):161-169.
- [26] Y. Wu, FDS Team. CAD-Based Interface Programs for Fusion Neutron Transport Simulation[J]. *Fusion Engineering and Design*, 2009, 84 (7-11):1987-1992.
- [27] Y. Wu, J. Song, H. Zheng, et al. CAD-based Monte Carlo program for integrated simulation of nuclear system SuperMC[J]. *Annals of Nuclear Energy*, 2015, 82:161-168.
- [28] Y. Wu, FDS Team. Development of Reliability and Probabilistic Safety Assessment Program RiskA[J]. *Annals of Nuclear Energy*, 2015, 83: 316-321.
- [29] Y. Wu, Z. Chen, L. Hu, et al. Identification of Safety Gaps for Fusion Demonstration Reactors[J]. *Nature Energy*, DOI: 10.1038/NENERGY.2016.154.
- [30] Y. Wu. Public Acceptance of Constructing Coastal/Inland Nuclear Power Plants in Post-Fukushima China[J]. *Energy Policy*,2017,101:484-491.

## 2 - Nuclear Waste Transmutation: the Potential Role of Hybrid Systems and Major Technical Requirements

**Phillip Finck and Massimo Salvatores**

*Idaho National Laboratory, Idaho Falls, USA*

The fission process used in nuclear reactors produces a number of isotopes that can be toxic to human beings and the environment. Since the start of the large scale deployment of nuclear energy, disposal of the long lived isotopes has been an issue that has had a priority in most nuclear countries.

We will first give an overview of the scale of that issue in terms of masses and relative toxicities of various isotopes, and will follow by a summary of the national strategies that have evolved to provide short and long term solutions.

From that summary we will point out that all national strategies are a combination – with nationally different weighting factors – of three technical approaches: temporary storage, transmutation, and permanent storage.

While transmutation is not a necessary element in these strategies, it can achieve a number of benefits, including the reduction in the mass of key isotopes, the reduction in the total toxicity, and the reduction in storage requirements, in particular a potential reduction in the storage time.

A number of studies, analyses, and experiments have been run in the world over the past several decades on various systems for transmutation, including transmutation in source driven systems – where the source (of neutrons) originates either from accelerators or fusion systems.

From these studies we will summarize what we believe are the major challenges related to the use of source driven systems, namely:

- the physics of the system where a delicate balance between the source neutron production and the multiplicity of the nuclear component
- source reliability
- the safety of the source driven systems remains of utmost concern when analyzed in detail
- engineering of the barriers between the source and the nuclear component has been demonstrated to be a particularly delicate achievement
- the development of the targets containing the nuclear waste, and their compatibility with nuclear safety rules
- The energy “cost” of the neutrons (characterized by ratio of the energy that should be spent to produce the source to the total fission energy to be used e.g. for transmutation) that should be kept to a minimum while keeping the fission blanket sub-critical (e.g.  $K \sim 0.95$ )
- finally, because the masses of the waste involved, this effort eventually will need to move to large scales, and economics of the various approaches will need to be considered.

### 3 - Feasibility of early fusion applications

#### A. Botrugno

*ENEA, Dipartimento FSN, C. R. Frascati, Via E. Fermi 45, 00044 Frascati (Roma), Italy*

A Magnetic Confinement Fusion (MCF) Neutron Source can produce high intensity ( $10^{12} < n/s < 10^{20}$ ) of high energy neutrons, approximately mono-chromatic at 2.45 MeV (using DD plasma) or 14.1 MeV (using DT plasma). These characteristics are different from those of all the other types of neutron sources currently in use, and open the way to both improvements of traditional neutron applications and to newer fast neutron applications.

Presently, several countries have strategies to exploit by now acquired MCF technology or its close extrapolation ( $0.5 < Q < 2.0$  and power level  $< 40$  MW) for non-electrical applications. In particular, programs are being carried out mainly in the USA, Russia, China, India and United Kingdom. Most promising applications are in the nuclear energy field, medical science, material science and nuclear industry such as fissile fuel production, nuclear waste transmutation and radioisotope production.

This work provides a preliminary analysis of the technical feasibility of each application based on their different physical, technological and regulatory requirements. Different applications can be carried out by facilities ranging from small DD devices with a specific purpose to a full large-scale multi-functional DT device; they present different degrees of technical and regulatory complexity, different classes of costs and risk factors. The analysis is guided by the well-established requirements for compact tokamaks, by the ITER experience and by the on-going technology development for DEMO.

Moreover, potential showstoppers and some related issues for fostering the development of non-electrical fusion applications will also be presented and discussed.

## 4 - Development of tokamak based fusion neutron sources and fusion-fission hybrid systems

**B.V. Kuteev**

National Research Centre "Kurchatov Institute", 123182 Moscow, Russia - email: Kuteev\_BV@nrcki.ru

The interest of nuclear research and industry in intense fusion neutron sources (FNS) and fusion-fission hybrid systems (FFHS) definitely has been growing up during the past decades. Major motivations for that are driven by the deficit of excess neutrons needed for controlling subcritical active cores and production of radionuclides in the nuclear industry, needs for deeper insight in fusion and fission nuclear science and technology, requirements for realization of neutron experiments and technologies with higher safety characteristics at higher neutron fluxes and lower level of radiotoxicity generated. This paper summarizes the results of Russian conceptual design activity in the development of FNS and FFHS.

### Introduction

Contemporary level of physics and technology allows us to realize tokamaks with DT-fusion neutron yields up to  $10^{18}$ - $10^{19}$  n/s. The modern technology is developed for those operating in a pulse mode with the duration of tens of seconds. A lot of design and research activity is still needed to make the device operational in steady state mode (SSO) and neutron environment that is extremely desirable for research and industrial applications [1].

From the technical point of view, FNS could be realized using beam-plasma fusion in a tokamak with copper coils or via mixed beam-plasma and thermonuclear fusion mode in a larger superconducting tokamak.

Both options have been considered in our design of spherical tokamak FNS-ST with major radius  $R = 0.5$  m and aspect ratio  $A = 1.67$  [2, 3] as well as conventional tokamak DEMO-FNS with  $R = 2.75$ - $3.2$  m and  $A = 2.75$ - $3.2$  [1, 4, 5]. According to system code analysis both are capable of producing the neutron loading of  $0.2$  MW/m<sup>2</sup> in SSO mode maintained by neutral beams and gyrotrons. The total power consumptions are  $60$  MW and  $200$  MW for FNS-ST and DEMO-FNS correspondingly.

Applications for FNS include material studies in fusion neutron spectra, fusion nuclear science, blanket module testing, production of thermal and cold neutrons, subcritical core control and nuclide production. A decade scale seems feasible for design and construction of such devices.

The mission of DEMO-FNS is the demonstration of SSO-tokamak and hybrid technologies at the semi-industrial level. Devices like that may appear by 2035. The cost for these facilities will be in B\$ range or higher.

### 1. Significance of Ignition, Controlled fusion and Hybrid Systems

From the very beginning of fusion research the major goal, namely, reaching ignition conditions, defined the development program. The parameter, characterizing the gap between the technology level reached and the ignition, is determined by the plasma density  $n_{20}$ , temperature  $T$  and energy confinement time  $\tau_E$ , the triple product of which should reach  $5 \times 10^{21}$  m<sup>-3</sup>keVs at ignition. Industrial level of fusion development requires device operation close to ignition under the fusion energy multiplication factor  $Q = P_{fus}/P_{AH} > 30$  - the ratio of fusion ( $P_{fus}$ ) and auxiliary heating ( $P_{AH}$ ) powers. Realization of Controlled Fusion requires additionally Steady State Operation (SSO) with duration  $t_{SS}$  in year scale, intensive fusion rate  $k_g$  in grams of neutrons per day (corresponds to  $\sim 20$  MW of DT-fusion power) and capacity factor  $C$  close to unity. It is convenient to evaluate the contemporary development level (tokamak JET, laser facility NIF), next future devices (ITER) and the Controlled fusion goal – reactors DEMO and PROTO using the Kurchatov factor  $K_g = n_{20} T \tau_E k_g t_{SS} C$ . As clearly seen from Table 1, the JET level is close to Breakeven  $Q=1$ , NIF is still far from that, ITER plans to reach  $Q=10$  or higher. Meanwhile, transition from modern tokamaks to PROTO still requires growth of the Kurchatov factor over 12 orders of magnitude.

Facility	$n_{20}$	$T_{keV}$	$\tau_E$	$k_g$	$t_{SS}$	$C$	$Q$	$K_g$
JET	1	10	0.3	0.35	$3.5 \times 10^{-7}$	0.1	1	$3 \times 10^{-8}$
NIF	$10^{12}$	0.2	$2 \times 10^{-11}$	$10^{-8}$	$10^{-6}$	0.1	0.015	$4 \times 10^{-15}$
ITER	1	10	3.5	25	$10^{-4}$	0.25	10	$2 \times 10^{-2}$
FNS-ST	1	2	0.05	0.2	1	0.3	0.2	$6 \times 10^{-3}$
DEMO-FNS	1	4	0.3	2	1	0.3	1	$7 \times 10^{-1}$
DEMO	1	15	5	50	1	0.5	25	$2 \times 10^3$
PROTO	1	15	6	150	1	0.8	30	$1 \times 10^4$

Table 1. Parameters of Fusion and Hybrid facilities

Below a conceptual design is considered for the two facilities, which may operate in the intermediate domain of Kurchatov factor  $10^{-3}$ - $10^{-1}$  and provide new information about SSO and fusion nuclear science FNS complementary to ITER information about burning plasma physics.

## 2. Hybrid Systems in Russian Fusion Program

Hybrid development program was presented at FEC-25 in Saint Petersburg by E.P. Velikhov [6]. The main stream of Strategy is associated with ITER-DEMO-PROTO line. The major facilities on the path to Industrial Hybrid Plant are shown in figure 1. Development of SSO and Molten Salts technologies require capital and operation cost \$1 B, that for supporting and integration of

Globus-M3 facility is \$100 M, for FNS-ST oriented to materials and components -\$1 B, for DEMO-FNS oriented to hybrid technology integration-\$5B. For hybrid power plant PHP with 500 MW(th) power we expect cost ~\$10 B like our US colleagues. Project cost of IHP incinerator program will be very close to evaluations of USA - \$100 B and will need ~100 years for realization. Basic parameters of FNS-ST, DEMO-FNS and ITER are compared in Table 2.

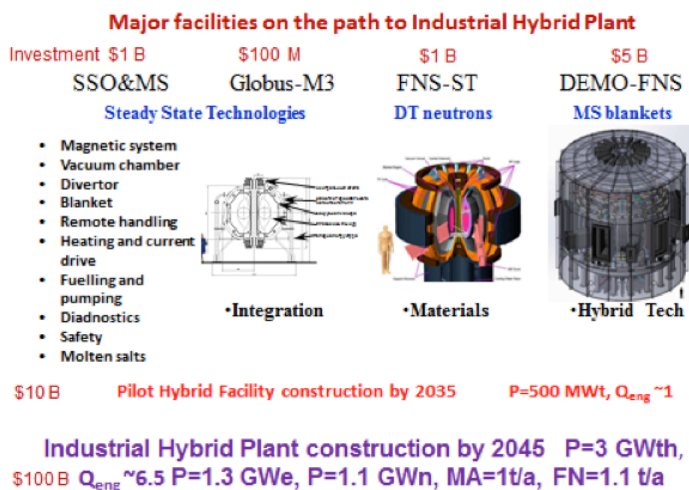


Fig. 1. Major Facilities on the path to industrial power plant.

	FNS-ST	DEMO-FNS	ITER
Major radius R, m	0.5	2.75-3.2	6.2
DT-Fusion option	Beam driven fusion	Beam driven and thermonuclear ~50:50 %	Thermonuclear fusion ~100%
Heat transfer from alphas to plasma	no	yes	yes
Divertor configuration	Double null	Double null	Single null
Toroidal magnetic field at VV center, T	1.5	5	5.3
Fusion power, MW	1-3	30-40	500
Auxiliary heating power P <sub>AH</sub> , MW	8-10	30-40	60-80
Fusion energy gain factor Q = P <sub>fus</sub> /P <sub>AH</sub>	~0.2	~1	~10
Shielding, m	No shield	0.50-0.70	0.6-0.8
Type of magnetic system	Cu	LTS	LTS
Neutron loading, MW/m <sup>2</sup>	0.2	0.2	0.5
Neutron fluence MWy/m <sup>2</sup>	~2	~2	0.3

Table 2. Basic parameters of FNS-ST, DEMO-FNS and ITER

FNS-ST should demonstrate and utilize the best features of beam-plasma fusion and no-shielding device with simplest copper coils design. The mission of DEMO-FNS is to reach transmutation range valuable energy applications and open the door to PHF and IHP.

Technical feasibility of DEMO-FNS construction by 2035 is supported by the following design and experimental information.

- 1 - Regimes with Q~1 are realized in tokamaks.
- 2 - Electron temperature sufficient for DT beam driven fusion T = ~4 keV has been demonstrated in numerous experiments.
- 3 - Non-inductive current drive has been demonstrated in conventional tokamaks and is close to demonstration in spherical devices.
- 4 - Reduction of technical requirements on neutron loading in PHF to 0.2 MW/m<sup>2</sup> and fluence value for operation time below 2 MWA/m<sup>2</sup> allows to use commercially available materials.
- 5 - Economics of PHP is acceptable in case of total products selling: MA incineration, electricity production, tritium breeding, fuel breeding for U-Pu and Th-U nuclear fuel cycles.
- 6 - System models and codes predict appropriate parameters of PHF.
- 7 - Russia has an appropriate cooperation of fusion and fission organizations and highly qualified staff.

## 3. FNS-ST conceptual design

New physics appears for FNS-ST due to the high specific heating power up to 10 MW/m<sup>3</sup> which is by a factor of 10 higher than that for ITER and even higher than that in the DEMO case. Steady state operation without inductive current drive is another R&D problem dealing with reaching the required currents, their maintenance and control. Stability of the plasma with a high fraction of fast ions and high pressure anisotropy is the additional issue that needs research activity. Meanwhile, the benefits of the low cost, simplicity and opportunity to use existing materials under reduced

neutron fluences are very attractive and maintain interest to such devices [7].

A cut-away view of FNS-ST device is shown in Fig. 2. Prospective technical solutions for tokamak systems have been validated, and choices of enabling technologies and materials of the basic FNS have been made. Spinel ( $MgAl_2O_4$ ) has been finally chosen as the insulating material and plasma spraying technology has been chosen for inter-loop insulation in toroidal magnetic coils with a twisted center post. The neutron fluence of approximately  $10^{26}$  n/m<sup>2</sup> will be tolerable from the viewpoint of both the degradation of insulation property and decreasing the conductivity of copper.

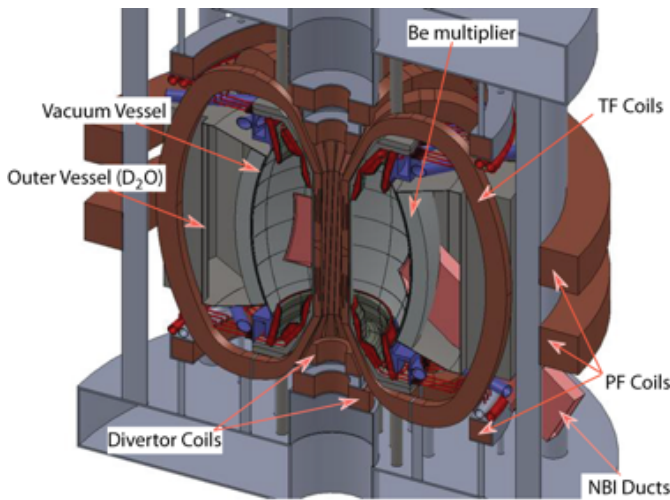


Fig. 2. FNS-ST cut-away view.

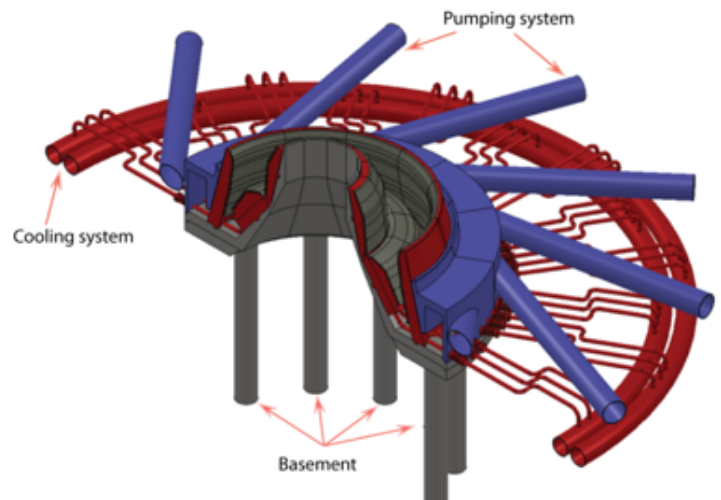


Fig. 3. Divertor basement with pumping.

Toroidal beryllium coils cooled down to the liquid nitrogen temperature offer the best characteristics both for the neutronics and the power consumption of the toroidal magnet system. Power consumption reduces by a factor of 3 compared with pure copper coils. The neutron flux in the thermal blanket grows up by a factor of 2 and this allows reaching fluxes similar to the highest ones produced by fission reactors  $\sim 10^{15}$  n/cm<sup>2</sup>s. However, additional analysis and R&D are needed to assess the manufacturing feasibility of this very attractive Be option. The design of the FNS-ST vacuum vessel has been upgraded and new solutions for the first wall (FW) structure and joints of the FW with divertor basement.

A concept of a double-null divertor for the FNS-ST has been suggested which is capable to withstand heat fluxes up to 6 MW/m<sup>2</sup>. The divertor basement with pumping is shown in Fig. 3. Lithium dust injection technology is proposed to control the border plasma radiation and plasma-surface interaction in the scrape-off layer [8].

Concepts of the FNS-ST blankets for the pure thermal neutron production and for the development of a thorium fuel cycle for fission reactors have been proposed and considered. It was shown that thermal neutron fluxes as large as  $10^{15}$  n/cm<sup>2</sup>s are feasible in the FNS-ST with Be coils. The radial structure, neutronics and thermal hydraulic characteristics as well as the U233 production rate and opportunities to self-breed tritium have been defined. Such a device may also be capable to test DEMO blanket modules in DT-fusion neutron spectra (Fig.4). The neutron flux as high as 0.2 MW/m<sup>2</sup> is provided at the outer wall. This allows materials and components to be tested under fluence of 2 MW\*year.

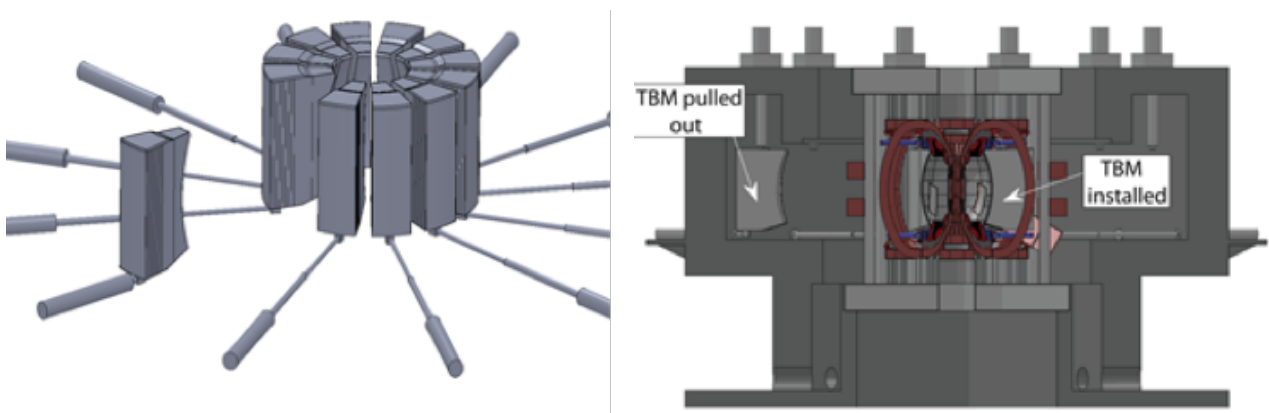


Fig. 4. Blanket maintenance approach, proposal for DEMO TBM tests

The one through approach was chosen for remote handling of the tokamak systems placed within the toroidal magnetic field coils. This means that only minor repairs and inspections will be maintained in this highly activated zone. The accidents requiring welding and reassembling will necessitate a total changing of these systems. The whole tokamak will be changed except removable blanket modules and systems beyond the toroidal magnetic field coils. As a backup approach the replacement of the injectors and blanket modules to a new machine hall is considered.

#### 4. DEMO-FNS status

**Fusion-fission hybrid facility** based on superconducting tokamak DEMO-FNS is developed in Russia for integrated commissioning of steady-state and nuclear fusion technologies at the power level up to 40 MW for fusion and 400 MW for fission reactions. Fusion-fission hybrid technologies tested on DEMO-FNS may accelerate the implementation of fusion technologies and are capable of improving the neutron balance in the global nuclear energy system. Implementation of hybrid technologies should also accelerate the development of Atomic energy reducing the radio-toxicity generated in nuclear fuel cycle and the level of pollution by fuel reprocessing. These problems are associated with the forthcoming transition of Nuclear Power to a closed nuclear fuel cycle.

The development of fusion neutron source DEMO-FNS based on a classical tokamak was launched in the NRC "Kurchatov Institute" in 2013. Design was aimed at reaching steady state operation of the plant with a neutron loading  $\sim 0.2 \text{ MW/m}^2$ , lifetime neutron fluence  $\sim 2 \text{ MWa/m}^2$ , with the plasma facing surface area of the blanket  $\sim 100 \text{ m}^2$ , sufficient for testing materials and components in the fusion neutron spectrum as well as for development of hybrid transmutation technology, fuel nuclides and tritium production, and energy generation (Fig.5).

It was found during design process that for reliable performance, durability and maintainability of fusion-fission complex it is necessary to increase the thickness of the radiation shield and to improve the strength characteristics of the electromagnetic system [1].

As a result, in this embodiment, the large radius  $R$  was increased from 2.5-2.7 m to 3.2 m. This modification has a little effect on plasma currents generated by the beam of neutral atoms, as well as on the total DT-fusion power and on the beam fusion part in it. However, it has led to several important corrections in the general layout of the tokamak, which have affected the overall configuration and design of the DEMO-FNS divertor and blanket.

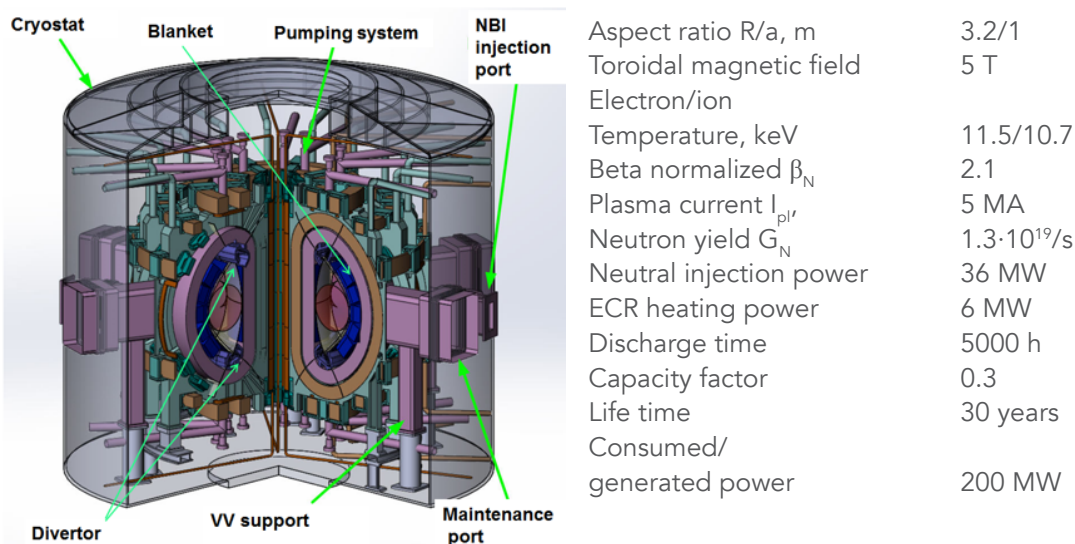


Fig. 5. Cut-away view of DEMO-FNS tokamak

Figure 6 shows the magnetic configuration and plasma parameters of DEMO-FNS.

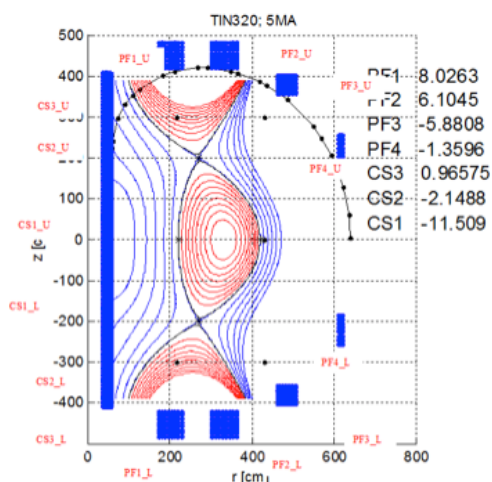


Fig.6. Vertical cross-sectional of DEMO-FNS.

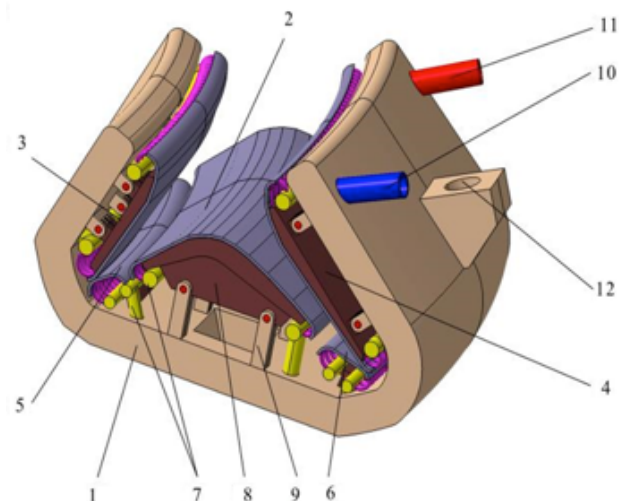


Fig. 7. Divertor cassette

**Divertor** of the DEMO-FNS tokamak is double null one. It is formed by a set of cassettes located inside the tokamak vacuum chamber in zones around the upper and lower X-points. Each divertor consists of 18 independent cassettes which form a continuous annular heat removal surface. Each divertor cassette is provided with a forcing and a drain pipes with the coolant, which are placed at the rear side of the cassette case. Coolant venting pipes are placed inside the equatorial tokamak ports. When replacing for repair the cassette and cooling pipes are replaced together. Welding of the coolant pipes is carried out in the zone of minimum neutron flux, preferably outside the vacuum chamber. The cassette contains a robust case made of nonmagnetic stainless steel, in which the ducts are made for circulating coolant through heat removal panel, as well as bayonet hole for the tensioning device and the holes for pumping. The schematic of the divertor cassette is shown in figure 7.

According to operation scenarios the superconducting magnet system (SMS) of DEMO-FNS should work with any direction of toroidal field in plasma. It should provide maintenance of thirty pulses with the duration up to 5000 hours at the current of 5 MA and the plasma fusion power up to 40 MW. Hybrid discharge scenario includes an inductive plasma current ramp-up to the reference value and the transition to steady maintenance of the plasma current using non-inductive heating methods and bootstrap current. The coils of the magnetic system must maintain the superconducting state during the plasma current disruptions, withstand 100 cycles of cooling / warming, 1000 cycles of the current feeds in toroidal field coils (TFC), and 50 rapid outputs of energy, including five TFC transitions to the normal state.

**Electromagnetic system** (EMS) of DEMO-FNS includes toroidal field system, consisting of eighteen coils; sectioned central solenoid (CS); five pairs of poloidal field coils (PFC); three groups (of 18 windings) correction coils (CC) and a vertical stability coil of the plasma column, disposed within the vacuum chamber. Interunit TFC mechanical structures also belong to the electromagnetic system. Cryogenic piping and current feedthroughs are made for superconducting coils of EMC. In normal operation, these components are maintained at liquid helium temperature. Coil wires for CS and TFC will be made on the base of the intermetallic compound Nb<sub>3</sub>Sn. It is permissible to use Nb<sub>3</sub>Sn and NbTi alloys for PFC and CC wires. Design solutions and operation modes of DEMO-FNS impose increased requirements onto conductors of EMS: coil

- Compactness EMS coils require high structural current density values;
- Serious electromagnetic forces provide mechanical loadings on EMS, so conductors must withstand to them without noticeable degradation;
- Steady state thermal (neutron) loadings on the EMS make it necessary well-arranged cooling;
- A high rate of the magnetic field variation under rapid (pulse) modes (discharge and ramp-up of the plasma current) imposes additional requirements to the stability wire and value of losses in them.

However, stress-strain analysis of the TFC coils leads us to the conclusion that technical feasibility (containing the required amount of structural material to withstand mechanical loads) of TF-coil design requires placing the winding wire into massive radial plates, as is shown in Figure 8. The cable for a thin-wall casing that is shown in Figure 5 should be made of Nb<sub>3</sub>Sn, carry the current of ~ 80kA and include about 1,000 strands with a critical current density (for non-copper fraction) not less than 1100 A / mm<sup>2</sup> (12 T, 4.2 K)

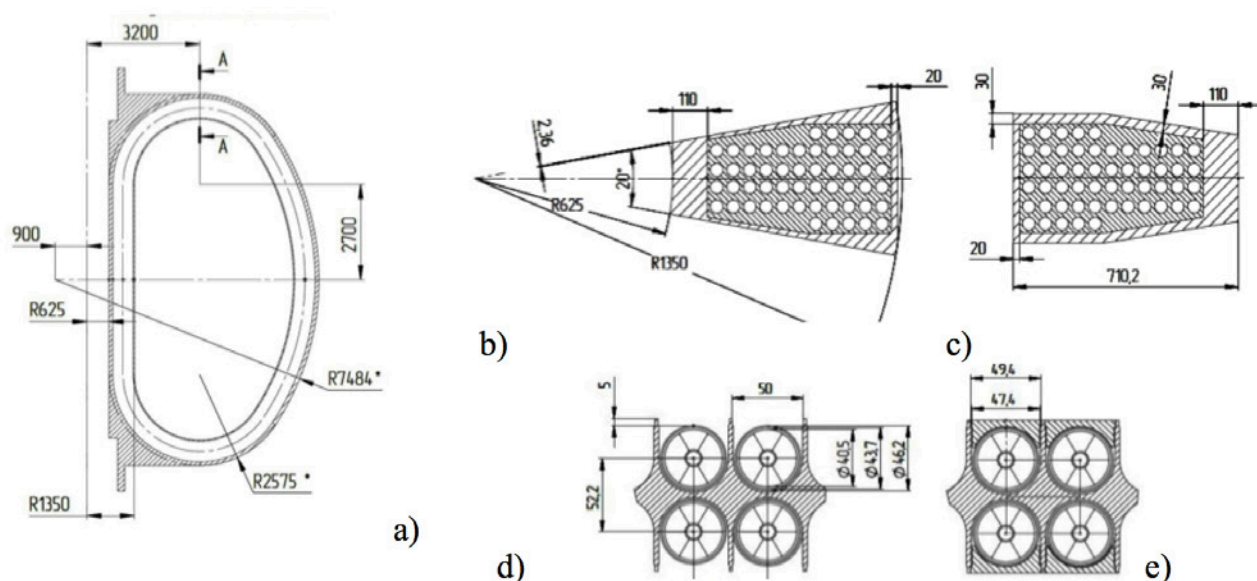


Fig. 8. The coil unit in a casing (a); cross-section of the inner "legs" (b); cross-sectional outer "legs" (c); conductors in radial plate (d, e).

Poloidal field coils are supposed to carry out a set of double-layer sections wound with two parallel conductors of circular cross-section. Taking into account the size (diameter 12 m) of coils and their operation conditions - as a rule the magnetic field on the conductor 6 T, winding from NbTi conductor cables are traditionally chosen.

According to optimization criteria for a tokamak central solenoid it must operate at the highest possible magnetic field 12-13 T. Obviously, with such a level of magnetic field CS conductors withstand a high mechanical stress (more than 400 MPa). CS sections are supposed to wind from conductors with square cross section, with subsequent heat treatment, insulating and repacking. To withstand loads the winding wire casing should be made of high-strength steel (316LN). According to preliminary estimates, the rate of magnetic field change on the conductor of CS is 10-15 T/s in the fastest modes.

Structural scheme of the **hybrid module blanket** is being developed with functions of transmutation of minor actinides (MA) and tritium breeding. Blanket consists of 120 modules (Fig. 9).

Drawing keys are as follows:

- 1 - module case;
- 2 - nuclear zone;
- 3 - breeding zone (ceramic breeder);
- 4 - coolant inlet collector;
- 5 - coolant outlet collector;
- 6 - inlet gas collector;
- 7 - outlet gas collector. The initial composition of the mixture of MA in nuclear zone is shown in Table 4. Initial MA loading ~ 40 ton. MA burning is expected about 0.5 % per year. TBR ~1.

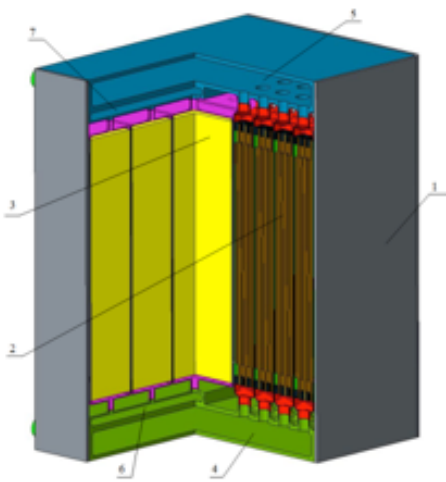


Fig. 9. A general view of the blanket module.

Nuclide	Mass content, %
Np237	44.5
Am241	48.6
Am242m	0.04
Am243	6.1
Cm243	0.02
Cm244	0.74

Table 3. Initial composition of MA mixture

Optimization of FC characteristics was aimed at reducing flows and inventory of hydrogen isotopes and tritium. Computer code TC-FNS was applied to estimate tritium distribution in FC systems and components of "tritium plant". The code evaluates tritium and deuterium flows and inventory. The separation of D/T mixture is not applied and use of 50:50

mixture of D and T. A small fraction of the fuel (<2%) delivered to the hydrogen isotopes separation system only for deprotonation. The separate deuterium loop (without tritium) for a neutral beam injection system is proposed.

Neutronic performance and inventory analyses were carried out to quantify the damage and gas production rates in candidate materials used in the first wall (FW) of DEMO-FNS. They are irradiated by the combined neutron energy spectrum formed by the two-component fusion-fission neutron source. Fusion neutrons are produced by plasma in front of the FW and the subcritical fission blanket acts from behind. As shown in [8] the damage and gas production rates are non-linear functions of the fission neutron source intensity. The D-T-neutron fluence value for DEMO-FNS is ~0.2 MWa/m<sup>2</sup> per one operation year (fpy) as measure of 14.1 MeV neutron current through the FW. According to the one-point approximation, the neutron multiplication factor Mn at the safe subcriticality limit of ~0.95 is about ~20. In this case the total fast neutron fluence ~4.4 x 10<sup>21</sup> cm<sup>-2</sup> per fpy is approximately a factor of ~2.2 higher than that from the initial D-T-neutron source only.

The radiation damage values are almost ~2 times higher compared with those for a pure fusion system at the same 14 MeV neutron FW loading. Both radiogenic hydrogen (H) and helium (He) gas atom production rates are practically at the same level except of about ~4-5 times higher He-production in austenitic and reduced activation ferritic martensitic steels.

## Conclusions

Increasing the geometric dimensions as compared to the previous version of DEMO-FNS has led to important changes, which have affected the design of the EMS, vacuum vessel, radiation shield and divertor of the tokamak.

The results of the discharge scenario modeling using DINA code, as well as the current ramp-up scenario in tokamak DEMO-FNS by ASTRA code confirm reaching the design goals.

Three-dimensional modeling the neutron fluxes from plasma and blanket sources has shown that the hybrid blanket makes an insignificant contribution to the radiative heating of TFC.

Issues of integrating the hybrid facility in the nuclear fuel cycle of Russian nuclear power are currently under consideration. Development of devices like FNS-ST and DEMO-FNS may make a significant input in development of DEMO and PROTO projects. Steady State Technologies of enabling systems: Magnets, Vacuum vessel, Divertor, Heating and Current drive, Fueling and pumping, Diagnostics, Control, Integration technologies can be tested at pilot plant level on such facilities. Faster experiments with tritium breeding and hybrid blankets, tritium handling, remote handling, radiochemistry, fusion materials and components will also be possible, complementing ITER activity on burning plasma physics. Such research will stimulate also safety analysis, licensing and legislation in the controlled fusion field.

## References

1. Kuteev, B.V., et al., Development of DEMO-FNS tokamak for fusion and hybrid technologies. Nucl. Fusion 55 (2015) 073035 (8pp).
2. Kuteev, B.V., et al., Steady state operation in compact tokamaks with copper coils. Nucl. Fusion 51(2011) 073013 (6pp).
3. Kuteev, B.V., et al., Intense fusion neutron sources. Plasma Phys. Rep. 36 (2010) 281.
4. Azizov, E.A., et al., Tokamak DEMO-FNS: concepts of magnet system and vacuum chamber. PAST ser. "Thermonuclear Fusion". 2015. Vol. 2 pp. 5-18 (in Russian).
5. Shpanskiy, Y.S., et al., Status of DEMO-FNS development. 26th IAEA Int. Conf. on Fusion Energy (Kyoto, Japan, 2016) FNS/1-1.
6. Velikhov, E.P., Fusion-Fission hybrid systems and molten salt technologies in large scale nuclear energy 25th IAEA Int. Conf. on Fusion Energy (St.Petersburg, Russia 2014) O3 keynote lecture.
7. Kuteev, B.V., et al., Conceptual Design Requirements and Solutions for MW-Range Fusion Neutron Source FNS-ST, IAEA FEC-2012, FTP/P7-07.
8. Sergeev, V.Yu., et al., Conceptual design of divertor and first wall for DEMO-FNS. Nucl. Fusion 55 (2015) 123013 (12pp).
9. Khripunov, V.I., First wall material damage induced by fusion-fission neutron environment. Fusion Eng. Des. 109–111 (2016) 7–12.

## 5 - The SABR TRU-Zr Fuel, Modular Sodium-Pool Transmutation Reactor Concept

W. M. Stacey, A. T. Bopp, J-P. Floyd, M. D. Hill, A. P. Moore, B. Petrovic, C. M. Sommer,  
C. L. Stewart and T. M. Wilks

Georgia Institute of Technology, Atlanta, GA 30332 USA

October, 2016

**Abstract.** The updated Georgia Tech design of the SABR fusion-fission hybrid spent nuclear fuel transmutation reactor and supporting analyses are summarized. SABR is based on tokamak fusion physics and technology that will be prototyped in ITER and the fast reactor physics and technology proposed for the Integral Fast Reactor and the PRISM Reactor, which has been prototyped in EBR-II. Introduction of SABRs in a 1-to-3 power ratio with LWRs would reduce the spent nuclear fuel HLWR capacity requirement by a factor of 10 to 100.

### 1. Introduction

The fusion group at Georgia Tech has worked (over the past two decades) to identify a practical, near-term application of a D-T fusion neutron source based on the fusion plasma physics and technology that will be demonstrated by the operation of ITER<sup>1</sup>. A D-T plasma producing the ITER design objective 500 MWth of fusion power will produce

$S_{fus}^{500} = 2.1 \times 10^{20} \text{ n/s}$  14 Mev neutron/s. If this fusion neutron source is surrounded by fissionable material in an assembly with multiplication constant  $k$  the total neutron transmutation (fission) rate will be<sup>2</sup>  $TR_{fis} = kS_{fus}/(1-k) \text{ fis/s}$ , provided  $k < 1$ . Thus, a constant transmutation (power production) rate can be maintained as  $k$  varies with fuel burnup by varying the fusion source level. The characteristics and performance capability of nuclear facilities driven by a tokamak fusion neutron source operating with essentially ITER-level physics and technology (but improved availability) have been characterized<sup>2-6</sup> and design concepts have been developed for different nuclear applications (transmutation of weapons-grade plutonium<sup>7</sup>, tritium production<sup>8</sup>, transmutation of transuranics (TRU) in spent nuclear fuel<sup>9-18</sup> and breeding of fissile material<sup>19</sup>) operating with such tokamak D-T fusion neutron sources. The fuel cycle performance<sup>20-27</sup> and dynamic safety<sup>28</sup> of the fission-fusion hybrid TRU transmutation reactors have been investigated, and the work has been summarized in Refs 29-31.

It would appear that the transmutation (destruction by fission) of TRU in spent nuclear fuel provides the most promising opportunity for fusion to contribute to nuclear energy in the first half of the present century. The realization that we must decrease burning of fossil fuels<sup>32</sup> is becoming widely accepted, and the dream of large-scale replacement of fossil fuel power with reliable baseline solar and wind power is slowly being confronted by the reality that these sources are environmentally problematical in other ways and inherently intermittent in nature, with only niche practical applications<sup>32</sup>. This leaves nuclear power as the only available option for displacing fossil fuel produced electricity on a large scale in the first half of this century<sup>32</sup>.

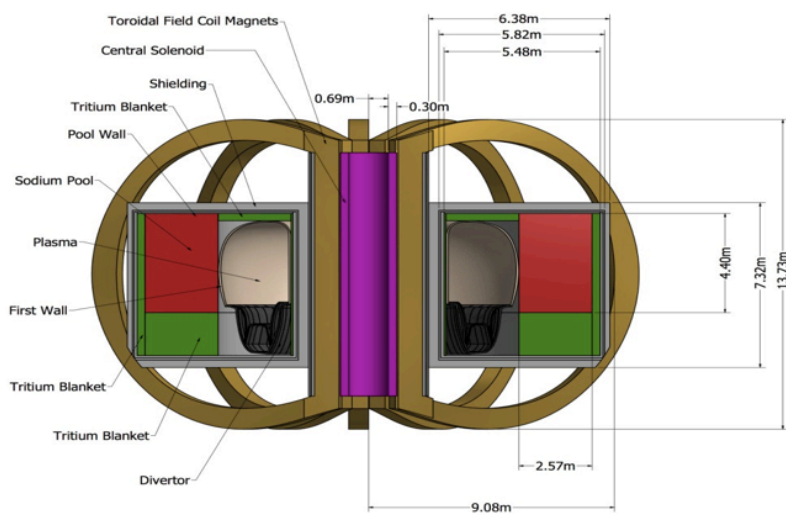
However, nuclear power has an unresolved problem that fusion can help solve—the disposal of spent nuclear fuel containing radioactive TRU elements with extremely long half-lives of 100,000 years or more. While disposal of this spent fuel by burial in secured repositories is technically feasible and not excessively expensive, this solution has been rejected in the US (at least temporarily) for political reasons. The burial solution also wastes the substantial energy source in the transuranics in the spent fuel. A better, but technically more difficult, solution is to separate the long-lived transuranics in spent nuclear fuel, which are fissionable in fast reactors, and use them as TRU fuel in special purpose “fast burner” or “transmutation” reactors, thus destroying the long half-life radioactive material, while extracting additional energy from the uranium fuel resource.

There are technical reasons why such transmutation reactors would work better if operated subcritical with a neutron source rather than operated critical. (In a critical reactor the neutron fission chain reaction is maintained entirely by the neutrons produced in fission, while in a subcritical reactor the neutrons produced by fission must be supplemented by source neutrons in order to maintain the neutron fission chain reaction.) One advantage of subcritical operation is that the neutron source strength can be increased to maintain the neutron fission chain reaction (power) level as the fissionable material is destroyed, allowing a longer fuel residence time in the reactor and more transuranic destruction before reprocessing. Another advantage of subcritical operation is that the margin of reactivity error to a runaway power excursion is much larger in a subcritical reactor than in a critical reactor where it is related to the small fraction of delayed fission neutrons which are not emitted instantaneously. Since this delayed neutron fraction is much smaller for the transuranics ( $\beta$ ; 0.002) than for uranium ( $\beta$ ; 0.006), prudence dictates that only a fraction (about 20%) of the fuel in a critical reactor be transuranics. The much larger margin of reactivity error with subcritical operation ( $\delta k_{sub} \approx 0.003$ ) would allow the subcritical transmutation reactor to be completely fueled with transuranics, resulting in 5 times fewer subcritical than critical transmutation reactors being needed to “burn” a given amount of transuranics.

## 2. The SABR TRU transmutation reactor design concept

There has been a substantial technical investigation<sup>9-12,16-18,20,22-31</sup> of fission-fusion transmutation reactors based on tokamak and sodium-cooled/metal-fuel fast reactor technologies. The reason that these technologies were chosen is that they are the most highly developed fusion and fission transmutation-applicable technologies, about which we know enough to make a realistic assessment of something that could be built in the next 25-30 years. The Subcritical Advanced Burner Reactor (SABR)<sup>16,18</sup> is based on ITER<sup>1</sup> fusion technology and physics, so in a sense ITER will be the prototype for the fusion neutron source for SABR. The fission reactor physics and technology for SABR is based on the Integral Fast Reactor (IFR)<sup>33,34</sup> and the GE PRISM<sup>35</sup> designs, so the successful operation of EBR-II and its associated pyro-processing system<sup>34,36</sup> were the prototype for the fission system.

It has been calculated that the ITER<sup>1</sup> tokamak magnetic and plasma support technology configuration, with a slightly smaller plasma operating with somewhat lesser performance parameters but with higher availability, could provide an adequate D-T fusion neutron source to maintain a 3000 MWth annular fast burner reactor surrounding the plasma<sup>4,16</sup> over an operating period of 2800 full power days in a 4-batch fuel cycle that would accumulate 200 dpa in the discharged fuel cladding, the design limit on the ODS steel fuel cladding. The SABR fusion neutron source is described in Fig.1 and Table 1.



Plasma	
Major radius	4.0m
Plasma radius	1.2m
Elongation	1.5
Toroidal magnetic field (on axis)	5.6T
Plasma current	10 MA
Inductive current startup	6.0 MA
Non-inductive current drive	4.5 MA
Bootstrap current fraction	0.55
Heating & current-drive power	110 MW (70 EC, 40LH)
Confinement factor $H_{98}$	1.2
Normalized $\beta_N$	3.2%
Safety factor at 95% flux surface	3.0
Max. and BOL fusion power	500 MW and 233 MW
Max. fusion neutron source strength	$1.8 \times 10^{20} \text{n/s}$
Fusion gain ( $Q_p = P_{\text{fusion}}/P_{\text{extheat}}$ )	4.6

Table 1 SABR plasma physic parameters

Fig. 1 SABR configuration

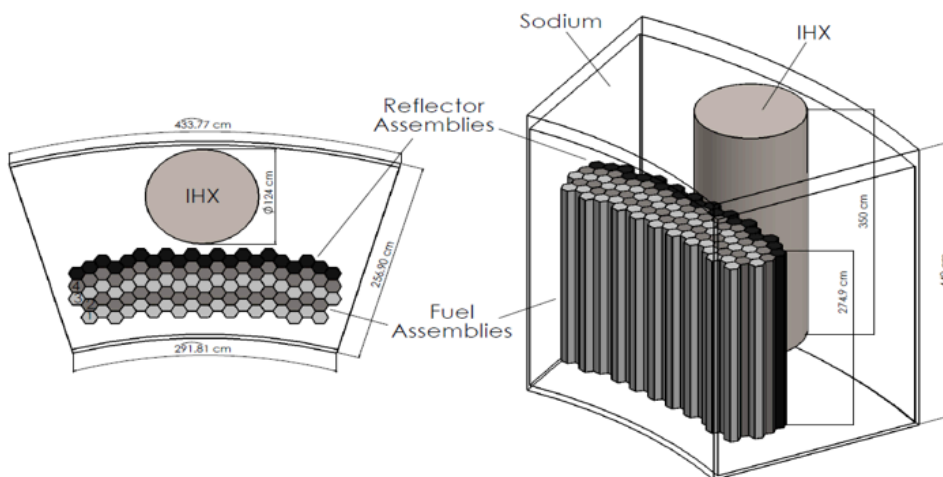


Fig. 2. SABR modular sodium pool with reactor and intermediate heat exchanger.

The ITER magnetic, first-wall and divertor systems (the latter two converted to Na coolant) were used with minimal alteration, and the heating-current drive system was adapted from that of ITER. The TRU-Zr fuel is clad with ODS steel in 0.54 cm OD fuel pins, 469 of which are contained in each of the 80 fuel assemblies, 13.9 cm across flats, in each of the 10 Na-pools. Each pool also contains an intermediate heat exchanger, as depicted in Fig. 2. A 3 mm thick SiC flow channel insert is placed within

each assembly to prevent current loops connecting through the duct wall, which would increase the MHD pressure drop.

The fuel pin design is depicted in Fig. 3. The pin is about 2 m in height, with the TRU fuel in the lower third and a fission gas plenum in the upper two-thirds.

The fuel assembly consists of 469 of these pins, arranged as indicated in Fig. 4. Note the SiC liner separating the fuels pins and sodium within the assembly from ODS steel duct in order to prevent current loops that would cause MHD pressure drops.

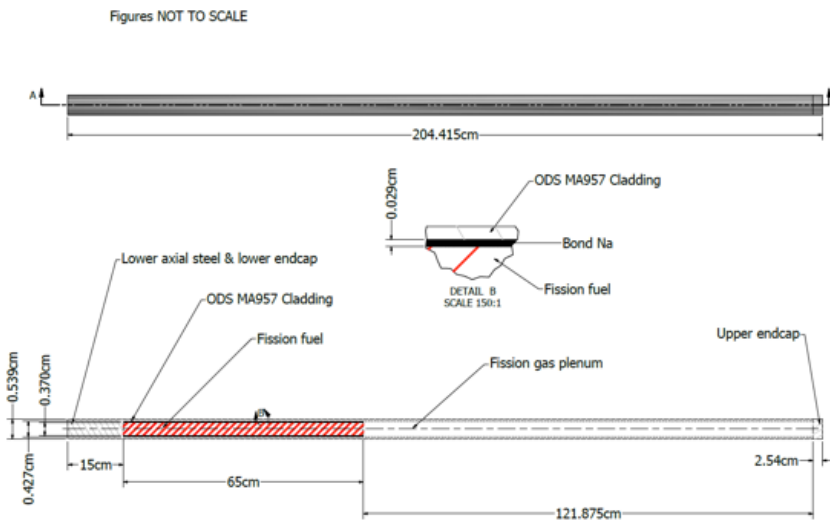


Fig. 3. TRU fuel pin configuration.

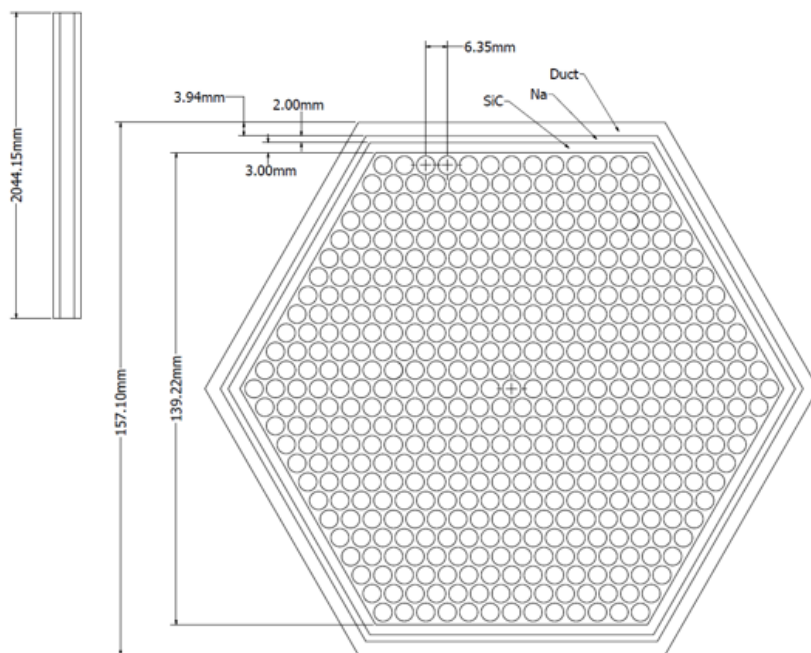


Fig. 4. TRU fuel assembly configuration.

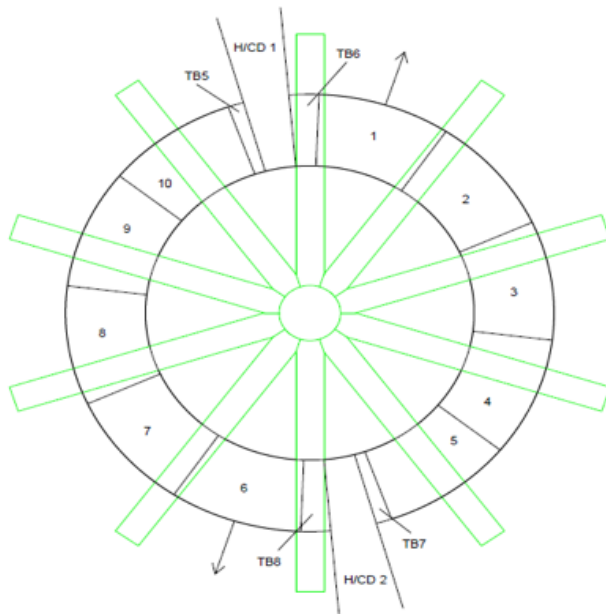


Fig. 5. Removal of Na-pools from modular pool configuration

<b>Sodium Pool</b>	
Number of modular pools	10
Mass of fuel per pool	1510.4 kg
Mass of Na per pool	22,067 kg
Power per pool	300 MWth
Power Peaking	1.27
Mass flow rate per pool	1669 kg/s
Number of pumps per pool	2
Pumping power per pool (EM pumps)	20 MW
Core Inlet/Outlet temperatures	628 K/769 K
Fuel Max Temp/Max Allowable Temp	1014 K/1200 K
Clab Max Temp/Max Allowable Temp	814 K/973 K
Coolant Max Temp/Max Allowable Temp	787 K/1156K

Table 2 SABR modular sodium pool parameters

Fuel assembly calculations were made in 1968 groups P1 transport theory to homogenize the fuel assemblies for a 2D, S8, 33-group ERANOS neutronics calculation, and RELAP-5 thermal-hydraulic calculations were made to obtain the parameters given in Table 2.

Refueling (removal and replacement) of the fuel assemblies located within the TF coil configuration is a challenging design issue that was addressed as illustrated in Fig. 5. Transport casks for removal of an individual Na pool to a hot bay are located between TF coils on the outboard at the locations of pools 1 and 6 in Fig. 5. The pools in these locations are removed radially, first, then the other pools are individually rotated to a port and removed. The secondary coolant system must be disconnected for the individual pool during its removal. The thermal capacity of the pool must absorb the decay heat during the removal to prevent clad damage, which places an upper limit on the allowed decay heating for a given decay heat fraction. We estimate the procedure will work for 1 h removal time and decay heat equal 1% of operating power, which it will reach about 3 h after shutdown.

### 3. Fuel cycle

Several fuel cycles based on pyroprocessing the fuel removed from SABR to separate the remaining transuranics in aggregate from the fission products and recycling of the TRU have been investigated<sup>22-27</sup>. The maximum fuel residence time in the reactor is limited to 700 days by the 200 dpa radiation damage limit on the fuel cladding. A 4-batch fuel cycle is indicated in Fig. 6. The maximum effective multiplication constant was  $k_{eff}^{BOL}$ ; 0,97 at BOL and the maximum fusion power required to maintain the 3000MWth fission rate was < 500 MW.

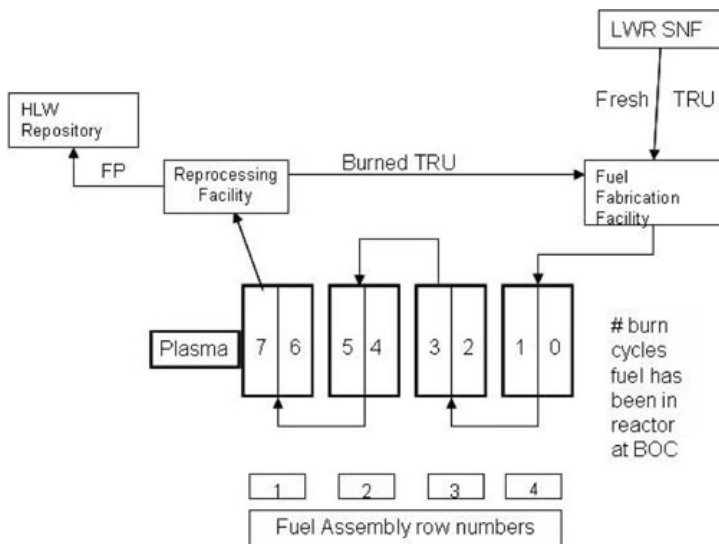


Fig. 6 The SABR 4-batch out-to-in fuel cycle.

A SABR, based on the sodium cooled, metal fuel technology developed at ANL<sup>33,34</sup> and proposed in the ANL IFR<sup>35</sup> and the GE PRISM reactor<sup>36</sup>, operating at 75% availability with a 4-batch out-to-in fuel cycle (with total fuel residence time limited by 200 dpa radiation damage in the clad) could destroy annually all the transuranics produced annually by three 3000MWth LWRs<sup>22,23,25</sup>. Thus, an equilibrium nuclear fleet could be envisioned in which 75% of the power is produced by advanced versions of the present LWRs and 25% is produced by SABRs burning the transuranics produced in the LWRs.

In an alternative fuel cycle in which the LWRs are phased out in favor of critical fast reactors, the Pu could be separated from the transuranics in spent fuel and used to fuel critical fast reactors, while the remaining "minor actinide" transuranics were used to fuel SABRs.

One 3000MWth SABR could destroy annually all the minor actinides produced annually in 25 3000MWth LWRs. With such SABR fleets, the relatively short-lived fission products (most with less than a few hundred year half-life), the few longer-lived fission products and trace amounts of transuranics would still need to be buried in secure repositories, but an order of magnitude fewer of them would be needed than for the direct burial of LWR spent fuel.

#### 4. Tritium self-sufficiency

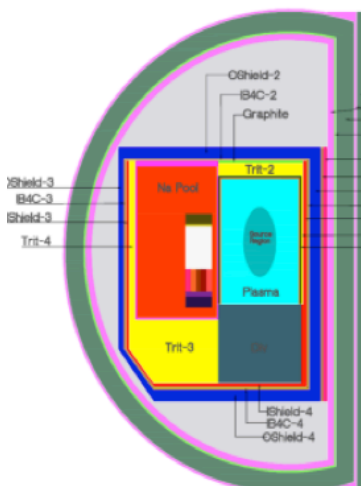
Modular sodium-cooled  $Li_4SiO_4$  blankets are located i) above the plasma, ii) below the sodium pools, iii) outboard of the sodium pools and iv) in two locations 180° apart in the ring of sodium pools shown in Fig. 3 (TB5, TB6, TB7, TB8). This tritium must migrate through the blanket to helium purge channels, which requires a blanket temperature in the range  $325\text{ C} < T < 925\text{ C}$ . Thermal-hydraulics calculations indicate that the nuclear heating can readily be removed to maintain temperatures in the blanket within this temperature window.

Neutron transport calculations (R-Z,  $S_8$ , 33-grp) indicate that this configuration produces an average TBR = 1.12. A time-dependent calculation of the tritium inventory in the  $Li_4SiO_4$  blankets, the tritium processing system, the tritium storage system and plasma demonstrated tritium self-sufficiency for an operational cycle based on one year of burn at 75% availability, followed by 90 days of downtime for the refueling operation. SABR consumes about 15 kg/yr of tritium.

#### 5. Shielding

The SABR shield design is indicated in Fig. 7. A 2D, R-Z MCNP-B Monte Carlo calculation confirmed that this shield design reduced the radiation damage to the TF Coils below the design limits shown in Table 3 for a 40 yr operational lifetime at 75% availability.

### SHIELDING (SABR MEETS 30FPY DESIGN OBJECTIVE)



Radiation Limit	Value	Units
Insulation Dosage	$1 \times 10^9$	rads
Nuclear Heating Rate	1.0 – 5.0	mW/cc
Neutron (>0.1MeV) fluence	$1.0 \times 10^{19}$	n/cm <sup>2</sup>
Copper Stabilizer Resistivity	1.2	nΩm

Fig. 7: SABR Shield Design

Table 3: SABR Shield Design Limits to TF Coils

## 6. Ongoing dynamic safety analysis

### a) Feedback Control of Plasma Power Excursions

The SABR must be designed to prevent or suppress any dynamic power surges that may inadvertently occur in the plasma neutron source or in the modular fission cores. The actions of various negative and positive reactivity feedback mechanisms for the fission cores are well-known, and in fact it was demonstrated in EBR-II that metal-fuel, sodium pool technology could be designed to be inherently safe (i.e. negative feedback mechanisms shut the reactor down without damage when pumps in the sodium pool and in the external heat removal system were intentionally shut down to increase the fuel temperatures<sup>33,37,38</sup>).

Earlier work<sup>28</sup> examined the transient response to loss-of-flow, loss-of-heat-sink and loss-of-power events in a single 3000MWth SABR core with a sodium-loop cooling system. The earlier loop-type cooling system has now been replaced by a modular sodium pool design with the intention of capturing the inherent safety features demonstrated by such a system. We are constructing a coupled-core, or nodal, neutron and coolant dynamics model of the 10 fission cores, the fusion neutron source and the associated heat removal systems in order to investigate whether these inherent safety features<sup>33,37,38</sup> can be retained by the SABR modular core design and to investigate if the modular fission core configuration might be subject to spatial power oscillations.

Power excursions in the plasma neutron source, due either to instabilities within the plasma or to the inadvertent turn-on of a modular plasma heating unit or pellet fueling unit or the inadvertent opening of a gas fueling valve, etc. are a concern because they would produce power excursions in the fission cores. We have recently begun an investigation of burn control mechanisms that could limit unanticipated D-T plasma power excursions. We are motivated by the observation that the edge plasma parameters have a strong impact on the core plasma parameters to search for possible burn control mechanisms in the plasma edge. Experimental and theoretical observations encourage us that it may be possible to use fueling of deuterium or a seeded impurity gas in such a way that the plasma would respond to an increase in edge temperature by momentarily dropping into the L-mode confinement regime and thereby to terminate or at least limit any plasma power excursion.

We are presently assembling a dynamic plasma-impurities-neutrals edge transport code coupled to a global plasma dynamics code, a wall recycling model and a 2-pt divertor model for the purpose of investigating the ability of modulated gas puffing (D) or impurity seeding (Ne, Ar, Xe) to create edge conditions in which an increase in edge temperature causes a momentary H-L transition to suppress the power excursion. For example, impurities seeded into a plasma edge that was somewhat cooler than the temperature for which the impurity radiation is maximum would respond to an increase in temperature with an increase in radiative power, hence a decrease in non-radiative power across the separatrix below the threshold  $P_{\min}^{H-L}$ , causing the plasma to drop momentarily into L-mode in response to a positive edge temperature excursion and thus serving as a burn control mechanism. Another possibility that will be investigated is that an increase in edge temperature would produce an increase in ion orbit loss of energy that would terminate a power excursion.

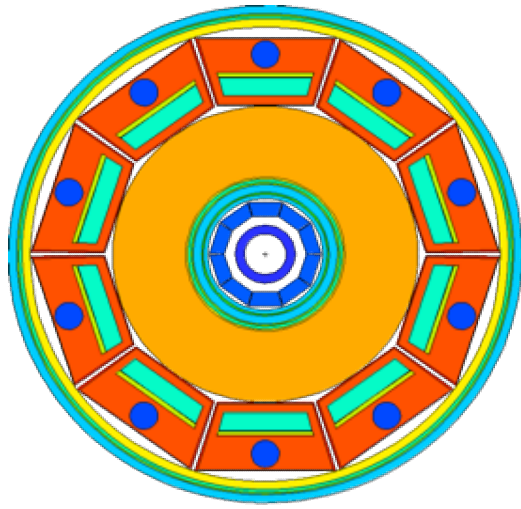
### b) Nodal Neutron Dynamics Model

We are developing a coupled nodal neutron dynamics model for the neutron population in the different sodium pools. A node is defined as all of the fuel assemblies and reflector assemblies in a given sodium pool. These nodal kinetics equations will be used to calculate the time-dependent power in each separate core during various accident scenarios such as Loss of Flow Accidents (LOFA) and Loss of Heat Sink Accidents (LOHSA). The neutron dynamics equations for the neutron density and for the delayed neutron precursor density in group  $i$  in each node  $j$ ,  $c_{i,j}$  are

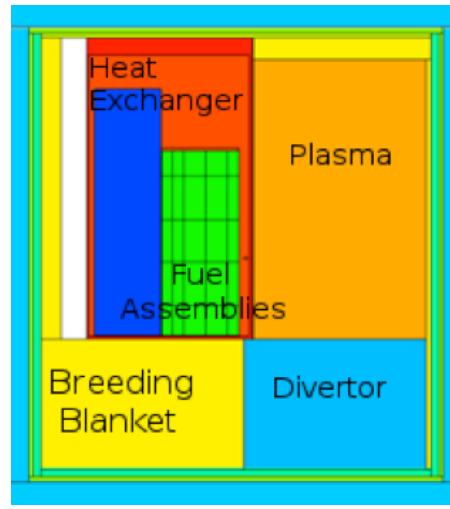
$$\frac{dn_j(t)}{dt} = \frac{(1 - \beta_j)}{\Lambda_j} n_j(t) + \sum_{i=1}^6 \lambda_{i,j} c_{i,j}(t) + \frac{n_j(t)}{\tau_j} + S_{\text{fus},j} + \sum_{k=1}^{10} \frac{\alpha_{k,j} n_k(t)}{l_{e,k}} - \frac{n_j(t)}{l_{e,j}} - \frac{n_j(t)}{l_{a,j}}$$

$$\frac{dc_{i,j}}{dt} = \frac{\beta_{i,j}}{\Lambda_j} n_j(t) - \lambda_{i,j} c_{i,j}$$

$\Lambda$  is the fission generation time,  $\tau$  is the n-2n generation time,  $l_a$  is the absorption lifetime,  $l_e$  is the escape lifetime,  $S_{\text{fus},j}$  is the rate at which fusion neutrons from the plasma enter node  $j$ , and  $\alpha_{k,j}$  is the nodal coupling coefficient (i.e. the probability that a neutron leaking from node  $k$  will enter node  $j$  before entering another node). These kinetics terms are calculated using MCNP6<sup>39</sup> in a 3D geometry shown in Fig.8. We also include in the model a calculation of how these kinetics parameters change during various perturbations such as fuel Doppler broadening, sodium voiding, fuel rod axial expansion, core grid plate expansion, and fuel bowing.



Top down view sodium pools in MCNP model



Side view of sodium pools in MCNP model

Figure 8 3D Geometry of Nodal Neutron Dynamics Model

The power is calculated in MATLAB by numerically solving the kinetics equations. This MATLAB model is coupled to COMSOL Multiphysics<sup>40</sup> which in turn solves all of the thermal and fluid calculations required for each accident scenario. For each of the 10 nodes, there is one neutron density equation and 6 precursor equations.

## 7. Economics

Over the past two years, the SABR research group has collaborated with Georgia Tech's Scheller College of Business and the law school at Emory University to investigate the economic viability of the SABR concept and explore potential commercialization strategies<sup>41</sup>.

This investigation initially focused on the United States as a target market for SABR, however the team later expanded to consider other markets (countries) around the world. The primary attributes for any suitable SABR market are: (1) a dependency on nuclear energy generation; (2) the existence of a "commercial" reprocessing program; (3) a favorable regulatory environment and public opinion; and (4) status as an ITER Party. Reprocessing, which is a method that separates the transuranic waste components of spent nuclear fuel, is a critical technology for any suitable SABR market. There are significant challenges in assessing the economic viability of a potential SABR implementation, not the least of which is the significant amount of uncertainty in the construction cost of a SABR. The determination of whether a SABR scenario could be economically viable vis-à-vis direct burial of SNF in HLWRs cannot be based on a simple cost comparison because, unlike geological repositories, SABRs would produce electricity, change the number of traditional nuclear reactors in operation, and even affect the cost of fuel for those traditional nuclear reactors.

To reduce these complex considerations to a single number, the energy industry uses the Levelized Cost of Electricity (LCOE). The LCOE can be thought of as the current price of electricity per kilowatt-hour from a power plant which, when adjusted for inflation throughout the lifetime of the plant, would result in the plant meeting all debt obligations incurred in constructing the plant and providing a reasonable return to equity investors. Calculations of the LCOE for nuclear power, such as that done by MIT in the 2003 report "The Future of Nuclear Power", typically stop short of accounting for the true societal cost of the SNF. Instead, they use the waste fee that nuclear plants are required to pay to the federal government. The team modified the calculation to compute a true, post-waste LCOE, which is better suited to evaluating the effects of a SABR program on the complex nuclear industry.

It is not feasible at this time to estimate the cost of a SABR and its prorated share of the associated fuel processing and re-fabrication facilities—a SABR+ cost. Instead, we are taking the approach of determining a "break-even" SABR+ cost with respect to direct burial of SNF in HLWRs. We will first determine the true LCOE of nuclear power with direct burial of SNF in HLWRs that can be secured indefinitely into the future. We will then determine the "break-even SABR+" cost for each SABR and its prorated share of the associated reprocessing and fuel fabrication facilities for which the electricity revenue and cost savings resulting from avoiding the construction of the majority of the repositories will result in a similar overall LCOE for nuclear energy, compared to the direct SNF burial in HLWRs (i.e. Yucca Mountains) scenario. A lower than "break-even" construction cost for a SABR and its prorated associated reprocessing and fuel re-fabrication facilities would result in a lower LCOE for nuclear power with SABRs than with HLWRs. If plutonium is separated during the reprocessing stage and used as fuel in critical fast reactors to produce additional electricity, the LCOE for the SABR scenario can be reduced; however this would mitigate the non-proliferation aspect of the reference SABR fuel cycle in which the transuranics and the plutonium are processed as an aggregate metal.

## 8. Summary

- SABR FISSION PHYSICS & TECHNOLOGY HAS BEEN PROTOTYPED BY EBR-2.
- SABR FUSION PHYSICS & TECHNOLOGY WILL BE PROTOTYPED BY ITER.
- SABR USES THE ITER MAGNET SYSTEM AND THE ITER FIRST-WALL AND DIVERTOR SYSTEMS, THE LATTER MODIFIED FOR NA-COOLANT.
- MODULAR DESIGN ALLOWS REFUELING OF FISSION REACTOR LOCATED WITHIN MAGNET SYSTEM.
- SiC INSERTS IN FUEL ASSEMBLIES REDUCES MHD EFFECTS OF NA FLOWING IN B-FIELD.
- SABR IS TRITIUM SELF-SUFFICIENT.
- SABR IS ADEQUATELY SHIELDED TO ACHIEVE 30 FPY.
- SABRS CAN REDUCE THE HLWR CAPACITY NEEDED FOR NUCLEAR POWER BY 10-100.
- 1 SABR CAN BURN THE ANNUAL TRU PRODUCTION OF 3, 1000MWE LWRS, OR THE ANNUAL MA PRODUCTION OF 25, 1000MWE LWRS.
- PASSIVE SAFETY POTENTIAL OF SABR FISSION & FUSION SYSTEMS IS BEING INVESTIGATED.
- THE BREAK-EVEN COST OF SABR + FUEL REPROCESSING/RE-FABRICATION FACILITIES IS BEING EVALUATED BY EQUATING THE LCOEs FOR NUCLEAR POWER WITH THE SABR BURN OPTION AND WITH THE DIRECT BURIAL OF SNF IN HLWRs.

### Appendix: the rationale for a subcritical advanced burner reactor (SABR)

1. Nuclear power is the only technically credible option for carbon-free electric power on the scale needed to impact climate change for at least the first half of the present century.
2. The major technical problem now confronting the widespread expansion of nuclear power is disposal of the extremely long half-life transuranics (TRU) in spent nuclear fuel (SNF) in high-level radioactive waste repositories (HLWRs) that can be secured for  $10^5$ - $10^6$  yrs .
3. TRU can be fissioned, much more readily in a fast than a thermal neutron spectrum reactor, to yield energy and short half-life fission products (FPs), most which only need to be stored in secured HLWRs for 10-100 years.
4. Reprocessing LWR SNF to separate TRU from the remaining U and FP for use as fuel in advanced fast burner reactors (ABRs) would reduce the required HLWR capacity for nuclear power to that needed to store the long-lived FPs and trace amounts of TRU due to inefficiencies in separation, at least by a factor of 10. (This means e. g. that the present level of nuclear power in the USA would require a new Yucca Mntn. every 300 years instead of every 30 years.)
5. Subcritical operation of ABRs with an external neutron source (e.g. SABR) would have certain advantages:
  - a. The reactivity margin of error to a prompt critical power excursion in a critical reactor is the delayed neutron fraction  $\beta$ , which is about 0.002 for TRU, as compared to about 0.006 for U. Prudence would probably dictate that a critical ABR be only partially fueled with TRU (maybe 20%). In a SABR the reactivity margin of error to a prompt critical power excursion is  $\Delta k_{sub} > 0.03 \gg \beta$ , so a SABR could be fueled 100% with TRU.
  - b. Since the power level (fission transmutation rate) can be maintained constant as the fuel depletes in a SABR by increasing the neutron source strength, the fuel can remain in the reactor until it reaches the radiation damage limit, thereby minimizing the number of fuel reprocessing steps and the trace amount of TRU in with the FPs that go to the HLWR. On the other hand, in a critical reactor additional reactivity must be built into the fuel to offset the fuel depletion.
6. The fission physics and technology for a SABR based on: a) a pool-type Na-cooled, TRU-Zr metal fuel has been prototyped by the EBR-2 program in the USA; and b) a Na-cooled oxide fuel has been prototyped in many countries.
7. In the pyro-processing fuel cycle that would be used with the TRU-Zr fuel all the TRU (Pu, Np, Am, Te) is separated from the FPs as an aggregate metal—the Pu is never separated from the other TRU—which greatly reduces any proliferation risk.

### References

1. [www.ITER.org](http://www.ITER.org)
2. W. M. Stacey, "Capabilities of a DT Tokamak Fusion Neutron Source for Driving a Spent Nuclear Fuel Transmutation Reactor" , Nucl. Fusion 41, 135 (2001).
3. W. M. Stacey, "Tokamak Neutron Source Requirements for Nuclear Applications", Nucl. Fusion 47, 217 (2007).
4. J. P. Floyd, S. M. Jones, M. Kato, J. C. Schultz, B. H. Schrader, J. B. Weathers, W. M. Stacey, Z. W. Friis and R. W. Johnson, "Tokamak Fusion Neutron Source for a Fast Transmutation Reactor" Fusion Sci&Techn 52, 727 (2007).
5. W. M. Stacey, "Subcritical Transmutation Reactors with Tokamak Neutron Sources Based on ITER", Fusion Sci&Techn. 52, 719 (2007).

6. W. M. Stacey, "Transmutation Missions for Fusion Neutron Sources", *Fus. Eng. Des.* 82, 11 (2007).
7. W. M. Stacey, B. L. Pilger, J. A. Mowrey, D. C. Norris, M. Dietsche, E. A. Hoffman, et al., "A Transmutation Facility for Weapons-Grade Plutonium Disposition Based on a Tokamak Fusion Neutron Source", *Fusion Techn.* 27, 326 (1995).
8. W. M. Stacey, J. A. Favorite, M. J. Belanger, R. D. Granberg, S. L. Grimm, F. A. Kelly, et al., "A Tokamak Tritium Production Reactor", *Fusion Techn.* 32, 563 (1997).
9. W. M. Stacey, J. Mandrekas, E. A. Hoffman, G. P. Kessler, A. N. Mauer, et al., "A Fusion Transmutation of Waste Reactor", *Fusion Sci&Techn.* 41, 116 (2002).
10. E. A. Hoffman and W. M. Stacey, "Nuclear Design and Analysis of the Fusion Transmutation of Waste Reactor", *Fusion Sci&Techn.* 63-64, 87 (2002).
11. W. M. Stacey, J. Mandrekas and E. A. Hoffman, "Subcritical Transmutation Reactors with Tokamak Fusion Neutron Sources", *FusionSci&Techn.* 47, 1210 (2005).
12. A. N. Mauer, J. Mandrekas and W. M. Stacey, "A Superconducting Transmutation of Waste Reactor", *Fusion Sci&Techn.* 45, 55 (2004).
13. W. M. Stacey, V. L. Beavers, W. A. Casino, J. R. Cheathan, Z. W. Friis, et al., "A Subcritical, Gas-Cooled Fast Transmutation Reactor with a Fusion Neutron Source", *Nucl. Techn.* 150, 162 (2005).
14. W. M. Stacey, Z. Abbasi, C. J. Boyd, A. H. Bridges, E. A. Burgett, M. W. Cymbor, et al., "A Subcritical Helium-Cooled Fast Reactor for the Transmutation of Spent Nuclear Fuel", *Nucl. Techn.* 156, 99 (2006).
15. W. M. Stacey, K. A. Boakey, S. K. Brashear, A. C. Bryson, K. A. Burns, et al., "Advances in the Subcritical Gas-Cooled Fast Transmutation Reactor Concept", *Nucl. Techn.* 159, 72 (2007).
16. W. M. Stacey, W. Van Roojen, T. Bates, E. Colvin, J. Dion, J. Feener, et al., "A TRU-Zr Metal-Fuel Sodium-Cooled Fast Subcritical Advanced Burner Reactor", *Nucl. Techn.* 162, 53 (2008).
17. W. M. Stacey, "Georgia Tech Studies of Sub-Critical Advanced Burner Reactors with D-T Fusion Tokamak Neutron Source for the Transmutation of Spent Nuclear Fuel", *J. Fus. Energy* (2009).
18. W. M. Stacey, C. L. Stewart, J-P. Floyd, T. M. Wicks, A. P. Moore, A. T. Bopp, M. D. Hill, S. Tandon and A. S. Erickson, "Resolution of Fission Fusion Technology Integration Issues: An Upgraded Design Concept for the Subcritical Advanced Burner Reactor", *Nucl. Techn.* 187, 15 (2014).
19. C. L. Stewart and W. M. Stacey, "The SABrR Concept for a Fission-Fusion Hybrid 238U-to- 239Pu Fissile Production Reactor", *Nucl. Techn.* 187, 1 (2014).
20. E. A. Hoffman and W. M. Stacey, "Comparative fuel cycle analysis of critical and subcritical fast reactor transmutation systems", *Nucl. Techn.* 144, 83 (2003).
21. J. W. Maddox and W. M. Stacey, "Fuel Cycle Analysis of a Subcritical Fast Helium-Cooled Transmutation Reactor with a Fusion Neutron Source", *Nucl. Techn.* 158, 94 (2007).
22. W. M. Stacey, C. S. Sommer, T. S. Sumner, B. Petrovic, S. M. Ghiaasiaan and C. L. Stewart, "SABR Fusion-Fission Hybrid Reactor Based on ITER", *Proc. 11th OECD/NEA info exchg mtg on Actinide Separation* (2010).
23. C. M. Sommer, W. M. Stacey and B. Petrovic, "Fuel Cycle Analyses of the SABR Subcritical Transmutation Reactor Concept" *Nucl. Techn.* 172, 48 (2010).
24. V. Romanelli, et al., "Comparison of the Waste Transmutation Potential of Different..." "Proc. 11th OECD/NEA info exchg mtg on Actinide Separation (2010).
25. C. M. Sommer, W. M. Stacey and B. Petrovic, "Fuel Cycle Analysis of the SABR Subcritical Transmutation Reactor Concept", *Nucl. Techn.* 172, 48 (2010).
26. V. Romanelli, C. Sommer, M. Salvatores, W. Stacey, W. Maschek, B. Petrovic, F. Gabrielli, A. Schwenk-Ferrero, A. Rinsiski and B. Vezzoni, "Advanced Fuel Cycle Scenario Study in the European Context Using Different Burner Reactor Concepts", *Actinide Separation mtg*, ISBN 978-92-64-99174-3, OECD/NEA (2012).
27. C. S. Sommer, W. M. Stacey, B. Petrovic and C. L. Stewart, "Transmutation Fuel Cycle Analyses of the SABR Fission-Fusion Hybrid Reactor for Transuranic and Minor-Actinide Fuels", *Nucl. Techn.* 182, 274 (2013).
28. T. S. Sumner, W. M. Stacey and S. M. Ghiaasiaan, "Dynamic Safety Analyses of the SABR Subcritical Transmutation Reactor Concept", *Nucl. Techn.* 171, 123 (2010).
29. W. M. Stacey, "Georgia Tech Studies of Sub-Critical Advance Burner Reactors", *J. Fusion Energy* 28, 328 (2009).
30. W. M. Stacey, "Principles and Rationale of the Fusion-Fission Hybrid Burner Reactor", *Fusion for Neutrons and Subcritical Nuclear Fission 1" AIP Conf. Proc.* 1442, 31 (2012).
31. W. M. Stacey, "A Strategic Opportunity for Magnetic Fusion Energy Development", *J. Fusion Energy* 35, 111 (2016).
32. B. Richter, "Beyond Smoke and Mirrors", 2nd ed., Cambridge Univ. Press, Cambridge (2014).
33. J. Sackett, "Operating and Test Experience with EBR-II, the IFR Prototype", *Prog. Nucl. Energy* 31, 111 (1997).
34. C. E. Till and Y. I. Chang, *Plentiful Energy: The Story of the Integral Fast Reactor*, (Create Space, Charleston) 2011.
35. Y. I. Chang, et al., "Advanced Burner Test Reactor Preconceptual Design Report", ANL-ABR-1, Argonne Nat. Lab. Report (2008).
36. A. E. Dubberly, et al., "Super-PRISM Oxide and Metal Fuel Core Designs", *Proc. ICONE 8* (2000).

37. S. Fistedis, "The Experimental Breeder Reactor-II Inherent Safety Demonstration", Nucl. Eng. Des. 101, 1 (1987).
38. D. C. Wade, R. A. Wigeland and D. J. Hill, "The Safety of the IFR", Prog. Nucl. Energy 31, 63 (1997).
39. "LANL Monte Carlo Working Group," <https://mcnp.lanl.gov/>, (Current as of Aug. 23 2016).
40. "COMSOL Multiphysics," <http://www.comsol.com/comsol-multiphysics>, (Current as of Aug. 23 2016).
41. M. Hill, L. Pratt, J. Collens, R. High and B. Warner, "SABR: The economically viable, socially responsible solution to the nuclear waste crisis", TiGR report, College of Business, Georgia Institute of Technology (2016).

## 6 - Plasma controls in FFH machines

**F. Crisanti**

*ENEA, Dipartimento FSN, C. R. Frascati, via E. Fermi 45, 00044 Frascati (Roma), Italy*

Control aspects are one of the fundamental aspects of any presently ongoing or planned fission and/or fusion device, consequently it is quite obvious that, in a integrated fusion/fission reactor, the control aspects will play even more a key role, from the machine performances point of view up to the safety point of view. Since an actual design of an hybrid reactor does not yet exist, obviously it is difficult to exactly define the necessary integrated control system, but a clear point can easily stated out. Differently from the ongoing commercial fission reactors, hybrid reactors are potentially inherently safe, because they remain deeply subcritical under all conditions and decay heat removal is possible via suitable passive mechanisms. Fission is driven by the neutrons provided by fusion reaction, consequently it is not self-sustaining. If the fusion process is interrupted for any reason (deliberately or by any casual event), the fission reaction stops immediately. This is in contrast to the forced shut off in a conventional fission reactor by controlling the rods to reduce the neutron flux below the critical, self-sustaining, level. In a hybrid configuration the fission and fusion reactions are decoupled, i.e. while the fusion neutron output drives the fission, the fission output has no effect whatsoever on the fusion reaction, completely eliminating any chance of a positive feedback loop. Under this frame it quite obvious that the main critical machine control aspects are inherent to the fusion part (the drive) of the reactor. In this talk all the present Tokamak control aspects will be described, starting from the plasma performances up to the necessary condition to guarantee a steady state (or quasi steady state) plasma scenario. Looking ahead to an experiment relevant for an hybrid reactor (at least  $Q \approx 2 \div 3$ ) the engineering most critical control aspects will be addressed, including the necessity to guarantee at least a  $TBR \approx 1.2$  and a neutron flux at least of the order  $2 \div 3 \text{ MW/m}^2$  in a safe a reliable way.

## 7 - Development and Experiment of Fusion Neutron Driven Zero Power Subcritical Fast Reactor

**Y. Wang\*, S. Chen, C. Liu, Q. Wu, Y. Wu, FDS Team**

*Key Laboratory of Neutronics and Radiation Safety, Institute of Nuclear Energy Safety Technology, Chinese Academy of Sciences, Hefei, Anhui, 230031, China*

A fusion neutron driven zero power sub-critical fast reactor (FDS-0) is now under construction, which consists of High Intensity D-T Fusion Neutron Generator (HINEG) and Lead-based Zero Power Sub-critical Reactor (CLEAR-0). HINEG serves as neutron source which produces fusion neutrons to drive the sub-critical reactor CLEAR-0. FDS-0 will be a significant experimental platform for fusion-fission hybrid systems and fast reactor studies.

The R&D of HINEG includes two phases: HINEG-I and HINEG-II. HINEG-I has been completed and commissioning with the D-T fusion neutron yield of up to  $10^{12}$  n/s. Furthermore, the neutron yield of  $10^{13}$  n/s is expected to be achieved in near future. HINEG-II aims to have a high neutron yield of  $10^{15}\sim 10^{16}$  n/s. CLEAR-0 is a multi-functional zero-power reactor for simulating neutronics process in various hybrid systems and fast reactors. The core of CLEAR-0 is designed to be flexible with sufficient safe considerations, which could loaded with various fuel and coolant materials, such as lead or lead-based alloy which is been chosen as potential coolant for hybrid blankets or fast reactor due to their many unique nuclear, thermal-physical and chemical attributes. CLEAR-0 and HINEG could be coupled to form FDS-0 through locating the target in the center of CLEAR-0.

The recent experiment plan of FDS-0 is focused on verification and validation (V&V) of nuclear design and control and measurement technology for hybrid system. The data acquired from experiment, such as fission rate, neutron flux, tritium-breeding ratio, sub-criticality and so on, are compared with the results of Monte Carlo calculation to validate the conceptual design, software and data library used in fusion-fission hybrid reactor development. Also, the experiment data from FDS-0 will be used to verify the control and measurement methods for hybrid system.

## 8 - Development and Application of Super Monte Carlo Simulation Program for Fusion and Fission Nuclear Energy Systems

**Jing Song\*, Liqin Hu, Pengcheng Long, Lijuan Hao, Mengyun Chen, Huaqing Zheng, Shengpeng Yu, Guangyao Sun, Bin Wu, Qi Yang, Tongqiang Dang, Chaobin Chen, Peng He, Yican Wu, FDS Team**

*Key Laboratory of Neutronics and Radiation Safety, Institute of Nuclear Energy Safety Technology, Chinese Academy of Sciences, Hefei, Anhui, 230031, China*

The Monte Carlo (MC) methods have been broadly adopted in nuclear design and radiation safety evaluation of fusion, fission and hybrid nuclear energy systems due to the great complexity and high requirements on the precision. However, for traditional MC methods, great challenges prevent the application of MC methods. Advanced capabilities and features of Super Monte Carlo Simulation Program for Nuclear and Radiation Process (SuperMC) were developed by FDS Team to solve the corresponding problems, especially focusing on the following points :

- 1) The geometry of fusion and hybrid nuclear energy systems is extremely complicated. Tediousness, intensive labor and error-prone in geometry modeling process makes the accurate analysis unrealistic. The automatic CAD-based geometry modeling methods were developed with outstanding capabilities of decomposition and conversion of very complex geometry, void free geometry description, processing of high order surfaces, visual-based hierarchical structure modeling and etc.
- 2) Deep penetration of radiation shielding is another challenge situation. Series of novel methods were proposed to accelerate the convergence. Global weight window generator was proposed and speeded up the global flux calculation 249 times for the ITER (International Thermonuclear Experimental Reactor) A-Lite model. In this method, the expected contribution to a uniform particle distribution was considered at a very fine level and an efficient automatic iteration scheme was employed. The Optimal Spatial Subdivision method and Bounding Box method were proposed for geometry processing acceleration based on particle location anticipation.
- 3) Neutrons in fusion and hybrid nuclear energy systems are strongly anisotropic in large energy range with complex energy spectrum structure. The hybrid evaluation nuclear data libraries in SuperMC include fine-group, coarse-group, fine-group and point-wise nuclear data with selecting suitable energy structure and weight functions were developed. The physical effect was corrected including resonance self-shielding, thermal neutron up-scattering and temperature Doppler effect.

SuperMC has been verified by more than 2000 benchmark models and experiments. Now SuperMC has been applied in more than 30 major nuclear engineering projects.

## 9 - Application of a new fast reactor for fission-fusion hybrid systems

**Fabio Panza<sup>a</sup>, Marco Ciotti<sup>b</sup>, Francesco Paolo Orsitto<sup>c</sup>, Mikhail Osipenko<sup>a</sup>,  
Jorge Manzano<sup>d</sup>, Aldo Pizzuto<sup>d</sup>, Giovanni Ricco<sup>a,e</sup>, Marco Ripani<sup>a,e</sup>**

<sup>a</sup> Istituto Nazionale di Fisica Nucleare - Sezione di Genova (Italy)

<sup>b</sup> ENEA Casaccia, S. Maria di Galeria (Italy)

<sup>c</sup> Consorzio CREATE Università di Napoli Federico II, Napoli (Italy)

<sup>d</sup> CR ENEA Frascati, Via E. Fermi 27, 00044, Frascati (Italy)

<sup>e</sup> Centro Fermi, Roma (Italy)

### 1. Tokamak general characteristics

The aim of this work is to perform a feasibility study on a fusion-fission hybrid system based on a schematic tokamak model with the following characteristics, as reported in fig. 1:

- The torus major radius is 350 cm (1);
- The orange region represents the D-T elliptical plasma (minor axis 120 cm (2), major axis 210 cm (3));
- The white region is (15 cm thick) the vacuum (4) between the plasma and the first wall;
- The light blue/green region is the first wall, composed by 5 cm AISI 316 steel, 3 cm light water and 5 cm AISI 316 steel (5);
- The yellow region is the 100 cm thick Lead-Lithium breeder;
- The green boundary is the 1.5 cm thick external wall (7);
- The ratio between major and minor axis is 1.75, in all elliptical sections.

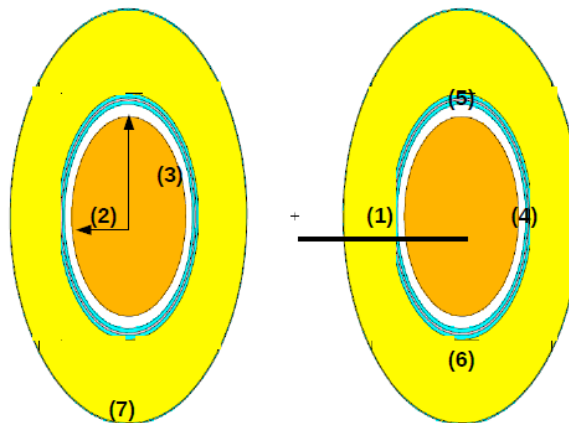


Fig. 1: Schematic tokamak side view.

### 2. Hybrid system

The first step was the study the properties of the hybrid system adding two 35 cm thick and 520 cm height cylindrical rings sub critical fission core around the first tokamak wall (black region) as shown in Fig. 2.

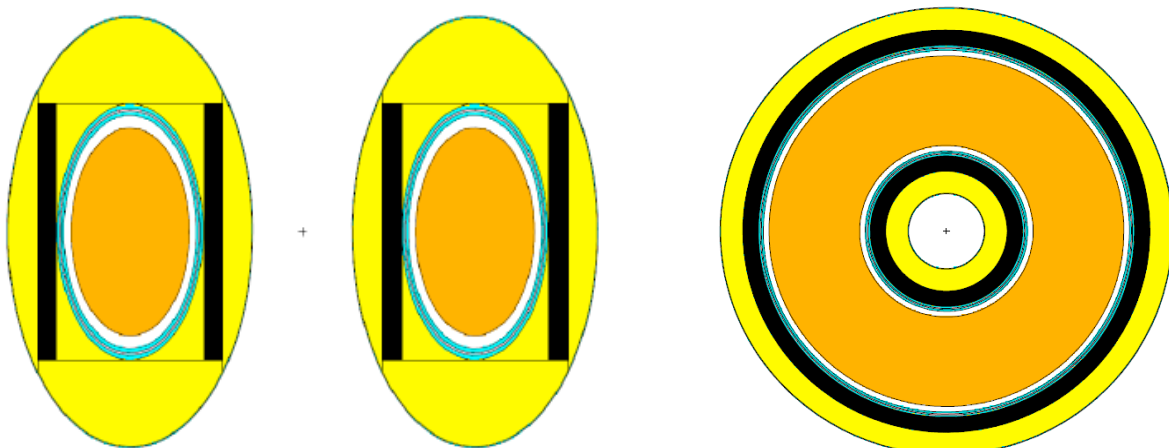
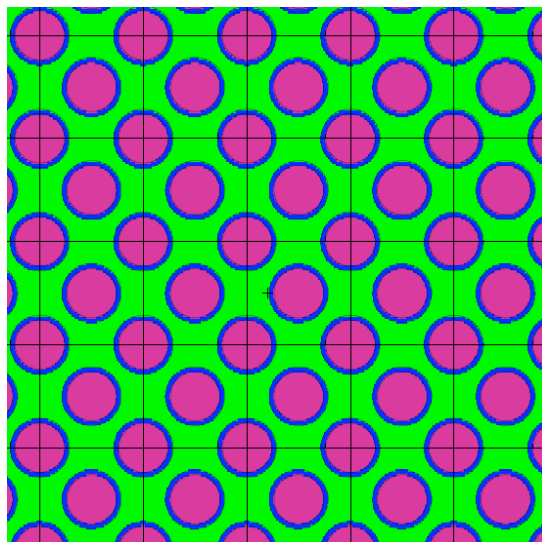


Fig. 2: Transverse (left) and horizontal (right) sections of the hybrid system.

A fission reactor core zoom is shown in Fig. 3 where it is possible to see, the 1.5 x 1.5 cm<sup>2</sup> elementary lattice, the 0.357 cm MOX (75% Uranium isotopes, 25% Pu isotopes) fuel pins (purple), the 0.07 cm thick AISI steel cladding (blue) and the liquid lead coolant (green). The composition of MOX fuel is reported in Table 1.



Nuclide	Percentage (%)
U-234	1.95E-3
U-235	2.63E-3
U-236	6.55E-3
U-238	6.67E+1
Pu-238	5.13E-1
Pu-239	1.26E-1
Pu-240	5.99E+0
Pu-241	1.36E+0
Pu-242	1.72E+0
Am-241	5.91E-2
O-16	1.20E+1

Fig. 3: Subcritical reactor core zoom, MOX fuel pins (purple), AISI steel cladding (blue), lead coolant (green).

Table 1: MOX fuel composition vector

The 14 MeV fusion neutrons are simulated as isotropically emitted from a mono-dimensional central 350 cm radius circumference (see Fig. 4).

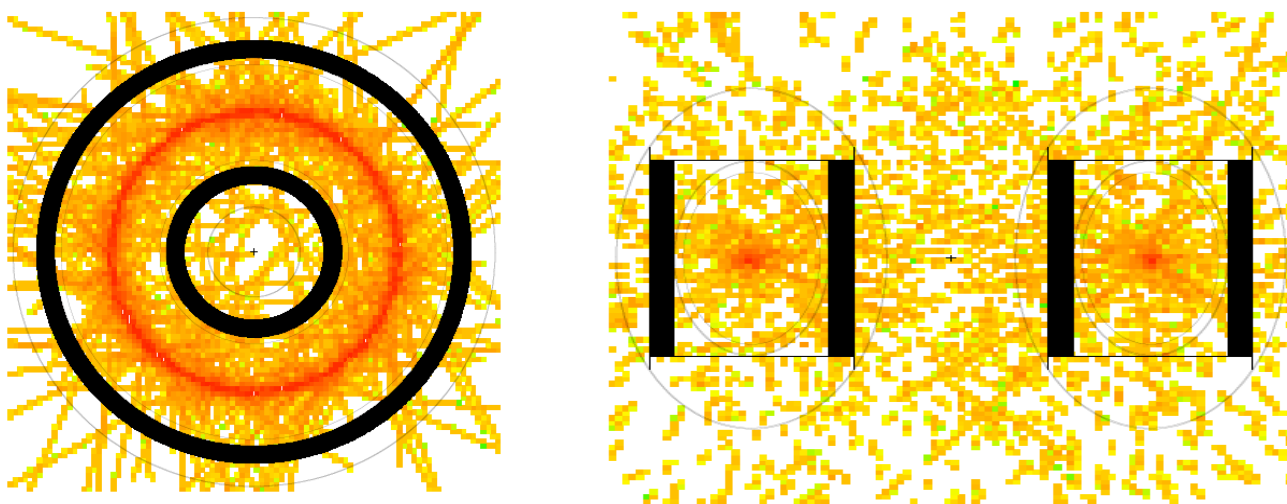


Fig. 4: Hybrid system horizontal (left) and vertical (right) sections in which it is possible to see the neutron source distribution.

The neutron source normalization factor has been evaluated assuming a monochromatic 14 MeV neutron flux impinging on the first tokamak wall, for a thermal load of 0.5 MW/m<sup>2</sup>. The neutron fusion source term, neglecting scattered and absorbed neutrons in the vacuum chamber, is  $5.83 \times 10^{19}$  n/s associated with a total fusion power of 160 MW.

The energy distribution of the neutron flux on the internal side (red line) and on the external side (blue line) of the tokamak first wall is reported in Fig. 5: the overall wall effect is an energy dependent attenuation.

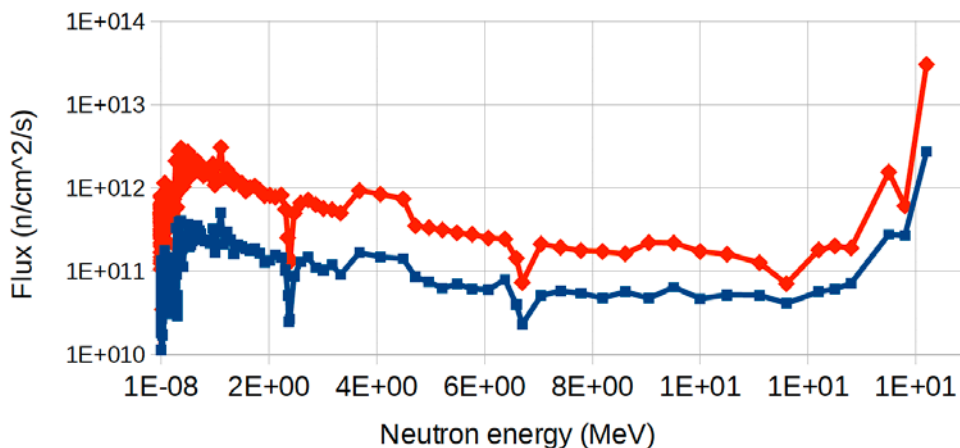


Fig. 5: Neutron flux energy distribution on the internal side (red line) and on the external side (blue line) of the first tokamak wall.

The effective multiplication factor  $k_{\text{eff}}$  and the thermal power behavior are reported as a function of the fission reactor core thickness in figures 6 and 7: a rapid power increase is observed for  $k_{\text{eff}} > 0.95$  corresponding to a core thickness  $> 34$  cm.

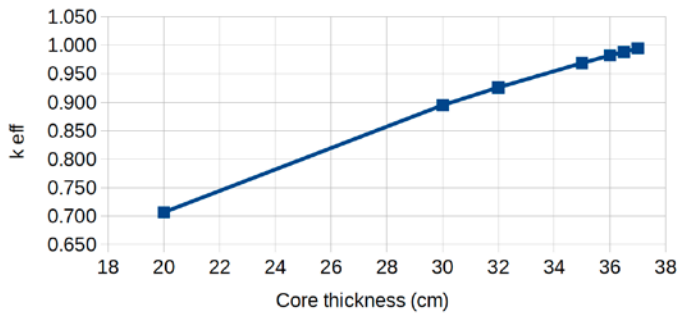


Fig. 6: Fission reactor effective multiplication factor as a function of the reactor core thickness.

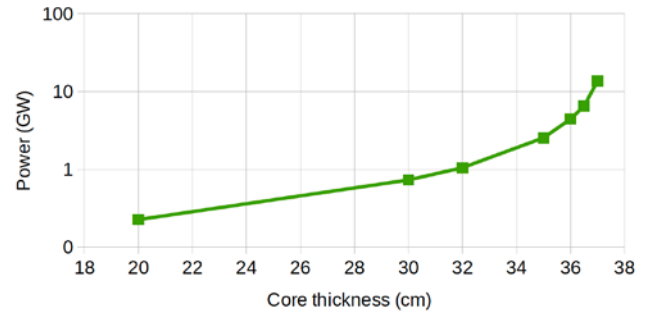


Fig. 7: Fission reactor thermal power as a function of the reactor core thickness.

For the following simulations, we have therefore chosen, as a reasonable safety level, a core thickness of 35 cm, corresponding to an effective multiplication factor of 0.97 and a 2.5 GW fission reactor thermal power. The amplification factor with respect to the fusion output power is 15.6.

The neutron flux and thermal power radial distributions are shown in figures 8 and 9 with the corresponding sampling positions.

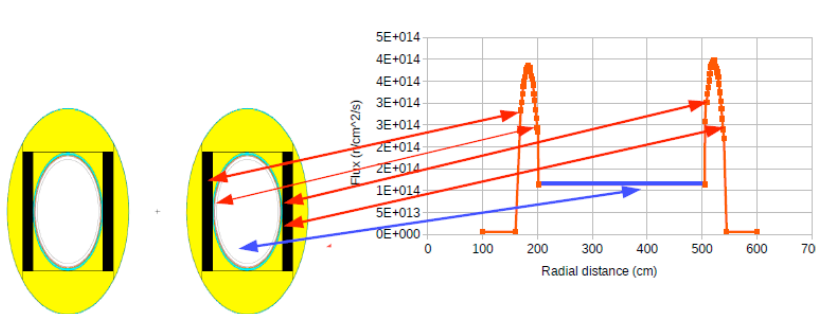


Fig. 8: Neutron flux radial distribution with the corresponding sampling positions.

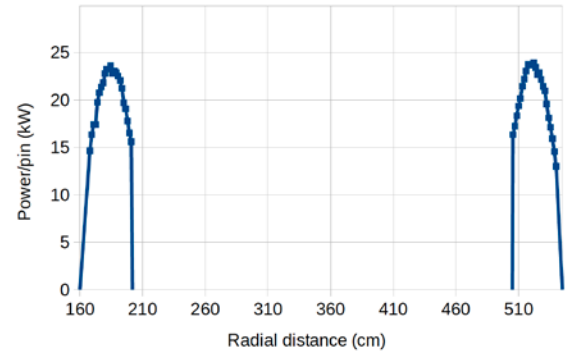


Fig. 9: Fission reactor thermal power radial distribution.

The energy distributions of the neutron flux for the innermost (red line) and the outermost (blue line) rod in the cylindrical ring of the sub critical assembly are shown in Fig.10: we can see a small residual 14 MeV component in the innermost position which is not present in the outermost position.

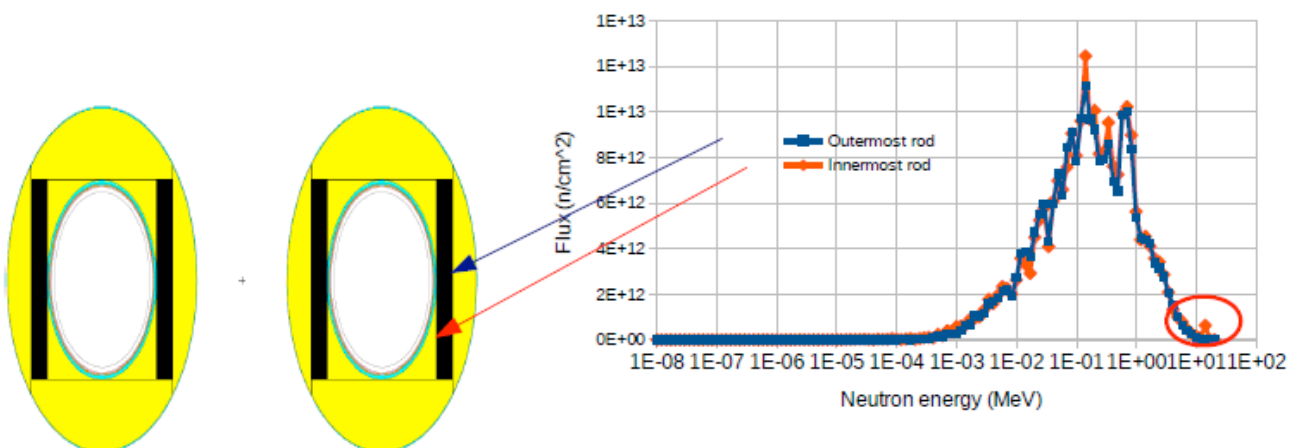


Fig. 10: Neutron flux energy distributions in the innermost position (red line) and in the outermost position (blue line) in the fission reactor core.

### 3. Tritium breeding

We had also evaluated the tritium breeding for the fusion (tokamak, without fissile blanket) and for the hybrid configurations: the tritium mass, as a function of the irradiation time for the two considered configurations, fusion (blue line) and hybrid (fusion+fission, red line) is reported in Fig. 11, where the masses behavior is normalized to the total Li/Pb (17% Li, 83% Pb) mixture mass ( $4.66 \times 10^6$  kg for the pure fusion configuration and  $3.82 \times 10^6$  kg for the hybrid configuration), which is different in the two considered configurations. For the hybrid case, during the evolution of the system the multiplication coefficient  $k_{eff}$  and the fission power are decreasing over time, due to the burn-up of the MOX fuel, without any fresh fuel replacement.

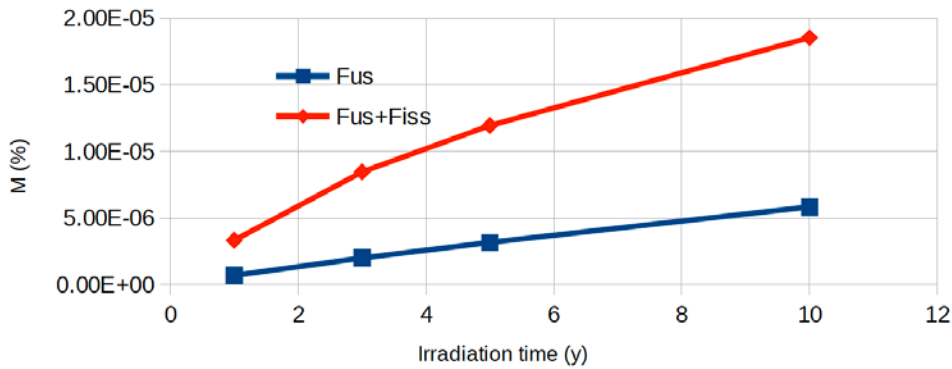


Fig. 11: Produced tritium mass in the breeder as a function of the irradiation time for the fusion configuration (blue line) and for the hybrid configuration (red line) normalized to the breeder masses.

For the considered tokamak (130 MW neutron power) we have a tritium production of about 3 kg/year which is not enough to sustain the tokamak tritium consumption (9 kg/year). In the hybrid case the breeding is about 13 kg/year, with a surplus of about 4 kg/year.

### 4. Preliminary evaluation and consequences of fuel burn-up

In the last part of this work we performed some preliminary studies of the fuel burn-up, in particular we simulated the actinides radiotoxicity as a function of the irradiation period (blue line) compared with the pure decay radiotoxicity (red line), as shown in Fig. 12. It is possible to see that, after an irradiation period of 10y, the actinides radiotoxicity returns close to its initial level.

The fuel burn-up also causes a decrease of the fission effective multiplication factor  $k_{eff}$  which is plotted as a function of the irradiation period in Fig. 13. Maintaining  $k_{eff}$  and power level at the same average values during burn-up will require periodical replacement of a part of the irradiated fuel with fresh one. Without refuelling, at the end of an irradiation period of 10 y, we would obtain a thermal power level of about 930 MW from fission reactor.

### 5. Preliminary accidental analysis

FDS ( Fusion Driven System) is an intrinsically safe system provided that criticality ( $k_{eff}=1$ ) is never reached. We have performed a preliminary accidental analysis considering as a scenario the complete loss of liquid metal in various regions of the reactor, namely liquid Lead in the core and Li/Pb mixture in some different breeding and

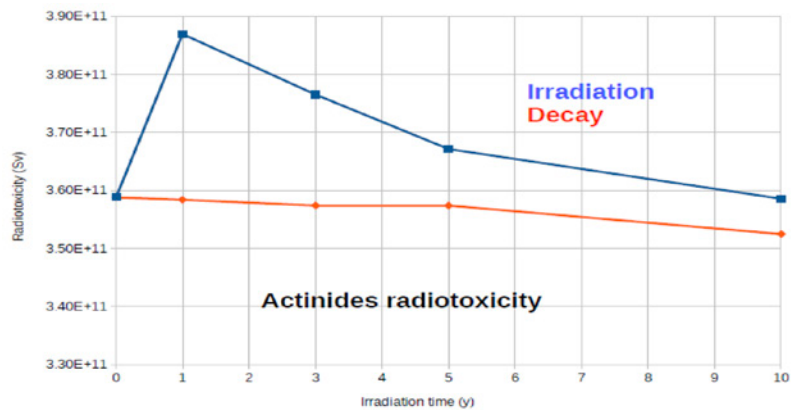


Fig. 12 Actinides behavior as a function of irradiation time (blue line) and as a function of decay time (red line).

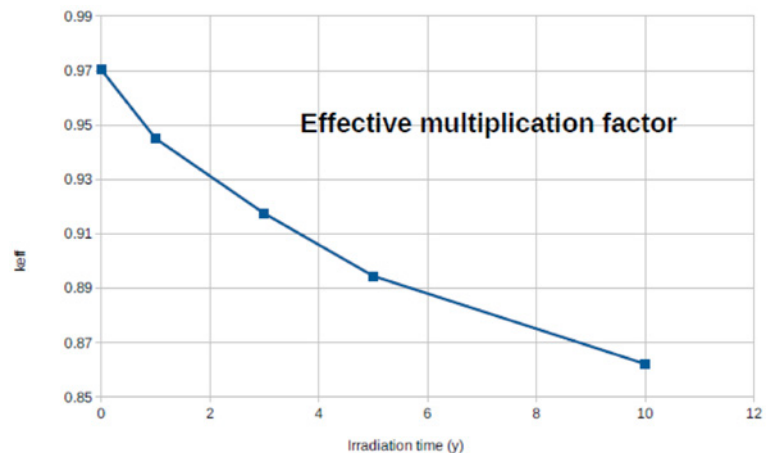


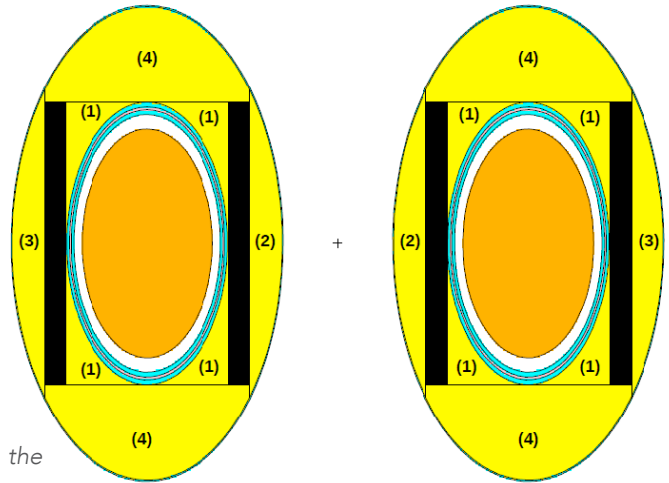
Fig. 13: Fission reactor effective multiplication factor as a function of the irradiation period.

cooling regions (see Fig.14) . The simulated  $k_{eff}$  values corresponding to these configurations are shown in table 2.

Depleted region	$k_{eff}$
1	0.962
2	1.040
3	0.968
4	0,969
1+2+3+4	0.993
Liquid lead in the core	0.956

Table 2: Effective multiplication factor evaluation in the different region without liquid metal.

Fig. 14 Hybrid system vertical view: the numbers indicate the Li/Pb region considered in the accidental analysis.



The highest impact is due to the breeding region (2 in Fig. 14 internal to the tokamak, likely due to neutrons traveling to this region not being absorbed anymore by the Lithium in the mixture. In order to obtain a higher safety level, we have modified the design by emptying this internal breeding region and reducing at the same time the internal fission reactor core thickness to 30 cm. In this configuration we got:

-  $k_{eff}=0.97$ , total power  $P=2.5$  GW, ( $k_{eff}$  is mostly dependent from the internal core size)

The tritium breeding behavior as a function of the irradiation time in this new configuration is shown in Fig. 15 (yellow line) compared with the previous configuration (red line) normalized to the total breeder mass. Tritium produced masses in the three selected configurations are reported in Table 3.

Irradiation period (y)	Tritium mass A (kg)	Tritium mass B (kg)	Tritium mass C (kg)
1	3.20	12.73	11.88
3	9.28	32.41	30.10
5	14.72	45.86	42.12
10	27.15	71.02	65.03

Table 3: Tritium mass as a function of the irradiation period for the three different configurations, pure fusion (A), hybrid (B) and hybrid depleted by Li/Pb mixture in region 2 of Fig. 14 (C)

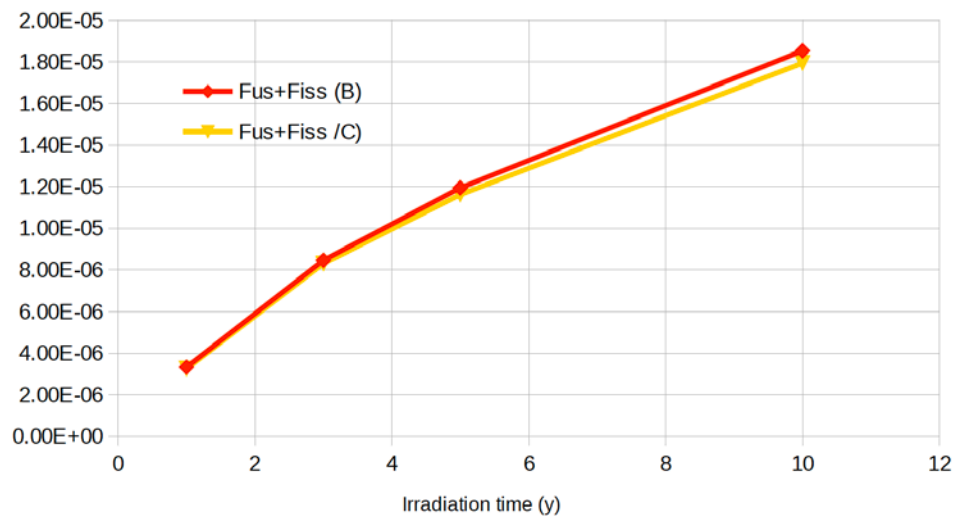


Fig. 15: Produced tritium mass in the breeder as a function of the irradiation time for the hybrid configuration (red line) and for the new hybrid configuration (yellow line) normalized to the breeder masses.

Therefore in this new configuration, a similar tritium breeding level is obtained, while our simple analysis seems to indicate that criticality accidents due to loss of liquid metal would be avoided.

## 6. Summary

We started from a tokamak of 130 MW neutron power corresponding to 0,5 MW/m<sup>2</sup> first wall density power to study a simple hybrid fusion-fission reactor model. The fission reactor is based on MOX fuel and liquid lead cooled. This configuration allows the presence of a lead/lithium breeder around the reactor core. The lithium breeding is increased in the fusion-fission configuration with respect to the fusion one due to the presence of a higher number of neutrons circulating in the system. A preliminary fuel burn-up analysis has been performed considering the actinides radiotoxicity in the fuel as a function of the irradiation time in the system, and, as a consequence, the effective multiplication factor of the fission reactor behavior as a function of the operation time. We finally performed a simple loss of coolant accidental analysis in which we studied the effects of the liquid metals in the different regions of the hybrid system in order to evaluate an eventual criticality scenario.

## Acknowledgements

We thank Dr. M. Angelone for the useful discussions and informations.

## 10 - ST40 as a prototype of the fusion core for FFH: design and status of construction

*M. Gryaznevich, S. McNamara, and Tokamak Energy Ltd. Team*

*Tokamak Energy Ltd, 120A Olympic Avenue, Milton Park, Abingdon, OX14 4SA, UK*

A new generation high field spherical tokamak, ST40, is currently under construction at Tokamak Energy Ltd. (TE). The main parameters of ST40 are:  $R_0=0.4\text{--}0.6\text{m}$ ,  $A=1.7\text{--}2.0$ ,  $I_{pl}=2\text{MA}$ ,  $B_t=3\text{T}$ ,  $\kappa=2.5$ . It will have liquid nitrogen cooled copper magnets, up to 2MW of auxiliary heating power, and a pulse length of  $\sim 1\text{s}$  when operating at full power. ST40 aim to demonstrate burning plasma condition parameters ( $nT\tau_E$ ) and may also be suitable for DT operations in future to provide up to  $3\times 10^{17}\text{n/s}$ , so could be a prototype of a compact Fusion neutron source or a core of a Fusion-Fission hybrid (FFH). The main physics and engineering challenges are caused by the high toroidal field, relatively high plasma current, and wall and divertor power loads and are discussed. The status of construction is presented.

Keywords: spherical tokamak, fusion neutron source, hybrid reactor.

### 1. Introduction

Advances in the development of high temperature superconductors (HTS) [1], and an indication of a strong favorable dependence of electron transport on higher toroidal field (TF) in Spherical Tokamaks (ST) [3], open new prospects for a high field ST as a compact fusion reactor. The combination of the high  $\beta$ , the ratio of the plasma pressure to magnetic pressure, which has been achieved in STs [4], and the high TF that can be produced by HTS TF magnets, could clear a path to lower-volume fusion devices, in accordance with the fusion power scaling proportional to  $\beta^2 B_t^4 V$ . Such compact high field STs have been considered as a Fusion neutron source [6,7] and a core of a Fusion-Fission hybrid.

STs have typically operated at toroidal magnetic fields around 0.3–0.5T. Recent upgrades to NSTX, Globus-M and MAST will bring them up to 1T fields. However, in order to reach high fusion performance in an ST, higher fields of 3–5T, or above, will be needed. Due to subsequent large forces and space limitations in a compact device, constructing an ST operating at such fields will require innovative engineering solutions and the use of HTS may resolve some of these issues. As a first step, to develop and test solutions to some of the major engineering challenges, TE has designed ST40, which uses conventional copper magnets cooled to liquid nitrogen (LN2) temperatures and will operate at fields up to 3T. At lower fields of  $\sim 1.5\text{T}$ , which is sufficient for an intense Fusion neutron source [7], much longer pulses may be performed, giving a chance to assess confinement at steady-state conditions and current drive.

### 2. ST40 design

The overall structure of ST40 is shown in Fig. 1. The main components are the inner and the outer vacuum chambers (described in Section 2.1.), and the toroidal and poloidal field coils (Section 2.2.). The outer vacuum chamber is supported by four legs and the entire assembly sits on top of the assembly platform (only partly visible in Fig. 1), which provides enough elevation to allow access underneath the device. The outer vessel acts as a cryostat to keep the TF and other coils at LN2 temperature. Outer PF coils will also be LN2 cooled.

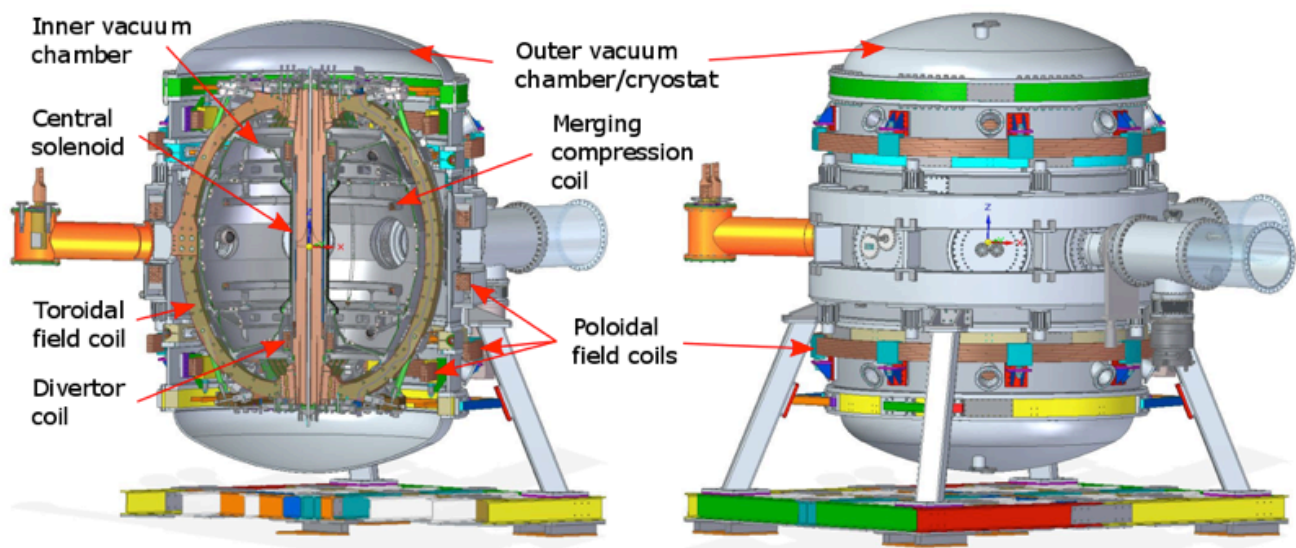


Fig. 1. Cutaway view (left) and outside view (right) of ST40 with the main components labelled.

## 2.1. Inner and outer vacuum chamber

ST40 will have a two-chamber vacuum system that consists of the inner vacuum chamber (IVC) and the outer vacuum chamber (OVC), illustrated in Fig. 1. The IVC is made of 10 mm thick stainless steel, apart from the centre tube (left panel of Fig. 2) that is made of 4 mm thick Inconel. On the high-field-side (HFS), the plasma will be limited by a set of eight fine grain graphite limiters (not shown in Fig.1 and not yet installed in Fig. 2) that cover the entire height of the centre tube. On the low-field-side (LFS) the stainless steel of the IVC is the main plasma facing surface.

For plasma operations, the IVC (cf. right panel of Fig. 2) will be pumped down to  $\sim 10^{-8}$  mbar pressure.  $3 \times 10^{-7}$  mbar has been already achieved with only a few hours of baking up to  $160^\circ\text{C}$  and before any glow discharge cleaning (GDC). The vacuum within the OVC will be substantially lower, around  $10^{-4}$  mbar. The main purposes of the secondary vacuum are: (i) to prevent icing of the TF magnets when they are cooled to LN2 temperatures, and (ii) to work as an insulator between the IVC and the OVC, particularly during the IVC baking.

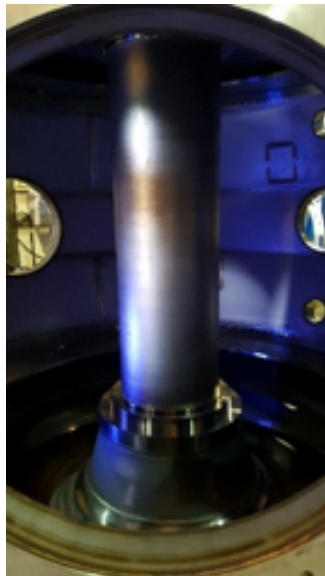


Fig. 2. Photos of the centre post of the device (left) and the entire ST40 inner vacuum chamber (right) ready to be baked in the baking stove

## 2.2. Coils

All the coils of ST40 are made of copper. It is a tried and tested magnet material with good structural strength and conductivity, particularly at liquid nitrogen temperatures.

The TF magnet of ST40 consists of 24 turns arranged in 8 limbs of 3 turns each, all connected in series. All the turns are connected to the centre post with flexible demountable joints. The centre post itself consists of 24 copper wedges with a 15-degree twist in each to allow connecting one TF turn to the next. This design avoids the need for a TF compensating coil. The centre post, with its 24 wedges, is shown in the bottom panel of Fig. 3. The central solenoid, to be wound on the centre post, is not shown in the photo.

Another innovative solution is to design the TF return limbs in the shape of constant tension curve. This design minimizes the difference in the vertical expansion of the centre post and the return limbs over the permitted temperature rise during operations. Consequently, it helps minimize movement in the critical flexi-joints that connect the return limbs to the centre post wedges. One of the three turns of the TF return limbs and one of a single limb are shown in the top panel of Fig. 3.

On the LFS of the device, ST40 has three pairs of poloidal field (PF) coils (cf. Fig. 1), each positioned symmetrically relative to the midplane. Together with the divertor coils, located near the high-field-side top and bottom corners of the IVC, the PF coils are used for controlling the plasma current, position, and shape.

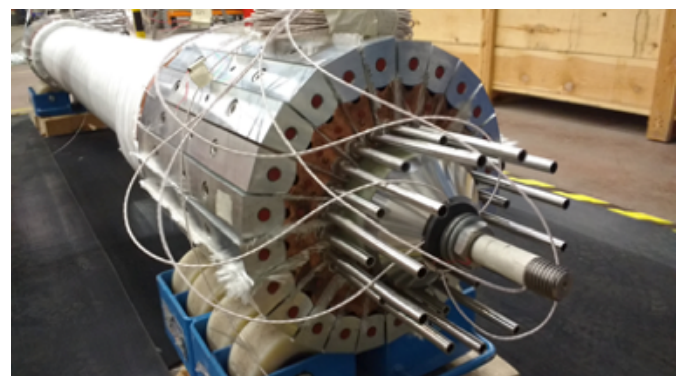


Fig. 3. Photos of a copper TF return limb (top) and of the entire centre post with its 24 TF wedges (bottom).

Operating a small device with strong magnetic fields will result in large forces on the TF coils both in-plane ( $J \times B$  forces due to the interaction between current in the TF coil and the toroidal magnetic field) and out-of-plane ( $J \times B$  forces due to TF coil current and poloidal magnetic field from the PF coils). To accommodate these forces, ST40 has two large stainless steel rings on the OVC. Each of the TF return limb is attached to both of these rings with two carbon fiber

straps. In addition, there are two torque plates, one at the top and one at the bottom of the device, with eight carbon fiber straps each, to add extra support against twisting.

In order to obtain high toroidal fields in the plasma, it is desirable to use most of the centre post for the TF coils. As a result, ST40 will only have a minimal central solenoid. Unlike in most conventional tokamaks, the solenoid is not used for inductive start-up. Instead, its purpose is to help maintain the flattop current and, thus, extend the length of the pulse.

For start-up, ST40 will use a method called merging compression (MC) [5] that was first developed for START [9] and later used on MAST [10]. For that purpose, the design includes two in-vessel merging compression coils (see Fig. 1). In the MC plasma start-up, the plasma is first formed as two rings around two MC coils by rapidly ramping down the current in them. As the current in the coils vanishes, they are no longer able to hold on to the plasma rings that at that point carry a significant amount of current. Due to the mutual attraction between the currents in the two rings, the rings then merge at the midplane. During the merging, reconnection of the magnetic fields of the two rings results in magnetic energy being converted into plasma thermal energy. This hot plasma is then compressed along the major radius using the PF coils.

All the coils are actively cooled, initially with water. Later on, liquid nitrogen can be used in all the coils except for the top two pairs of PF coils. This will enable extending the pulse length from  $\sim 1$ s to  $\sim 5$ s.

### 2.3. Power supplies

All ST40 power supplies incorporate capacitors for storing energy to enable their short pulsed outputs. The merging compression power supply (PS) uses high voltage metallised polypropylene capacitors, while the power supplies for all the other coils use ultracapacitors due to their ability to store large amount of energy. The merging compression PS is a simple power supply: it has a thyristor single shot high voltage system with a diode freewheel. When the thyristor is triggered, the stored energy from the capacitors resonates with the coil to generate a damped sine wave current waveform.

The power supplies connected to the other coils are more sophisticated. Their output can be controlled during a pulse using a differential input signal. The power supply of the TF coils uses multiple parallel buck converters with Insulated Gate Bipolar Transistor (IGBT) switches to create a maximum 250kA output current, whilst the others have H-Bridge inverters and, hence, benefit from full 4-quadrant output capability.



Fig. 4. TF power supply charger (left) and part of the TF ultracapacitor banks (right).

### 2.4. Diagnostics

The diagnostic setup of ST40 consists of a wide array of diagnostics from machine monitoring (e.g. vacuum measurements, mass spectrometer, fast ion gauge, thermocouples, position monitoring, TF joint testing) to plasma diagnostics. An extensive set of magnetic diagnostic, together with controllable power supplies (recall Sec. 2.3.), will allow current, position, and shape control during the pulse. Signals from the magnetic diagnostic will also be used for post-pulse equilibrium reconstruction. ST40 will have: two sets of poloidal magnetic field probes (34 probes per set), 19 flux loops, Rogowski coils (two for plasma current, one for each magnet, one for OVC, four for MC coil supports), 44 saddle coils, and two diamagnetic coils.

Several cameras will also be installed. There are two visible light cameras: a fast camera with a frame rate of 10000fps (with the resolution of  $256 \times 256$  pixels), and a high resolution camera with 90fps ( $2048 \times 2048$  pixels). In addition, an infrared camera and a multifoil soft X-ray (SXR) camera system with three cameras will be available. Every SXR camera will have four diodes with different filters, each detecting the signals from the same 20 lines-of-sight. The viewing cones of the three cameras overlap and, hence, lend themselves for tomographic reconstruction.

Other diagnostics include a spectrometer with impurity Doppler measurements,  $195\mu\text{m}$  interferometer with two lines-of-sight (one vertical and one horizontal), hard X-ray spectrometer, neutron spectrometer, NPA, ECE imaging, and ECE Doppler radiometer. The toroidal locations of some of the above-mentioned diagnostics are shown in Fig. 5.

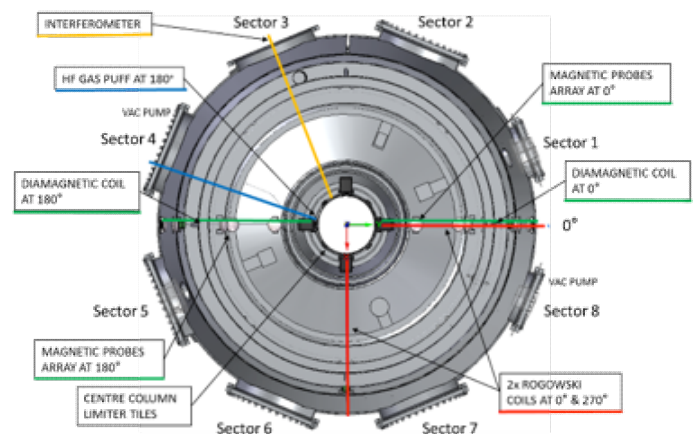


Fig. 5. Top-down view of ST40 indicating the locations of some of its diagnostics.

## 2.5. Divertor

One of the challenges for compact fusion reactors are the potentially prohibitively high power loads on the divertor. In spherical tokamaks, operating in a double-null divertor (DND) configuration practically isolates the inner scrape-off-layer (SOL) from the outer scrape-off-layer. As particles and energy mostly escape the plasma from the HFS, most of the power loads are shared by the upper and lower outer divertor plates. This helps with the power loads because the outer divertor has more surface area than the inner divertor. It also has more space in which to implement advanced divertor configurations.

ST40 will operate in a DND configuration with graphite divertor tiles and cryo-pumping of the divertor region. Active vertical control will be used, and liquid nitrogen cooled passive plates will be installed to stabilise the highly elongated plasma.

## 3. ST40 operational objectives

The goals of ST40 are: (i) to demonstrate the feasibility of constructing and operating a high field ST, (ii) to show the benefits of a high field in an ST, and (iii) to achieve fusion relevant conditions, i.e., a high  $n\tau E$ .

As mentioned earlier, ST40 will use the merging compression plasma formation method. Empirical scaling, based on experimental data from existing devices predicts that the plasma temperature resulting from merging compression is proportional to the square of the merging poloidal magnetic field [11][12][12]. In ST40, this field will be at least three times higher than in MAST, which demonstrated electron and ion temperatures up to 1.2keV. Therefore, the expectation of multi-keV temperatures is justified. Moderate extrapolation of the achievable plasma current from MAST and START data predicts achievement of 2MA in ST40 with the support from the central solenoid and the current driven by neutral beam injection. As the ST40 operating regime assumes densities in  $1-5 \cdot 10^{20} \text{m}^{-3}$  range, conditions close to burning plasma requirements ( $n\tau E > 3 \cdot 10^{21}$ ) are expected, providing that the plasma confinement will follow optimistic predictions based on MAST and NSTX data.

## 4. Fusion as a neutron source

A potential near term application of nuclear fusion is as a powerful source of energetic neutrons. No longer bound by the stringent requirement to produce commercially competitive net energy a fusion neutron source (FNS) could explore novel operating regimes and be developed relatively quickly, using current, or near-term technologies. ST40, as a prototype FNS, would be an invaluable proof of principle and intermediary commercial application of fusion.

For devices designed for non-electrical applications the critical performance measure is the fusion power density,  $P_f$ . A high  $P_f$  allows the device size and ultimately the cost to be minimised and enables deployment across a diverse range of potential applications. A general FNS design procedure is presented below, comprised of two key sections. Firstly, it is instructive to determine the plasma conditions that maximise  $P_f$ . These optimum plasma conditions are then used as the basis of a FNS design by applying established tokamak stability and operational limits, and a guidance for the operational window of ST40.

### 4.1 Maximising $P_f$ at a fixed plasma pressure

In a purely thermonuclear system, operating with equal parts deuterium and tritium  $P_f$  scales with the plasma pressure, as  $P_f \sim p^2$ , with the performance dictated by the maximum  $p$  at which the device can stably operate. In the 1970s it was demonstrated [13,14] that at fixed pressure  $P_f$  can be raised above the equivalent thermonuclear level by taking advantage of the high reactivity of beam-plasma reactions. In these beam-driven systems the fusion output is dominated by beam-plasma reactions and the primary role of the confined plasma is to act as a suitable target for the beam to react with while thermalising. The requirements on the plasma confinement are, therefore, significantly more lenient than those of high gain operation. This result is encapsulated by Fig.6, which shows the dependence of  $P_f$  and the energy gain,  $Q_f$ , on the target plasma confinement, quantified as  $n_e \tau_e$  in a fixed pressure system sustained against energy losses by deuterium neutral beam injection (NBI). At high confinement, the heating power is low and the system resembles a conventional thermonuclear one. As  $n_e \tau_e$  is reduced more heating power is required to maintain  $p$  and

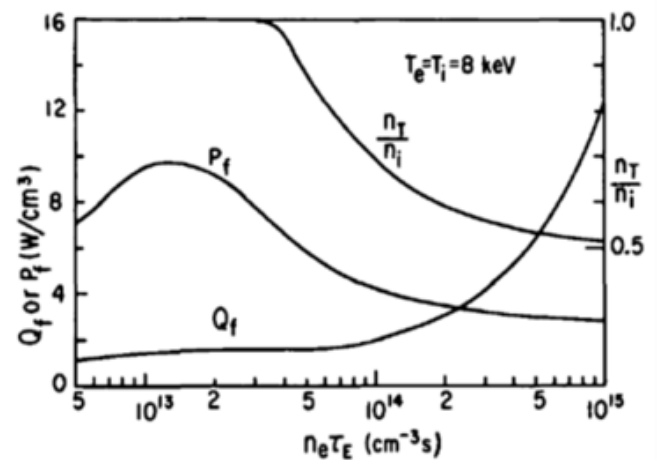


Fig.6 Originally published in [13]. Dependence of  $P_f$  and  $Q_f$  on confinement. The conditions for maximising  $P_f$  are markedly different from those required for high gain.

beam-plasma reactions become increasingly significant. This is reflected by the increase in the optimum target plasma tritium composition,  $n_T/n_i$ , top curve in Fig.6.

A further notable characteristic of such systems is the temperature dependence of  $P_f$  and the corresponding optimum  $n_e \tau_e$ , both of which favour lower target plasma temperatures, scaling approximately as  $P_f \sim p^2/T^2$  and  $n_e \tau_e \sim T$ . Other considerations, such as the reduction in  $Q_f$  and increase in the target density at lower  $T$ , mean the optimum temperature for maximising  $P_f$  at fixed plasma pressure is in the range  $T = 4\text{--}8\text{keV}$  [13,14].

While this appears to represent a highly desirable optimisation, its applicability to practical device design is limited, the large increase in the applied beam power needed to raise  $P_f$ , not previously given due consideration and particularly relevant to compact devices, means any optimisation at fixed pressure ultimately requires further restrictions on the beam power to be applied, to make more feasible a practical application on ST40.

## 4.2 Restricting the power

The externally applied heating power density,  $P_{\text{ext}}$  is related to the total thermal power density escaping the plasma via the scrape off layer by  $P_{\text{thermal}} = P_{\text{ext}} + f_\alpha P_\alpha - P_{\text{rad}}$  where  $P_\alpha$  and  $P_{\text{rad}}$  are, respectively, the alpha and radiated power densities and  $f_\alpha$  is the fraction of confined alphas. For a fixed plasma and device geometry  $P_{\text{thermal}}$  is limited by either materials or stability considerations. Fixing  $P_{\text{thermal}}$  along with  $p$  restricts the operational space and yields a different set of optimum conditions to those at fixed  $p$  only. This can be seen in Fig.7, which shows  $P_f$  as a function of  $n_e \tau_e$  at fixed  $p$  only and under the additional constraint of fixed  $P_{\text{thermal}}$ .

At fixed  $P_{\text{thermal}}$ ,  $P_f$  no longer scales as  $T^{-2}$ , as reducing  $T$  no longer allows for an increase in the beam power. The optimum plasma conditions of maximising  $P_f$  reduce to a single point, with the optimum  $T$ ,  $n_T/n_i$ ,  $Q_f$  and  $n_e \tau_e$  all being approximately constant along contours of  $p^2/P_{\text{thermal}}$ . This ratio is related to the ratio of thermonuclear ( $\sim p^2$ ) to beam-plasma ( $\sim p_b \sim P_{\text{thermal}}$ ) fusion reactions. Rather than varying smoothly from a beam driven to a thermonuclear system as  $p^2/P_{\text{thermal}}$  is increased, there exist two distinct regimes of operation, separated by a discontinuity in the optimum conditions. The defining characteristics of each regime are summarised in Table.1. In the beam-plasma regime maximum  $P_f$  is realised when operating with a pure tritium target plasma and precise control of the level of edge recycling and prompt loss of the thermalised beam ions is required. In the thermonuclear regime, the system is less sensitive to  $n_T/n_i$ , but higher confinement is needed. At the boundary between the two regimes there is a discontinuity in the optimum plasma conditions, with  $n_T/n_i$  jumping from 0.81 to 1.

	Beam-plasma regime	Thermonuclear regime
Confinement	Low - modest	Modest - high
$n_T/n_i$	1	0.5 – 0.81
$p^2/P_{\text{thermal}}$	Low	High
Ratio of $P_f$ with and without alpha confinement	$(1 + 0.2Q_f)^{-1}$	80%
Change in $Q_f$ due to alpha confinement	Unchanged	Increased

Table.1 Characteristics of the two distinct operating regimes.

The first wall neutron flux and total fusion power output are specified. Taking the triangularity as  $\delta = 0.5$  and the elongation as  $\mathcal{K} = 0.9 \mathcal{K}_{\text{max}}$ , where  $\mathcal{K}_{\text{max}} = 2.4 + 65 \exp[-A/0.376]$  [15] and  $A$  is the aspect ratio, allows the range of possible device geometries to be determined and quantified by the major radius,  $R_0$ . As  $R_0$  is increased  $A$ , and therefore  $\mathcal{K}$ , must be reduced to maintain the plasma surface area and first wall neutron flux. As a result, the plasma volume is inversely related to  $R_0$ . By imposing a limit on  $P_{\text{thermal}}$ , the plasma pressure at which the device must operate

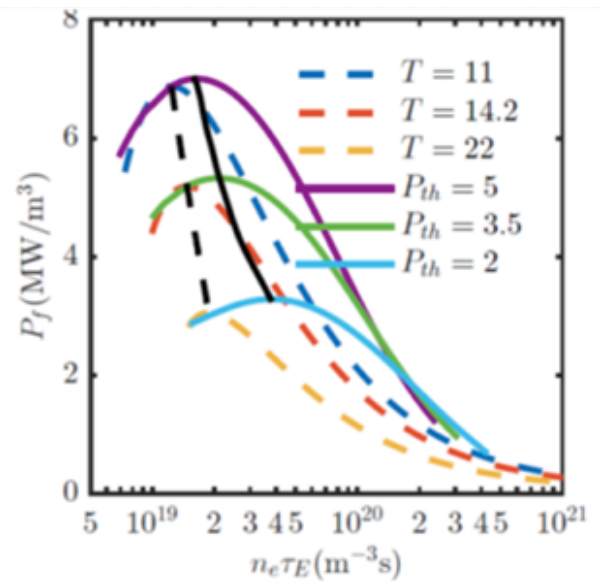


Fig.7  $P_f$  at fixed  $p$  only (dashed curves) and at fixed  $P_{\text{thermal}}$  (solid curves).

## 4.3 High power density device optimisation

By applying established tokamak stability and operational limits the optimum plasma conditions are used to inform a high  $P_f$  device design study. The optimisation procedure aims to reduce the dimensionality of the possible design space to simplify what would otherwise be a perplexing search for the optimal configuration. A summary of the model is given here before being applied to an example device design, which could be a next step after ST40.

Within the model there is significant scope to apply different stability and operational limits. The optimisation procedure applied here is as follows.

to achieve the specified fusion output can be determined using the optimum conditions already derived. For this investigation,  $P_{\text{thermal}}$  is limited by the thermal power flux crossing the separatrix,  $\Gamma_{\text{thermal}}$ , although another limit, such as the power flowing to the divertor region, could be imposed.

The normalised plasma beta is taken as  $\beta_N = 2/3 \beta_N^{\text{ideal}}$ , where  $\beta_N^{\text{ideal}}$  is the ideal-wall beta limit given in [16]. As the plasma conditions ( $T$ ,  $n_e$ ,  $P_{\text{NBI}}$ , etc) are already known, the NBI driven current,  $I_{\text{NBI}}$ , can be estimated using standard expressions (either based on kinetic estimates [17], as used here, or using a dimensionless current drive efficiency, such as [18]). This current can be reduced by increasing the component of the beam that is injected perpendicular to the magnetic field and this initial injection angle acts as a further optimisation parameter that serves to modify  $I_{\text{NBI}}$ . Assuming fully non-inductive current drive,  $f_{\text{bs}} + f_{\text{NBI}} = 1$ , taking  $f_{\text{bs}} = 0.04 \epsilon^{-0.5} \beta_N q_a$  [19], where  $q_a$  is the edge safety factor, and applying the Sykes-Troyon beta limit [20] the safety factor can be determined as a function of  $R_0$ ,  $\Gamma_{\text{thermal}}$  and  $I_{\text{NBI}}$ . The toroidal beta,  $\beta_T$ , may then be calculated, which in turns gives the toroidal field,  $\beta_{T0} = \sqrt{P/\beta_T}$ . Finally, the total plasma current is found using  $I_p = I_{\text{NBI}} / (1 - f_{\text{bs}})$ . This procedure reduces the dimensionality of the design space to 3 parameters:  $\Gamma_{\text{thermal}}$ ,  $I_{\text{NBI}}$  and  $R_0$ . In this design space, various physics checks are applied, such as ensuring that  $q_a > 2.2$  and the electron density is below the Greenwald density limit,  $n_{e,20} < n_G = I_p / \Pi \alpha^2$ .

For fixed values of  $R_0$  the confinement enhancement factors,  $H_{\text{fac}}$ , relative to both the ITER-98P(y,2) and Petty  $\beta$ -independent [21] confinement time scalings are calculated as a function of  $\Gamma_{\text{thermal}}$  and  $I_{\text{NBI}}$ . Along contours of fixed,  $H_{\text{fac}}$  the optimum point is chosen as that which minimises the value of  $P_{\text{thermal}}$ . An example of the optimisation output is shown in Fig. 8 and Fig. 9. In the example considered, the first wall neutron flux is  $1 \text{ MWm}^{-2}$  and the total fusion power output is 75MW.

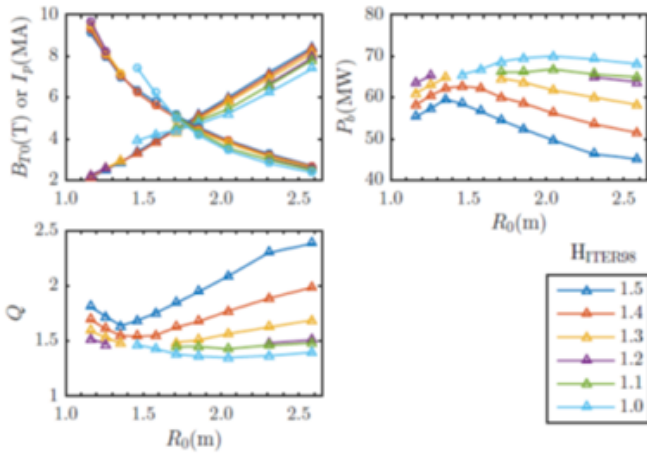


Fig.8 Optimum device parameters as a function of  $R_0$  and  $H_{\text{fac}}$  when applying the ITER-98p(y,2) confinement scaling. In the top right plot the triangle markers show  $B_{T0}$  and the circles  $I_p$ .

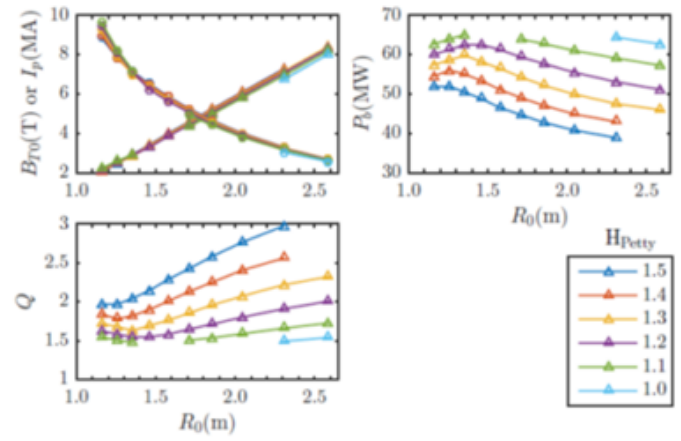


Fig.9 Same as Fig.8 but with the Petty  $\beta$ -independent confinement time scaling applied.

For the design point considered the optimum plasma conditions were predominantly those that allowed for contributions to  $P_f$  from both beam-plasma and thermonuclear reactions (ie in the 'thermonuclear' regime of Table.1). Only at the lowest levels of confinement and when applying the ITER-98P(y,2) confinement scaling did the optimum point lie in the pure beam-plasma regime, where  $n_T/n_i = 1$ . The toroidal field and plasma current are only weakly dependent on the level of confinement and predominantly determined by the device size. At larger  $R_0$  the plasma pressure must increase to compensate for the reduced plasma volume which, coupled with the reduced  $\beta_T$  at lower aspect ratio, leads to the increased  $\beta_{T0}$ . The parameter most sensitive to the confinement is the applied beam power and, therefore,  $Q_f$ . Larger devices benefit from increased energy gain, however, the additional electrical and cryogenic power required to produce the increased toroidal field would result in a reduction in the overall plant efficiency and a higher 'cost per neutron'. The optimisation presented could easily be extended to include more sophisticated parameter dependencies and additional considerations and significantly simplifies the multidimensional search for the optimum device configuration.

## 5. Summary

Tokamak Energy Ltd. is currently constructing ST40, a spherical tokamak with  $R_0 = 0.4\text{--}0.6\text{m}$ ,  $A = 1.7\text{--}2.0$ ,  $I_{p1} = 2\text{MA}$ ,  $B_t = 3\text{T}$ ,  $\kappa = 2.5$ . The device will be equipped with up to two 40keV, 1MW neutral beam injectors, and could be suitable for DT operations in future. The ultimate goal of ST40 is to demonstrate burning plasma condition parameters ( $n_T \tau_E$ ). It will also be used to develop and test solutions to some of the major engineering challenges in constructing compact high field spherical tokamaks and to demonstrate feasibility of a compact high-field ST as a FNS and a core of a FFH reactor. The pulse length in the first stage with water-cooled magnets will be  $\sim 1\text{s}$  of full power operation but, later on, when using LN2 cooling, that can be substantially increased to address confinement and current drive issues. The presented

optimisation procedure, extending the work done in 1970<sup>th</sup> by Jassby et al, results in more realistic requirements for future next steps.

## Acknowledgments

The members of the Tokamak Energy Ltd. who provided the images for this publication are thankfully acknowledged: P. Tigwell (Fig. 1), G. Dunbar (Figs. 2 and 3), A. McFarland (Fig. 4), and G. Whitfield (Fig. 5).

## References

- [1] M. Gryaznevich et al., Progress in application of high temperature superconductor in tokamak magnets, *Fusion Engineering and Design* 88 (2013) 1593
- [2] W. Fietz et al., Prospects of High Temperature Superconductors for fusion magnets and power applications, *Fusion Engineering and Design*, 88 (2013) 440-445
- [3] M. Valovic et al., Scaling of H-mode energy confinement with  $I_p$  and BT in the MAST spherical tokamak, *Nuclear Fusion* 49 (2009) 075016
- [4] A. Sykes, High  $\beta$  produced by neutral beam injection in the START (Small Tight Aspect Ratio Tokamak) spherical tokamak, *Physics of Plasmas* 4 (1997) 1665
- [5] M Gryaznevich, et al., Achievement of Record beta in START Spherical Tokamak. *Phys. Rev. Lett.* v.50, n.15, (1998) 3972
- [6] M.P. Gryaznevich, et al., Options for a Steady-State Compact Fusion Neutron Source. *Fusion Science and Technology* 61 1T (2012) 89
- [7] B.V. Kuteev, et al., Steady-state operation in compact tokamaks with copper coils. *Nucl. Fusion* 51 (2011) 073013
- [8] P. Buxton et al., Merging Compression start-up in ST40, P1.047, 29th Symposium on Fusion Technology (SOFT 2016)
- [9] A. Sykes et al., First results from the START experiment, *Nuclear Fusion* 32 (1992) 694
- [10] A. Sykes et al., First results from MAST, *Nuclear Fusion* 41 (2001) 1423
- [11] Y. Ono et al., High power heating of magnetic reconnection in merging tokamak experiments, *Physics of Plasmas* 22 (2015) 055708
- [12] M. Gryaznevich and A. Sykes, Merging-compression formation of high temperature tokamak plasma, Submitted to *Nuclear Fusion* "Special issue of papers arising from ICCP 2016"
- [13] DL Jassby. Optimization of fusion power density in the two-energy-component tokamak reactor. *Nuclear Fusion*, 15 (1975) 453
- [14] JM Dawson, HP Furth, and FH Tenney. Production of thermonuclear power by non-Maxwellian ions in a closed magnetic field configuration. *Physical Review Letters*, 26 (1971) 1156
- [15] RD Stambaugh, LL Lao, and EA Lazarus. Relation of vertical stability and aspect ratio in tokamaks. *Nuclear Fusion*, 32 (1992) 1642
- [16] YR Lin-Liu and RD Stambaugh. Optimum equilibria for high performance, steady state tokamaks. *Nuclear Fusion*, 44 (2004) 548
- [17] DFH Start and JG Cordey. Beam-induced currents in toroidal plasmas of arbitrary aspect ratio. *Physics of Fluids* (1958-1988), 23 (1980) 1477-1478
- [18] Luce T.C. et al, *Phys. Rev. Lett.* 83 (1999) 4550
- [19] CE Kessel. Bootstrap current in a tokamak. *Nuclear Fusion*, 34 (1994) 1221
- [20] F Troyon, R Gruber, H Saurenmann, S Semenzato, and S Succi. MHD-limits to plasma confinement. *Plasma Physics and Controlled Fusion*, 26 (1984) 209
- [21] C Petty. Sizing up plasmas using dimensionless parameters. *Physics of Plasmas* (1994-present), 15 (2008) 080501

## 11 - The Reversed Field Pinch as Neutron Source for Fusion-Fission Hybrid Systems: Strengths and Issues

**R. Piovan<sup>1\*</sup>, C. Bustreo<sup>1</sup>, L. Carraro<sup>1</sup>, D. Escande<sup>1</sup>, S. Martini<sup>1</sup>, M.E. Puiatti<sup>1</sup>, M. Valisa<sup>1</sup>, G. Zollino<sup>1</sup>**

<sup>1</sup>Consorzio RFX – C.so Stati Uniti 4, 35127 Padova (Italy)

The fusion reactor remains one of the long term, ultimate solution of energy production. This requires to control fusion reaction with an energy gain  $Q > 30 - 40$ . The tokamak configuration is nowadays the most investigated path to this goal.

Meanwhile a proposed interim carbon-free solution, with the merit of nuclear waste transmutation, is the hybrid fusion-fission reactor, in which sub-critical fission is activated by fast neutron generated in a fusion reactor. In this case fusion could be produced in a device with lower  $Q$ , roughly of the order of one.

The Reversed Field Pinch (RFP) is an alternative configuration to tokamak and stellarator for the future fusion reactor. Its disruption-free configuration, the need of a much weaker toroidal magnetic field and the capability of reaching thermonuclear temperatures without additional heating, are significant advantages in a commercial reactor.

While RFP plasmas have yet an energy confinement too low for a high  $Q$  reactor, reaching  $Q$  near 1 might be reasonable for a RFP machine with an appropriate R&D activity. Starting from the present knowledge in RFP configuration, the experimental results from the different machines and the theoretical advancement obtained in the last years, an analysis is presented on the possibility to use the RFP configuration as a fast neutron generator. The advantages of this solution with respect to the tokamak – no disruption, toroidal field coils at room temperature and reduced size with more space for breeding blanket, superconductors limited to the magnetizing coil and no divertor - and the possible issues- steady state operation, for example - will be highlighted in the paper.

## 12 - Analysis of safety problem in Fusion Reactors

**A. Malizia<sup>1\*</sup>, J.F. Ciparisse<sup>1</sup>, L.A. Poggi<sup>1</sup>, R. Rossi<sup>1</sup>, M. Gelfusa<sup>1</sup>, A. Murari<sup>2</sup> and P. Gaudio<sup>1</sup>**

<sup>1</sup>Department of Industrial Engineering, University of Rome Tor Vergata

<sup>2</sup>Consorzio RFX, Padova

Given the urgent need to converge on precise guidelines for accident management in nuclear fusion plants, in this paper, the authors will analyze the problem related to the choice of possible candidate materials for the nuclear fusion plants like International Thermonuclear Experimental Reactor (ITER), DEMOnstration power plant (DEMO), or PROTOtype power plant (PROTO). Fusion power is a promising long-term candidate to supply the energy needs of humanity. From the safety point of view, nuclear fusion holds inherent and potential safety advantages over other energy sources. In magnetic confinement devices, the plasma edge and surrounding material surfaces provide a buffer zone between the high temperature conditions in the plasma core and the normal “terrestrial” environment. The interaction between the plasma edge and the surrounding surfaces profoundly influences the conditions in the plasma core and is the principal key engineering issue. Robust solutions to plasma–material interactions (PMIs) issues are required to realize a commercially attractive fusion reactor. PMIs critically affect tokamak operation in many ways. Erosion by the plasma determines the lifetime of plasma-facing components (PFCs) and generates a source of impurities, which cool and dilute the plasma. Deposition of material onto PFCs alters their surface composition and can lead to long-term accumulation of large in-vessel tritium inventories. Dusts are currently produced in the existing plants like JET (and will also be in the future ones like ITER, DEMO, and PROTO) by PMIs. Thus, the issues related to the PFCs of the first wall of the nuclear fusion plants area topic that the Quantum Electronics and Plasma Physics Research Group (QEP) have been studying for more than a decade. The QEP has developed, in collaboration with ENEA FUS-Tech Department, a facility (STARDUST) to study the problem of dust mobilization and resuspension and after that has implemented the facility into the new one (STARDUST-U). In this paper the authors will present the main scientific achievements get with this experiments together with an analysis on how huge and important are the uses of these results in different scientific fields.

## 13 - Safety assessment of critical and subcritical systems with fast neutron spectrum

**A.Rineiski**

*Karlsruhe Institute of Technology - andrei.rineisky@kit.edu*

New designs for critical and subcritical systems with fast neutron spectrum are considered currently. Many are not in their most reactive configuration. In case of a strong material redistribution due to a hypothetical accident the reactivity may increase and lead to a power excursion. Then a possible mechanical energy release should be evaluated. Several fast spectrum neutron system types and possible accident scenarios are considered in the presentation. Methods and codes for their safety assessment are highlighted. Possible design measures for particular fast reactor types are discussed. Some results of safety assessments are shown.

## 14 - MYRRHA Project Status and New Implementation Plan. A new Large Research Infrastructure in a Small Innovative Country. Challenges & Opportunities

**Hamid Aït Abderrahim, Didier De Bruyn**

*SCK-CEN Boeretang 200, BE-2400, Mol, Belgium*

### Abstract

Since 1998 SCK•CEN is developing the MYRRHA project as an accelerator driven system (ADS) based on the lead-bismuth eutectic (LBE) as a coolant of the reactor and a material for its spallation target. MYRRHA is a flexible fast-spectrum pool-type research irradiation facility, also serving since the FP5 EURATOM framework as the backbone of the Partitioning & Transmutation (P&T) strategy of the European Commission concerning the ADS development in the third pillar of this strategy. MYRRHA is proposed to the international community of nuclear energy and nuclear physics as a pan-European large research infrastructure in ESFRI to serve as a multipurpose fast spectrum irradiation facility for various fields of research. In this paper, we present the current design of MYRRHA and the updated implementation strategy, showing that challenges can be turned into opportunities.

### Introduction

SCK•CEN is at the forefront of Heavy Liquid Metal (HLM) nuclear technology worldwide with the development of the MYRRHA ADS. MYRRHA (Aït Abderrahim et al, 2007, 2012, 2013) is a flexible fast-spectrum pool-type research irradiation facility cooled by LBE, and was identified by SNETP ([www.snetp.eu](http://www.snetp.eu)) as the European Technology Pilot Plant for the Lead-cooled Fast Reactor. MYRRHA is also serving since the FP5 EURATOM framework as the backbone of the P&T strategy of the European Commission based on the "Four Building Blocks at Engineering level" and fostering the R&D activities in EU related to the ADS (in the third building block) and the associated HLM technology developments. MYRRHA is proposed to the international community of nuclear energy and nuclear physics as a pan-European large research infrastructure in ESFRI to serve as a multipurpose fast spectrum irradiation facility for various fields of research such as: transmutation of High-Level Waste (HLW), material and fuel research for Generation IV reactors, material for fusion energy, innovative radioisotopes development and production. As such, MYRRHA is since 2010 on the high priority list of the ESFRI roadmap (<http://www.esfri.eu/roadmap-2016>).

Since 1998 SCK•CEN is developing the MYRRHA project as an ADS based on the LBE as a coolant of the reactor and a material for its spallation target. The nominal design power of the MYRRHA reactor is 100 MWth. It is driven in sub-critical mode ( $k_{\text{eff}} = 0.95$ ) by a high power proton accelerator based on LINAC technology delivering a proton beam in CW mode of 600 MeV proton energy and 2.5 mA intensity. The choice of LINAC technology is dictated by the unprecedented reliability level required by the ADS application. In the MYRRHA requirements, the proton beam delivery should be guaranteed with a maximum number of 10 beam trips lasting more than 3 seconds for a period of 3 months corresponding to the operating cycle of the MYRRHA facility. Since 2005, SCK•CEN and Belgium opened the MYRRHA project for the EU Member States for participation as well as to the major nuclear power countries for participation in the development of MYRRHA and further on during the construction and operation periods.

In this paper, we present the present status of the MYRRHA project in terms of design of its sub-critical reactor and high-level power accelerator, licensing, and perspective of implementation. We develop the new implementation strategy of the MYRRHA project as endorsed by Belgian authorities from end of 2015 on. We also present some of the many challenges an innovative project has to face and how some of them can be turned into opportunities.

### ADS Activity in Europe

R&D activities in the field of P&T are conducted in Europe in major nuclear energy countries since the beginning of the 60's and interest for ADS gained a larger interest from the 90's on, for energy production combined with HLW transmutation or for each objective separately.

Many ADS programmes, designs and experimental facilities helping to understand and to master the various aspects of ADS were conducted during the last two decades in Europe; several of them leading to the physical construction of an ADS facility, like the MUSE experiments in France (M. Salvatores et al., "MUSE-1: A First Experiment at MASURCA to Validate Physics of Sub-critical Multiplying Systems Relevant to ADS," IAEA Technical Document No. 985, Vienna, Austria, pp. 430-436, 1997), the YALINA experiments in Belarus (H. Kiyavitskaya . et al., H. Kiyavitskaya (Experimental and Theoretical Research on Transmutation of Long-Lived Fission Products and Minor Actinides in a Sub-critical Assembly Driven by a Neutron Generator," Evaluation Form for Annual Reports of ISTC Projects: Project #B-070-98, 1 September 1998) and the GUINEVERE facility at SCK•CEN Mol in the frame of a partnership between Belgium and France (H. Aït Abderrahim, P. Baeten, et al (2007); The GUINEVERE-project at the VENUS facility, Conference

proceedings "Utilisation and Reliability of High Power Proton Accelerators", Mol, Belgium, May 2007).

## The European framework programmes and strategy

Since the beginning of the years 2000, many European member states are conducting strong national programmes in P&T with innovative nuclear systems with fast reactors or ADS among others. In the FP5 framework programme (2000 – 2005) many projects related to the same topics were conducted but with a loose coordination or streamlining and no objectives towards the realisation of common large facilities for P&T.

In Europe there is a strong interest to explore the potential scientific, technical and industrial possibilities of P&T. Integrating the total European efforts (European Commission & Member States) was therefore compulsory in order to speed up the development and put the European R&D at lead in this field. A Thematic Network project, called ADOPT, was launched in the second call of FP5, fostering the efforts within the EC FP5 projects and also in structuring the national programmes towards joint objectives.

The specific objectives of ADOPT were:

- to promote consistency between P&T FP5 projects and national programmes;
- to define rules for dissemination of information and access to national R&D programme data;
- to review results of the P&T FP5 projects and avoid duplications;
- to identify gaps in the overall programme;
- to inform the members about the ongoing activities in P&T and ADS outside the EU (International Organisations, USA, Japan, Korea, among others) and finally
- to give input to future research proposals and guidelines for further R&D orientation.

To fulfil its objectives ADOPT was organised in five Clusters:

- PARTITION with the projects PYROREP, PARTNEW and CALIXPART (all lead by CEA);
- FUETRA with the projects CONFIRM (lead by KTH), THORIUM (lead by NRG) and FUTURE (lead by CEA);
- TRANSMUTATION: DESIGN with the project PDS-XADS (lead by AREVA NP);
- BASTRA with the projects MUSE (lead by CEA), N\_TOF-ND-ADS (lead by CERN) and HINDAS (lead by UCL);
- TESTRA with the projects SPIRE (lead by CEA), TECLA (lead by ENEA), MEGAPIE -TEST (lead by FZK) and ASCHLIM (lead by SCK•CEN).

The return of experience from ADOPT led in the next framework programme (FP6) to the creation of the largest ever project in EURATOM FP: the EUROTRANS Integrated Project (2005 – 2010), with 48 partners, a total budget of ~43 M€ (from which ~23 M€ budget from EC), subdivided in five technical domains and one management and coordination domain. EUROTRANS (Knebel et al, 2009, De Bruyn et al, 2010, Mansani et al, 2010) was coordinated by FZK with support of SCK•CEN, ENEA, CEA and CIEMAT.

More important is the establishment of the EC strategy for industrial deployment of P&T, where the EC and EU Member States R&D activities were fostered towards moving the level of demonstration from lab scale to pre-industrial engineering level for the four steps so called four "building blocks" (BB), listed below:

1. Demonstration of the capability to process a sizable amount of spent fuel from commercial LWRs in order to separate plutonium, uranium and minor actinides (MA);
2. Demonstration of the capability to fabricate at a semi-industrial level the dedicated fuel needed MA heavily loaded for dedicated transmuter;
3. Design and construction of one or more dedicated transmuters, MYRRHA (for ADS route) and ASTRID (for SFR route);
4. Development of Pyro-reprocessing of the dedicated fuel unloaded from the transmuter.

The EC contributes to the four BB and fosters the national programmes towards this strategy for demonstration at engineering level. Belgium contributes to the EC P&T strategy by focusing on the third BB through the realisation of MYRRHA as a pre-industrial ADS demonstrator and R&D facility.

## MYRRHA at a glance

The project consists in the creation of a large international research infrastructure (LRI) in the field of nuclear sciences, which will be used for the next 40 years at least. This facility consists of a 600 MeV – 2.5 mA proton linear accelerator (LINAC), a spallation target and a LBE cooled reactor able to operate in subcritical and critical mode.

This highly innovative and multidisciplinary research infrastructure will be used for:

- Testing and developing the transmutation of long-life and most toxic radionuclides in spent nuclear fuel in order to reduce their radiotoxicity in volume (with a factor 100) and in time (from hundreds of thousands

of years to a few centuries – a factor 1,000) compared to the current management options. The need for geological waste disposal still exists but transmutation reduces the technical requirements because a smaller volume is stored for a smaller amount of time. That way, transmutation has a positive impact on safety as well as on the economic cost;

- Securing the continuous production of radio-isotopes for medical applications due to an increasing demand worldwide, and in order to produce more efficient and high-quality radio-isotopes;
- Carrying out materials research and tests for the current and future nuclear fission reactors as well as nuclear fusion technology;
- Providing a multifunctional accelerator for fundamental and applied research.

In 2010, the Belgian Government took the decision to support the MYRRHA project for further development with a specific endowment of 60 M€2010. Furthermore, it was envisaged to contribute to its construction at a level of 40% of the total cost. The MYRRHA design as worked out in the FP7 Central Design Team project (D. De Bruyn, R. Fernandez, L. Mansani, A. Woaye-Hune, M. Sarotto & E. Bubelis (2012) The Fast-spectrum Transmutation Experimental Facility FASTEF: Main Design Achievements (Part 1: Core & Primary System) Within The FP7-CDT Collaborative Project Of The European Commission, 2012 International Congress on Advances in Nuclear Power Plants (ICAPP '12), Chicago (Illinois, USA), American Nuclear Society (CD-ROM), paper 12014, 1122-1130), the successor for design activities of the EUROTRANS project in FP6), served as a starting point for the further design work of the MYRRHA primary system, the accelerator as well as for the design of the auxiliary systems.

This resulted in mid-2014 in an updated MYRRHA primary system design called "Rev. 1.6". This version takes into account stringent safety requirement imposed after the Fukushima accident as well as a more advanced design of the primary system based on design mechanical codes after the conceptual stage. As a result of these elements, "Rev. 1.6" showed a substantial increase in the size of the MYRRHA primary system and projected cost of construction (1.6 G€2014).

This led the SCK•CEN Board of Directors to request at the end of 2014 the MYRRHA design team to revisit "Rev. 1.6" with the objective to reduce the total of the cost of the project. At the same time, it has been also requested to consider various implementation scenarios for the realisation of the project for spreading the investment costs and mitigating the technological, cost and planning risks namely:

1. Accelerator first and reactor later;
2. Reactor first and accelerator later;
3. Accelerator and reactor jointly deployed.

Two separate Evaluation Panels recommended as follows:

- On the MYRRHA Primary System design:
  - o To continue developing the Primary System Design with a 100 MWth pool-type reactor derived from Rev. 1.6 with one innovative "In-vessel Fuel Handling Machine" (IVFHM) and an innovative Pressurised Heat Exchanger system consisting of external double-wall heat exchangers with a monitored gap containing a conductive medium.
  - o In parallel to further explore as backup option a 100 MWth innovative loop-type primary system with bottom

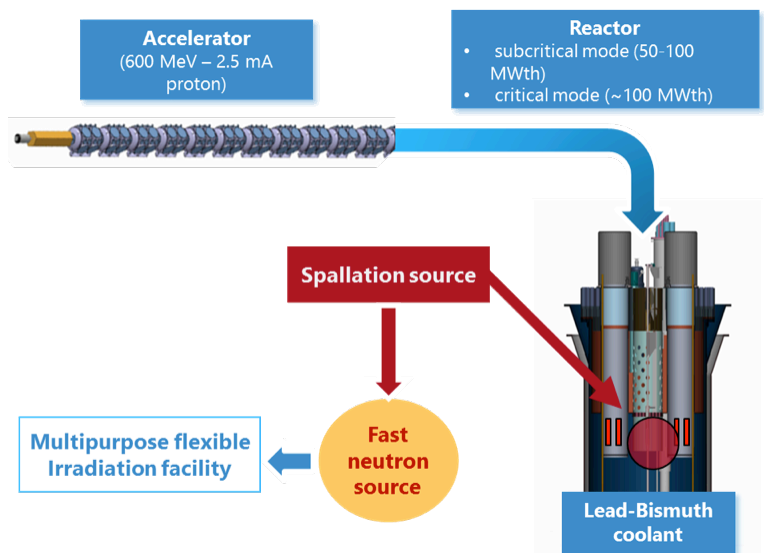


Fig. 1 : The three components of the MYRRHA facility

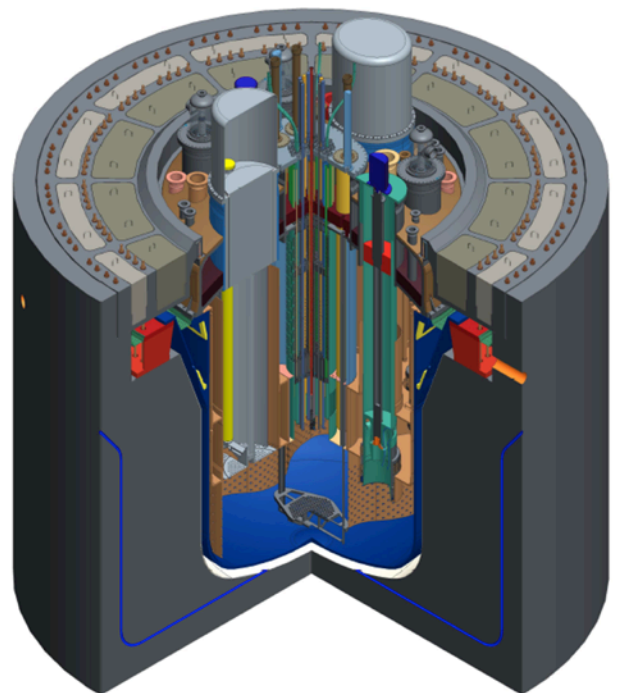


Fig. 2 : The MYRRHA reactor vessel and its internals

loading and employing conservative technical choices. This option includes more conventional double-wall heat exchangers and will use an existing IVFHM concept.

- *On the MYRRHA Implementation Scenarios*

- o To pursue scenario 1 for realisation of MYRRHA, i.e. a phased implementation with Accelerator first & Reactor later. In this scenario, the construction of the MYRRHA accelerator happens in two consecutive phases: 0-100 MeV (phase 1) followed by the 100-600 MeV sections (phase 2). The reactor (phase 3) is a separate phase and can be executed in parallel with or after phase 2.

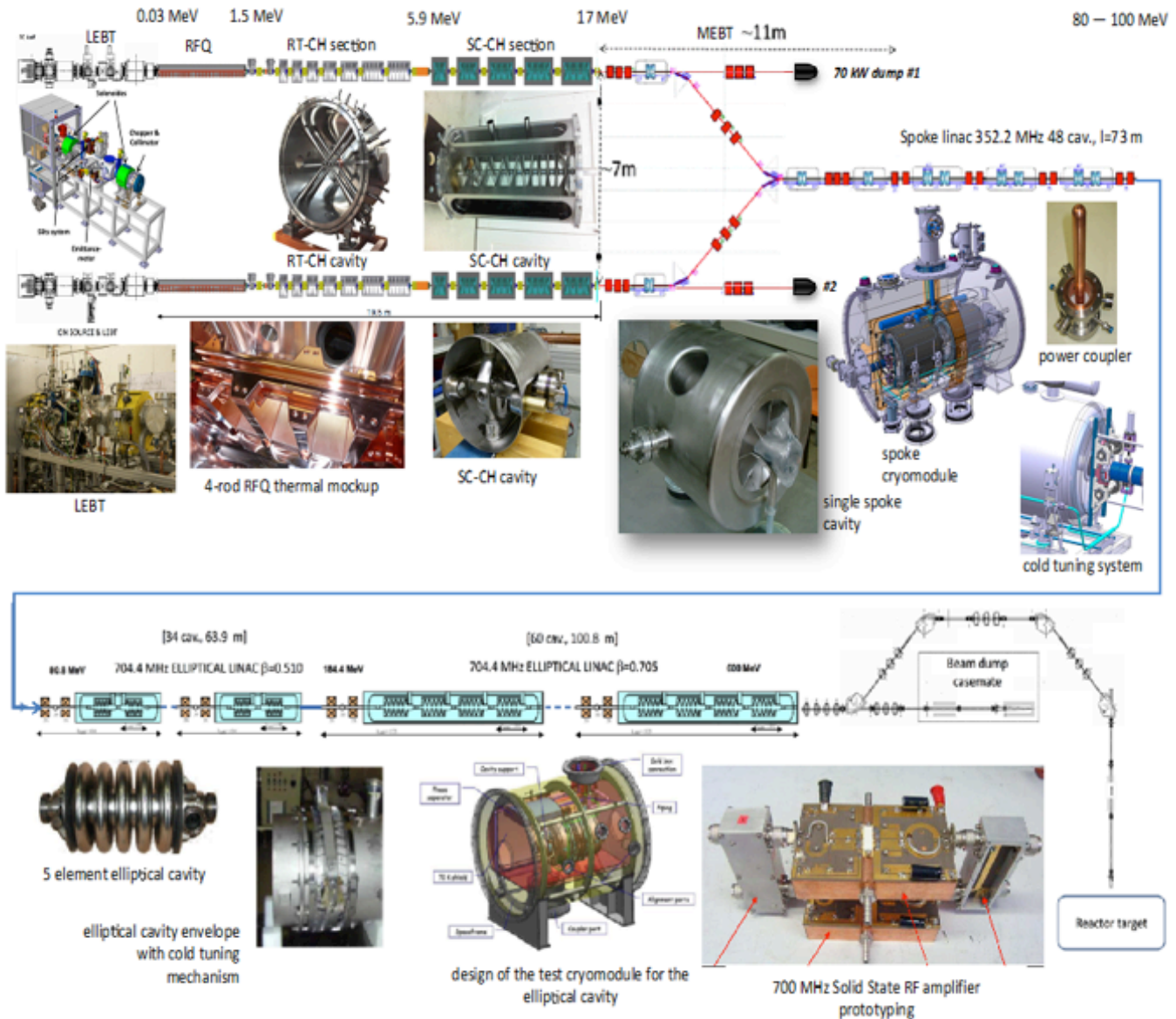


Fig. 3: The MYRRHA accelerator (upper part is Phase 1, bottom part is Phase 2)

This strategy was then confirmed by the SCK•CEN Board of Directors. Based on the Final report of the Ad-hoc evaluation group for the period 2010-2014, the Belgian Government decided in the meantime continuing to support MYRRHA and granted SCK•CEN a new dedicated MYRRHA endowment of 40 M€ for 2016-2017 and has put forward a milestone for decision by the end of 2017 by the Belgian Government for the further implementation of the MYRRHA along the above mentioned deployment scenario.

The major key dates in the planning for the Phase 1 are:

- 2017: Conclude the contracts for components manufacturing
- 2022: End of components manufacturing by contractors
- 2022: Buildings exist on the Mol site
- 2022: Components assembly on the Mol site
- 2023-2024: Commissioning, reliability & operational tests
- 2025: Start of operation of 100 MeV facility at full power

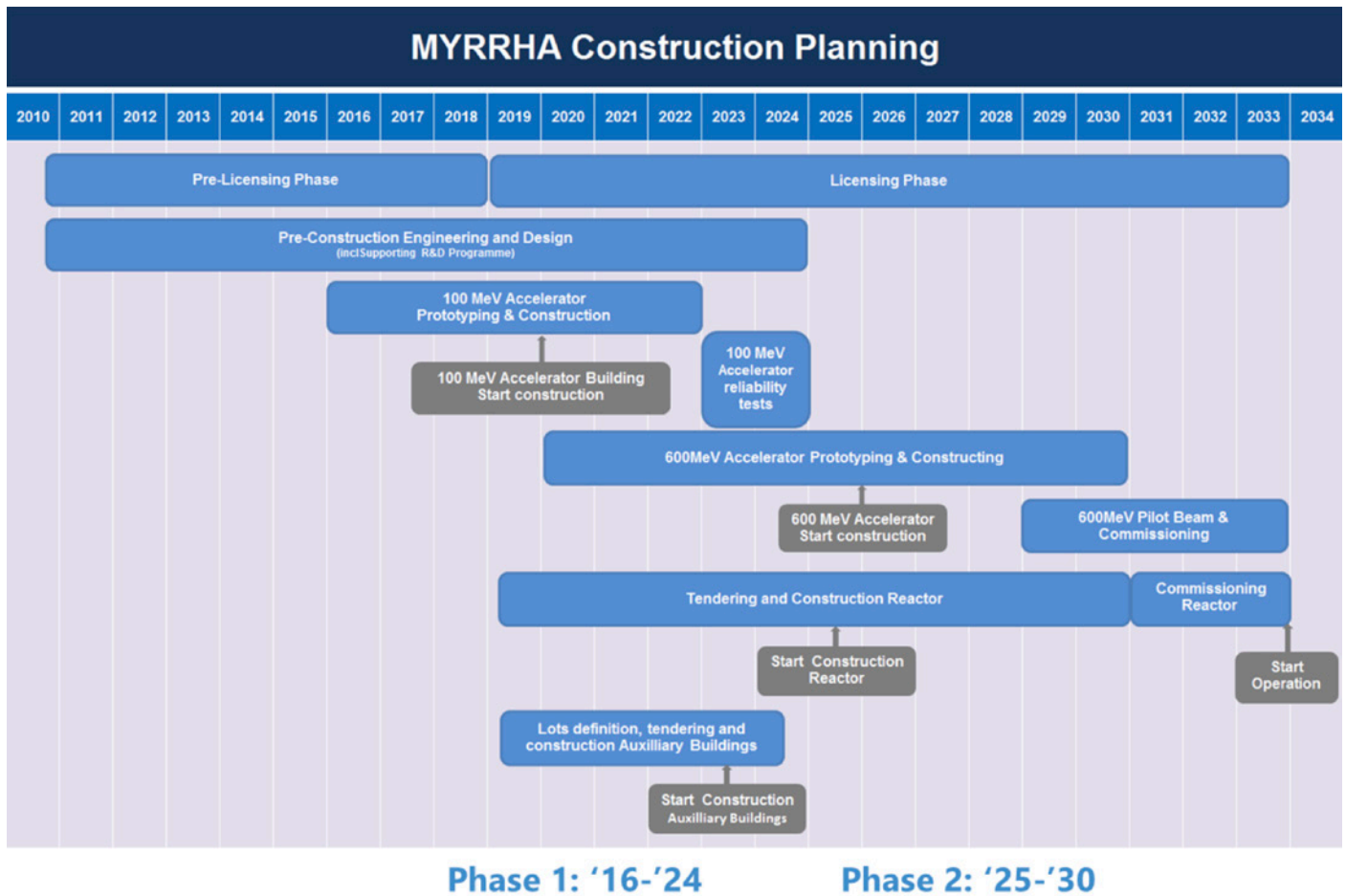


Figure 4: High-level planning 2016 - 2030

### Challenges and opportunities

Aiming to build a new LRI in a Small but Innovative Country is a very challenging task as one has to face:

- National competition with other innovative research sectors, with the handicap of being a “nuclear” project in a country aiming to phase out nuclear power;
- European competition with the large countries (Germany, France, United Kingdom, Italy) when it comes to pretending to host a LRI;
- Nuclear energy heavy conservatism when it comes to technology choices (ADS vs Reactor, LBE vs Sodium, Solid vs Liquid for the the spallation target, cyclotron vs LINAC, ...);

It is therefore necessary to turn those challenges into opportunities through “endurance and perseverance to achieve excellence” as such for SCK•CEN we created a worldwide Centre of Excellence in HLM technology addressing various aspects related to the use of the LBE in reactor technology such as; chemistry, instrumentation, material corrosion, robotics, CFD, components development, advanced materials development and qualification.

### Conclusions

The high level waste (HLW) management through advanced option such as P&T, is a multinational problem and endeavour and request an international collaboration. Joining efforts in this field will enhance the role of nuclear power in the green energy mix of tomorrow. Addressing the nuclear waste issue through innovative solutions allows to attract the young generation to the nuclear sector, guaranteeing the further successful use of nuclear technology if they dare to challenge their elder mentors.

Belgium is contributing to an innovative approach for the treatment of the spent nuclear fuel of present nuclear power plants under development within the EU strategy for P&T through the unique project MYRRHA. MYRRHA is based on a sub-critical reactor Generation IV Lead Fast Reactor (LFR) technology requesting very unique expertise and facilities in reactor as well as accelerator technologies. The MYRRHA reactor and its associated R&D facilities can benefit to the LFR Generation IV deployment in particular for the Small Modular Reactor-LFR.

## References

- H. Aït Abderrahim, D. De Bruyn & M. Giot (2007) From MYRRHA to XT-ADS – Development of Pb-Bi cooled ADS and Perspective of Implementation in Europe, International Conference "Nuclear Energy for New Europe 2007", Portorož (Slovenia), 901.01 – 901.10.
- H. Aït Abderrahim, P. Baeten, D. De Bruyn & R. Fernandez (2012) MYRRHA, a multi-purpose fast spectrum research reactor, *Energy Conversion & Management* Volume 63, 4-10.
- H. Aït Abderrahim, D. De Bruyn, G. Van den Eynde & S. Michiels (2013) Transmutation of High Level nuclear Waste by means of Accelerator Driven System (ADS).- In: *Encyclopedia of Nuclear Physics and its Applications*, Frankfurt, Germany, Wiley-VCH - Reinhard Stock, 689-704, ISBN: 9783527407422.
- F. Bianchi, C. Artioli, K. W. Burn, G. Gherardi, S. Monti, L. Mansani, L. Cinotti, D. Struwe, M. Schikorr, W. Maschek, H. Aït Abderrahim, D. De Bruyn & G. Rimpault (2006) Status and trend of core design activities for heavy metal cooled accelerator driven system, *Energy Conversion & Management* Volume 47, 2698 – 2709.
- D. De Bruyn, S. Larmignat, A. Woaye Hune, L. Mansani, G. Rimpault & C. Artioli (2010) Accelerator Driven Systems for Transmutation: Main Design Achievements of the XT-ADS and EFIT Systems within the FP6 IP-EUROTRANS Integrated Project, 2010 International Congress on Advances in Nuclear Power Plants (ICAPP'10), San Diego (California, USA), paper 10112, 1808 – 1816.
- J. U. Knebel, H. Aït Abderrahim, M. Caron-Charles, D. De Bruyn, F. Delage, C. Fazio, M. Giot, E. Gonzalez, G. Granget, L. Mansani, S. Monti & A. C. Mueller (2009) EUROTRANS : European Research Programme for the Transmutation of High Level Nuclear Waste in an Accelerator Driven System: Towards a Demonstration Device of Industrial Interest, FISA 2009 "EU Research and Training in Reactor Systems", Prague (Czech Republic). Published by the European Commission, EUR 24048 EN (2010) 286 – 316, ISBN 13-978-92-79-13302-2.
- L. Mansani, M. Reale, C. Artioli & D. De Bruyn (2010) The designs of an experimental ADS facility (XT-ADS) and of an European Industrial Transmutation Demonstrator (EFIT), OECD Nuclear Energy Agency International Workshop on Technology & Components of Accelerator Driven Systems (TCADS), Karlsruhe (Germany). Published by OECD (2011) NEA n° 6897, ISBN 978-92-64-11727, 321-334.

## 15 - Stellarator-mirror fusion-fission hybrid systems

V.E. Moiseenko<sup>1\*</sup>, V.V. Nemov<sup>1</sup>, S.V. Chernitskiy<sup>1</sup>, O. Ågren<sup>2</sup>, A.N. Shapoval<sup>1</sup>, V.S. Voitsenya<sup>1</sup>, I.E. Garkusha<sup>1</sup>

<sup>1</sup> National Science Center "Kharkiv Institute of Physics and Technology", Kharkiv, Ukraine

<sup>2</sup> Ångström Laboratory, Uppsala University, Uppsala, Sweden

### Abstract

The development of stellarator-mirror fission-fusion hybrid concept is reviewed. The hybrid comprises a fusion neutron source and a powerful sub-critical fast fission core. It is aimed for transmutation of spent nuclear fuel and safe fission energy production. The stellarator part of the neutron source offers relatively good confinement for warm Maxwellian deuterium plasma. The hot minority tritium ions are sustained in the plasma by radio-frequency heating or neutral beam injection (NBI). Since high energy ions are poorly confined in stellarators, it is proposed to embed into the stellarator a mirror trap with lower magnetic field. A scheme with NBI at the mirror ends is considered and studied numerically, and the neutron generation intensity spatial distribution is computed. Energy balance calculations for the stellarator-mirror system are performed. In a power plant scale the plasma part of the considered hybrid machine is rather compact with a size comparable to existing fusion devices. An experimental device could be built in small scale for a proof-of-principle purpose, and even under these conditions it may have a positive power output. Neutron calculations have been performed with the MCNPX code, and the principal design of the reactor part is made. Neutron leakage at outer parts of the reactor is sufficiently reduced by employment of the borated water. The transmutation rates for the fuel components are computed. A candidate for a combined stellarator-mirror system is a DRACON magnetic trap. For high energy ions of tritium, computations of collisionless losses in the mirror part of a specific design of the DRACON type trap indicate a sufficient level of tritium confinement. The Uragan-2M stellarator type device is used to check key points of the stellarator-mirror concept. The magnetic configuration of a stellarator with an embedded magnetic mirror is arranged by switching off one toroidal coil. The magnetic surfaces for such a case are predicted numerically and measured experimentally. Plasma confinement is observed. The motion of fast particles magnetically trapped in the embedded mirror is analyzed numerically with use of motional invariants. It is predicted that a weak radial electric field is necessary to provide the confinement.

### Introduction

Fast neutron reactors are likely to play a key role in future nuclear power production. Such reactors consume the abundant U238 instead of the scarce U235 and could supply the world with energy for many centuries. It is foreseen that the majority of the reactors would be critical, i.e. self-sufficient in neutron balance. A most important reactor characteristic,  $k_{eff}$ , the effective neutron multiplication factor, is unity for the stationary regime of the critical reactor operation. In transient regimes  $k_{eff}$  should not exceed the value of  $1+\beta$ , where  $\beta$  is the delayed neutron fraction. The value of  $\beta$  is not big, e.g. for U235 and thermal neutrons it is  $6.4 \times 10^{-3}$ . If the fuel is plutonium the number of delayed neutrons is almost triple less. Americium fuel has even lesser. So, the critical fast reactors have much narrower frame of safe operation than the light water reactors. It should be also mentioned that stabilizing effect of Doppler broadening is absent for fast reactors.

The sub-critical reactors which are controlled by an external neutron source are more costly, but have certain advantages before critical reactors. They offer an improved controllability of the chain fission reaction that boosts reactor safety. In a sub-critical reactor the delayed neutrons are not as important as in a critical reactor, and, therefore, sub-critical reactors can operate with a wider variety of fuels and also incinerate nuclear waste. Here a sub-critical fast reactor with a plasma neutron source, i.e. a fusion driven system or fission-fusion hybrid (FFH), is considered. Several different concepts of this type (see, e.g. [1-4]) are studied in the literature.

Fusion neutron source is a bit special since fusion, to be self-sufficient, requires more neutrons than it produces. Each neutron generated in D-T fusion reaction is needed to produce an atom of tritium in a neutron reaction with lithium. The tritium production could be moved to fission part of the hybrid. This is feasible since fission is rich in neutrons. In other words, an external fusion neutron source is needed rather for fission reactor control than for neutron supply. The neutrons are generated in hot magnetically confined D-T plasma. Since the fusion reaction is affected by a strong Coulomb barrier between D and T nuclei, it becomes efficient starting from high plasma temperature, 5-10 keV. Such a temperature can be obtained only in big plasma devices. This results in big amount of generated neutrons, sometimes bigger of that is necessary for subcritical reactor control.

Another possibility exists to arrange neutron generation in more cold plasma with temperature 1-3 keV. This background plasma could be chosen deuterium. Inside it, a hot minority population of tritium ions can be sustained with average energy 60-150 keV which is optimum for neutron generation. Lower background plasma temperature means that a smaller plasma device is necessary, and also neutron output is lower. The hot tritium ions should be heated continuously

to compensate their energy losses in Coulomb collisions with the background plasma. Operation of FFH could be considered as amplification of fusion power by fission reactions. The amplification factor can be calculated from the global neutron balance in fission reactor:

$$Q_{f/f} = \frac{P_{fis}}{P_{fus}} = \frac{E_{fis}}{E_{fus}} \frac{1}{\bar{\nu}} \frac{k_{eff}}{1 - k_{eff}} \varphi^* \quad (1)$$

Here  $E_{fis} \approx 200$  MeV and  $E_{fus} \approx 17.6$  MeV are fission and fusion energy release,  $\bar{\nu}$  is the average number of neutrons released in fission reaction,  $\varphi^*$  is the efficiency of fusion neutron penetration to the reactor core. For the value of  $k_{eff}$  which can prevent its increase over unity during lost-of-coolant-accident,  $k_{eff} = 0.95$ , power amplification is  $Q_{f/f} \approx 70$ . If the fusion neutron source is aimed for compensation of lacking delayed neutrons only (this opportunity is less studied), the amplification is one order of magnitude greater. This means that that even with a small fusion Q factor (Q is the ratio of released fusion power to the power of plasma heating) net power production is possible because the fission mantle has high power amplification [5]. The majority of power production of FFH is provided by fission that could be more than one order of magnitude larger than the contribution from fusion. Also, the fission energy yield in a single fission reaction is substantially higher than in fusion. The characteristic range of the power amplification coefficient is  $Q_{f/f} = 20 \dots 200$ . Thereby, the corresponding range for the fusion Q is  $Q = 0.1 \dots 2$  in a hybrid reactor.

### SM hybrid description

A proposal for a hybrid device, stellarator-mirror hybrid (SM hybrid), is described in Ref. 6. The fusion neutrons are generated in a deuterium-tritium plasma confined magnetically in a stellarator-type system (see Figure 1). The plasma contains a warm electron component, and the majority of ions (deuterium) is in thermal equilibrium with the electrons. The stellarator provides steady-state operation and offers relatively good confinement for such a warm Maxwellian plasma. The hot minority tritium ions are sustained in the plasma by radio-frequency (RF) heating (see Refs. 7-10). Since high energy ions are poorly confined in stellarators, it is proposed in Ref. 6 to embed into the stellarator a mirror trap with lower magnetic field. The hot ions have predominately perpendicular kinetic energy. Because of the mirror trapping effect, the hot ion motion is restricted to the mirror part of the device. This localization of the hot sloshing ions and the neutron production zone to the mirror part is favorable: With this localization of the neutron production, it is sufficient to surround with a fission mantle only the mirror part. Furthermore, all sensitive plasma diagnostics and plasma control devices can be placed outside the fission reactor, where the high neutron flux is avoided.

Not only RF heating is capable of sustaining sloshing ions. Continuous neutral beam injection (NBI) is an alternative option for this. It is practiced both in stellarators [11] and mirror machines [12].

For mirrors a quasi-tangential injection to the midplane is typical. In comparison with normal injection, it allows one to increase the injection energy. However, a midplane injection would severely influence on the reactor design: either the reactor would be split into two independent nuclear reactor cores [13] or, in case of a single reactor core, beamlines inside the reactor core must be introduced. Both cases would result in serious technical problems.

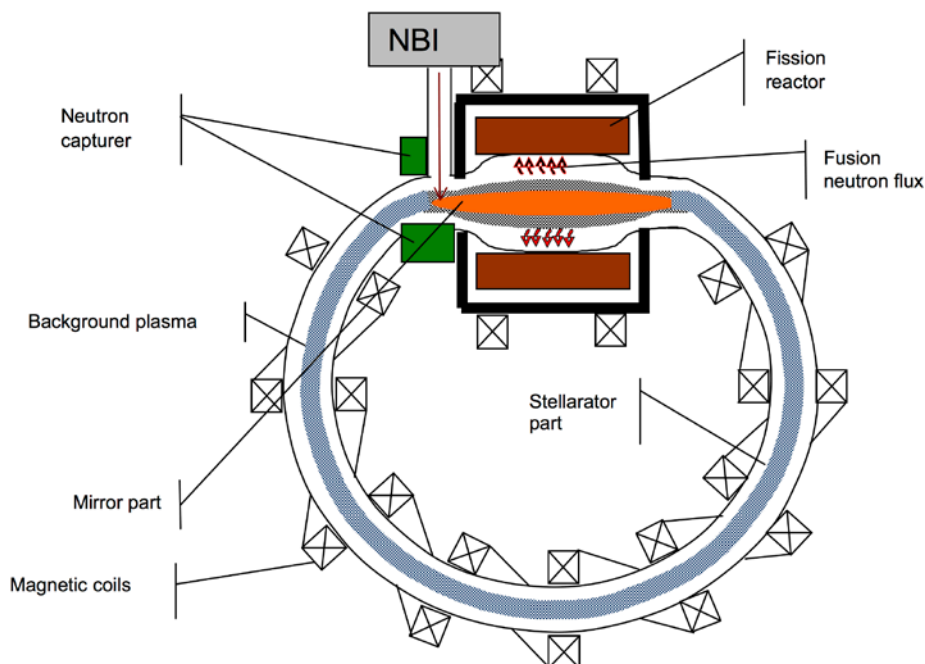


Figure 1. Sketch of the fission-fusion hybrid

Use of normal injection is favourable because it provides less neutron loss from fission core and allows one to put beamlines outside the reactor core. To avoid beam shine-through, the shorter beam-plasma interaction distance is compensated by a tolerable increase of the plasma density. A scheme with NBI at the mirror ends is adopted here, similar to the scheme addressed in Ref. 14. The NBI is normal to the magnetic field and targets plasma just near the fission mantle border (see Fig. 1). The shined-through atoms, which are in minority compared to the amount of injected atoms, hit the armor placed opposite to the NBI port.

A first step for the study of SM hybrid is a power balance analysis [15,16]. It provides estimates of the plasma machine size, magnetic field strength, necessary power for hot ion sustaining and the overall power efficiency. In the calculations the ISS04 stellarator scaling and kinetic calculations results are used. The three versions of the SM hybrid are presented in Table 1. Following the data in this table, the stellarator-mirror hybrid could be realized either in small or big versions. The calculated plasma parameters, magnetic field values and the machine sizes are within a reachable range. Such values of the parameters are either already achieved in fusion experiments or could be achieved with moderate extrapolation. The magnetic field is somewhat higher for a smaller device. This is a consequence of the restriction for the plasma target density for the neutral beam to decrease beam shine-through. In case of ICRH usage the magnetic field could be chosen lower. The estimate for costs is made only for the second version. The estimated cost is anyhow much less than for a fusion reactor.

### DRACON, as plasma part of SM hybrid

Straightforward local decrease of the magnetic field in the stellarator results in an embedded magnetic mirror, but this mirror is handicapped. It follows from the obtained in [16] results that the symmetry of the magnetic field for the mirror part is strongly broken under the influence of the magnetic field of the stellarator part, and poor confinement of trapped hot ions occurs. Therefore, improvement of the trapped particle confinement is necessary. In particular one can expect that such an improvement can be obtained by constructing rectilinear section (sections) of the magnetic system of the device and placing mirror trap (traps) at this section (these sections). Up to present time a number of the stellarator type configurations with rectilinear sections have been proposed. These are, e. g., the DRACON stellarator type device [17], a linked mirror configuration [18], and a theoretically developed configuration EPSILON [19]. The DRACON system [17], for which a method of calculating the real-space magnetic field has already been developed in Ref. 20, seems more suitable. The derivation from the standard DRACON is that the SM hybrid needs not long, but short mirror part and it should be single.

Parameter	Version 1	Version 2	Version 3
Stellarator beta	0.01	0.01	0.01
Mirror beta	0.15	0.15	0.15
Tritium injection energy	150 keV	150 keV	150 keV
Beam shine-through parameter (ratio of ion mean-free path to plasma radius)	1.5	1.5	1.25
Background plasma temperature	1 keV	1.6 keV	3keV
Stellarator part magnetic field	4.4 T	4.1 T	3.1 T
Mirror ratio	1.7	1.7	1.7
Angle of rotational transform	0.8	0.8	0.8
Inverse aspect ratio	0.05	0.05	0.05
Plasma density	$3 \cdot 10^{14} \text{cm}^{-3}$	$1.5 \cdot 10^{14} \text{cm}^{-3}$	$6 \cdot 10^{13} \text{cm}^{-3}$
Minority concentration (in mirror part)	0.11	0.11	0.11
Heating power	10 MW	20 MW	60 MW
Fission power	140 MW	570 MW	3.3 GW
Plasma minor radius	12 cm	20 cm	60 cm
Torus major radius	2.4 m	4 m	12 m
Mirror length	1.9 m	3.2 m	9.6 m
Electric efficiency $Q_{el}$ (for nuclear mantle with $k_{eff}=0.95$ )	2.4	4.8	9.3
Estimated costs, M\$	-	500	-

Table 1. Parameters of 3 versions of stellarator-mirror hybrid (see Ref. 16).

The equilibrium stellarator configuration DRACON [17] consists of two rectilinear regions and two curvilinear elements (known as CREL), which close the magnetic system and whose parameters are chosen such as to keep the Pfirsch-Schlüter currents within the CREL and to prevent them from penetrating into the rectilinear sections. In order to improve the plasma confinement, the magnetic field in the CRELs is higher than the field in the rectilinear parts. In SM hybrid scenario good confinement of hot ions is important. It could be provided by mirror symmetry of the magnetic field in the mirror parts analogous to the axial symmetry of an open mirror trap. However, such a symmetry can be broken under the influence of CRELs.

For high energy ions of tritium with an energy of 70 keV comparative computations of collisionless losses in the mirror part of a specific design [21] of the DRACON type trap are carried out. Two variants of the trap are considered with different lengths of the rectilinear sections (initial and shortened). Also the total number of current-carrying rings in the magnetic system is varied. The results indicate that high energy ions can be satisfactorily confined in the mirror part during much longer time (1 s) than the time of fast ion slowing down in plasma by electron drag (0.025 s).

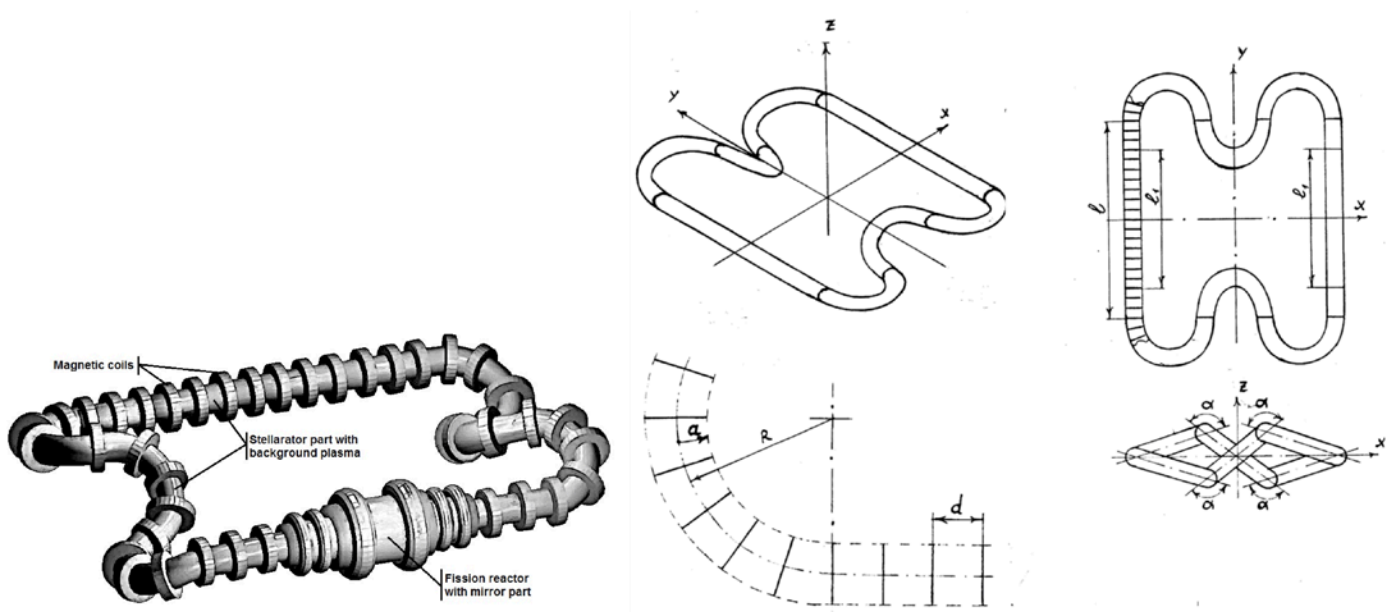


Figure 2. A sketch (left) and scheme (right) of the DRACON type trap.

Another notable result is that the majority of passing ions are confined less than 0.01 s. This is favorable in sense of necessity to suppress fusion neutron generation at the stellarator part. The calculations confirm suitability of DRACON for plasma part of SM hybrid.

### Fission reactor part

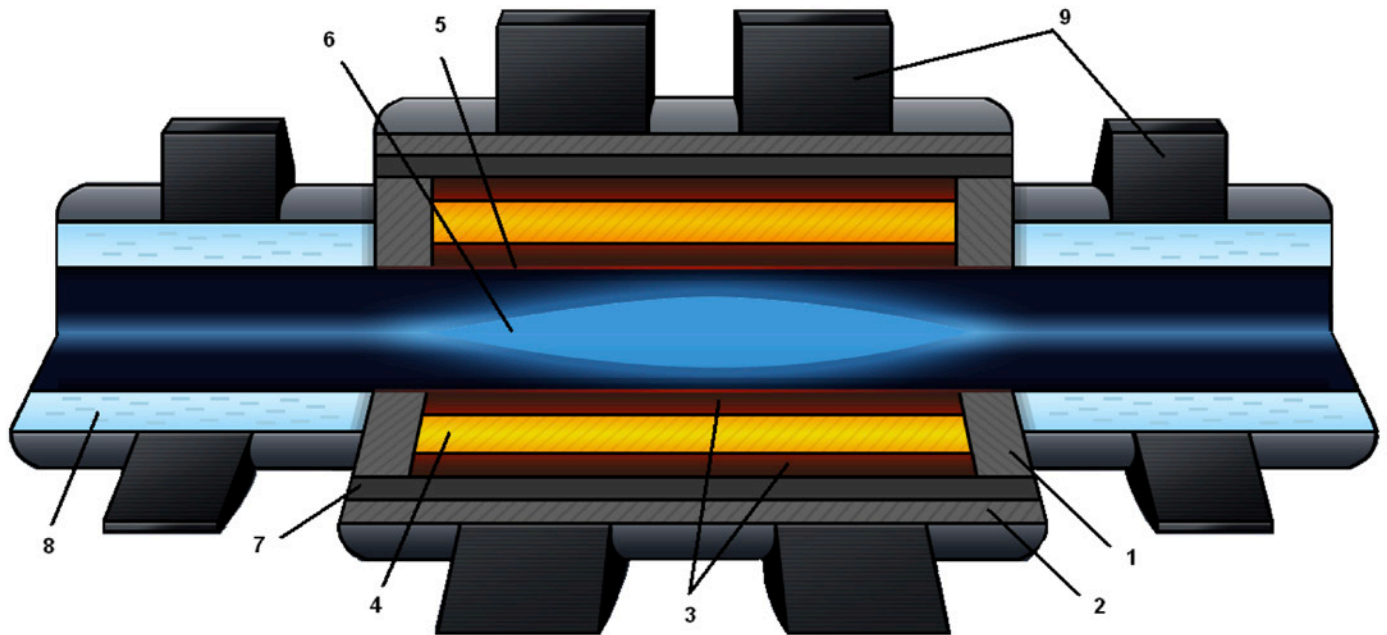
The acquired knowledge on fusion neutron source parameters gives starting conditions to a preliminary design of the fission mantle part of the hybrid. The design of the mantle is mainly based on the developments described in Ref. 22. The major difference from the described there reactor is that the device length must be much shorter in our case. A task is to clarify whether it is possible to achieve an appropriate value of the effective neutron multiplication factor  $k_{\text{eff}}$  in such conditions.

As in Ref. 22, the fission reactor core is cylindrical. In the center there is a vacuum chamber that contains the D-T plasma which supplies fusion neutrons. First wall which separates the vacuum chamber and the reactor suffers from high-energy neutron load and, in contrast to pure fusion devices, fission as well as fusion neutrons contribute to wall damage. In order to get a longer lifetime of the first wall, its damage rate must be low.

In the reactor, the inner radius of the vacuum chamber was fixed to 50 cm. For the first wall a thickness of 3 cm was chosen. The first wall is made of HT-9 steel with a mass density of 7.7 g/cm<sup>3</sup> and its isotopic composition was taken from the ORNL Fusion materials data bank [23]. A buffer has been introduced between the first wall and the fission blanket in order to increase the neutron flux in the core using the reaction  $^{207}\text{Pb}(n,2n)^{206}\text{Pb}$  which has a large cross section for the incident neutron energies above 7 MeV. Besides, the buffer reduces the flow of fission neutrons from the reactor core to the first wall and the vacuum chamber.

The reactor core goes next to the buffer. Its thickness was determined by critically calculations. A thickness of 27.8 cm was found to provide the effective multiplication factor  $k_{\text{eff}} \approx 0.95$ . The length of the core is 3 m. There are axial reflectors on both sides. They contain HT-9 steel and the lead and bismuth eutectic (LBE) -coolant with the volume fractions 70% and 30%, respectively.

The active zone of the reactor contains fuel, structure/cladding and coolant. HT-9 steel and LBE were used as structure/cladding and coolant materials, respectively. The actual fuel material is the alloy (TRU-10Zr) which consists of the transuranic elements with 10 wt.% of zirconium [24]. The alloy has a mass density of 18.37 g/cm<sup>3</sup>. The fuel is made of the spent nuclear fuel from PWRs after the removal of uranium. The fuel is of disperse type, (see e.g. the Ref. 25) and is practically free of fertile isotopes.



- |  |  |
|--|--|
| 1. Axial reflector: HT-9 steel - 70% and LBE-30%   | 6. Neutron source (D-T plasma)   |
| 2. 60:40 Vol.% mixture of the stainless steel S30467 type 304B7 with water. The steel contains 1.75 wt% of natural boron | 7. Radial reflector: HT-9 steel - 70% and Li17Pb83 - 30% (enrich. 20% Li6) |
| 3. Coolant (Lead and Bismuth eutetic)  | 8. Borated water with B (10g/kg) B10 - 20% and B11 - 80%                   |
| 4. Fission blanket   | 9. Magnetic coils  |
| 5. First wall  |  |

Figure 3. Scheme of the reactor part of SM hybrid.

The fission blanket is surrounded by the core expansion zone. Its thickness was put to 15 cm. This zone is filled by LBE. Effective multiplication factor of neutrons in the core will decrease in the time. This is due to the fact that the transuranic isotopes (primarily <sup>239</sup>Pu) will burn out and production of the fissile isotopes is absent (note here that the fuel composition does not contain <sup>238</sup>U). To maintain the effective multiplication factor on an acceptable level one should add new fuel assemblies into the reactor core.

For this reason core expansion zone has been added. The radial reflector in the model is a homogeneous mixture of HT-9 steel and Li17Pb83 (20% enriched <sup>6</sup>Li) with the volume fractions 70% and 30%, respectively. This mixture is aimed for tritium breeding from the reaction with <sup>6</sup>Li(n,T)<sup>4</sup>He.

A shield is used to reduce the neutron and gamma loads of the stellarator-mirror magnetic coils needed for the plasma confinement. The shield contains a 60:40 vol% ratio of the stainless steel alloy S30467 type 304B7 (see Ref. 18) with water. The steel contains 1.75 wt% of natural boron. The shield thickness is of 25 cm.

The total length of the main part of the nuclear reactor is 4 m. The energy multiplication factor calculated by neutron kinetic model of MCNPX code is  $Q_{eff}=65$  [26] which is close to the above given theoretical estimate. The borated water shield sufficiently decreases the neutron release to outer space and the stellarator part. This lowers the neutron heat load to the superconducting magnetic windings. The tritium breeding ratio reaches 1.8.

### Uragan-2M contribution for SM hybrid concept: magnetic surfaces and particle motion

There are several principal problems concerning this concept of fusion-fission hybrid which could be investigated experimentally on existing stellarators and mirrors. The Uragan-2M stellarator (IPP, Kharkiv) offers feasible possibilities for this: The first problem to solve is whether it is possible to find a combination of magnetic mirror and stellarator with a system of nested magnetic surfaces. A more general question is how a stellarator magnetic configuration reacts to the local ripple of the toroidal magnetic field. Uragan-2M has coils for the toroidal magnetic field, and switching off one of them results in a local magnetic mirror with the mirror ratio about 1.5.

For such a case the magnetic configuration of Uragan-2M is calculated (see [16]). Such strong perturbation as switching

off one of the toroidal coils makes destructive influence on the magnetic configuration: the magnetic surfaces do not exist in case of high rotational transform. But, fortunately, the magnetic surfaces can be found if the rotational transform is approximately 1.5 times lower. This is approved by the experimental measurements [27].

It would be good to generate fast sloshing ions trapped in the mirror part of Uragan-2M device, but this could not be successful if radial drifts ruin confinement. The study of particle confinement [16] confirms this. But it did not account for a radial electric field which may improve the confinement.

The numerical study [28] is based on Biot-Savart calculations of the magnetic field of the device and the analysis of the parallel adiabatic invariant  $J_{||}$ . The influence of the static radial electric field is taken into account in the calculations. The results are presented in figure 4. All quantities are normalized by product of magnetic moment and the magnetic field strength at the stellarator part. So, the normalized energy of the particle for this calculation is 0.8.  $A$  represents the normalized energy of an ion in the electrostatic field at the plasma column edge.

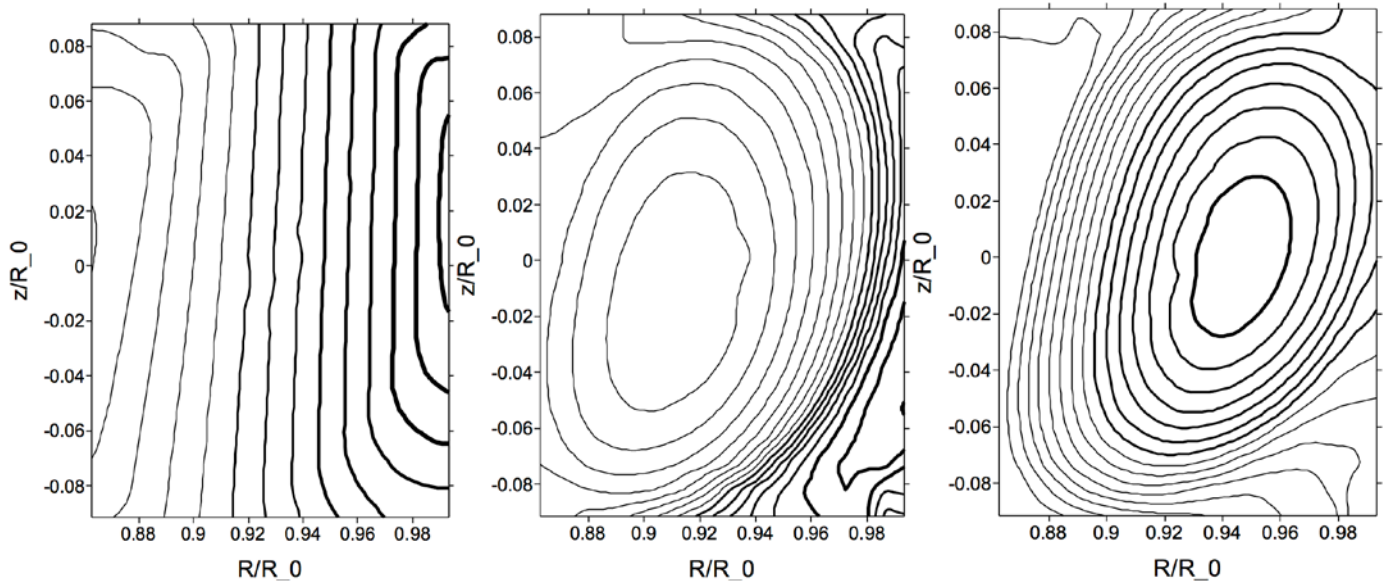


Figure 4. Contours of  $J_{||}$  for  $A=0$  (left),  $A=0.1$  (center) and  $A=-0.1$  (right). Thicker lines correspond to bigger  $J_{||}$  values.

Figure 4 (left) shows contours of  $J_{||}$  for the case of zero electric field. Drift surfaces are not closed in this case. This is because of the toroidal drift that forces particles to drift in vertical direction. Starting from some  $A$  value, a maximum of the parallel invariant appears. This maximum is surrounded by closed mean drift surfaces. In case of negative  $A$ ,  $J_{||}$  has a minimum point shifted inside the torus (see Figure 4, right).

The calculations indicate that radial electric field can improve the situation substantially. It causes particle drift in the poloidal direction which is competing with the vertical magnetic drift. Above a certain value of the electric field, mean drift surfaces become closed, and particle confinement improves. This value can be estimated from the formula

$$|e\Phi| \sim \mu\Delta B$$

where  $\Delta B$  is the variation of the magnetic field across the confinement volume.

This estimate is confirmed by the above calculations. Since  $\Delta B/B \sim \langle r \rangle_{last} / R_0 \ll 1$

a radial variation of the potential energy in the electrostatic field, which is much smaller than the kinetic energy of the particle, is sufficient to achieve the confinement. Another remarkable feature is that confinement improves for both, positive and negative point charges.

To establish the potential in the plasma column, a very small amount of lost ions is sufficient. The potential seems to be small enough to destroy the diffusive character of confinement of the bulk plasma. However, when the potential energy of bulk electrons and ions in the electric field reaches the values of their kinetic energies, the diffusive fluxes may be sufficiently altered which may increase the hot ion losses.

### Uragan-2M contribution for SM hybrid concept: plasma confinement

A first attempt was made to create plasma in Uragan-2M device with embedded mirror. The discharge was initiated by RF pulse of the crankshaft antenna [29]. The generator frequency was 4 MHz, neutral gas pressure  $10^{-3}$  Pa, magnetic field at the stellarator part was 0.37 T.

The start-up of the discharge was successful: the plasma is created with density about  $10^{12}$  cm<sup>-3</sup>. The  $H_{\alpha}$  line indicates

full ionization of hydrogen. The OII line immediate appearance could be explained by presence of volatile impurities. No decrease of its intensity during emission of higher excitation threshold lines, OV and CV, indicates high impurity influx from the chamber wall. The OV and CV lines appear with some delay and quickly die out. Their intense emission, especially of CV, indicate some electron temperature not less than 100 eV. The discharge starts to fade at 20<sup>th</sup> ms and finally collapses due to impurities.

## Conclusions

The concept of SM hybrid is developed. It has the following attractive features:

- The hybrid is capable to provide steady-state operation (for a year or more) .
- It is expected that the full control on plasma could be achieved: there would be no any disruption or spontaneous instabilities which seriously influences on neutron generation.
- The neutron outflow is tuneable and the response time is short enough to provide full control on power generation.
- The design and operation of all plasma device systems is facilitated with a localization of the neutron emission.
- In a wide range of the machine parameters, a high electric Q is calculated.
- In a power plant scale SM hybrid machine is compact enough with a size comparable to existing fusion devices.
- An experimental device could be built in small scale for a proof-of-principle purpose, and even under these conditions it may have a positive power output.
- Reproduction of tritium can be provided.

The studies on SM hybrid concept are underway. Based on the power balance analysis and kinetic calculations, the parameters of several versions of SM hybrid are calculated. The plasma part of the hybrid could be a DRACON-like with a single short embedded mirror. The calculations predict good fast trapped ion confinement in the mirror part. The proposed reactor part is compact enough to integrate it into the plasma part. It is strongly shielded and is able to reproduce tritium in sufficient amount. A series of studies in support of SM hybrid concept has been carried out at and for Uragan-2M device including magnetic configuration studies, hot ion and background plasma confinement. The studies made indicate good prospects for this concept.

## References

1. Kuteev B V et al 2011 Nucl. Fusion 51 073013
2. Wu Bin 2003 Fusion Engineering and Design 66-68 181.
3. Noack K, Rogov A, Ivanov A A, Kruglyakov E P 2007 Fusion Science and Technology 51·No 2T 65.
4. Ågren O, Moiseenko V E, Noack K 2010 Fusion Science and Technology 57 No 4 326.
5. Noack K, Ågren O, Moiseenko V E, Hagnestål A 2013 Annals of Nuclear Energy 59 261.
6. Moiseenko V E, Noack K, Ågren O 2010 J. Fusion Energy 29 65.
7. Moiseenko V E, Ågren O 2007 Journal of Physics: Conference Series 63 012004
8. Moiseenko V E, Ågren O 2005 Phys. Plasmas 12 102504.
9. Moiseenko V E, Ågren O 2007 Phys. Plasmas 14 022503.
10. Moiseenko V E and Ågren O 2012 AIP Conf. Proc 1442 199 doi:<http://dx.doi.org/10.1063/1.4706869>.
11. Yamada H et al 2003 Nucl. Fusion 43 749.
12. Zuev A A et al 2002 Plasma Phys. Rep. 28 268.
13. Noack K., et al 2008 Annals of Nuclear Energy 35 1216.
14. Ryutov D D, Molvik A W, Simonen T C 2010 J. Fusion Energy 29 548.
15. Moiseenko V E, Ågren O 2013 Fusion Science and Technology 63 no. 1T 119.
16. Moiseenko V E, Kotenko V G, Chernitskiy S V, et al 2014 Plasma Phys. Control. Fusion 56 094008 (11pp).
17. Glagolev V M et al 1981 Proceedings of 10-th European Conference on Controlled Fusion and Plasma Physics, Moscow, Vol. 1 E-8.
18. Pastukhov V P and Berk H L 1993 Nucl. Fusion 33 1471.

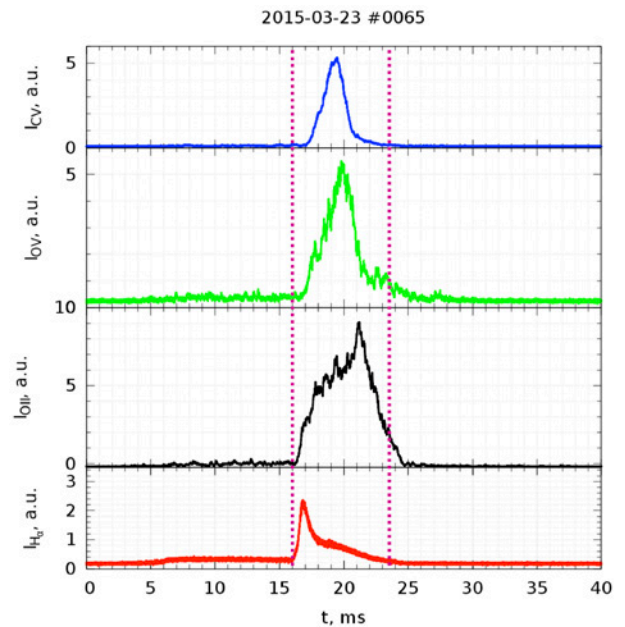


Figure 5. Optical line emissions from plasma of Uragan-2M with embedded mirror. Dotted vertical lines indicate beginning and end of RF pulse.

19. Arsenin V V et al 2001 Nucl. Fusion 41 945.
20. Némov V V 1989, 16th European Conf. on Controlled Fusion and Plasma Phys., Venice, 13B, Part II, 599.
21. Glagolev V M et al 1985 Nucl. Fusion 25 881.
22. Noack K, et al, 2011 Annals of Nucl. Energy 38 578.
23. ORNL, Fusion Materials, 1999.
24. Stacey W M, et al, 2002 Fusion Science and Technology 41 116.
25. Park W S, et al, 2003 IAEA-Tecdoc, 1348 195.
26. Chernitskiy, S V, et al, 2014 Annals of Nucl. Energy 72 413.
27. Lesnyakov G G, et al, 2013 Problems of Atomic Science and Technology, Series: Plasma Physics (83). № 1 57.
28. Moiseenko V E, et al, 2016 Plasma Phys. Control. Fusion 58 064005 (8pp).
29. Moiseenko V E, et al, 2016 Nukleonika 61(2) 91.

## 16 - Current status of R&D of Accelerator-Driven System for minor actinide transmutation in JAEA

K. Tsujimoto

Japan Atomic Energy Agency

### Abstract

To continue the utilization of the nuclear fission energy, the management of the high-level radioactive waste (HLW) is one of the most important issues to be solved. Partitioning and Transmutation technology of HLW is expected to be effective to mitigate the burden of the HLW disposal by reducing the radiological toxicity and heat generation. The Japan Atomic Energy Agency (JAEA) has been conducting the research and development (R&D) on accelerator-driven subcritical system (ADS) as a dedicated system for the transmutation of long-lived radioactive nuclides. The ADS proposed by JAEA is a lead-bismuth eutectic (LBE) cooled fast subcritical reactor with thermal output of 800 MW. For ADS to play important roles in the nuclear fuel cycle, several critical issues have to be resolved. Items of R&D are divided into three technical areas peculiar to the ADS : (1) superconducting linear accelerator (SC-LINAC), (2) LBE as spallation target and core coolant, and (3) subcritical core design and technology. For these technical areas, various R&D activities are progressing in JAEA. In this paper, the present status of the R&D activities in JAEA is reported.

### 1. Introduction

To continue the utilization of the nuclear fission energy, the management of the high-level radioactive waste (HLW) is one of the most important issues to be solved. The difficulty of the HLW management exists in its long-lasting radioactive toxicity which has to be isolated more than millions years and heat generation which may affect the structural integrity of the deep geological repository. Partitioning and Transmutation (P&T) technology of HLW is expected to be effective to mitigate the burden of the HLW disposal by reducing the radiological toxicity and heat generation. The Japan Atomic Energy Agency (JAEA) has been continuously implementing research and development (R&D) on P&T technology to reduce the burden of the backend of the nuclear fuel cycle. The R&D on P&T in JAEA are basing on two kinds of concepts: one is the homogeneous recycling of minor actinide (MA) in commercial fast breeder reactors and the other is the dedicated MA transmutation, so-called "double-strata" strategy, using an accelerator-driven system (ADS). JAEA have promoted the R&D to perform the feasibility study. In this paper, the present status of the R&D activities in JAEA is reported.

### 2. General Description of JAEA proposed ADS

JAEA's reference design of ADS2) is a tank-type subcritical reactor, where lead-bismuth eutectic (LBE) is used as both the primary coolant and the spallation target, as shown in Fig.1. The central part of the core is the spallation target region. The target region is provided by substituting central seven assemblies to a target module. In the target region, LBE is flowing from the core bottom. The proton linac with the proton energy of 1.5 GeV is used for the accelerator to operate the ADS. A tank-type system is adopted to take advantage of a simple design and to eliminate the necessity of heavy primary piping. All primary components, including primary pumps, steam generators, and auxiliary heat exchangers, are accommodated within the reactor vessel. The primary cooling system includes two mechanical pumps and four steam generators. The heat generated in the target and the core is removed by forced convection of the primary LBE, and transferred through the steam generators to a secondary water/steam system for power conversion. The auxiliary cooling system is provided as a backup system for decay heat removal. The inlet and outlet temperature of the LBE coolant were set to 300 and 407 °C, respectively. For the core fuel, (MA,Pu)-nitride is used. As inert matrix, zirconium-nitride (ZrN) is used

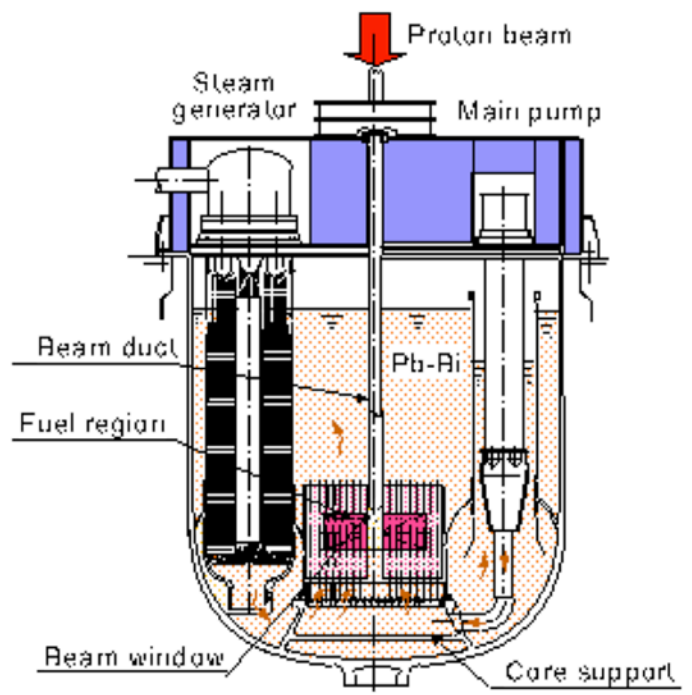


Fig.1 JAEA proposed LBE-cooled 800MWth ADS for transmutation of MA

with the fuel. To minimize the burnup swing and the power peaking, the fuel region is divided into two zones with the different initial Pu loading. The MA inventory is about 2500 kg. Since the transmutation rate of MA is 250 kg/yr as described before, the relative transmutation efficiency of MA is about 10 %/yr. The maximum keff during whole burnup cycles was set to 0.97. The burnup swing in whole cycles is about 3 %Δk/k. The maximum beam current is 20 mA (30 MW).

### 3. R&D of Proton Accelerator for ADS

The proton accelerator for the ADS should have high intensity of power, more than 20 MW, with good economical efficiency and reliability. To realize such an accelerator, energy efficiency should be enhanced to assure the self-sustainability for electricity of the whole system. Taking account of these requirements, the superconducting linac (SC-linac) is regarded as the most promising choice. The SC-LINAC consists of a series of cryomodules, which contain two units of superconducting cavities made of high-purity niobium. JAEA has a prototype cryomodule to test the performance of the electric field and the helium cooling. In addition to the development of the cryomodule, the system study for the SC-LINAC was also performed.

#### 3.1 Estimation of Acceptable Beam Trip Frequency of Accelerator for ADS

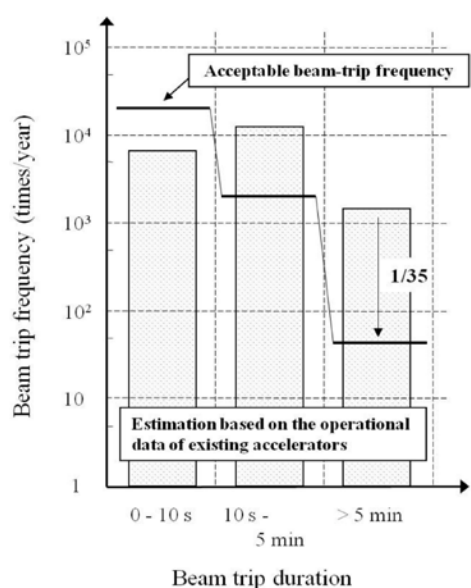


Fig. 2 Comparison of the acceptable frequency of beam trips and the estimated frequency of the JAEA's SC-linac for ADS

Although the high reliability is necessary for the accelerator of ADS, frequent beam trips are experienced in existing high power proton accelerators. The beam trip may cause thermal fatigue problems in ADS components which may lead to degradation of their structural integrity and reduction of their lifetime. To achieve the high reliability for the accelerator, the requirements for the beam trip frequencies were estimated<sup>3,4)</sup>. For this object, thermal transient analyses were performed to investigate the effects of beam trips on the reactor components. These analyses were made on the thermal responses of four parts of the reactor components; the beam window, the fuel clad, the inner barrel, and the reactor vessel. The results indicated that the acceptable frequency of beam trips ranged from 42 to 2 × 10<sup>4</sup> times per year depending on the beam trip duration. The former corresponded to the beam trip duration exceeding five minutes. On the other hand, the latter corresponded to the beam trip duration of 10 seconds or less. And the plant availability was estimated to be 70 % or greater in cases where the beam trip frequency decreased to the acceptable frequency of beam trips.

In order to consider measures to reduce the frequency of beam trips on the high power accelerator for ADS, the acceptable frequency of beam trips were compared with the operation data of existing accelerators. In this analysis, operation data of a proton linac of LANSCE<sup>5,6)</sup> and an electron/positron injector linac at High Energy Accelerator Research Organization (KEK 7). By using the distribution of beam trip durations obtained from the data of the LANSCE and the KEK, the down time distribution of the SC-linac for ADS was estimated and compared with the acceptable beam trip frequencies. The results are shown in Fig.2. The comparison showed that even at the present technological level of accelerators, the beam trip frequency for durations of 10 seconds or less is within the acceptable level. On the other hand, the beam trip frequency for durations of exceeding five minutes should be reduced to about 1/35 to satisfy the plant availability conditions.

#### 3.2 J-PARC LINAC

JAEA is conducting a multi-purpose high-intensity proton accelerator program called J-PARC collaborating with KEK. The proton accelerators consist of three stages, the linac, 3 GeV Synchrotron (Rapid Cycling Synchrotron, RCS) and 50 GeV Synchrotron (Main Ring, MR). The linac accelerates negative hydrogen beams for injection to the 3 GeV RCS at beam energy of

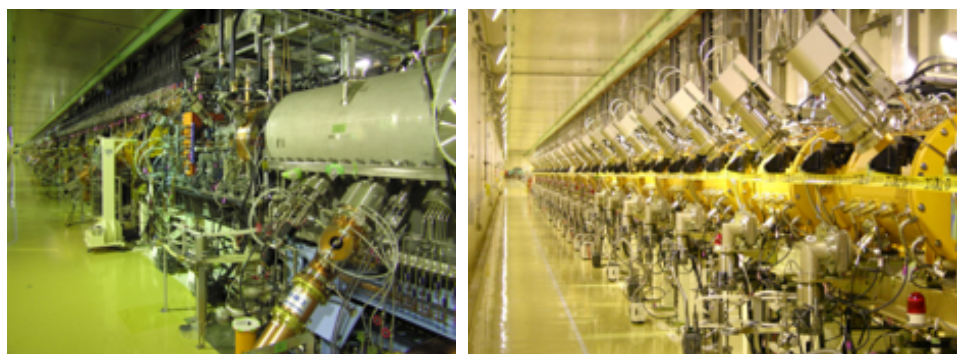


Fig 3. J-PARC LINAC (Left) Low energy part (RFQ and DTL) and (Right) Medium energy part (SDTL up to 181 MeV)

181 MeV, which will be upgraded to 400 MeV. The nominal peak current is 30 mA, which will be increased to be 50 mA to achieve a 1-MW beam power at the RCS. The repetition rate and the pulse width are 25 Hz and 500  $\mu$ s, respectively. The linac consists of the front-end part, a drift-tube linac (DTL), a separated-type DTL (SDTL), an ACS, and beam transport between the linac and the RCS (L3BT). The front-end part consists of the negative hydrogen ion source (IS), the radio-frequency quadrupole linac (RFQ), low-energy beam transport between the IS and the RFQ, and medium-energy beam transport between the RFQ and the DTL. Figure 3 shows the photos of linac part. It consists of IS, RFQ, DTL, and SDTL. Protons were successfully accelerated to 181 MeV in January 2007, to the designed energy of the RCS in October 2007, and to the initial goal in the MR of 30 GeV by December 2008.

#### 4. Feasibility Study of Beam Window

The beam window, which forms a boundary between the vacuum proton beam tube and the subcritical core, is one of the most important technical issues in the engineering feasibility of ADS. The beam window will be used in the severe conditions; (a) external pressure by LBE, (b) heat generation by the proton beam, (c) creep deformation by high temperature, (d) corrosion by LBE, and (e) irradiation damage by neutrons and protons.

##### 4.1 Design of Beam Window

The design study for the beam window<sup>8)</sup> was performed considering the results of thermal-hydraulic and structural analysis. The external pressure and the heat generation were considered and feasible concepts have been determined. Hence, the shape and the thickness of the beam window were optimized to prevent the buckling failure by the parametric survey.

The structural analysis was performed by a finite element method. Elastic-plastic large deformation buckling calculation without the effects of the creep and the irradiation was performed. Mod. 9Cr-1Mo (T91) steel was assumed as the window material in this study. The generalized calculation model was employed in the parametric survey. This model is an ellipse model, which consists of a top part, a transient part and a cylinder part, as shown in Fig. 4.

In the parametric study,  $t_1$ ,  $t_2$ , and  $t_3$ , which were the thicknesses at the top,  $\theta_f=60^\circ$ , and a connection between the transient and cylinder parts, were treated as parameters ( $t_1 \leq t_2 \leq t_3$ ). The survey calculations for  $1.0 \leq t_1 \leq 3.0$  mm,  $2.0 \leq t_2 \leq 5.0$  mm and  $2.0 \leq t_3 \leq 5.0$  mm were performed with the condition  $t_1 \leq t_2 \leq t_3$ . In each calculation case, detailed temperature distribution was calculated considering a heat density and a coolant temperature under the condition with a 1.5GeV-20mA Gaussian ( $1\sigma=11.16$  [cm]) proton beam. The calculation results were evaluated under the criteria in which Factor of Safety (FS) of 3 and the design external pressure 1.0 MPa. FS of 3 is based on the initial imperfection analysis and ASME B&PV Code Section III Case N-2849). The results show that the ellipse shape concepts with the thickness of 2.0-2.4[mm] at the top and the thickness of 2.0-4.0[mm] at the transient part were acceptable under the current ADS design parameters. It was also confirmed that the structural robustness would be kept when the uniform change of the beam window thickness would occur due to the corrosion.

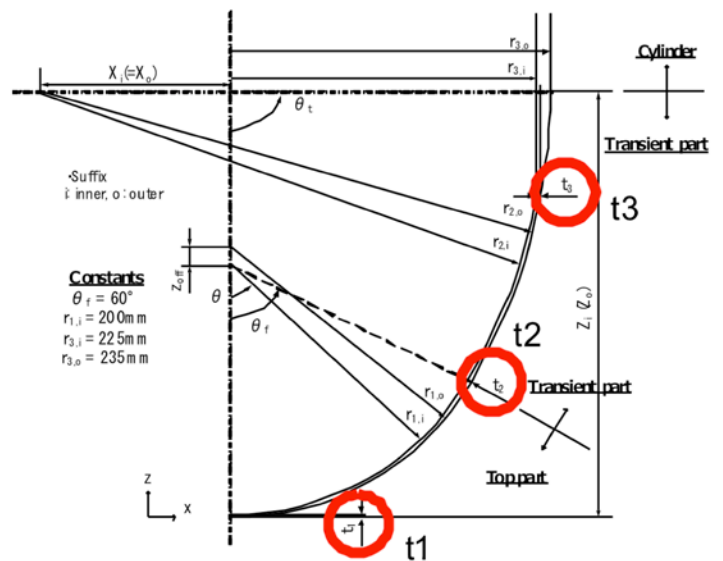


Fig.4 Generalized calculation model for the ellipse concept

##### 4.2 Development of Measurement Techniques

It is of great importance to measure and predict the detailed flow distribution of LBE for the reliable design of ADS. In JAEA, measurement technique of LBE flow velocity profile have been developed by using the Ultrasonic Velocity Profiler (UVP) technique. UVP is a suitable tool to measure an instantaneous space-time velocity profile especially on a velocity measurement of an opaque liquid flow, such as liquid metal. Developed UVP measurement system was applied to the JAEA Lead Bismuth Loop-2(JLBL-2).

As a result of an experiment, the flow velocity profile was successfully measured, and it was found that there were periodical releases of eddy from the re-circulation region formed near the wall surface of the inner cylinder<sup>10)</sup>. In the next step, a measurement for non-parallel directions with the centerline was carried out, and 3-dimensional structure of LBE flow configuration was found. Moreover, a new technique, which enables the measurement of the velocity vector in multi-dimensions on a line in the flow field, was developed. It was named Vector-UVP. This system was successfully

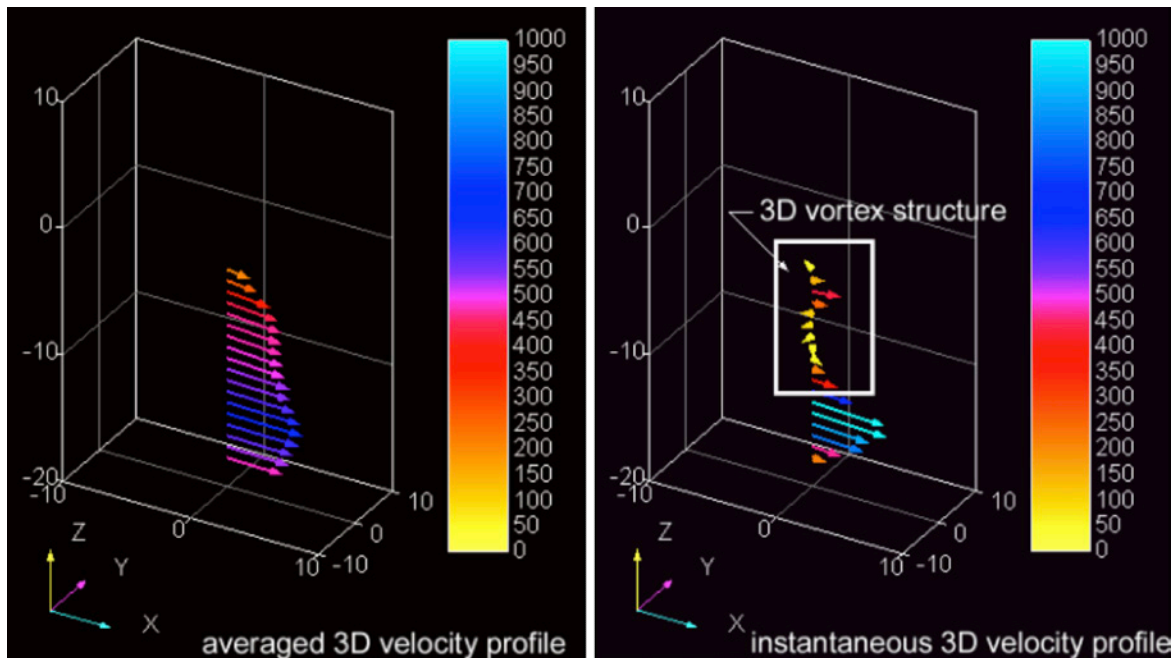


Fig.5 Averaged and instantaneous three-dimensional velocity vector profile in LBE loop measured by Vector-UVP system

applied to an actual liquid metal flow for three-dimensional velocity vector measurements. Figure 5 shows an example of the experimental result. The working fluid was LBE which was kept at 150 °C constant. The spatial-resolution was 0.88 mm, and the time-resolution was 50 msec.

The time averaged result had an orderly flow like a Poiseuille flow. However, Vector-UVP system was able to measure the instantaneous flow which had a vortex flow with three-dimensional structure caused by the velocity different. In future, this system will realize the measurement of the various liquid metal flows in an actual temperature condition by development of the high-temperature ultrasonic transducer.

### 4.3 Material Corrosion Test in LBE

The compatibility of materials with liquid LBE is one of the main technical issues in R&D of ADS. It is considered that temperature, oxygen concentration, types of steels, flow rate of LBE and temperature difference between high and low temperature part in loop tests have great influence on corrosion behavior in liquid LBE. In JAEA, two kinds of activities are under way: the static corrosion test and the loop test.

In the static corrosion equipment, specimens can be soaked in LBE of 450 °C to 600 °C with the oxygen concentration controlled. According to test results of many candidate steels for 3000 hours using the static corrosion equipment, the good corrosion resistance of steel with additional elements such as Si and Al, which are expected to form protective oxide films. In Si-containing steels and Al-containing steels, it is anticipated that these elements also affect their mechanical and irradiation properties. In contrast, coating and surface treatment are promising as the method by which only high corrosion resistance is added to steels with good mechanical and irradiation properties. According to results of the corrosion tests at 550 °C in liquid LBE, the good corrosion resistance of the Al-alloy coating layers on 316SS was shown (Fig. 6) because the Al-alloy coating prevent severe corrosion attack<sup>11)</sup>. Based of the experimental results, it is

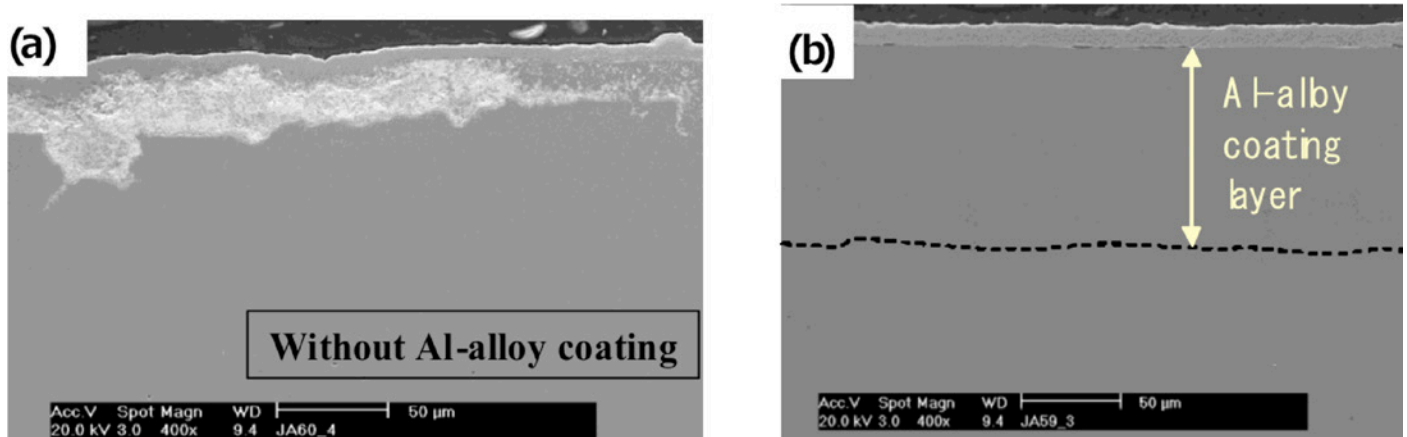


Fig. 6 SEM images of cross sections of 316SS after the corrosion test, (a) without Al-alloy coating and (b) with Al-alloy coating. The corrosion test was conducted at 550 °C for 3000h in liquid LBE

estimated that the range of the adequate Al concentration in the coating layer is from 4 to 12 wt%. The loop corrosion test aims at the acquisition of the corrosion data in the flowing LBE with temperature gradient and to test the feasibility of mechanical devices such as an electromagnetic pump and an electromagnetic flow meter. To meet these purposes, the JAEA Lead Bismuth Loop-1 (JLBL-1) was installed. The maximum flow rate is 5 liter/min. and the maximum flow speed at the test tube section is 1 m/s. Recently, corrosion test of solution annealed (SA)-JPCA and 20% cold worked (CW)-JPCA pipe specimen was conducted for 1,000 hours using JLBL-1. TIG welds were applied for joining SA-JPCA and 20%CW-JPCA, and its compatibility in flowing LBE has also been investigated. The results showed that LBE penetrated superficially into the matrix of SA-JPCA through a thin ferrite layer which was formed because of nickel and chromium dissolution. As for 20%CW-JPCA, dissolution attack occurred only partially, and localized superficial pitting corrosion was observed. It was found that the different corrosion behaviour was due to the structure transformation of the austenitic caused by the cold working.

#### 4.4 Material Irradiation Studies

The beam window of the ADS is subjected to proton/neutron irradiation. The irradiation damage of the structural material by protons and neutrons, especially for the beam window, is one of the crucial issues for the feasibility of the ADS. JAEA is participating in the irradiation program for the spallation target material using the SINQ facility at the Paul Scherrer Institute in Switzerland. Small pieces of samples irradiated by 580 MeV protons were transported to JAEA. The tensile tests and the bending fatigue tests were done at the hot cell facility. The results for the austenitic steel irradiated up to about 10 dpa (displacement per atom) at 90°C to 380°C showed the hardening and decrease in ductility of the material by the irradiation. Change of microstructures of proton/neutron-irradiated steels is investigated by means of transmission electron microscope (TEM) observation. The characteristics of the proton/neutron irradiated materials are affected by dpa by high displacement energy particles and amount of produced helium and hydrogen atoms. Recently, samples of 316SS, JPCA and F82H irradiated at higher dpa levels and higher temperatures were prepared at the SINQ facility and transported to JAEA. JAEA participated the MEGAPIE (MEGAWatt Pilot Experiment) project<sup>12)</sup> which is the world's first megawatt-class lead-bismuth target. The MEGAPIE was successfully operated and dismantled in a hot-lab in PSI. The PIE samples cutting from the MEGAPIE target material were transported to JAEA and PIE studies have been performed.

### 5. Reactor Physics of ADS dedicated for MA Transmutation

Neutronics design is important issue for R&D of ADS. In the reactor physics characteristics of ADS, large burnup reactivity swing and significant power peaking are considerable problems. The problem of the peaking factor is closely related to the burnup reactivity swing. Since the peaking factor depends on the effective multiplication factor ( $k_{\text{eff}}$ ), increase of the minimum keff value during burnup cycle, namely the minimization of the burnup reactivity swing, is important to reduce the peaking factor. Moreover, the minimizing burnup reactivity swing also means reduction of proton beam current, since the proton beam current required to keep predefined power level is directly related to keff. Therefore, calculation accuracy for keff is important in neutronics design of ADS.

#### 5.1 Present Status of Neutronics Design of ADS

To understand current accuracy of neutronics calculation for the ADS, a benchmark activity was performed in the Coordinated Research Project (CRP) on "Analytical and Experimental Benchmark Analyses of Accelerator Driven Systems" held by the International Atomic Energy Agency (IAEA). JAEA proposed the "800MW ADS" benchmark problem<sup>13)</sup> as one of problems discussed in the IAEA CRP. In this benchmark, the calculation results using the newest version of JENDL, JENDL-4.0<sup>14)</sup>, were compared with those with the previous version, JENDL-3.3. The calculation results are shown in Fig. 7. The results show that a large difference by 2 to 3 % $\Delta k$  in  $k_{\text{eff}}$  at both BOC and EOC.

To discuss the nuclear design accuracy, the uncertainty analysis using covariance data for evaluated nuclear data and sensitivity analysis is effective<sup>15)</sup>. The JENDL-4.0 contains the covariance data for all nuclear data of all actinides, which is one of the major updates from JENDL-3.3 that includes only few covariance data for MA. The results of the uncertainty analysis are summarized in Table 1. In this table, the  $k_{\text{eff}}$  and the coolant void reactivity are shown with their uncertainties deduced from each library. The coolant void reactivity is defined as a reactivity insertion when all of the coolant in the active core vanishes. In the analysis with JENDL-3.3, the provisional covariance data, which are rough data

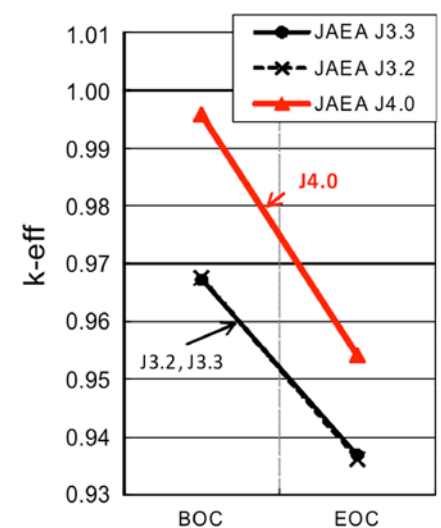


Fig. 7 Comparison of calculation results for  $k_{\text{eff}}$  with different version of JENDL libraries (BOC=beginning of cycle, EOC=end of cycle)

preliminary supplied by the experts, were used. As shown in Table 1, the uncertainties estimated by the two libraries, 1.1% and 1.3%, are equivalent. However, the estimated uncertainties by the covariance data are much smaller than the dispersion of  $k_{eff}$  between the results with different libraries. This tendency is extreme in the results for the coolant void reactivity. This discrepancy of the uncertainty means that the difference in the cross section evaluated by the individual evaluator is larger than the covariance data. The comparison of covariance data and difference of cross section among the libraries is necessary in the future work.

	JENDL-4.0	JENDL-3.3
Criticality ( $k_{eff}$ )	$0.999 \pm 1.1\%$	$0.971 \pm 1.3\%$
Coolant void reactivity [pcm]	$5330 \pm 8.1\%$	$3880 \pm 6.8\%$

Table 1 Calculation results of criticality and coolant void reactivity with uncertainties

## 5.2 Preliminary Safety Analysis of ADS

For the basic study of safety performance for ADS<sup>15)</sup>, investigations for abnormal events and safety analysis were performed from a view point of the possibility of Core Disruptive Accident (CDA). The investigation for abnormal events was carried out by Level 1 PSA (Probabilistic Safety Assessment). The safety analysis was performed by the transient analysis code SIMMER-III<sup>16)</sup>.

Level 1 PSA was used to quantify a frequency of an abnormal event. The frequency was analyzed by the initiating event and the mitigation function. The initiating events and the frequencies for the selected events were referred from the study for the fast reactor<sup>17)</sup>. As the inherent events for the ADS, "Beam over power" and "Beam window breakage" were assumed. The frequencies of these two events were assumed 0.1 [/reactor-year] for which relatively high frequencies were assumed. The mitigation functions also present the unreliability, which means a probability to fail its function. Based on these initiating events and the mitigation functions, the frequencies of the abnormal events were estimated. The results were sorted into "design basis accident (DBA)" and "beyond design basis accident (BDBA)". DBA is the accident to evaluate the design or to determine the design condition. BDBA is the accident exceeded DBA. A criteria of  $1 \times 10^{-6}$  [/reactor-year] was employed to determine DBA or BDBA. As the result of Level1 PSA, only two cases became DBA. The first one was Unprotected Transient Over Power (UTOP) caused by the beam window breakage and the failure of the scram signal. The second one was Protected Loss of Heat Sink (PLOHS) caused by the loss of external power supply and the failure of the emergency power supply. The discussion for BDBA from the viewpoint of CDA was also performed and BOP (Beam over power) and ULOF (Unprotected Loss of Flow) were supposed to have a possibility to induce CDA. Though the frequencies of these two accidents were exceedingly smaller than DBA, detailed calculations for these were also carried out to confirm a possibility of CDA. The SIMMER-III code is an advanced safety analysis code, which has been developed to investigate postulated core disruptive accidents in fast reactors. The SIMMER-III code is a two-dimensional three-velocity field, multi-phase, multi-component, Eulerian fluid dynamics codes coupled with a structure model and a space-, time- and energy-dependent neutron kinetics model. For BOP, a transient with doubled intensity of the external neutron source was analyzed. For ULOF, a transient with the external neutron source without a pump driving force was performed. The coast down of the pump was assumed from 0sec to 15sec. In the calculation result of BOP, the maximum temperature of the fuel was about 2500°C and that of the fuel clad was about 900°C by the doubled intensity of the external neutron source. From these results, it was found that there was little possibility to occur a pin failure with the doubled intensity of the external neutron source since the melting points of the nitride fuel and the fuel pin (SS316) are 2780°C and 1400°C, respectively. However, it was considered that there was the possibility of the creep rupture of the cladding tube. In the calculation result of ULOF, the power was increased by about 2% at 15sec and slightly decreased. Figure 8 shows the fuel clad temperature changes. The maximum

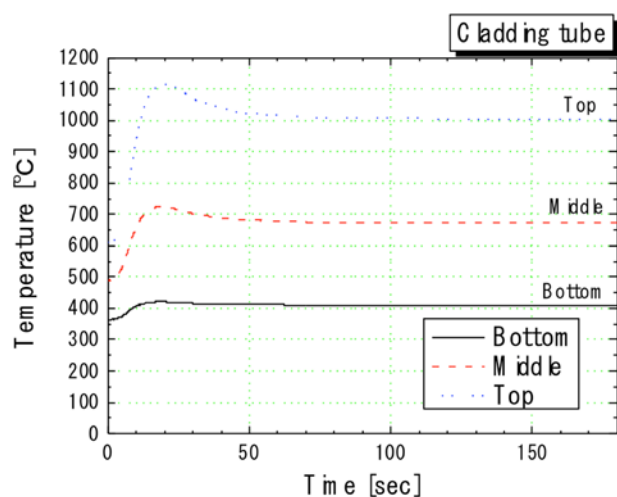


Fig. 8 Temperature change of the fuel clad during ULOF

temperature of the fuel reached about 1800°C and that of the fuel clad reached 1100°C. These analysis results indicated that there was very little possibility of CDA in ULOF since both the fuel and the fuel clad temperatures were lower than their melting points. On the other hand, the possibility of the creep rupture of the cladding tube was also considered. These safety analysis results indicated that there was very little possibility of CDA in the ADS. On the other hand, it was supposed that there was the possibility of the creep rupture of the fuel clad tube in both BOP and ULOF. However, it is concluded that the ADS had very little possibility of CDA or the re-criticality accident.

## 6. Outline of Transmutation Experimental Facility

JAEA is conducting a multi-purpose high-intensity proton accelerator program called J-PARC (Japan Proton Accelerator Research Complex) collaborating with High Energy Accelerator Research Organization (KEK). To study the basic characteristics of the ADS and to demonstrate its feasibility from viewpoints of the reactor physics and the spallation target engineering, JAEA plans to build the Transmutation Experimental Facility (TEF) in the Tokai site under a framework of the J-PARC Project as shown in Fig.9. TEF consists of two buildings: the Transmutation Physics Experimental Facility (TEF-P) and the ADS Target Test Facility (TEF-T). TEF-P is a zero-power critical facility where a low power proton beam is available to research the reactor physics and the controllability of the ADS. TEF-T is a material irradiation facility which can accept a maximum 400MeV-250kW proton beam into the spallation target of LBE. Using these two facilities, basic physical properties of subcritical system and engineering tests of spallation target will be studied.

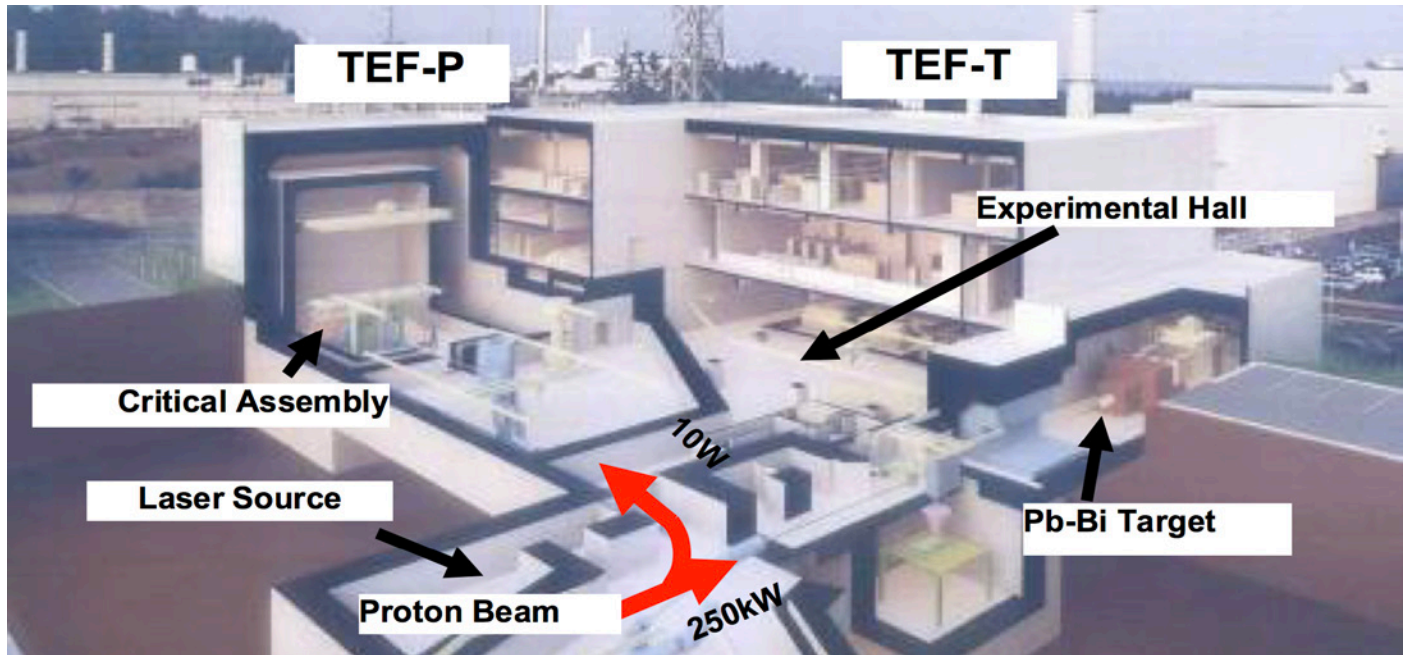


Fig.9. Transmutation Experimental Facility

### 6.1. Transmutation Physics Experimental Facility (TEF-P)

Several kinds of experiments to investigate the neutronic performance of the ADS have been performed using existing facility worldwide. In Japan, subcritical experiments were carried out at the Fast Critical Assembly (FCA) by using a  $^{252}\text{Cf}$  and DT neutron source. Moreover, many experimental studies have been performed to the neutronics of the spallation neutron source with various target material such as lead, tungsten, mercury and uranium. These experiments for spallation target are not directly related to the ADS, but they are also useful to validate the neutronic characteristics of ADS. There has been, however, no experiment aiming at the research and the demonstration of the fast subcritical system combined with a spallation source. Therefore, taking above mentioned situation into consideration, TEF-P is designed to cover the fields of R&D for:

- 1) reactor physics aspects of the subcritical core driven by a spallation source,
- 2) demonstration of the controllability of the subcritical core including a power control by the proton beam power adjustment, and
- 3) investigation of the transmutation performance of the subcritical core using certain amount of MA and LLFP.

For above mentioned purposes, the high thermal power is not necessary; a power level of critical experiments such as 100 W is optimal from viewpoints of accessibility to the core. Although the necessity of thermal feedback effect of the core might be insisted, such experiments can be performed by using an electrical heater which simulates the reactor power without real fission energy nor accompanying fission products. The maximum thermal power is temporarily decided as 500 W. The most serious problem to build a new nuclear facility is how to prepare the fuel, since tons of low-enriched uranium or plutonium are necessary to simulate the ADS (e.g.  $k_{\text{eff}} = 0.95$ ) in the fast neutron system. We expect to use the plate-type fuel of the FCA in JAEA/Tokai, or preferably to merge FCA into TEF-P. Various simulation materials required to simulate fast reactor and ADS such as lead and sodium for coolant, tungsten for solid target, ZrH for moderator, B<sub>4</sub>C for absorber, and AlN for nitride fuel will be prepared. TEF-P is therefore designed with referring to FCA; the horizontal table-split type critical assembly with a rectangular lattice matrix. Figure 10 shows a conceptual view of the assembly. Proton beam was introduced horizontally from the center of the fixed half assembly.

As for the neutronics in the subcritical system, power distribution,  $k_{\text{eff}}$ , effective neutron source strength, and neutron spectrum are measured by changing parametrically the subcriticality and the spallation source position. The material of

the target will also be altered with Pb, LBE, W, and so on. The reactivity worth is also measured for the case of the coolant void and the intrusion of the coolant into the beam duct. It is desirable to make the core critical in order to ensure the quality of experimental data of the subcriticality and the reactivity worth. As for the demonstration of the hybrid system, feedback control of the reactor power is examined by adjusting the beam intensity. Operating procedures at the beam trip and the re-start are also examined. As for the transmutation characteristics of MA and LLFP, fission chambers and activation foils are used to measure the transmutation rates. Several kinds of MA and LLFP samples

are also prepared to measure their reactivity worth, which is important for the integral validation of cross section data. Ultimate target of the facility is to install a partial mock-up region of MA nitride fuel with air cooling to measure the physics parameters of the transmutation system. The central rectangular region (28cm x 28cm) will be replaced with a hexagonal subassembly.

The distinguished points of TEF-P in comparison with existing experimental facilities can be summarized as follows: (1) both the high energy proton beam and the nuclear fuel are available, (2) the maximum neutron source intensity of about  $10^{12}$  n/s is strong enough to perform precise measurements even in the deep subcritical state, and, is low enough to easily access to the assembly after the irradiation, (3) wide range of pulse width (1ns - 0.5ms) can be available by the laser charge exchange technique and, (4) MA and LLFP can be used as a shape of foil, sample and fuel by installing an appropriate shielding and a remote handling devise.

## 6.2 ADS Target Test Facility (TEF-T)

To solve technical difficulties for liquid LBE application, construction of TEF-T is planned to complete the datasets which required for LBE target/cooled ADS design. The experiments to obtain the material irradiation data for beam window are the most important mission of TEF-T.

TEF-T mainly consists of a LBE spallation target, a secondary cooling circuit, and an hot cells to handle the spent spallation target vessel and irradiation test pieces. LBE is filled into a sealed double annular cylindrical tube made by type 316 stainless steel or 9Cr steel. An effective size of the target unit is about 15cm diameter and 3 to 4 meter long as shown in Fig.11. The target head is designed to be changed according to the objective of the experiments. One of the target head is designed to irradiate several kinds of samples in the flowing LBE environment.

A primary LBE loop is designed to allow LBE flow up to 2 meter per second of velocity and 500°C of the maximum temperature of the LBE. LBE is circulated by electro-magnetic pump (EM pump) that is independent from the target tube. When the trouble is occurred around the EM pump, target unit can be replaced by withdrawing the electro-magnetic flow meter and EM pump.

Design study of the target head to realize TEF-T target system is performed. To set up the parameters, future ADS concepts are taken into account. In the reference case of the target which is supposed to be used for various material irradiation, 20 mA/cm<sup>2</sup> of proton beam current density was assumed that equals to the maximum beam current density of JAEA proposed 800MWth ADS. Through the analyses of neutronics, thermal-hydraulics, and structural strength, target can be applicable with reference operation condition with maximum coolant temperature up to 450°C.

However, by introducing 400MeV-250kW proton beam, with 20 μA/cm<sup>2</sup> of beam current density, about 7 to 8 DPA/year of irradiation can be obtained in the irradiation sample which is set in flowing LBE environment. Because

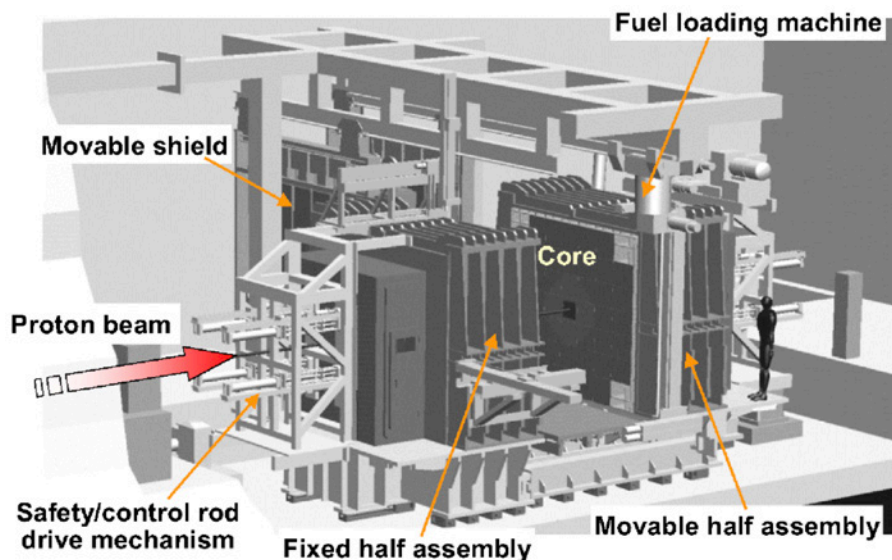


Fig.10 Conceptual view of TEF-P

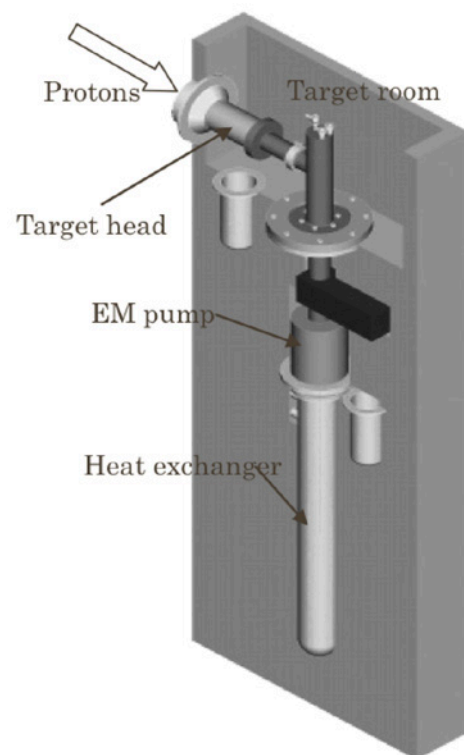


Fig.11. Sealed annular type spallation target

this value is about 20% of DPA considered in the beam window of JAEA-ADS, studies for focusing the injected proton beam up to 40  $\mu\text{A}/\text{cm}^2$ , and reduction of beam window temperature by changing LBE flow is underway.

## 7. Conclusion

JAEA has been promoting various R&D activities on ADS. The preliminary system design of the superconducting part of the SC-LINAC was performed. Based on the preliminary design, the frequency of unexpected beam trip was estimated by referencing the performance of existing accelerators to discuss the feasibility of the SC-LINAC for ADS. In the design of ADS, the critical issues are in the engineering feasibility of the beam window for the high power spallation target in terms of thermal-hydraulic and structural design. The engineering feasibilities of the beam window was evaluated. While LBE is regarded as the prime candidate for the spallation target and the core coolant of the ADS, the technology to use LBE in the nuclear system is not well-established. Some small test loops using LBE were built in JAEA to investigate the corrosion of structural material and the thermal-hydraulics characteristics. In the neutronics design of ADS, present status of nuclear data was evaluated with the uncertainty analysis using covariance data for the evaluated nuclear data. The effect on uncertainty reduction of TEF-P, which is a critical facility capable to contain kg-order MA planned in J-PARC, was assessed. Preliminary safety analyses were also carried out for typical initiators.

## References

1. Atomic Energy Commission of Japan, "Concerning the Report Entitled –Current Status and a Way Forward to Promote the Research and Development of Partitioning and Transmutation Technologies–," April 28, 2009, <http://www.aec.go.jp/jicst/NC/senmon/bunri/kettei-090428e.pdf>.
2. K. Tsujimoto, H. Oigawa, K. Kikuchi, Y. Kurata, M. Mizumoto, T. Sasa, S. Saito, K. Nishihara, M. Umeno, and H. Takei, "Feasibility of Lead-Bismuth-Cooled Accelerator-Driven System for Minor-Actinide Transmutation," *Nucl. Tech.*, 161, 315-328 (2008).
3. H. Takei, K. Nishihara, K. Tsujimoto, and H. Oigawa, "Estimation of Acceptable Beam Trip Frequencies of Accelerators for ADS and Comparison with Performances of Existing Accelerators," *Proc. of Technology and Components of Accelerator-driven system*, Karlsruhe, Germany, 15-17 March 2010 (2010).
4. H. Takei, K. Nishihara, K. Tsujimoto, and H. Oigawa, "Estimation of Acceptable Beam-trip Frequencies of Accelerators for Accelerator-Driven System and Comparison with Existing Performance Data," *J. Nucl. Tech.*(to be published).
5. LANSCE, Los Alamos Neutron Science Center, (online) available from <http://lansce.lanl.gov/> (accessed 2008-10-27).
6. M. Eriksson, "Reliability Assessment of the LANSCE Accelerator System," M.Sc. thesis at the Royal Institute of Technology, Stockholm, Sweden (1998).
7. Abe, I., et al., "The KEKB injector linac," *Nucl. Instrum. Methods Phys. Res.*, A499, 167 (2003).
8. T. Sugawara, K. Nishihara, H. Obayashi, Y. Kurata, and H. Oigawa, "Conceptual Design Study of Beam Window for Accelerator-Driven System," *J. Nucl. Sci. Technol.*, 47(10), 953-962 (2010).
9. ASME, "2004 ASME Boiler & Pressure Vessel Code Section III", (2004).
10. H.Obayashi, Y.Tasaka, S.Kon, Y.Takeda, "Velocity vector profile measurement using multiple ultrasonic transducers", *Flow Meas. & Inst. Volume 19, Issues 3-4, June-August 2008*, 189-195, (2008).
11. Y. Kurata, H. Yokota, and T. Suzuki, "Development of Aluminum Alloy Coating for Advanced Nuclear Systems using Lead Alloys," *Proc. of ASME Small Modular Symposium (SMR 2011)*, Washington DC, USA, 28-30 September 2011 (2011).
12. Ch. Latge, F. Groeschel, P. Agostini, M. Dierckx, C. Fazio, A. Guertin, Y. Kurata, G. Laffont, T. Song, K. Thomsen, W. Wagner, K. Woloshun, "MEGAPIE SPALLATION TARGET : Irradiation of the first prototypical spallation target for future ADS," *Proc. of GLOBAL2007*, Boise, Idaho, September 9-13, 2007 (2007).
13. K. Nishihara, T. Sugawara, H. Iwamoto, F. A. Velarde, and A. Rineiski, "Investigation of Nuclear Data Accuracy for the Accelerator-Driven System with Minor Actinide Fuel," *Proc. of 11th OECD/NEA information exchange meeting*, San Francisco, USA, 1-4 November 2010 (2011).
14. K. Shibata, O. Iwamoto, T. Nakagawa, N. Iwamoto, A. Ichihara, S. Kunieda, S. Chiba, K. Furutaka, N. Otuka, T. Ohsawa, T. Murata, H. Matsunobu, A. Zukeran, S. Kamada, and J. Katakura, "JENDL-4.0: A New Library for Nuclear Science and Engineering," *J. Nucl. Sci. Technol.* 48(1), 1-30 (2011).
15. T.Sugawara, K.Nishihara, K.Tsujimoto, Y. Kurata, and H. Oigawet, "Investigation of Safety for Accelerator Driven System," *Proc. of Technology and Components of Accelerator-driven system*, Karlsruhe, Germany, 15-17 March 2010 (2010).
16. Y. Tobita, Sa. Kondo, H. Yamano, K. Morita, W. Maschek, P. Coste, T. Cadiou, "The Development of SIMMER-III, An Advanced Computer Program for LMFR Safety Analysis, and Its Application to Sodium Experiments", *Nuclear Technol.*, 153, 245-255 (2006).
17. K. Hioki, K. Kurisaka, T. Mihara, "Level 1 PSA on Large Fast Breeder Reactor", PNC TN9410 93-134, (1993) [In Japanese].

# 17 - The SFLM Concept for Fusion Driven Energy Production by Incineration of Spent Nuclear Fuel

O. Ågren<sup>1,\*</sup>, V.E. Moiseenko<sup>2</sup>, K. Noack<sup>1</sup>, S. V. Chernitskiy<sup>2</sup>

<sup>1</sup> Uppsala University, Ångström Laboratory, Box 534, SE-751 21 Uppsala, Sweden

<sup>2</sup> Institute of Plasma Physics, National Science Center "Kharkiv Institute of Physics and Technology", 61108 Kharkiv, Ukraine

\*email: Olov.Agren@angstrom.uu.se

## Abstract

Major results from the studies on the SFLM (Straight Field Line Mirror) concept are presented. Motivations for the SFLM research are to identify a steady state device design where obstacles for a future commercial use would not be ruled out by insufficient plasma confinement, material problems, accessibility for diagnostics, tritium consumption and breeding, as well as reactor safety issues. Some of the important results are on the existence of a radial constant of motion (necessary for confinement) which could be controlled by biased potential plates, on the plasma heating (ICRH can be applied in steady state), on material loads (from neutrons and plasma bombardment), on a high power amplification by fission (preferably as high as possible within safety constraints) and on reactor safety. Geometries are carefully selected to identify a design with a potential for commercial use. Critical problems are avoided by the choices for the compact superconducting coil design, the flux tube expander, the openings for accessibility, the method for plasma heating and the reactor blanket arrangements. The geometrical arrangements for the SFLM may offer possibilities to obtain solutions to these challenges.

Keywords: Hybrid reactor, fusion neutron source, magnetic mirror, SFLM

PACS: 52.55

## Introduction

Hybrid reactors [1] offer a possibility for application of fusion in a not too distant future. A main reason is that the plasma confinement requirements are relaxed compared to a stand-alone fusion reactor if there is a high power amplification by fission. Steady-state operation on a time scale of a year without interruption is essential for such applications, but pulsed operation enforced by a need to induce a plasma current could prevent a commercial application of tokamak and main stream toroidal fusion devices. In response to this, we analyze a mirror machine concept [2-15], where a key advantage is the potential for steady state operation. In several aspects, predictions for the SFLM (Straight Field Line Mirror) concept are encouraging. Our studies address several critical issues on particle confinement, plasma heating, plasma stability and magnetic coil design. Reactor safety and engineering requirements of the design are also addressed in Monte Carlo computations for the neutrons.

The overall design [8,9] is reasonably compact (a 25 m long device with an outer coil radius of 3 m and a mid plane plasma radius of 0.4 m), see Figures 1 and 2. This design is considered for a 1.5 GWth reactor. Damage of equipment is reduced by avoiding ports for diagnostics and plasma heating [5-7] in sensitive areas. The top and bottom of the device is intended for access, with feeding of plasma heating and diagnostics. On opposite sides of the plasma confinement region, the magnetic flux tube expands and directs plasma to large receiving plates with a radius of 4 m, which replace the "divertor plates" in a toroidal device. The large area of the end plates enables a tolerable (about 0.6 MW/m<sup>2</sup>) heat deposition. Electric potential control can be installed at sectioned endplates, and a small radial electric field, which is needed for improvement of confinement, can in this way be enforced on the plasma [15]. This results in a weak plasma rotation, which is expected to eliminate collision-less radial drifts. Each particle then moves closely to a single magnetic surface, and from this we have identified a *radial constant of motion* for magnetic mirror systems, even for mirror fields with a strong stabilizing quadrupolar field component [15]. In the collision-free approximation, all particles are predicted to be confined radially for an infinite time. This attractive feature results from the weak plasma rotation which is controlled by the biased electric potentials. An additional useful property is that the confinement sensitivity to field errors, which can cause particles to radially drift out from the confining magnetic flux tube, is strongly suppressed by the weak plasma rotation. Elimination of such loss is crucial for any magnetic confinement concept.

The compact 3D superconducting coils [10, 12] have 2 m inner radii (which provide sufficient space for the fusion device and the fission reactor core) and only 3 m coil outer radii. The curved 3D coils have been inspired by the coil design of a helias stellarator, i.e. Wendelstein 7X, but the strong gradients of a mirror field (with a mirror ratio of 4 or more) have imposed a particular challenge for the coil design of a mirror machine with strong asymmetries from the stabilizing quadrupolar magnetic field, see Figures 2 and 3. Antennas for ICRH (ion cyclotron resonance heating) are located on both sides of the mirror ends of the device [5, 6, 7]. These regions can be protected from neutron bombardment.

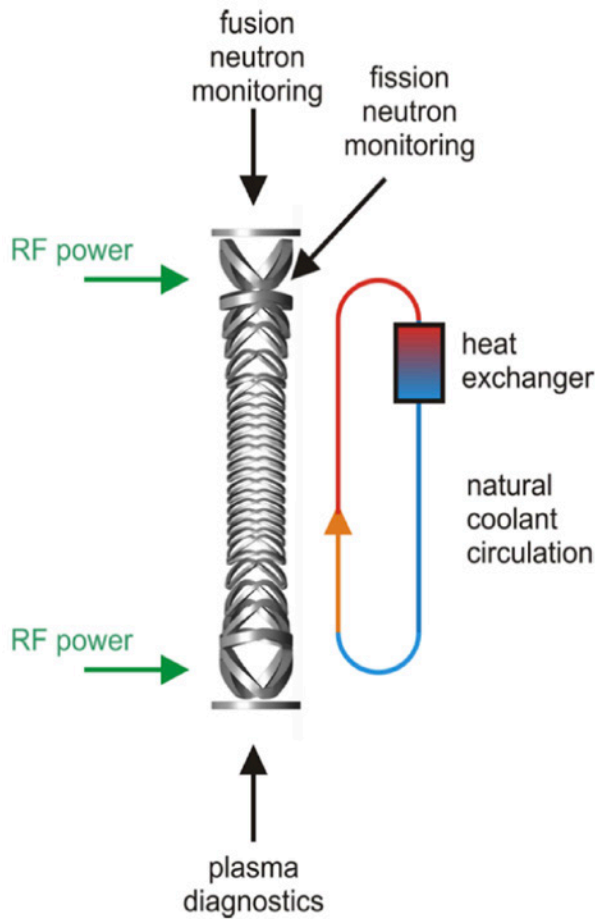


Figure 1. Outline of arrangements for an SFLM reactor, with the 3D coils shown. Diagnostics and monitoring equipment are located on the top and bottom of the device to protect sensitive equipment from neutron and particle bombardment. RF heating is fed through openings near the magnetic mirror ends. An annular (or tubular) fission reactor core is located in between the plasma confinement region and the coils, where the arrangement with minimized holes for diagnostics is beneficial for neutron economy. A vertical orientation enables passive coolant circulation.

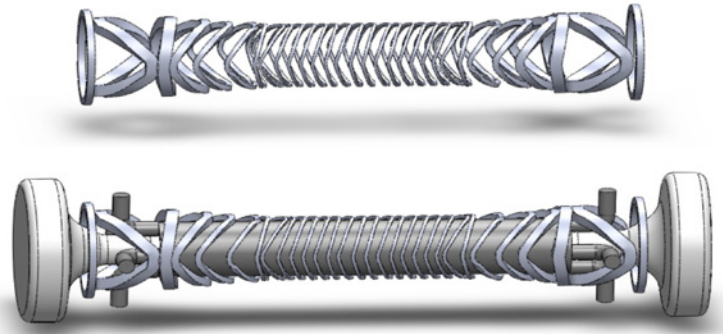


Figure 2. Superconducting coils for the SFLM. The upper figure shows the superconducting coils. The lower figure indicates location of fission reactor part between the coils and the vacuum chamber for the plasma and the expander plates which are intended as plasma receiving "divertor plates".

ICRH heating has the advantage that it can be applied over long times, which is necessary when the ambition is steady state operation for a time scale of a year.

Neutrons produced from fusion reactions can be further utilized for fission (and incineration) in a reactor surrounding the fusion part of the device [8, 9, 13]. The avoidance of holes in this region is one reason why a high power amplification by fission (up to a value as high as 150) may be achievable with the SFLM-geometry. This enables a very small fusion  $Q$  factor for a mirror based hybrid reactor. Even a fusion  $Q$  factor as low as  $Q=0.15$  may be sufficient for efficient power production. This is about ten times lower than predicted for axisymmetric toroidal devices.

### Radial constant of motion

The identification of motional invariants is crucial to obtain an overall understanding of particle motion and to control confinement in magnetic fields [15]. Magnetic confinement is necessary both along the longitudinal and along the radial direction of a magnetic flux tube. We need to identify constants of motion which assure confinement in both directions [15]. The longitudinal confinement in a mirror machine is governed by two constants of motion, i.e. the energy of the particle and its magnetic moment. The aim is to identify conditions for the existence of a radial invariant  $I_r$  which makes the radial motion across a magnetic flux tube bounded [15]. Such a constant of motion would correspond to perfect confinement in the collision free approximation. However, predictions on radial confinement are subtle to carry out, and depend sensitively on the confining fields. Even small field errors (for instance deviations from axisymmetry) worsen radial confinement in tokamaks and axisymmetric mirrors. Even more obvious concerns can be made on quadrupolar mirrors, since there is no global symmetry in such fields, although there exist certain fields where each guiding center motion is restricted to move on a single magnetic surface in the long-thin limit, compare [11]. For representative parameters of a fusion reactor, confinement for about 10 000 longitudinal bounces are required for power production

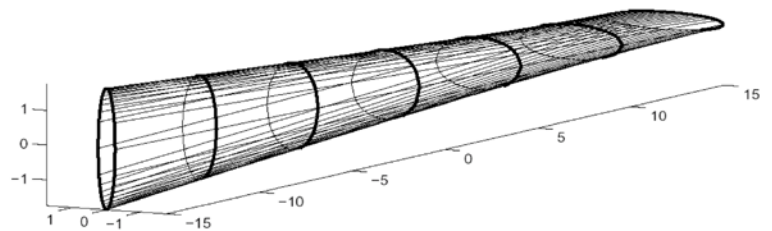


Figure 3. The magnetic field lines of the SFLM are straight and non-parallel. With straight field lines, there is no guiding center drift, and each guiding centers move on a single magnetic field line. The stronger magnetic field modulus at the opposite ends provide longitudinal confinement by the mirror effect.

in a stand-alone fusion reactor. This restricts the tolerable radial net drift in each longitudinal bounce to less than 0.1 mm in a 100 m long device with 1 m plasma radius. This is indeed a challenging demand, which is hard to meet in any confining scheme! The idealized SFLM field has straight nonparallel magnetic field lines [2], where each gyro center is restricted to move on a single magnetic field line [4], see Figure 3. The concern for radial confinement is deviation by field errors from this ideal field. That causes radial excursions from the initial magnetic surface, which in many cases corresponds to oscillatory radial drifts for the imperfect SFLM field, see Figure 4, and then poses no major threat on confinement [11]. However, certain field errors cause net radial magnetic drifts which would quickly ruin confinement [14].

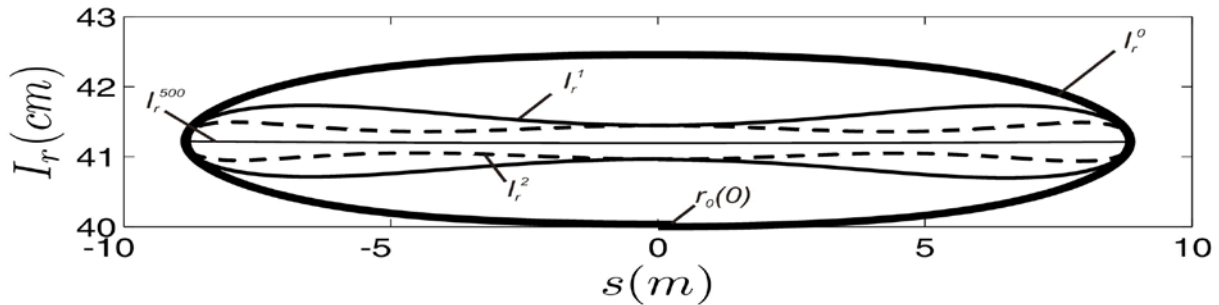


Figure 4. Variations of the lowest order radial invariant describe “banana” excursions from a magnetic flux surface during a longitudinal bounce. In the radial invariant, banana widths are accounted for by bounce harmonic terms. Notice that the longitudinal scale is much larger than the radial scale, which demonstrates small radial excursions of the particle. The “banana” widths can be reduced further by applying a radial electric field.

Several experiments in various devices have demonstrated that a radial electric field can improve confinement, and this is applied in toroidal devices, at the GDT (Gas Dynamic Trap) axisymmetric mirror [16] as well as in the anchor cells of the Gamma10 tandem mirror. A very high ellipticity (around 50) is required in the Gamma 10 anchor cells to provide gross plasma stability by the quadrupolar field, which has a drawback of introducing large radial magnetic drifts. For this reason, it has been necessary to introduce biased electric potential plates to reduce the radial drift loss in Gamma10. One suggested interpretation [16] for the biased electric potential experimental results in GDT is that a shear rotational plasma rotation “chops” large plasma structures originating from flute instabilities into smaller structures near the region of opposite plasma rotation, which may produce improved overall confinement in a similar manner as an ITB (internal transport barrier). A complete stabilization of the large scale flute mode is however preferable, and this is a motivation to consider an average minimum B field such as the SFLM field with its quadrupolar magnetic field component. The ambition for the SFLM is quiescent elimination of non-oscillatory radial drifts.

Mirror machines offer the flexibility to control the radial electric field by potential plates outside the confinement region. Our derivations predict that a radial constant of motion could be arranged by applying a controlled radial electric field, which enforces a slow plasma rotation which easily can overcome the radial magnetic drifts in an imperfect SFLM field. The radial invariant

$$I_r(\mathbf{x}, \mathbf{v}) = \langle r_0 \rangle$$

corresponds to an average radial motion on a mean magnetic surface [15]. Here,  $r_0$  is the radial Clebsch coordinate for the magnetic field, and a magnetic surface is determined by  $r_0 = \text{const}$ . If the oscillatory radial drifts are small, which can be arranged by slightly increasing the strength of the radial electric field, each guiding center moves close to a single magnetic surface. In this case, the radial invariant approaches the guiding center value of the radial Clebsch coordinate, and in

$$I_r(\mathbf{x}, \mathbf{v}) \approx \bar{r}_0 = r_0 - r_{0, \text{gyro}}(\mathbf{x}, \mathbf{v})$$

such a case [15]

where  $r_0$  is the radial coordinate of the particle (not the guiding center) and  $r_{0, \text{gyro}}$  is the gyro oscillation (or “gyro ripple”) of the particle. The dependence on this gyro oscillation in a distribution function corresponds to the self-consistent diamagnetic current in equilibria with pressure gradients [11].

## Plasma heating

For a deuterium-tritium plasma with about 40 % deuterium and 60 % tritium, the minority deuterium ions can be heated by an antenna at one mirror end with the antenna frequency matched to the fundamental deuterium cyclotron frequency at the resonance region [5]. Tritium is heated by second harmonic heating by an antenna at the opposite end [7]. To sustain a sloshing ion distribution, the resonance regions are chosen to be at about half the maximum magnetic field strength, corresponding to locations of sloshing ion peaks. Computations have predicted good coupling between the antennas and the plasma, and efficient heating can occur.

The antenna locations near the mirror ends is favorable for protection from particle bombardment. The waves propagate towards lower magnetic field with conversion between fast and slow waves, with absorption near cyclotron resonances. Heating efficiencies around 70 % is typically obtained in the computations [5, 6, 7].

### Neutron computations, power amplification and reactor safety

Monte Carlo simulations for the neutrons have been carried out based on a model with the cross section divided into annular sections [9,13], see Figure 5. The innermost region ( $r < 0.95$  m) is the vacuum chamber where the fusion neutron production occurs, covered by a first wall with 3 cm thickness. A buffer region, about 15 cm wide, outside of this is introduced to obtain a 30 % increase of incident neutron flux, a decrease of fission neutron leakage and a softening of the energy spectrum of the neutrons. That arrangement is essential to protect the first wall by reducing the dpa (displacement per atom) rate, where it is necessary to account both for the neutrons originating from fission as well as fusion. The core (about 22 cm thick) contains the fuel and eutectic lead-bismuth coolant. The fuel considered in the computations is based on the average content of spent fuel from fission reactors, with fission products and U238 removed to minimize production of minor actinides. External to these regions are a core expansion zone, a radial reflector and a lithium coolant (not shown in the Figure 5) to breed tritium. Detailed material choices and geometrical arrangements are given in [9].

The computations are based on an arrangement where the neutron multiplicity  $k_{eff}$  is subcritical (i.e. below unity). This implies that fission power generation can be stopped by turning off the fusion neutron source, which is a safety arrangement for subcritical fast reactors. As high a value of  $k_{eff}$  as possible is desirable for power production, but safety requirements impose an upper bound on  $k_{eff}$ . We have in the computations focused on the value  $k_{eff} = 0.97$ , which has a 3 % margin to a critical state, and made a number of studies to investigate if this value is within safety requirements [9].

A first result is that with this value, the power amplification by fission, i.e. ratio  $Q_{PAF} = P_{fis} / P_{fus}$  of power generated

$$Q_{PAF} \equiv \frac{P_{fis}}{P_{fus}} \approx 150$$

by fission and fusion, can be surprisingly high for the SFLM arrangements [9, 13]:

This implies that a fusion power of only [8]

$$P_{fus} = 10\text{MW}$$

would then correspond to 1.5  $\text{GW}_{th}$  total power production, which can be estimated to 0.5  $\text{GW}_{el}$  electric power generation. Even a fusion  $Q$  factor as low as [8]

$$Q=0.15$$

may be sufficient for efficient power production. With that value for the  $Q$  factor, the "divertor plates" should be capable of receiving 60 MW power from plasma leaking to the end walls. In this low field region, the gyro radii of the ions reaching the walls are large (exceeding 50 cm) and the heat deposition would then be evenly distributed over the receiving end plates. With a wall radius of 4 m of both end tank walls, which adds up to 100  $\text{m}^2$  area at the end plates, the power deposition is about 0.6  $\text{MW}/\text{m}^2$ , which is within a tolerable range for the heat load.

The arrangement with a buffer has resulted in more than a 30 years computed limit for the 200 dpa rate for the first wall. Neutrons originating from the reactor as well as from the fusion neutron source have to be included in that computation [9].

Reactor safety studies have investigated scenarios with loss of coolants (LOCA), void of coolant and other events. The most severe case found corresponds to loss of coolant in the core region (where the fuel is located) combined with replacement by water (which moderates the neutrons and increase the fission with Pu239), which can result in an increase in  $k_{eff}$  by 8 %, which is outside the safety margin. However, such events could be avoided by joining the coolant loops in the core and buffer regions, and a LOCA combined with water replacement is with such an arrangement not predicted to lead to  $k_{eff} > 1$ . Although no supercritical scenario has been identified in our model [8, 9], it should be emphasized that here is still need to deepen the reactor safety studies!

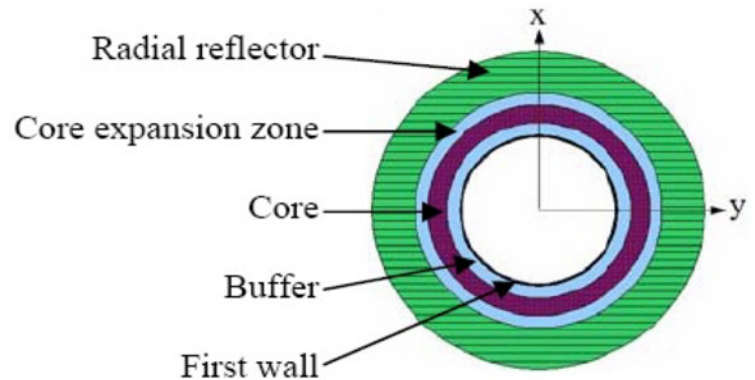


FIGURE 5. Outline of annular arrangements for the neutron computations

The possibility to quickly turn off the fusion neutron source is a safety arrangement. There is still a need to remove decay heat, which can be of the order of 10 % of the full power on a short time scale after the reactor is switched off. With a vertical orientation of the reactor, passive coolant circulation is predicted to be capable of removing a decay heat of 150 MW [18], which increases safety. External pumps would however be required to remove heat when the reactor is switched on. The blocking of the fuel rods on the coolant flow is an important factor for the required pumping power. The calculated pumping power to remove a heat of 1.5 GW<sub>th</sub> is well below 50 MW [18].

Tritium consumption is reduced to about 1 % of the consumption in a stand-alone fusion reactor, but it is still essential to avoid the cost of the tritium fuel. A lithium coolant loop has been introduced outside the radial reflector region to predict the tritium breeding ratio. A tritium breeding ratio exceeding unity is easily obtained for the SFLM hybrid reactor studies, where a value around 1.5 is a representative number for the computations.

## Discussions and conclusions

Mirror machines have several attractive features, among them a high  $\beta$  (ratio of plasma pressure to magnetic field pressure) and flexible geometrical arrangements. The major obstacle for mirror machines has been the tendency to be limited by a too low electron temperature, compare [3], which by electron drag leads to a too rapid cooling of the fuel ion temperatures. This has by many fusion researchers been considered as a show-stopper for mirror machines. However, increased electron temperatures have been reported in recent years in several mirror machines, i.e. the multimirror GOL 3 and GDT experiments at the Budker Institute in Russia and at the Gamma10 experiment in Japan. The results in GDT has a particular relevance for our studies [16]. A doubling of the electron temperature (to 230 eV) was first achieved by using biased control plates to feed a shear plasma rotation which resulted in enhanced confinement, and the electron temperature was increased further to about 430 eV by increasing the power of NBI (neutral beam injection). Thompson scattering has been used to measure the electron temperature. More recent reports for GDT [16] claim an electron temperature around 650 eV when electron cyclotron heating (ECR) is applied, where even the electron temperature reaches 900 eV in a few shots. This is approaching a range where the electron temperature would be sufficient for power production in a hybrid reactor.

Geometrical arrangements to avoid critical problems have been a guide for the SFLM-studies, and several of the results can also be transferred to the steady-state stellarator-mirror concept studied by researchers at KHIPT at Kharkiv in Ukraine [17]. In the experiments in the stellarator Uragan 2M, a local mirror region is established by switching off a toroidal field coil, whereby a stellarator-mirror configuration is obtained. A radial electric field, which may be spontaneously generated by a small initial escape of particles, is predicted to have a favorable influence on radial confinement also for that toroidal system, although the option to use electrical biased end plates is not an available option for a toroidal stellarator-mirror system.

Results from the SFLM are summarized in this paper. Major predictions from the studies are:

1. Gross plasma stability at high  $\beta$  is predicted from the minimum  $\beta$  property of the SFLM magnetic field.
2. Collision free radial drift loss is predicted to be eliminated by applying a radial electric field which can be controlled by biased plates outside the confinement region. Each guiding center motion then approaches a motion on a single magnetic surface. A radial constant of motion exist in such situations.
3. Steady-state operation for a time scale over a year is not ruled out by a need for pulsed operation.
4. Plasma heating by ICRH is predicted to be efficient.
5. A compact design is possible with superconducting 3D coils.
6. The geometry of the SFLM design is aimed to satisfy reactor requirements for accessibility and avoidance of damage of sensitive equipment.
7. Reactor safety studies are favorable, but more studies are required in this area.
8. A tritium breeding ratio above unity is predicted.
9. Neutron computations predict that only a small fusion power (about 10 MW) could be sufficient for a power generation of 1.5 GW<sub>th</sub>.

## References

1. H.A. Bethe, *Physics Today*, 44 (1979).
2. O.Ågren, N. Savenko, "Magnetic mirror minimum B field with optimal ellipticity", *Phys. of Plasmas* 11, p. 5041 (2004).
3. O.Ågren, N. Savenko, "Theoretical study of increased electron temperature in mirror machines by tuned ICRH cycles", *Phys. Plasmas* 12, 022506 (2005)
4. O.Ågren, V. Moiseenko and N. Savenko, "Constants of motion in a minimum B field", *Phys. Rev. E* 72, 026408 (2005).
5. V. Moiseenko, O. Ågren, "Radio-frequency heating of sloshing ions in a straight field line mirror", *Phys. Plasmas* 12, 015510 (2005).

6. V.E. Moiseenko and O. Ågren, "A numerical model for radio-frequency heating of sloshing ions in a mirror trap", *J. Plasma Phys* 72, 1133 (2006).
7. V.E. Moiseenko and O. Ågren, "Second harmonic ion cyclotron heating of sloshing ions in a straight field line mirror", accepted for *Phys. Plasmas* (2006).
8. O. Ågren, V.E. Moiseenko, K. Noack and A. Hagnestål, "Studies of a Straight Field Line Mirror with emphasis on fusion-fission hybrids", *Fusion Science and Technology* 57, 326 (2010).
9. K. Noack, V.E. Moiseenko, O. Ågren and A. Hagnestål, "Neutronic model of a mirror based fusion-fission hybrid for the incineration of the transuranic elements from spent nuclear fuel and energy amplification", *Annals of Nuclear Energy* 38, 578 (2011).
10. Anders Hagnestål, Olov Ågren, V. E. Moiseenko, "A Compact Non-Planar Coil Design for the SFLM Hybrid", *Journal of Fusion Energy* 31, 379, doi:10.1007/s10894-011-9479-z (2012).
11. O. Ågren, V.E. Moiseenko, K. Noack and A. Hagnestål, "Radial drift invariant in long-thin mirrors", O. Ågren, V.E. Moiseenko, K. Noack and A. Hagnestål, "Radial drift invariant in long-thin mirrors", *Eur. Phys. J. D.* 66, 28, DOI 10.1140/epjd/e2011-20477-4 (2012).
12. Anders Hagnestål, Olov Ågren, V.E. Moiseenko, "Theoretical Field and Coil Design for a Single Cell Minimum-B Mirror Hybrid Reactor", *Fusion Science and Technology* 59, Number 1T, January 2011, Pages 217-219
13. K. Noack, O. Ågren, V.E. Moiseenko, A. Hagnestål, "Comments on the power amplification factor of a driven subcritical system", *Annals of Nuclear energy*, DOI 10.1016/j.anuence.2012.06.020, (2012).
14. A. Hagnestål, O. Ågren, V.E. Moiseenko, "Radial confinement in non-symmetric quadrupolar mirrors", *Journal of Fusion Energy* DOI:10.1007/s10894-012-9573 (2012).
15. O. Ågren, V.E. Moiseenko, "Radial constant of motion for particles in magnetic mirror fields", *Plasma Phys. and controlled fusion* 56, 094008 (2014).
16. P.A. Bagryansky et. al., "Threefold Increase of the Bulk Electron Temperature of Plasma Discharges in a Magnetic Mirror Device", *Phys Rev. Letters* 114, 205001 (2015).
17. V.E. Moiseenko, V.G. Kotenko, S.V. Chernitskiy, V.V. Nemov, O. Ågren, K. Noack, V.N. Kalyuzhnyi, A. Hagnestål, J. Källne, V.S. Voitsenya and I.E. Garkusha, "Research on stellarator-mirror fusion-fission hybrid", *Plasma Physics and contr. Fusion* 56, 094008 (2014).
18. H. Anglert, *Principles of Passive and Active Cooling of Mirror-Based Hybrid Systems Employing Liquid Metals*, Proceedings of the International Conference, Varenna, Italy, editors Jan Källne, Dimitri Ryutov, Giuseppe Gorini, Carlo Sozzi and Marco Tardocchi, ISBN 978-0-7354-1038-1, September 12-15 2011.

## 18 - Conceptual Design of Z-pinch Driven Fusion-Fission Hybrid Reactor

**Wang Zhen<sup>1</sup>, Peng Xianjue<sup>2</sup>, Li Zhenghong<sup>1</sup>, Huang Hongwen<sup>1</sup>, Wang Min<sup>3</sup>, Zhao Yinkui<sup>3</sup>, Li Maosheng<sup>3</sup>  
Guo Haibin<sup>1</sup>, Ma Jimin<sup>1</sup>, Chen Xiaojun<sup>1</sup>, Qi Jianmin<sup>1</sup>**

<sup>1</sup> Institute of Nuclear Physics and Chemistry, Mianyang, Sichuan, China, 621900

<sup>2</sup> China Academy of Engineering Physics, Mianyang, Sichuan, China, 621900

<sup>3</sup> Institute of Applied Physics and Computational Mathematics, Beijing, China, 100084

We presented a conceptual design of Z-pinch driven fusion-fission hybrid reactor (Z-FFR). In the concept, plasma kinetic energy is used to compress the DT capsule in a dynamic hohlraum, producing fusion yield from multi hundreds to thousand of mega-Joules. A sub-critical blanket using natural uranium or depleted uranium as fuels and light water as heat-exchange medium, can provide energy magnification factor of 10-20 and Tritium breeding ratio of larger than 1.15. The reactor can produce hundreds of mega-watts to a million kilo-watts electric power driven by an accelerator 40MA-60MA in peak current.

Dynamic hohlraum is used to convert cylindrical plasma kinetic energy to radiation ensuring spherical compression of DT fuels. In the capsule, DT ice fuels are separated into two parts and isolated from each other by high-Z materials. Inner DT fuels, less than 5% of the total fuel mass, will be compressed holistically to ignition condition. While the rest burns after the ignition of inner fuels to obtain a high G factor. It can tolerate hohlraum radiation unsymmetry as worse as 10%. Numerical simulation indicates fusion yield of 1.5GJ driven by a plasma liner with 4.6MJ/cm kinetic energy in a 60MA accelerator.

The sub-critical blanket is comprised of 18 modules, using 825 tons of uranium fuels and 45 tons of  $\text{Li}_4\text{SiO}_4$  tritium breeding materials. In each module, 15.5Mpa light water flows in Zr alloy pipes array embedded in U-10Zr alloy fuels. A volume ratio of 2:1, i.e., uranium versus light water, is suggested to obtain a high F/B ratio of fissile nuclei to maintain the nucleonic performance for more than 200 years without refuelling. Reprocessing of fuels is simple and convenient, where the fuels is only needed to be heated to remove fission gas, without any separation of isotopes, especially separation of the uranium and the plutonium elements.

## 19 - A short overview of ITER-like pulsed MCF reactors application as hybrid nuclear systems for actinides transmutation

**Guglielmo Lomonaco<sup>1,2\*</sup>, Walter Borreani<sup>1,2</sup>, Barbara Caiffi<sup>2</sup> and Davide Chersola<sup>1,2</sup>**

<sup>1</sup> GeNERG - DIME/TEC, University of Genova, via all'Opera Pia 15/A, 16145 Genova – ITALY

<sup>2</sup> INFN, via Dodecaneso 33, 16146 Genova – ITALY

\*Corresponding author: [guglielmo.lomonaco@unige.it](mailto:guglielmo.lomonaco@unige.it)

### Abstract

The fusion-fission hybrid reactor is a promising technology that is likely to assume more and more importance in the global energy scenario in the coming years. Although this kind of nuclear system dates back to the earliest times of the fusion projects (when it was recognized that using fusion neutrons to “support” nuclear fission fuel cycle could widely increase the exploitation of the fusion plants), it appears to receive relatively limited attention since the mid-1980s. Notwithstanding, hybrid fusion fission systems have been already studied for some decades, in the most prominent laboratories and a relatively large bibliography was produced. Obviously much more papers on this topic have been published in more recent years.

The fusion-fission hybrid concept can use both the nuclear fusion and fission processes: in a typical application, neutrons from fusion reactions can be used to sustain the fission chain of a sub-critical system. This is the basis of the hybrid reactor concept: neutron generation is not produced just in neutron-induced fissions, but also as a “by-product” of the fusion reactions inside the nuclear fusion reactor “core” (i.e., respectively, the void chamber for MCF or the fuel particles for ICF). This method allows to have an intrinsically safe facility (with a higher efficiency than a fusion reactor itself and a harder neutron energy spectrum than a fission reactor) which could be suitable for nuclear waste transmutation, too. In the last years, many initiatives on nuclear waste transmutation were proposed in order to reduce the long-term radiotoxicity of the wastes by eliminating a high fraction of the TRU from the SNF before their final disposal. In this frame, as already anticipated, hybrid fusion-fission systems could have an additional degree of freedom because of the independent source: this means that the neutron spectrum can be (reasonably) tailored for the transmutation purposes. In the present study a special focus has been devoted to the transmutation of SNF from fission reactors loaded in a fusion system, operated under the hypothesis to take into account the behaviour of a planned “real” (i.e. pulsed) MCF (ITER-like) plant.

### Keywords

Nuclear fission fuel cycle closure, ITER, pulsed fusion reactors, minor actinides, hybrid reactors.

### List of Acronyms

ADS	Accelerator-Driven System
ASIPPC	Institute of Plasma Physics Chinese Academy of Science
BoC	Begin of Cycle
CCFE	Culham Centre for Fusion Energy
DEMO	DEMOstration fusion power plant
ENEA	Italian National Agency for New Technologies, Energy and Sustainable Economic Development
EoC	End of Cycle
FDS	Advanced Nuclear Energy Research team (China)
FR	Fast Reactor
FW	First Wall
ICF	Inertial Confinement Fusion
ITER	International Thermonuclear Experimental Reactor
JAEA	Japan Atomic Energy Agency
LWR	Light Water Reactor
MA	Minor Actinide
MCAM	Monte Carlo Automatic Modeling
MCF	Magnetic Confinement Fusion
MCNP	Monte Carlo N-Particle
OTTO	Once Through Then Out
SNF	Spent Nuclear Fuel
TBM	Test Blanket Module
TRU	Transuranic element

## 1. Introduction

In a subcritical system, the nuclear properties of the nuclear fuel and other components are unable to keep the chain reaction going on, and both the neutron population and the fission reaction rate vanish in a very short time [1].

There are some artificial heavy nuclei and some mixtures of heavy radioactive nuclei with a non-negligible strength of neutron emission. However, more powerful sources are needed to feed a subcritical system if we want to have a power density similar to that of a critical reactor. Generally speaking, there are two kind of reactions useful as (potential) independent neutron sources:

- A spallation reaction induced by accelerated charged particles impinging in a target of a heavy element (e.g. lead) [30][31][32][33]
- A fusion reaction

Between these two potential choices, also the latter is receiving more and more attention by the international scientific community. This is the basis of the hybrid reactor concept, where neutron generation is not produced just in neutron-induced fissions, but also as a “by-product” of the fusion reactions inside the nuclear fusion reactor “core” (i.e. respectively, the void chamber for MCF or the fuel particles for ICF). Although the fusion-fission hybrid concept dates back to the earliest times of the fusion projects (when it was recognized that using fusion neutrons to “support” nuclear fission fuel cycle could vastly increase the exploitation of the fusion plants), it appears to receive relatively limited attention since the mid-1980s [2]. Notwithstanding, hybrid fusion fission systems have been already studied for some decades, in the most prominent laboratories and a large bibliography was produced [3][4][5][6][7][8][9][10][11][12][13][14][15][16][17][18][19][20][21][22][23][24][25][26][27][28][29]. Obviously much more papers on this topic have been published in more recent years (just to give some examples, see [34][35][36][37][38][39][40][41][42][43][44][45][46][47][48][77]).

On the other hand, in the last years, many initiatives on nuclear waste transmutation were proposed in order to reduce the long-term radiotoxicity of the wastes by eliminating a high fraction of TRU from the SNF before their final disposal (e.g. [49][50][51][52][53][54][55][56][57][58][59][60][61][62][63][64][65][76][79]). In this frame, as already anticipated, hybrid fusion-fission systems have an additional degree of freedom because of the independent source: this means that the neutron spectrum can be (reasonably) tailored for the transmutation purposes [1].

## 2. Hybrid fusion-fission systems

As already anticipated, fusion can also be combined with fission in what is referred to as hybrid fusion-fission system, where the blanket surrounding the core represents a “subcritical fission reactor” (i.e. the neutrons are captured, resulting in fission reactions taking place); instead, the fusion reaction acts as a source of neutrons for the surrounding blanket. These fission reactions would also produce more neutrons, thereby assisting further fission reactions in the blanket itself.

The concept of hybrid fusion-fission systems can be compared with an ADS. The blanket of a hybrid fusion system could therefore contain the same fuel as an ADS: for example, the abundant element Th [52] or the long-lived heavy isotopes present in the SNF could be used as fuel (see, as examples, [39][41][42][47]).

To synthesize, some potential benefits of a fusion-fission hybrid plant could be [66][75][80]:

- Hybrid configuration minimizes the risk of criticality excursions, and relaxes many control requirements (good passive and inherent safety features: when the plant shuts down no runaway fission reactions are possible)
- Reduction of hazardous materials (the plant would transmute most of the long lived isotopes present in SNF): the need for high-level waste repositories is strongly reduced (only about 5 % as much repository space would be needed, compared with current OTTO fuel cycle in LWRs). Additionally no fertile material that could otherwise produce additional actinides needs to be added, so the system can be designed maximizing the burning efficiency
- Proliferation resistance: the plant does not require any enrichment or fuel reprocessing with isotopic separation, so the fuel would not be suitable for use in weapons. What’s more, it is possible to obtain the destruction of initial fertile and no new fissile creation (fertile-free fuel cycle)
- There is a great flexibility in the fueling, which (at least ideally) allows for the design of different actinides burners
- More generally, it can benefit both fusion and fission (fill in the gap, solve still open fission problems, promote fusion)

### 2.1. Transmutation capabilities of hybrid systems: ICF vs. MCF

In order to evaluate which kind of fusion confinement could be more suitable for transmutation purposes in a hybrid fusion-fission system, a brief comparison between hybrid systems based on MCF and ICF transmutation features could be reported [80]:

- Hybrid MCF based systems have a higher percentage of transmutation than those based on ICF

- The transmutation efficiency is generally higher for MCF based systems
- In the ICF based systems, the neutrons are usually attenuated before reaching the end of the transmutation zone
- The two main advantages of ICF systems are:
  - the transmutation of Cm244 is achieved much more than by MCF
  - Pu associated radiotoxicity are reduced for ICF more than MCF
- Finally, the highest Th fertile-to-fissile conversion rate is reached in the MCF systems

## 2.2. Which transmutation process?

In order to design in a proper way the engineering aspects related to the plant (e.g. heat removal, shielding, etc.), it is important to quantify the power source inside the hybrid modules; so we need to know which kind of nuclear processes are more likely to happen. In general terms we can say that [80]:

- The nuclides with high probability to be transmuted by fission reaction in hybrid fusion-fission systems are:
  - Pu239
  - Pu241
  - Cm243
- Nuclides with similar transmutation probability by radiative capture or fission reactions are:
  - Np237
  - Pu240
  - Pu242
- Th transmutes mostly by radiative capture

## 3. Preliminary calculations and results

Differently from almost all the studies carried out in the past on this topic, in the present study the burnup calculations have been performing under the hypothesis to consider the “real” behavior of a planned fusion plant (namely ITER), i.e. the pulsed steps considered in our burnup calculations have the same duration of those ones planned for the real reactor.

But why to choose ITER? First of all because ITER design provides the possibility to test some innovative solutions in ad-hoc blanket positions (TBM) using a machine that should be (hopefully) available in a (relatively) limited time; in this way it could be possible:

- To confirm results obtained by previous thermo-mechanic simulations and/or experiments
- To test neutronics, tritium production, fission and integration performances
- Last but not the least, to experimentally validate the transmutation capabilities of a («realistic») hybrid system

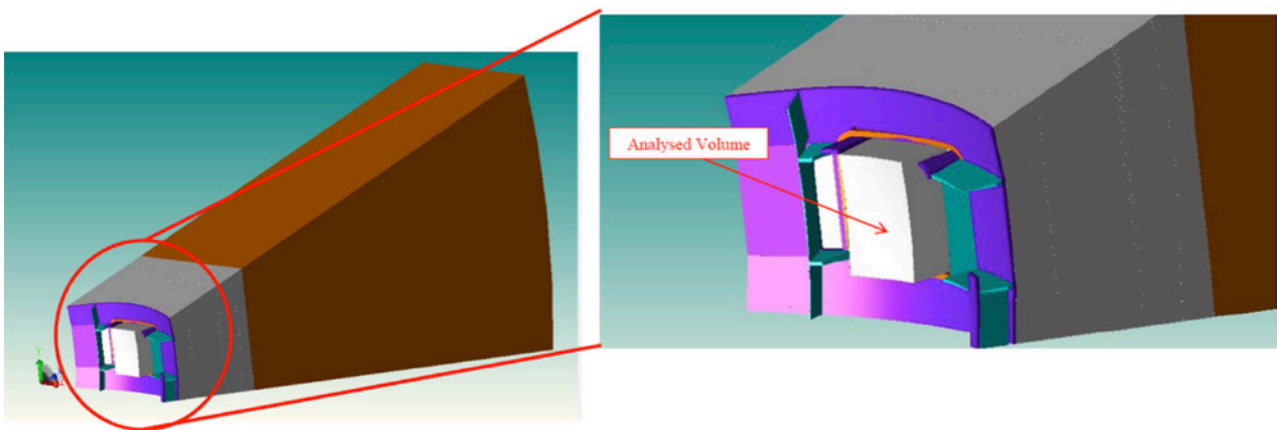


Figure 1 – FW and blanket sector analyzed in the burnup calculations

Starting from a complete and very detailed neutronic model of ITER [78] (on which we have performed a general MCNP [67] calculation with a FENDL based neutronic cross sections dataset [72]), we have extracted (by MCAM [74] code) a single sector (fig. 1) representative of a potential TBM where some MA (with a typical composition used for a FR [76]) have been inserted.

Then we have performed a burnup calculation limited to this sector by Serpent [68][69][70][71] code (imposing the boundary conditions obtained by previous general MCNP calculation) with a JEFF based neutronic cross sections dataset [73] obtaining the preliminary results in detail reported in [75]. Among the others, it is useful to highlight the spectra (at BoC and EoC) inside analyzed sector (fig. 2) and the transmutation results for some key MA (fig. 3, 4 and tab. 1).

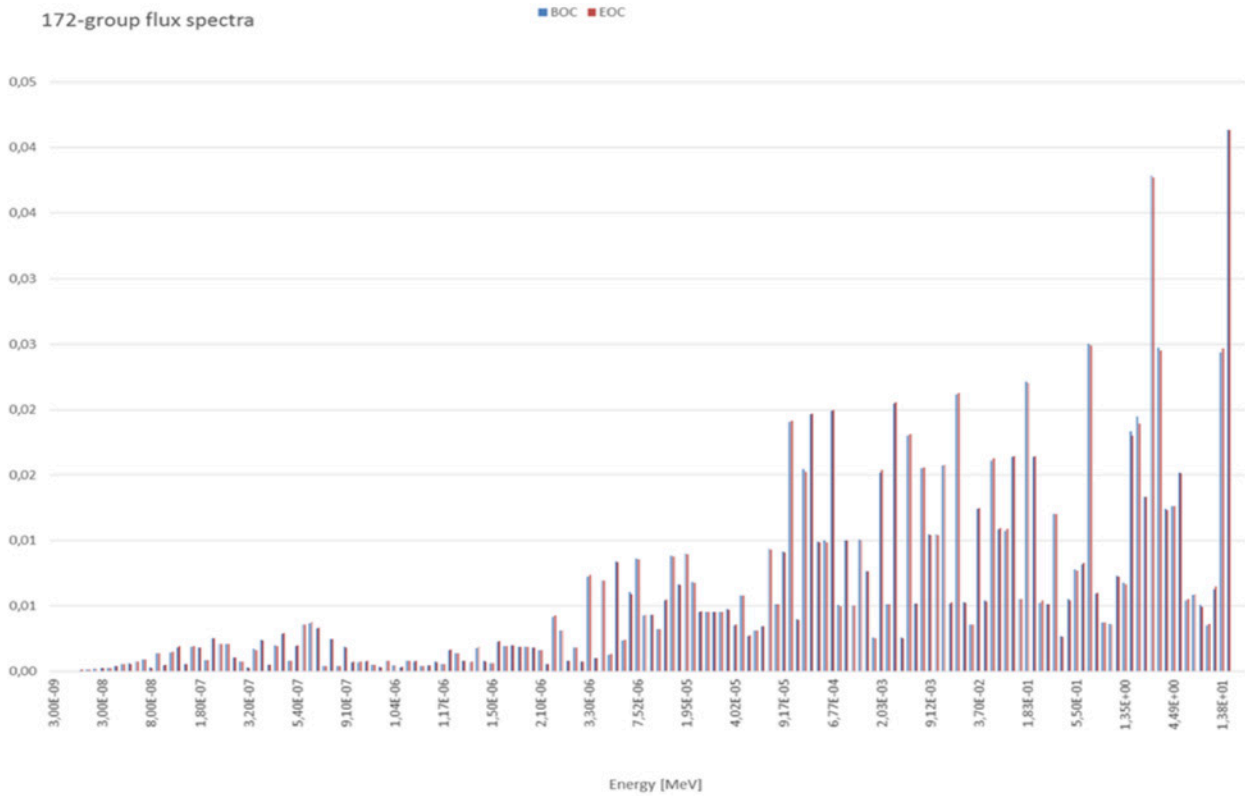


Figure 2 – 172-groups spectrum at BoC and EoC

<i>Nuclides</i>	<i>Initial value</i>	<i>Reduction</i>	<i>Variation [%]</i>
<b><i>Am<sup>241</sup></i></b>	~ 63642 g	~ 4 g	~ - 0.01 %
<b><i>Cm<sup>244</sup></i></b>	~ 570 g	~ 0.6 g	~ - 0.1%

Table 1 – *Am<sup>241</sup>* and *Cm<sup>244</sup>* variations during the whole irradiation period

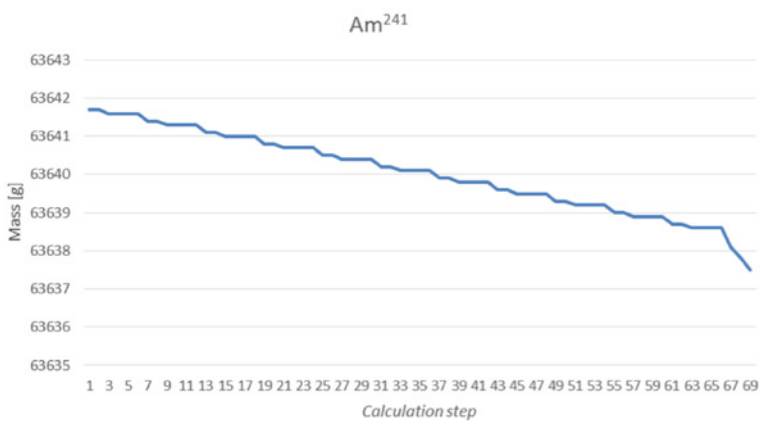
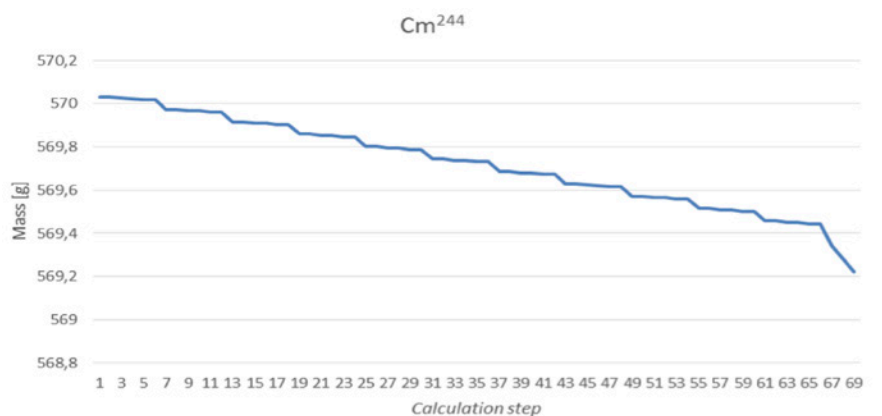


Figure 3 – *Am<sup>241</sup>* mass vs. calculation step

Figure 4 – *Cm<sup>244</sup>* mass vs. calculation step



#### 4. Discussion

As already found in previous publications, also our preliminary calculations and results confirm the feasibility and the potentiality of transmutation in hybrid fusion-fission reactors. However, looking at fig. 3. 4 and at tab. 1, the Am241 and Cm244 variations due to transmutation (and not to pure decay) seem very limited (at least for the supposed pulsed regime with very long inactivity periods).

So, also on the basis of the previous considerations, some important questions remain still open in view of the design of a possible "roadmap" for implementing a TBM loaded with MA in ITER:

- Heat removal:
  - Additional heat produced by MA fissions in blanket
  - Decay heat to be removed (also when fusion reactors is not working)
- Additional MA related problems:
  - Radioprotection issues
  - Blanket materials compatibility
  - Post-irradiation TBM «reprocessing»
- Capability to evaluate transmutation processes effects separately by pure MA decays

#### 5. Conclusions

Hybrid fusion-fission systems could be an interesting opportunity to be exploited in order to fully close the nuclear (fission) fuel cycle.

Unfortunately, at least at the moment, only fusion machines that work in a pulsed regime (with very long inactivity periods) should be available in the next future.

The transmutation results with this kind of systems seem not so encouraging (no substantial improvements with respect to pure decay).

Additionally, the insertion of MA dedicated modules inside a «pure» fusion machine implies the rise of additional materials compatibility, heat removal and radioprotection related issues.

#### Acknowledgements

First of all we like to thank Ing. D. Scarfò for his fundamental past contribution to this research activity.

This work was carried out using an adaptation of the B-lite MCNP model which was developed as a collaborative effort between the FDS Team of ASIPP China, University of Wisconsin-Madison, ENEA Frascati, CCFE UK, JAEA Naka, and the ITER Organization. We want to thank all these organizations.

We want to thank the FDS Team members also for their precious collaboration in MCAM installation, configuration and application.

Our thank goes to Dr. J. Leppänen of VTT for his continuous support in SERPENT configuration and documentation supply.

Finally, special thanks go to Ing. A. Muzzioli of GeNERG-DIME/TEC (University of Genova) for her help in computational issues, Dr. Ing. R. Marotta of Nucleco S.p.A. and Ing. M. Dellabiancia of RC-Rež for their suggestions.

#### References

- [1] J. M. Martinez-Val, M. Piera, A. Abánades, A. Lafuente, Hybrid Nuclear Reactors, in: S. B. Krivit, J. H. Lehr, T. B. Kingery, Nuclear Energy Encyclopedia - Science, Technology, and Applications, pp. 435÷455, J. Wiley & s., 2011
- [2] Y. Wu, Progress in fusion-driven hybrid system studies in China, Fusion Engineering and Design vol. 63÷64, 2002
- [3] H. A. Bethe, The fusion hybrid, Physics Today, vol. 5, 1979
- [4] D. J. Bender, Performance parameters for fusion-fission power systems, Nuclear Technology, vol. 44, 1979
- [5] M. Z. Youssef, R. W. Conn, W. F. Vogelsang, Tritium and fissile fuel exchange between hybrids, fission power reactors and tritium produce reactors, Nuclear Technology, vol. 47, 1980
- [6] J. K. Presley, A. A. Harms, M. Heindler, Nuclear fuel trajectories of fusion-fission symbionts, Nuclear Science and Engineering, vol. 74, 1980
- [7] S. I. Abdel-Khalik, P. Jansen, G. Kebler, P. Klumpp, Impact of fusion-fission hybrids on world nuclear future, Atomkernenergie, vol. 38, 1981
- [8] D. H. Berwald and J. Maniscalco, An economics method for symbiotic fusion-fission electricity generator systems, Fusion Science and Technology, vol. 1, 1981
- [9] R. P. Rose, The case for the fusion hybrid, Journal of Fusion Energy, vol. 1, 1981
- [10] J. D. Lee and R. W. Moir, Fission-suppressed blankets for fissile fuel breeding fusion reactors, Journal of Fusion Energy, vol. 1, 1981

- [11] E. Greenspan and G. H. Miley, Fissile and synthetic fuel production ability of hybrid reactors, *Atomkernenergie*, vol. 38, 1981
- [12] A. A. Harms and C.W. Gordon, Fissile fuel breeding potential with paired fusion-fission reactors, *Annals of Nuclear Energy*, vol. 3, 1976
- [13] S. Taczanowski, Neutron multiplier alternatives for fusion reactor blankets, *Annals of Nuclear Energy*, vol. 8, 1981
- [14] A. A. Harms and M. Heindler, *Nuclear Energy Synergetics*, Plenum Press, 1982
- [15] R. W. Moir, The fusion breeder, *Journal of Fusion Energy*, vol. 2, 1982
- [16] R. W. Moir, Design of a He-cooled, molten salt fusion breeder, *Journal of Fusion Energy*, vol. 8, 1985
- [17] R. W. Moir, J. D. Lee, M. S. Coops, F. J. Fulton, W. S. Neef, Jr., D. H. Berwald, R. B. Campbell, B. Flanders, J. K. Garner, N. Ghoniem, J. Ogren, Y. Saito, A. Slomovik, R. H. Whitley, K. R. Schultz, G. E. Benedict, E. T. Cheng, R. L. Creedon I. Maya, V. H. Pierce, J. B. Strand, C. P. C. Wong, J. S. Karbowski, R. P. Rose, J. H. Devan, P. Tortorelli, L. G. Miller, P. Y. S. Hsu, J. M. Beeston, N. J. Hoffman, D. L. Jassby, Fusion breeder reactor design studies, *Fusion Science and Technology*, vol. 4, 1983
- [18] J. D. Lee, US-DOE fusion breeder program-blanket design and system performance, *Atomkernenergie*, vol. 44, 1984
- [19] S. J. Piet, Safety evaluation of the blanket comparison and selection study, *Fusion Technology*, vol. 8, 1985
- [20] J. Garber, and I. Maya, Safety assessment of the fusion breeder, *Fusion Technology*, vol. 8, 1985
- [21] B. R. Leonard Jr., A review of fusion-fission (hybrid) concepts. *Nuclear Technology*, vol. 20, 1973
- [22] C. Powell and D. J. Hahm, Energy balance of a hybrid fusion-fission reactor, *Atomkernenergie*, vol. 21, 1973
- [23] L. M. Lidsky, Fusion-fission systems: hybrid symbiotic and Augean, *Nuclear Fusion*, vol. 15, 1975
- [24] A. A. Harms, Hierarchical systematics of fusion-fission energy systems, *Nuclear Fusion*, vol. 15, 1975
- [25] N. G. Cook and J. A. Maniscalco, Uranium-233 breeding and neutron multiplying blankets for fusion reactors, *Nuclear Technology*, vol. 30, 1976
- [26] J. A. Maniscalco, Fusion-fission hybrid concepts for laser induced fusion, *Nuclear Technology*, vol. 28, 1976
- [27] V. L. Blinkin and V. M. Novikov, Symbiotic system of a fusion and a fission reactor with very simple fuel reprocessing, *Nuclear Fusion*, vol. 18, 1978
- [28] H. Takahashi, P. Grand, J. R. Powell, M. Steinberg, H. J. C. Kouts, Fissile fuel production by linear accelerator, *Transaction of American Nuclear Society*, vol. 43, 1982
- [29] S. Sahin, Neutronic analysis of fast hybrid thermoionic reactors, *Atomkernenergie*, vol. 39, 1981
- [30] P. Saracco, R. Marotta, G. Lomonaco, D. Chersola, L. Mansani, A preliminary study of an improved area method, adapted to short time transients in sub-critical systems, *Proceedings of the International Conference on Physics of Reactors (PHYSOR 2014)*, Kyoto, Japan, September-October 2014
- [31] S. Dulla, M. Nervo, P. Ravetto, P. Saracco, G. Lomonaco, M. Carta, Reflector effects on the kinetic response in subcritical systems, *Proceedings of the Joint International Conference on Mathematics and Computation, Supercomputing in Nuclear Applications and the Monte Carlo Method (ANS M&C+SNA+MC 2015)*, Nashville, USA, April 2015
- [32] P. Saracco and G. Ricco, Various Operating Regimes of a Subcritical System as a Function of Subcriticality in One Group Theory, *Nuclear Science and Engineering*, vol. 162, 2009
- [33] M. Ripani, S. Frambati, L. Mansani, M. Bruzzone, M. Reale, S. Monti, M. Ciotti, M. Barbagallo, N. Colonna, A. Celentano, M. Osipenko, G. Ricco, P. Saracco, C. M. Viberti, O. Frasciello, P. Boccaccio, J. Esposito, A. Lombardi, M. Maggiore, L. A. C. Piazza, G. Prete, R. Alba, L. Calabretta, G. Cosentino, A. Del Zoppo, A. Di Pietro, P. Figuera, P. Finocchiaro, C. Maiolino, D. Santonocito, M. Schillaci, D. Chiesa, M. Clemenza, E. Previtali, M. Sisti, A. Kostyukov, A. Cammi, S. Bortot, S. Lorenzi, M. Ricotti, S. Dulla, P. Ravetto, G. Lomonaco, A. Rebora, D. Alloni, A. Borio di Tigliole, M. Cagnazzo, R. Cremonesi, G. Magrotti, S. Manera, F. Panza, M. Prata, A. Salvini, Study of an intrinsically safe infrastructure for training and research on nuclear technologies, *European Physical Journal – Web of Conferences*, vol. 79, 2014
- [34] D. Ridikas, R. Plukiene, A. Plukis, E. T. Cheng, Fusion–fission hybrid system for nuclear waste transmutation (I): Characterization of the system and burn-up calculations, *Progress in Nuclear Energy*, vol. 48, 2006
- [35] R. Plukiene, A. Plukis, D. Ridikas, E. T. Cheng, Fusion–fission hybrid system for nuclear waste transmutation (II): From the burn-up optimization to the tests of different data libraries, *Progress in Nuclear Energy*, vol. 48, 2006
- [36] T. A. Mehlhorn, B. B. Cipiti, C. L. Olson, G. E. Rochau, Fusion–fission hybrids for nuclear waste transmutation: A synergistic step between Gen-IV fission and fusion reactors, *Fusion Engineering and Design*, vol. 83, 2008
- [37] T. C. Simonen, R. W. Moir, A. W. Molvik, D. D. Ryutov, A 14 MeV fusion neutron source for material and blanket development and fission fuel production, *Nuclear Fusion*, vol. 53, 2013
- [38] M. Kotschenreuthera, P. M. Valanjua, S. M. Mahajana, E. A. Schneider, Fusion–Fission Transmutation Scheme-Efficient destruction of nuclear waste, *Fusion Engineering and Design*, vol. 84, 2009
- [39] J. Zhao, Y. Yang, Z. Zhou, Study of thorium–uranium based molten salt blanket in a fusion–fission hybrid reactor, *Fusion Engineering and Design*, vol. 87, 2012
- [40] M. Ni, Y. Song, M. Jin, J. Jiang, Q. Huang, Design and analysis on tritium system of multi-functional experimental

- fusion–fission hybrid reactor (FDS-MFX), *Fusion Engineering and Design*, vol. 87, 2012
- [41] X. B. Ma, Y. X. Chen, G. P. Quan, L. Z. Wang, D. G. Lu, Neutronics analysis of the power flattening and minor actinides burning in a thorium-based fusion–fission hybrid reactor blanket, *Fusion Engineering and Design*, vol. 87, 2012
- [42] X. B. Ma, Y. X. Chen, Y. Wang, P. Z. Zhang, B. Cao, D. G. Lu, H. P. Cheng, Neutronic calculations of a thorium-based fusion–fission hybrid reactor blanket, *Fusion Engineering and Design*, vol. 85, 2010
- [43] M. Piera, A. Lafuente, A. Abánades, J. M. Martínez-Val, Hybrid reactors: Nuclear breeding or energy production?, *Energy Conversion and Management*, vol. 51, 2010
- [44] M. Günay, Assessment of the neutronic performance of some alternative fluids in a fusion–fission hybrid reactor by using Monte Carlo method, *Annals of Nuclear Energy*, vol. 60, 2013
- [45] Y. Zheng, T. Zu, H. Wu, L. Cao, C. Yang, The neutronics studies of a fusion fission hybrid reactor using pressure tube blankets, *Fusion Engineering and Design*, vol. 87, 2012
- [46] M. Wang, J. Jiang, J. Liu, Y. Bai, Y. Hu, Neutronics performance evaluation of fast-fission fuel breeding blankets for a fusion–fission hybrid reactor, *Fusion Engineering and Design*, vol. 85, 2010
- [47] M. Matsunaka, S. Shido, K. Kondo, H. Miyamaru, I. Murata, Burnup calculation of fusion–fission hybrid energy system with thorium cycle, *Fusion Engineering and Design*, vol. 82, 2007
- [48] E. Gerstner, Nuclear energy: The hybrid returns, *Nature*, vol. 460, 2009
- [49] G. Lomonaco, O. Frasciello, M. Osipenko, G. Ricco, M. Ripani, An intrinsically safe facility for forefront research and training on nuclear technologies – Burnup and transmutation, *European Physical Journal – Plus*, vol. 129, 2014
- [50] N. Cerullo, G. Lomonaco, Generation IV reactor designs, operation and fuel cycle, in: I. Crossland, *Nuclear Fuel Cycle Science and Engineering*, pp. 333–395, Woodhead Publishing, 2012
- [51] E. Bomboni, N. Cerullo, G. Lomonaco, V. Romanello, A Critical Review of the Recent Improvements in Minimizing Nuclear Waste by Innovative Gas-Cooled Reactors, *Science and Technology of Nuclear Installations*, vol. 2008
- [52] G. Mazzini, E. Bomboni, N. Cerullo, E. Fridman, G. Lomonaco, E. Shwageraus, The Use of Th in HTR: State of the Art and Implementation in Th/Pu Fuel Cycles, *Science and Technology of Nuclear Installations*, vol. 2009
- [53] E. Bomboni, N. Cerullo, G. Lomonaco, Assessment of LWR-HTR-GCFR Integrated Cycle, *Science and Technology of Nuclear Installation*, vol. 2009
- [54] E. Bomboni, N. Cerullo, G. Lomonaco, Erratum for “Assessment of LWR-HTR-GCFR Integrated Cycle”, *Science and Technology of Nuclear Installations*, vol. 2009
- [55] D. Chersola, G. Lomonaco, R. Marotta, G. Mazzini, Comparison between SERPENT and MONTEBURNS codes applied to burnup calculations of a GFR-like configuration, *Nuclear Engineering and Design*, vol. 273, 2014
- [56] N. Cerullo, D. Bufalino, G. Forasassi, G. Lomonaco, P. Rocchi, V. Romanello, The capabilities of HTRs to burn actinides and to optimize plutonium exploitation, *Proceedings of the 12th International Conference on Nuclear Engineering (ICONE '04)*, vol. 1, Arlington, USA, April 2004
- [57] D. Castelliti, E. Bomboni, N. Cerullo, G. Lomonaco, C. Parisi, GCFR Coupled Neutronic and Thermal-Fluid-Dynamics Analyses for a Core Containing Minor Actinides, *Science and Technology of Nuclear Installation*, vol. 2009
- [58] B. Vezzoni, N. Cerullo, G. Forasassi, E. Fridman, G. Lomonaco, V. Romanello, E. Shwageraus, Preliminary Evaluation of a Nuclear Scenario Involving Innovative Gas Cooled Reactors, *Science and Technology of Nuclear Installation*, vol. 2009
- [59] G. Lomonaco, W. Grassi, N. Cerullo, The Influence of the Packing Factor on the Fuel Temperature Hot Spots in a Particle-Bed GCFR, *Science and Technology of Nuclear Installation*, vol. 2009
- [60] E. Bomboni, N. Cerullo, G. Lomonaco, Analysis of pebble fuelled zone modeling influence on HTR core calculations, *Nuclear Science and Engineering*, vol. 162, 2009
- [61] E. Bomboni, N. Cerullo, G. Lomonaco, Simplified models for pebble-bed HTR core burn-up calculations with Monteburns2.0©, *Annals of Nuclear Energy*, vol. 40, 2012
- [62] E. Bomboni, N. Cerullo, E. Fridman, G. Lomonaco, E. Shwageraus. Comparison among MCNP-based depletion codes applied to burnup calculations of pebble-bed HTR lattices, *Nuclear Engineering and Design*, vol. 204, 2010
- [63] N. Cerullo, D. Chersola, G. Lomonaco, R. Marotta, The GFR in the frame of advanced fuel cycles: the use of DA as an improved way to minimize the MA content in the SNF, *Journal of Energy and Power Sources*, vol. 1, 2014
- [64] D. Chersola, G. Lomonaco, G. Mazzini, Cross Sections Influence on Monte Carlo Based Burnup Codes, *Proceedings of the 22nd International Conference on Nuclear Engineering (ICONE22)*, Prague, Czech Republic, July 2014
- [65] D. Chersola, G. Lomonaco, G. Mazzini, Cross Sections Influence on Monte Carlo Based Burnup Codes Applied to a GFR-like configuration, *Nuclear Engineering and Radiation Science*, vol. 1, 2015
- [66] E. Moses, T. Díaz de la Rubia, E. Storm, J. Latkowski, J. Farmer, R. Abbott, K. Kramer, P. Peterson, H. Shaw, R. Lehman II, A Sustainable Nuclear Fuel Cycle Based on Laser Inertial Fusion Energy, *Fusion Science and Technology*, vol. 56, 2009
- [67] T. Goorley, M. James, T. Booth, F. Brown, J. Bull, L. J. Cox, J. Durkee, J. Elson, M. Fensin, R. A. Forster, J.

- Hendricks, H. G. Hughes, R. Johns, B. Kiedrowski, R. Martz, S. Mashnik, G. McKinney, D. Pelowitz, R. Prael, J. Sweezy, L. Waters, T. Wilcox, T. Zukaitis, Initial MCNP6 Release Overview, Nuclear Technology, vol. 180, 2012
- [68] J. Leppänen, and A. Isotalo, Burnup Calculation methodology in the Serpent2 Monte Carlo Code, Proceedings of PHYSOR 2012 (Advances in Reactor Physics Linking Research, Industry, and Education), Knoxville (Tennessee), USA, April 2012
- [69] J. Leppänen, M. Pusa, T. Viitanen, V. Valtavirta, T. Kaltiaisenaho, The Serpent Monte Carlo code: status, development and applications in 2013, Annals of Nuclear Energy, vol. 82, 2015
- [70] M. Pusa and J. Leppänen, Computing the Matrix Exponential in Burnup Calculations, Nuclear Science and Engineering, vol. 164, 2010
- [71] A. E. Isotalo and P. A. Aarnio, Higher order methods for burnup calculations with Bateman solutions, Annals of Nuclear Energy, vol. 38, 2011
- [72] M. E. Sawan and T. D. Bohm, Impact of FENDL-2.1 Updates on Nuclear Analysis of ITER and Other Fusion Systems, Journal of the Korean Physical Society, vol. 59, 2011
- [73] O. Cabellos, Processing of the JEFF-3.1 Cross Section Library into a Continuous Energy Monte Carlo Radiation Transport and Criticality Data Library, OECD NEA Data Bank, 2006
- [74] Y. Wu and FDS Team, CAD-based interface programs for fusion neutron transport simulation, Fusion Engineering and Design, vol. 84, 2009
- [75] D. Scarfò, B. Caiffi, D. Chersola, G. Lomonaco, A Preliminary Assessment of the Transmutation Potentialities for an ITER-like FW Sector Loaded with MA, Global Journal of Energy Technology Research Updates, vol. 2, issue 2, 2016
- [76] D. Chersola, G. Lomonaco, R. Marotta, The VHTR and GFR and their use in innovative symbiotic fuel cycles, Progress in Nuclear Energy, vol. 83, 2015
- [77] Y. Wu, J. Jiang, M. Wang, M. Jin and FDS Team, A fusion-driven subcritical system concept based on viable technologies, Nuclear Fusion, vol. 51, 2011
- [78] ITER Organization et al., ITER Internal Report "Blite v3 R121217", IDM 9KKVQR, December 2012
- [79] D. Chersola, G. Lomonaco, R. Marotta, G. Mazzini, Comparison between SERPENT and MONTEBURNS codes applied to burnup calculations of a GFR-like configuration, Nuclear Engineering and Design, vol. 273, 2014
- [80] C. E. Velasquez, C. Pereira, M. A. F. Veloso, A. L. Costa, G. de P. Barros, Fusion–Fission Hybrid Systems for Transmutation, Journal of Fusion Energy, vol. 35, 2016

## 20 - The possible role of the Italian Universities consortium CIRTEN for the engineering study of a fission-fusion hybrid reactor

M. Ricotti<sup>1</sup>, A. Cammi<sup>1</sup>, L. Luzzi<sup>1</sup>, M. Mariani<sup>1</sup>, E. Zio<sup>1</sup>, A.P. Di Maio<sup>2</sup>, G. Vella<sup>2</sup>, B. Bozzini<sup>3</sup>, G. Caruso<sup>4</sup>  
R. Gatto<sup>4</sup>, S. Dulla<sup>5</sup>, M. Ferraris<sup>5</sup>, P. Ravetto<sup>5</sup>, L. Savoldi<sup>5</sup>, G. Vecchi<sup>5</sup>, R. Zanino<sup>5\*</sup>

\*Corresponding author. E-mail roberto.zanino@polito.it

<sup>1</sup> Politecnico di Milano, Italy  
<sup>2</sup> Università degli Studi di Palermo, Italy  
<sup>3</sup> Università del Salento, Italy  
<sup>4</sup> Università di Roma "Sapienza", Italy  
<sup>5</sup> Politecnico di Torino, Italy

### Abstract

The fission-fusion hybrid reactor (FFHR) constitutes a challenging playground for nuclear engineers. The CIRTEN consortium is responsible today for essentially all of the nuclear engineering research and education efforts in the Italian academia, with a spread of competences going from ITER, DEMO and, more generally, different fusion engineering applications, to fission applications like Generation IV reactors, ADS, SMR etc, including different enabling technologies and cultures, like materials and safety. In the paper a brief summary of the multi-disciplinary know-how inside CIRTEN is presented. It is argued that CIRTEN could give a non-negligible contribution to the further development of the FFHR concept, provided a suitable national and, especially, international collaboration framework could be envisaged.

### 1. Introduction

The fusion-fission hybrid reactor (FFHR) is a powerful idea [1] that attempts to combine the best features of fission and fusion towards the achievement of a multiplicity of targets, which are not limited to power production but include also nuclear waste transmutation and others. Major efforts in this field are being carried out in China [2], Russia [3] and the US [4], among others.

### 2. The CIRTEN consortium and the Nuclear Engineering (NE) education programs in Italy

CIRTEN is a consortium of universities, see Fig. 1, which was founded in 1994 to foster research and education in the field of nuclear technologies in Italy.



Figure 1. Italian Universities contributing to CIRTEN

Almost all faculty in the field of NE, see Fig. 2, belong to CIRTEN universities.



Figure 2. Nuclear engineering faculty in Italy (data from <http://cercauniversita.cineca.it/php5/docenti/cerca.php> 05nov2016)

Notwithstanding the very significant difficulties for anything NE-related following the two referenda in Italy, a total of 100+ students a year, which for a Country without nuclear power plants (NPPs) can be considered, we believe, quite a big number, are enrolled in the educational programs either fully or at least partly devoted to NE, which are at this time the following:

- BSc level
  - NE track inside Energy engineering (UniPa)
- MSc level
  - Energy and NE (UniPa, PoliTo)
  - NE (PoliMi, UniPi)
  - NE track inside Energy engineering (UniRm1)
  - Poly2Nuc joint NE program between PoliMi and PoliTo
- PhD programs.

Of course, notwithstanding the strong involvement and success of Italian industries and agencies in the fusion field, the fact that Italy does not and also will not have any NPPs, at least in the short term, implies that our (best) students are often finding after graduation a position in some of the (best) nuclear institutions around the world, see Fig. 3 for an example. While this may be a cause of pride, as it is clearly a sign of the quality of our graduates, it also raises some questions as to the cost-benefit ratio and associated trade-off between the obvious pros of an international network of alumni and the cons associated to this brain drain for our Country.

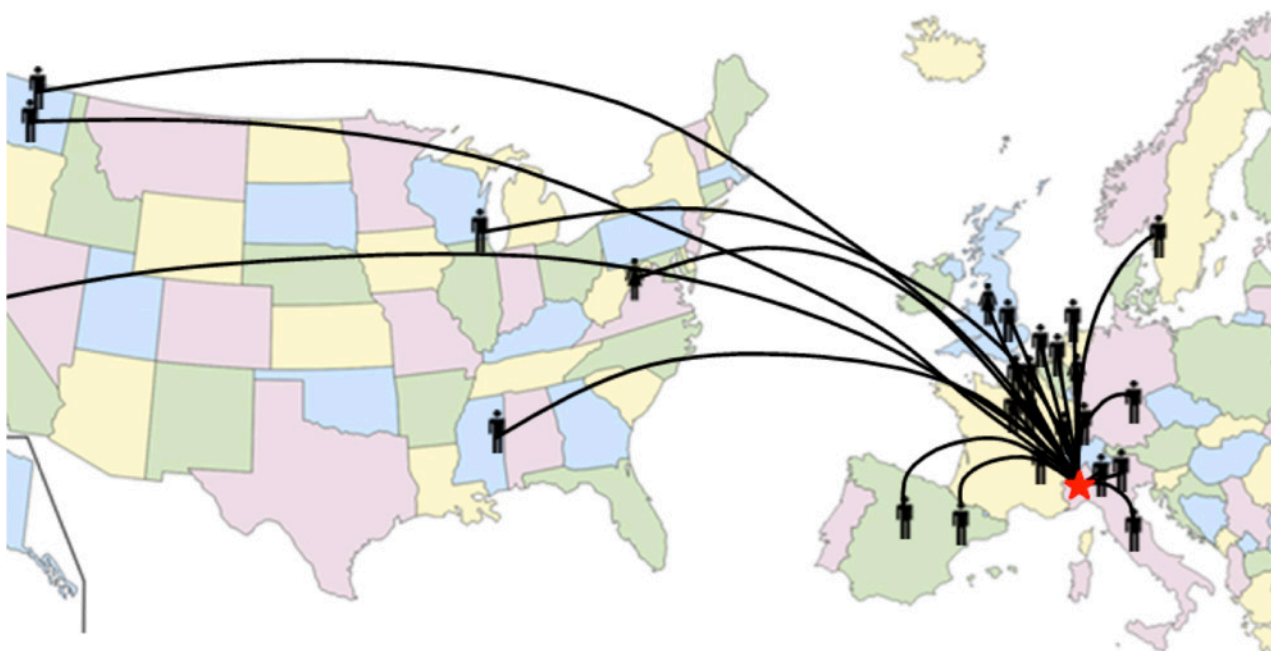


Figure 3. An example of CIRTEN "fallout": Export of PoliTo alumni towards nuclear institutions in the EU and in the US.

### 3. FFHR-relevant know-how inside CIRTEN

The FFHR can be seen as an excellent opportunity to bring together the fission and fusion research&education communities in Italy, especially considering that the most critical aspects in the design of such a reactor are likely to be related to the fission-fusion interfaces and require therefore by definition both competences.

The CIRTEN universities have built a significant experience and background in the NE field from the participation to

several international projects and namely

- In fission, LFR (ELSY, LEADER), ADS (IABAT, MUSE, XADS, EFIT), MSR (MOST, ALISIA, EVOL, SAMOFAR), P&T (NEWPART, PARTNEW, EUROPART, ACSEPT, SACSESS)
- In fusion, ITER, the EU-DEMO and several of the present tokamaks, including e.g. JET and KSTAR.

The typical know-how that the CIRTEN universities could offer in the framework of a collaboration on the FFHR pertains to the following fields

- Neutronics / Thermal-hydraulics (TH) / Thermo-mechanics (fission&fusion blanket, ...)
- Fusion
  - Superconducting magnets
  - Plasma-wall interactions and management of high heat fluxes
  - Radio-Frequency heating of the plasma
- Materials and nuclear fuel cycle
- Safety.

In the remaining part of this Section, a few selected contributions of CIRTEN universities in the above-mentioned fields will be briefly summarized.

In the field of multi-physics modeling, a major effort has been devoted at PoliTo, over the last 20 years or so, to the development and/or application of different, state-of-the-art computational tools, which could all be relevant in the design phase of an FFHR, e.g.

- The 4C (coil, conductor and cryogenic circuit) code [5], for the analysis of TH transients in superconducting magnets for fusion reactor applications, validated against experimental data from different machines (EAST, KSTAR, ITER Model and Insert Coils, W7-X), and also applied to several future tokamaks (ITER, EU-DEMO, JT-60SA, DTT),
- The GETTHEM (general tokamak thermal-hydraulic modeling) code, for the system-level TH analysis of the tokamak, based on the object-oriented Modelica language, currently applied to the design verification of the HCPB and WCLL solutions for the breeding blanket of the EU-DEMO [6],
- The different CFD modeling tools (ANSYS Fluent, STARCCM+, OpenFoam), applied to the TH modeling of different water cooled ITER components like the vacuum vessel [7], the first wall panels, the gyrotron collector and cavity,
- The FRENETIC (fast reactor neutronic/thermal-hydraulic) code [8], a computationally efficient, multi-physics modelling tool for liquid-metal cooled fast reactor cores, suitable for design and safety studies, recently validated against experimental data from EBR-II [9] and applied to the study of the LFR demonstrator ALFRED,
- The TOPICA code [10], for the design of ICRF antennas.

At PoliMi, PoliTo, UniPa and UniRm1, different models for the fission blanket could be developed

- to establish configuration, sub-criticality level and fission distribution of the subcritical system in steady-state, using the Serpent code and inverse models for reactivity monitoring [11],
- to evaluate the transmutation properties of the system, using the Fispack code, as well as the uncertainties due to nuclear data and models (using state-of the art UQ methods like GPT and reduced-order modelling),
- to compare the performances of LFR vs. MSR-like blankets, including the fluid/nuclear fuel non-linear coupling between fuel and neutron dynamics in the case of the latter [12]-[15],
- to compute the distribution of neutrons and heat load (using MCNP) [16], [21],
- to perform thermomechanical analyses (using Abaqus) [17],
- to evaluate the feasibility of selected blanket design concepts by means of preliminary TH estimates (using Relap5-3D) [18],
- to perform MHD calculations of the flow of liquid metals in a background B field for LFR-like blankets (using Ansys CFX and OpenFOAM).

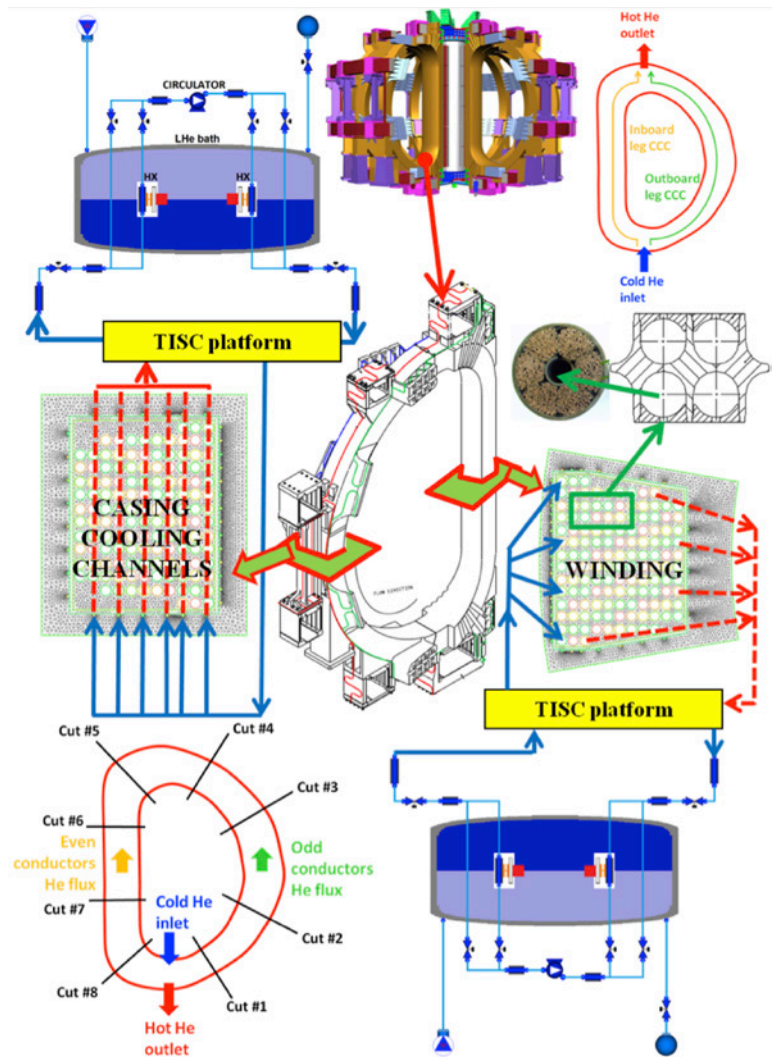


Figure 4. Architecture of the 4C code for thermal-hydraulic simulation of superconducting coils.

Some of the relevant TH features could also be studied taking advantage of the DYNASTY facility (first test end of 2016) developed at PoliMi for studying the stability of a closed molten salt loop with distributed heat generation.

In the field of nuclear materials several efforts are ongoing in the CIRTEN or related universities, among which some of the most FFHR-relevant ones include

- The analysis of chemical compatibility between MS and structural components, where a computational approach combining DFT simulations and Molecular Dynamics is coupled to (and partly validated by) an experimental approach, combining in turn the synthesis of compounds, thermal analyses, X-ray diffraction and solubility experiments, performed in the New Integrated Nuclear Laboratories at PoliMi [22],
- The study of pyrometallurgical reprocessing [23] and waste confinement [24], again in the same PoliMi laboratories,
- The development of joined or coated components and their experimental characterization at PoliTo, in collaboration with a series of international institutions [25]-[27],
- The experimental study of the corrosion of structural metallic components in contact with MS at UniSalento, where preliminary tests on W corrosion in molten NaCl have been performed [28]-[30].

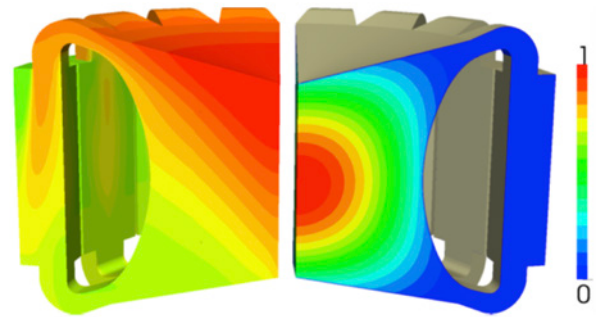


Figure 5. Spatial distribution of the delayed (left) and prompt (right) neutron sources (arbitrary units) computed with a 3D OpenFOAM simulation of an MSFR at nominal flow rate.

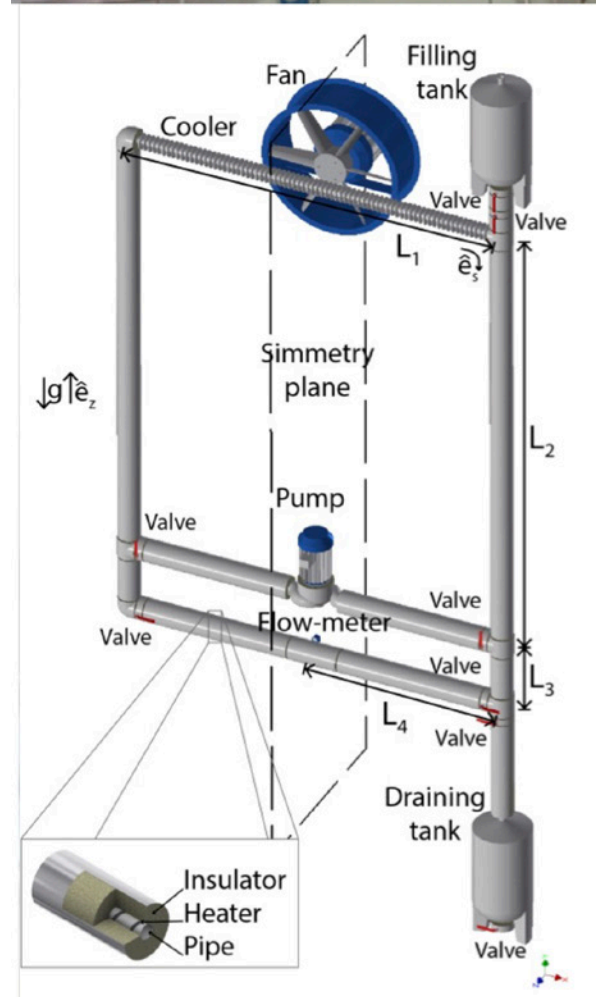


Figure 6. The DYNASTY facility at PoliMi.

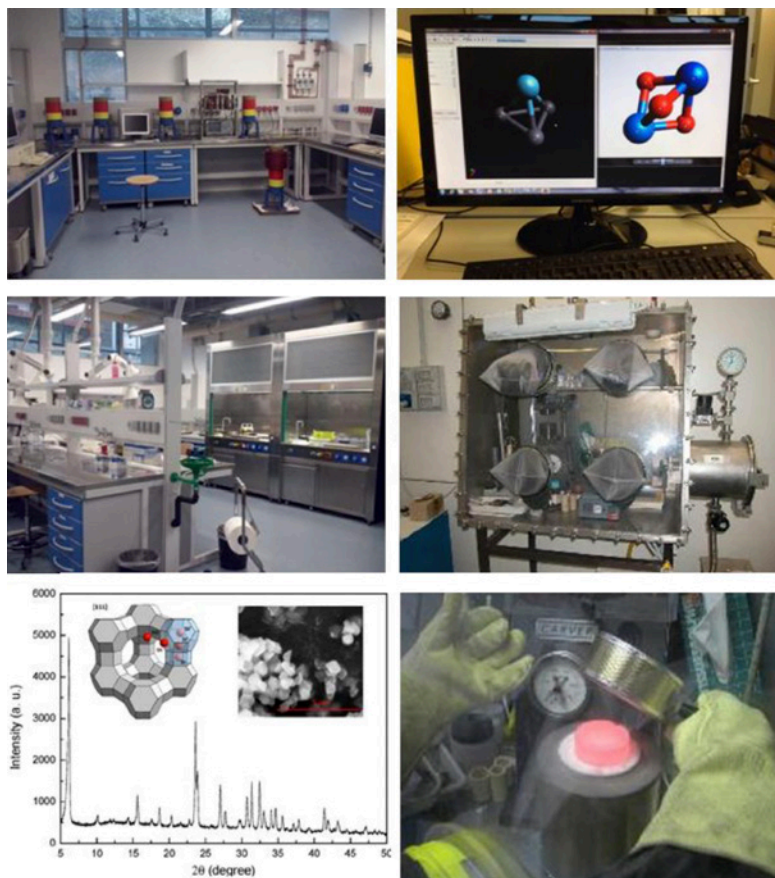


Figure 7. The Integrated Nuclear Laboratories at PoliMi.

Last, but definitely not least, the CIRTEN universities could contribute to the safety assessment of the FFHR different, complementary points of view, namely the analysis of operational transients at different power levels, the identification of the Postulated Initiating Events, based on the peculiar characteristics

of the subcritical assembly, and the ensuing accident analysis of the most relevant scenarios, using for the operational/accident transients both TH and multi-physics codes (like FLUENT, RELAP, FRENETIC, CONSEN [20]), or dedicated codes (like MELCOR 1.8.6-FUS and 2.1) in the case of severe accidents, and the integrated deterministic and probabilistic risk assessment of the entire system [31]-[33].

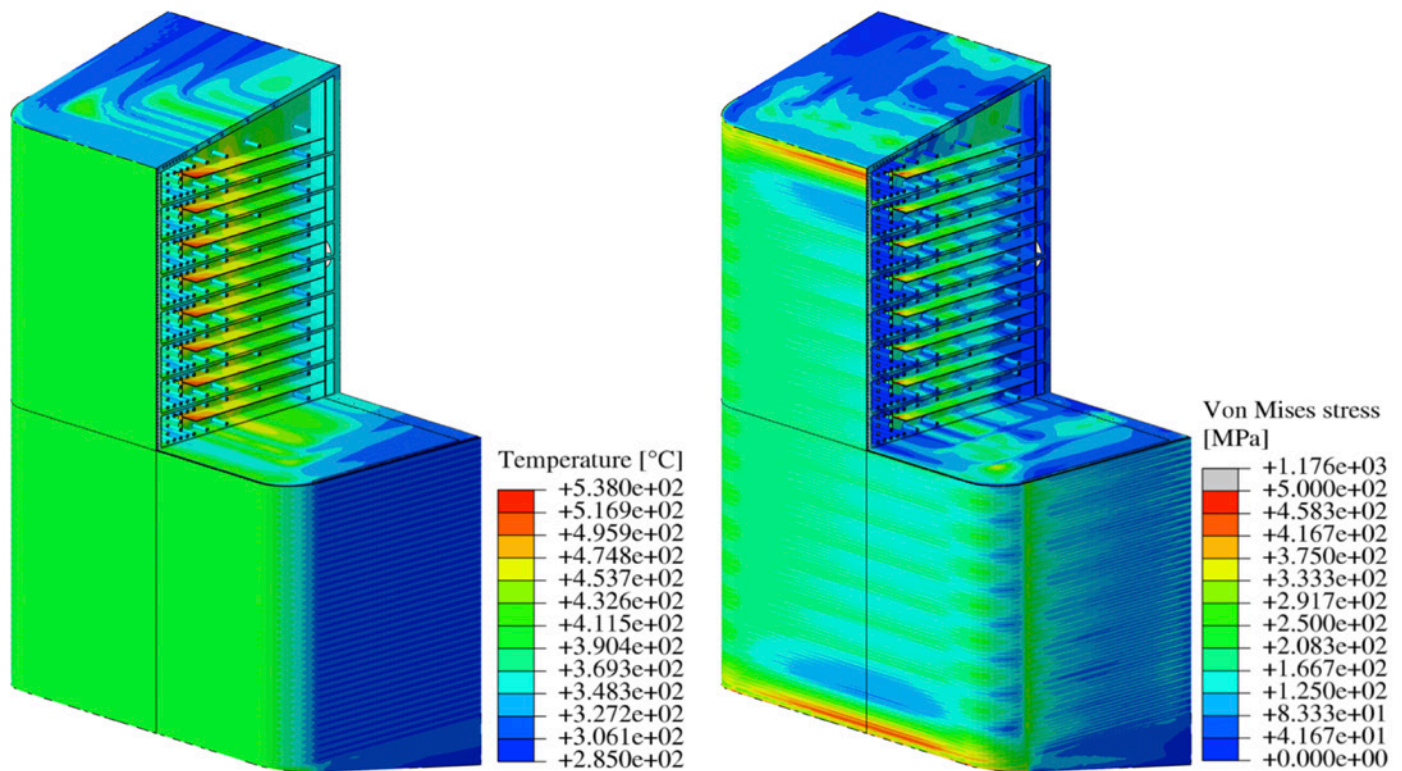


Figure 8. Temperature (left) and Von Mises equivalent stress (right) field distributions in the WCLL equatorial outboard blanket module.

#### 4. Conclusions and perspective

NE programs in CIRTEN universities were born more than 50 years ago and are still alive and quite active, notwithstanding three major NPP accidents in the US, Ukraine and Japan, and two referenda against nuclear power production in our Country, over the last 40 years or so.

The competences of the Italian academic NE community inside the CIRTEN consortium could be interestingly applied to the FFHR, if/when a suitable collaboration framework will be established with the major national and international players.

Considering the long-term nature of all nuclear endeavors (FFHR included ...), it is crucial for the survival of any program not only to confirm but also to increase the support for the education and training of the future generation of nuclear engineers and scientists.

#### References

- [1] H. A. Bethe, The fusion hybrid, *Physics Today* (May 1979) 44-51.
- [2] Y. Wu, et al., Fusion-Fission Hybrids Driven Research in China, Fusion-Fission Research Needs Workshop, Sept. 29-Oct.1, 2009, Gaithersburg, Maryland, USA.
- [3] B. V. Kuteev, et al., Development of DEMO-FNS tokamak for fusion and hybrid technologies, *Nucl. Fusion* 55 (2015) 073035 (8pp).
- [4] J. P. Freidberg, et al., Fusion-fission hybrids revisited, *Nature Physics* 5 (2009) 370-372.
- [5] L. Savoldi Richard, et al., The 4C code for the Cryogenic Circuit Conductor and Coil modeling in ITER, *Cryogenics* 50 (2010) 167-176.
- [6] A. Froio, et al., Dynamic thermal-hydraulic modelling of the EU DEMO HCPB breeding blanket cooling loops, to appear in *Progress in Nuclear Energy* (2016).
- [7] R. Zanino, et al., CFD analysis of a regular sector of the ITER vacuum vessel. Part II: Thermal-hydraulic effects of the nuclear heat load, *Fus. Eng. Des.* 88 (2013) 3248-3262.
- [8] R. Bonifetto, et al., A full core coupled neutronic/thermal-hydraulic code for the modeling of lead-cooled nuclear fast reactors, *Nuclear Eng. Des.* 261 (2013) 85-94.

- [9] D. Caron, et al., Full-core coupled neutronic/thermal-hydraulic modelling of the EBR-II SHRT-45R transient, *Int. J. Energy Res.* (2016) DOI: 10.1002/er.3571.
- [10] V. Lancellotti, et al., TOPICA: an accurate and efficient numerical tool for analysis and design of ICRF antennas, *Nucl. Fusion* 46 (2006) S476-S499.
- [11] S. Dulla, et al., A method for the continuous monitoring of reactivity in subcritical source-driven systems, *Annals of Nuclear Energy* 87 (2016) 1-11.
- [12] S. Dulla, et al., Random effects on reactivity in molten salt reactors, *Annals of Nuclear Energy* 64 (2014) 353-364.
- [13] M. Aufiero, et al., Development of an OpenFOAM model for the Molten Salt Fast Reactor transient analysis, *Chemical Engineering Science* 111 (2014) 390-401.
- [14] A. Pini, et al., Analytical and numerical investigation of the heat exchange effect on the dynamic behaviour of natural circulation with internally heated fluids, *Chemical Engineering Science* 145 (2016) 108-125.
- [15] A. Cammi, et al., The influence of the wall thermal inertia over a single-phase natural convection loop with internally heated fluids, *Chemical Engineering Science* 153 (2016) 411-433.
- [16] P. Chiovaro, et al., Study of the helium-cooled lithium lead test blanket module nuclear behaviour under irradiation in ITER, *Fus. Eng. Des.* 84 (2009) 2178-2186.
- [17] P. A. Di Maio, et al., On the optimization of the first wall of the DEMO water-cooled lithium lead outboard breeding blanket equatorial module, *Fus. Eng. Des.* 109-111 (2016) 335-341.
- [18] S. Kim, et al., Draining and drying process development of the Tokamak Cooling Water System of ITER, *Fus. Eng. Des.* 109-111 (2016) 272-277.
- [19] R. Gatto, et al., Self-consistent electron transport in tokamaks, *Phys. Plasmas* 14 (2007) 092502.
- [20] G. Caruso, et al., Modeling of a confinement bypass accident with CONSEN, a fast-running code for safety analyses in fusion reactors, *Fus. Eng. Des.* 88 (2013) 3263-3271.
- [21] N. Burgio, et al., Monte Carlo simulation analysis of integral data measured in the SCK-CEN/ENEA experimental campaign on the TAPIRO fast reactor. Experimental and calculated data comparison, *Nucl. Eng. Des.* 273 (2014) 350-358.
- [22] M. Cerini, et al., DFT-GGA Prediction of Thermodynamic Parameters in Solid Phase for Binary Compounds of Actinides and Fission Products, *Proceedings Global Nuclear Fuel Cycle for Low-Carbon Future* 5451 (2015) 1361-1366.
- [23] G. De Angelis, et al., Pyroprocess Experiments at ENEA Laboratories, *JNFCWT* 13 (2015) 19-27.
- [24] E. Macerata, et al., Immobilization of radioactive isotopes in fluorapatite matrices, *MRS-Symposia* 1193 (2009) 95-102.
- [25] L. Gozzelino, et al., He-irradiation effects on glass-ceramics for joining of SiC-based materials, *Journal of Nuclear Materials* 472 (2016) 28-34.
- [26] Y. Katoh, et al., Radiation-tolerant joining technologies for silicon carbide ceramics and composites, *Journal of Nuclear Materials* 448 (2014) 497-511.
- [27] M. Ferraris, et al., Effects of neutron irradiation on glass ceramics as pressure-less joining materials for SiC based components for nuclear applications, *Journal of Nuclear Materials* 429 (2012) 166-172.
- [28] B. Bozzini, et al., Corrosion of Stainless Steel Grades in Molten H<sub>2</sub>O/KOH 50% at 120°C: AISI304 Austenitic and 2205 Duplex, *Mater. Corros.* 64 (2013) 988-995.
- [29] B. Bozzini, et al., Corrosion of Stainless Steel Grades in Molten NaOH/KOH Eutectic at 250°C: AISI304 Austenitic and 2205 Duplex, *Mater. Corros.* 63 (2012) 967-978.
- [30] B. Bozzini, et al., Numerical modelling of MCFC cathode degradation in terms of morphological variations, *Int. J. Hydrogen Energy* 36 (2011) 10403-10413.
- [31] E. Zio, Challenges in the vulnerability and risk analysis of critical infrastructures, *Reliability Engineering and System Safety* 152 (2016) 137-150.
- [32] E. Zio, Some challenges and opportunities in reliability engineering, *IEEE Trans. On Reliability* PP (99) (2016) 1-14.
- [33] E. Zio, Integrated deterministic and probabilistic safety assessment: Concepts, challenges, research directions, *Nucl. Eng. Des.* 280 (2014) 413-419.

## 21 - First Wall Lifetime Extension with Flowing Liquid Zone for Fusion Reactors

Sümer ŞAHİN

Faculty of Engineering, Near East University, Turkish Republic of Northern Cyprus  
E - Mails: [sumer.sahin@neu.edu.tr](mailto:sumer.sahin@neu.edu.tr); [sumersahin@yahoo.com](mailto:sumersahin@yahoo.com)

### Abstract

At first, a fusion-fission (hybrid) with a multi-layered spherical blanket has been investigated, which is composed of a first wall made of oxide dispersed steel (ODS, 2 cm); neutron multiplier and coolant zone made of LiPb; ODS-separator (2 cm); a molten salt FLiBe coolant and fission zone; ODS-separator (2 cm); graphite reflector. In the second phase, LiPb coolant zone behind the first wall has been removed, and a flowing liquid protective first wall is included in front of the solid first wall. Without an internal liquid wall protection, major damage mechanisms have been calculated as DPA = 50 and He = 170 appm per year at the ODS first wall.

### Introduction

Innovative concepts with a protective liquid wall inside the fusion plasma chamber can unify several advantages, namely (1) achieving very high neutron load values, (2) along with low maintenance costs due to the largely extended lifetime of the first wall structure (the most sensitive and very expensive component of a fusion reactor), using (3) low cost steels structures, (4) based on wide technological data base, and (5) with a low residual radioactivity. A FLiBe zone of ~ 50 cm thickness as flowing wall liquid protection in front of the solid ODS first wall reduces material damage below permissible limits. It allows shallow burial of structure after final reactor decommissioning.

Controlled fusion energy appears to have potential in providing unlimited energy for mankind. A fusion energy system has attributes of an attractive product with respect to safety and environmental advantages compared to other energy sources and it has clear safety and environmental advantages over fission energy. Fusion fuels are abundantly available in the nature, contrary to relatively scarce fission fuel resources. Hence, growing efforts have been invested in fusion energy research in the past 40 years.

Selection of structural materials plays a key role in enhancing the economic competitiveness of fusion reactors. Structural materials for fusion reactors are subjected to thermal, mechanical, chemical and radiation loads. A selection study for candidate materials may be extrapolated based on the experiences gained from fission reactors only to a very limited degree. The expected conventional loads appear higher for economically competitive fusion reactors. This includes (1) higher operating temperatures, (2) chemically aggressive coolants as energy carrier, such as molten salts, liquid lithium metal or eutectic lithium-lead, lithium-tin, and (3) furthermore magneto-hydro-dynamic effects. In addition to that, nuclear radiation loads for fusion reactors differ greatly from fission reactors. The latter are subjected to fission neutron flux with an average energy ~ 2 MeV and to gamma-ray radiation. In a fusion reactor, first wall around the fusion chamber must withstand to high energetic charged particle fluxes, Bremsstrahlung and gamma-ray radiation, and most importantly to unconventionally high energetic intense neutron fluxes with a mean energy ~ 14 MeV. The latter are expected to lead to much higher material damage than observed by fission reactors, not only due to higher neutron kinetic energy, but also, and even more important due to detrimental threshold reactions for structural materials in MeV range. *Any maintenance and repair work on fusion chamber first wall will cause a long-term plant shutdown and will be very costly.* Hence, a selection study for structural fusion reactor materials must be conducted under consideration of various unconventional aspects. Structural materials of fusion reactors are subjected to unconventional loads, such as higher operating temperatures, chemically aggressive coolants, such as molten salts, liquid lithium metal or eutectic lithium-lead, lithium-tin, and magneto-hydro-dynamic effects. Furthermore, nuclear radiation loads for fusion reactors differ greatly from fission reactors. Especially at the first wall around the fusion chamber must withstand high energetic charged particle fluxes, Bremsstrahlung and gamma-ray radiation, and most importantly high energetic intense neutron fluxes of 14 MeV. Moreover, the structure should be compatible with lithium bearing coolants, such as natural lithium,  $\text{Li}_{17}\text{Pb}_{83}$ ,  $\text{Li}_{25}\text{Sn}_{75}$ ,  $\text{Li}_2\text{BeF}_4$ ,  $\text{NaF}\cdot\text{LiF}\cdot\text{BeF}_2$ ,  $\text{Li}_2\text{BeF}_4 + \text{UF}_4$  and  $\text{Li}_2\text{BeF}_4 + \text{ThF}_4$ . A protective flowing liquid wall between plasma and solid first wall in these reactors can relax to a great degree the material selection. In this work, the nuclear waste actinide transformation, breeding capability of fusion hybrids, different structural materials and the effects of a protective flowing liquid wall are subject of investigations.

### Structural materials

Structural materials of fusion reactors are subjected to thermal, mechanical, chemical and radiation loads during reactor operation. Information and experiences coming from fission reactors related to the performance of structural materials

can only be used at a very limited degree in material selection for fusion reactors as the expected loads will be higher for fusion reactors. This involves higher operating temperatures, chemically aggressive coolants, such as molten salts, liquid lithium metal or eutectic lithium–lead, lithium–tin, and magneto-hydro-dynamic effects. Furthermore, nuclear radiation loads for fusion reactors differ greatly from fission reactors. The latter are subjected to fission neutron flux with an average energy of ~2 MeV and to gamma-ray radiation. However, structural material of fusion reactor, especially at the first wall around the fusion chamber must withstand high energetic charged particle fluxes, Bremsstrahlung and gamma-ray radiation, and most importantly high energetic intense neutron fluxes with a mean energy of 14 MeV, which are expected to lead to much higher material damage than observed by fission reactors, not only due to higher neutron kinetic energy, but also, and even more important due to detrimental threshold reactions for structural materials in MeV range. Moreover, the structure should be compatible with lithium bearing coolants; natural lithium,  $\text{Li}_{17}\text{Pb}_{83}$ ,  $\text{Li}_{25}\text{Sn}_{75}$ ,  $\text{Li}_2\text{BeF}_4$ ,  $\text{NaF}\cdot\text{LiF}\cdot\text{BeF}_2$ ,  $\text{Li}_2\text{BeF}_4 + \text{UF}_4$  and  $\text{Li}_2\text{BeF}_4 + \text{ThF}_4$ . In addition to those, the structural material should have the properties given briefly as below:

- 1) Attractive high temperature physical and mechanical properties, i.e., tensile strength, creep strength, impact toughness, and fatigue.
- 2) Reliable, predictable behavior for low rate deterioration of materials properties (ageing, corrosion), and tolerance for overloads.
- 3) Short repair and replacement periods.
- 4) Stability and recirculation for renewed application.
- 5) Suitability for shallow burial. Compatibility of the Activation criteria with 10CFR61 regulations
- 6) Broad compatibility with cooling fluids and gases.
- 7) Low neutron absorption cross sections.
- 8) Easy fabrication with multiple processes.
- 9) Acceptable inspectability of components.
- 10) Resistant to 14 MeV neutrons induced displacement damage (strength, ductility and toughness).
- 11) High heat conductivity, independent of radiation damage level.
- 12) Low swelling or void formation, dimensional stability.
- 13) Adequate mechanical properties before and after irradiation.
- 14) Operation at a wide temperature window.
- 15) Working at high temperatures.
- 16) Resistant to atomic displacement and helium generation damage.
- 17) Low activation property under 14 MeV neutrons.

Various engineering materials; austenitic stainless steels, ferritic/martensitic steels, vanadium alloys, refractory metals and composites have been suggested as candidate structural materials for nuclear fusion reactors. Among these structural materials, austenitic steels have an advantage of extensive technological database and lower cost compared to other non-ferrous candidates. Furthermore, they have also advantages of very good mechanical properties and fission operation experience. Moreover, modified austenitic stainless (Ni and Mo free) have relatively low residual radioactivity. Nevertheless, they can't withstand high neutron wall load which is required to get high power density in fusion reactors. On the other hand, a protective flowing liquid wall between plasma and solid first wall in these reactors can eliminate this restriction.

Material damage types under neutron irradiation can be cited as;

- A) Microscopic radiation damage effects
  - \* Atomic displacement under neutron irradiation (DPA).
  - \* Gas production "(n,p); (n,d); (n,t); (n, $\alpha$ )".
  - \* Nuclear transmutation (Foreign atoms production).
  - \* Micro melting: local formation of hard, brittle martensite!
  - \* Ionization effects of gamma rays, or charged particles (insulators, dielectrics, plastics, lubricants, hydraulic fluids, and rubber are sensitive to ionization).

Main macroscopic radiation damage effects are:

- \* High-temperature embrittlement: Dimensional changes; swelling and irradiation creep. ( $> 0.5 T_M$ )
- \* Low-temperature embrittlement: agglomeration by radiation-induced defects, increase in the yield stress! ( $< 0.5 T_M$  "melting temperature in °K). Shift in the DBTT "Ductile-Brittle Transition Temperature".
- \* Degradation of material properties

Table I shows the temperature range of the main macroscopic radiation damage effects.

## Numerical calculations

The calculations are conducted for a fusion power generation of 1 GW<sub>el</sub> over 30 years of reactor operation with a thermos-dynamical conversion efficiency of 35 % leading to 2.857 GW<sub>th</sub> by a capacity factor of 100 %. One of the candidates as structural material is the oxide dispersed steel (ODS).

At first, a fusion-fission (hybrid) with a multi-layered spherical blanket has been investigated, which is composed of a first wall made of oxide dispersed steel (ODS, 2 cm); neutron multiplier and coolant zone made of LiPb; ODS-separator (2 cm); a molten salt FLIBE coolant and fission zone; ODS-separator (2 cm); graphite reflector. In the second phase, LiPb coolant zone behind the first wall has been removed. But instead, a flowing liquid protective first wall is included in front of the solid first wall in order to reduce material damage and residual radioactivity after final disposal of the latter. Without an internal

liquid wall protection, major damage mechanisms have been calculated as DPA = 50 and He = 170 appm per year at the ODS first wall. This will oblige to change the ODS first wall every ~ 3 years. Hydrogen production is calculated as 650 appm/year. Hydrogen will diffuse out of the structure by high operation temperatures. The alternative version to include a FLIBE zone of ~ 50 cm thickness as flowing wall liquid protection in front of the solid ODS first wall reduces material damage below permissible limits. It allows shallow burial of structure after final reactor decommissioning.

SS-304 type steel, SiC and graphite were also selected as structural materials of a magnetic fusion energy (MFE) reactor. Different types of liquid coolant with tritium breeding capabilities (FLIBE, Li<sub>17</sub>Pb<sub>83</sub>, natural lithium, all with natural lithium component) are investigated to protect the first wall from neutron- and Bremsstrahlung radiation and fusion reaction debris. With SS-304 as structural material, calculations have led to the following liquid wall thickness requirements under consideration of the mainline design criteria:

1. ~ 60 cm FLIBE, ~ 160 cm Li<sub>17</sub>Pb<sub>83</sub>, ~ 180 cm natural lithium and for material protection measured on displacement per atom (DPA < 100 after 30 years of operation), and ~ 60 cm FLIBE, ~ 60 cm Li<sub>17</sub>Pb<sub>83</sub>, ~ 150 cm natural lithium measured on helium gas production (He < 500 appm after 30 years of operation),
2. ~ 40 cm FLIBE, ~ 80 cm Li<sub>17</sub>Pb<sub>83</sub>, ~ 40 cm natural lithium for sufficient tritium breeding (TBR = 1.1),
3. ~ 50 cm FLIBE, ~ 160 cm Li<sub>17</sub>Pb<sub>83</sub>, ~ 140 cm natural lithium for a shallow burial index (SBI = 1).

Such a blanket would strongly reduce the shielding for super conducting coils around the fusion plasma chamber and would open the possibility of utilization of conventional stainless steel for fusion reactors due to the sufficiently low residual radioactivity in the structural materials after decommissioning of the plant.

Utilization of the molten salt mixture FLIBE+ThF<sub>4</sub> produces a precious nuclear fuel <sup>233</sup>U with a conservative value of 300,000 \$/kg. The additional revenue through fuel production can become 360, 600 and 825 M\$/a for 2% ThF<sub>4</sub>, 4% ThF<sub>4</sub> and 6% ThF<sub>4</sub> content, respectively, reducing the total electricity cost per kWh significantly. With the molten salt FLIBE+UF<sub>4</sub> and for a market value of 80 M\$/kg for <sup>239</sup>Pu, the additional revenue through fuel production becomes 90 M\$/a for 2% nat-UF<sub>4</sub> and can increase up to 400 M\$/a for 12% UF<sub>4</sub> content. The lower fuel revenue with nat-UF<sub>4</sub> is amply compensated through the significant energy amplification and more electricity generation for the same fusion power production.

## Conclusions

We have also investigated the ferritic steel (9Cr-2WVtTa), the vanadium alloy (V-4Cr-4Ti) and the SiC<sub>f</sub>/SiC composite also as structural materials for fusion reactors. A protective liquid wall with variable thickness, containing FLIBE + heavy metal salt (UF<sub>4</sub> or ThF<sub>4</sub>) is used for first wall protection. The content of heavy metal salt is chosen as 4 and 12 mol%. A flowing wall with a thickness of ~ 60 cm can extend the lifetime of the solid first wall structure to a plant lifetime of 30 years for 9Cr-2WVtTa and V-4Cr-4Ti, whereas the SiC<sub>f</sub>/SiC composite as first wall needs a flowing wall with a thickness of ~ 85 cm to maintain the radiation damage limit.

Effect	Temperature	Important for
segregation and changes in precipitation structure	$T > 0.2 T_M$	Corrosion, weldability
increase of DBTT	$0.1 T_M < T < 0.3 T_M$	BCC steels and refractory alloys for pressure vessels
Irradiation creep under mechanical load	$0.2 T_M < T < 0.4 T_M$	Most nuclear materials
Irradiation growth	$0.1 T_M < T < 0.3 T_M$	Non-cubic materials (Zr and its alloys, U, graphite)
Void swelling	$0.3 T_M < T < 0.5 T_M$	Austenitic steels
Helium high temperature embrittlement under creep and fatigue loads	$T > 0.45 T_M$	First wall structures

## 22 - Thorium blanket driven by fusion neutron source: generation for fission reactors of a unique fuel characterized by super high fuel burn-up

G.G. Kulikov\*, A.N. Shmelev, E.G. Kulikov, V.A. Apse

National Research Nuclear University MEPhI (Moscow Engineering Physics Institute),  
Departments of "Theoretical and experimental physics of nuclear reactor" and "Technology of closed nuclear fuel cycle"

\*Corresponding author: ggkulikov@mephi.ru

### Abstract

The paper considers neutron-physical peculiarities of nuclear fuel generation in thorium blanket of Fusion Neutron Source (FNS). It is demonstrated that nuclear fuel generated in thorium FNS blankets is characterized by very stable neutron-multiplying properties during LWR lifetime and enhanced proliferation resistance. Involvement of thorium-blanketed FNS into an international closed nuclear fuel cycle (NFC) can offer some significant advantages.

### Introduction

Traditionally, technology of controlled thermonuclear fusion (CTF) was considered and is being considered now as a practically inexhaustible energy resource. However, development, mastering and wide deployment of fast breeder reactors with closed NFC can substantially extend fuel base of nuclear power industry (NPI) up to unlimited scales. Under these conditions, it seems reasonable to introduce the works oriented on some principal problems of large-scale NPI with closed NFC into a circle of main CTF-related studies. The following two problems may be mentioned here.

The first problem concerns a scale of operations in NFC back-end that could be decreased by significantly deeper fuel burn-up in nuclear power reactors. As it was shown in Ref. 1, the use of ( $^{231}\text{Pa}$ - $^{232}\text{U}$ - $^{233}\text{U}$ -Th)-based fuel in LWR opens a possibility to reach high (up to 30% HM) and even ultra-high values of fuel burn-up.

The second problem concerns proliferation resistance of fissile materials in closed NFC. As is known, remarkable content of  $^{232}\text{U}$  in uranium fraction can form a really insurmountable barrier against unauthorized diversion of such a fuel from energy utilization to illegal purposes.

As it was shown in our studies [2-3], FNS involvement into NFC structure can render a fruitful assistance in resolving these problems. It seems reasonable to recognize that main FNS mission in NFC should be not energy generation but production of advanced fuel with specific nuclide compositions for nuclear power reactors.

### 1. Neutron-physical peculiarities of fuel generation in FNS blankets

#### 1.1. Inter-comparison of thorium and uranium blanket

As is known, the FNS concepts presume that high-energy fusion neutrons from (D,T)-reaction ( $E_n = 14.1$  MeV) are used to irradiate uranium or thorium in FNS blanket. Just thorium blanket allows to demonstrate with the most brightness high potential of fusion neutrons in threshold (n,2n)- and (n,3n)-reactions because micro cross-sections of these reactions for  $^{232}\text{Th}$  are larger than those for  $^{238}\text{U}$ . At the same time, fission cross-sections of  $^{232}\text{Th}$  are substantially lower than those of  $^{238}\text{U}$  (see Figs. 1 and 2).

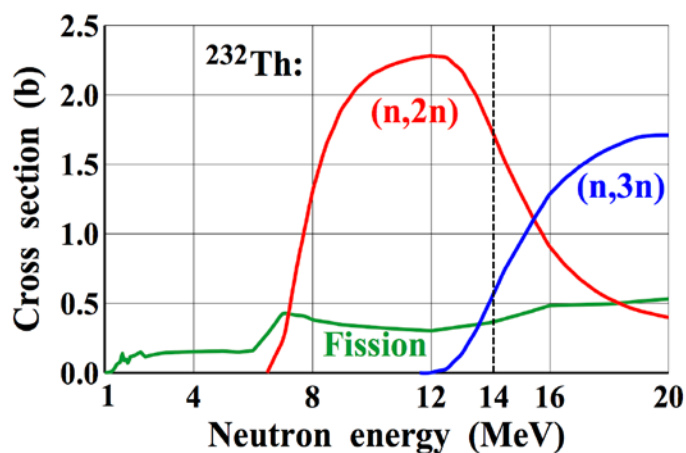


Fig. 1. Energy dependencies of fission cross-section and cross-sections of threshold (n,2n)- and (n,3n)-reactions for  $^{232}\text{Th}$

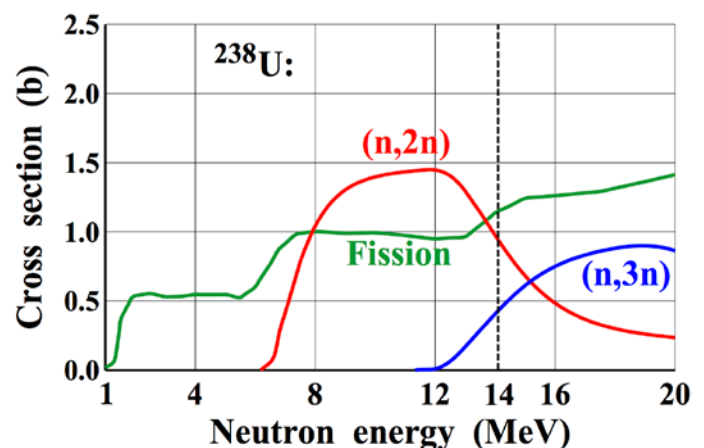


Fig. 2. Energy dependencies of fission cross-section and cross-sections of threshold (n,2n)- and (n,3n)-reactions for  $^{238}\text{U}$

Some experimental data [4-7] on bombardment of  $^{232}\text{Th}$  and  $^{238}\text{U}$  by fusion neutrons are pre-sented in Table 1. These results confirm the relationships between micro cross-sections.

Reaction	Thorium experiment	Reaction*	Uranium experiment
$^{232}\text{Th}(n,2n)\dots^{231}\text{Pa}$ ,	$0.42 \pm 0.04$	$^{238}\text{U}(n,2n)\dots^{237}\text{Np}$	$0.277 \pm 0.008$
$^{232}\text{Th}(n,3n),^{230}\text{Th}$	$0.30 \pm 0.05$	$^{238}\text{U}(n,3n),^{236}\text{U}$	$0.327 \pm 0.052$
$^{232}\text{Th}(n,f)$	$0.174 \pm 0.01$	$^{238}\text{U}(n,f)$	$1.18 \pm 0.06$
		$^{235}\text{U}(n,f)^*$	$0.281 \pm 0.017$
$^{232}\text{Th}(n,\gamma)\dots^{233}\text{U}$	$1.63 \pm 0.10$	$^{238}\text{U}(n,\gamma)\dots^{239}\text{Pu}$	$4.08 \pm 0.24$
Neutron leakage	$0.78 \pm 0.04$	Neutron leakage	$0.41 \pm 0.02$

\*) Metal natural uranium (0.71%  $^{235}\text{U}$ ) was irradiated in experimental assemblies [6, 7]

Table 1 - Reaction rates (per one 14-MeV neutron) in experimental thorium and uranium assemblies

As it follows from micro cross-sections and experimental data presented above, fusion neutrons are multiplied in thorium FNS blanket preferably by threshold (n,xn)-reactions while fusion neutrons are multiplied in uranium FNS blanket by chain fission reactions. Saying by another words, the yields of ( $^{231}\text{Pa}+^{230}\text{Th}$ ) nuclides in thorium FNS blanket (essentially, in fresh FNS blanket) per one fission or per two nuclei of fission products are larger than the yields of ( $^{237}\text{Np}+^{236}\text{U}$ ) nuclides in uranium FNS blanket. All these nuclides are produced through threshold channels in both blankets. This also means that energy generation in thorium FNS blanket (per one (D,T)-reaction) is lower than that in uranium FNS blanket. It should be noted that design of FNS blanket with weak energy generation rate is substantially simpler and better from economical viewpoint. Neutron-multiplying properties of the secondary  $^{233}\text{U}$ -containing fuel produced in thorium FNS blanket can provide the better fuel for thermal reactors than the secondary Pu-containing fuel produced in uranium FNS blanket [8].

## 1.2. Chains of nuclide transformations under thorium irradiation in FNS blanket

The following chains of nuclide transformations can be initiated in thorium FNS blanket under FNS operation (Fig. 3):

1. "Traditional" chain that begins from neutron capture by thorium, the capture channel:
  - $^{232}\text{Th}(n,\gamma)\dots^{233}\text{Pa}(\beta^-, T_{1/2}=27\text{ days})^{233}\text{U}(n,\gamma)^{234}\text{U}(n,\gamma)\dots$
2. "Non-traditional" chain that begins from threshold  $^{232}\text{Th}(n,2n)$  and  $^{232}\text{Th}(n,3n)$ -reactions, the threshold channel:
  - $^{232}\text{Th}(n,2n)^{231}\text{Th}(\beta^-, T_{1/2}=26\text{ hours})^{231}\text{Pa}(n,\gamma)^{232}\text{Pa}(\beta^-, T_{1/2}=1.3\text{ days})^{232}\text{U}(n,\gamma)^{233}\text{U}(n,\gamma)\dots$
  - $^{232}\text{Th}(n,3n)^{230}\text{Th}(n,\gamma)^{231}\text{Th}(\beta^-, T_{1/2}=26\text{ hours})^{231}\text{Pa}(n,\gamma)^{232}\text{U}(n,\gamma)\dots$

Besides  $^{233}\text{U}$ , these reactions can produce  $^{231}\text{Pa}$  and  $^{232}\text{U}$  in irradiated thorium. It can be seen from Table 1 that intensities of threshold (n,2n)- and (n,3n)-reactions are at the level of 40% from intensity of the capture channel leading to generation of main fissile isotope  $^{233}\text{U}$ .

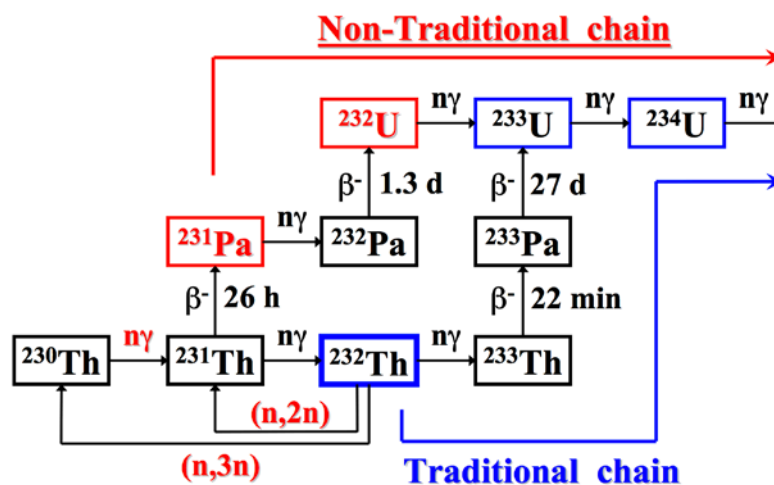


Fig. 3. Chains of nuclide transformations in thorium FNS blanket

### 1.3. Nuclide composition of fuel generated in thorium FNS blanket

As it can be seen from Table 2 [9], the longer irradiation time of thorium can result in larger content of  $^{230}\text{Th}$  and  $^{231}\text{Pa}$ . Nuclide  $^{231}\text{Pa}$  can be extracted from irradiated thorium by radiochemical technologies while nuclide  $^{230}\text{Th}$  remains in total thorium mass. This indicates on reasonability of multiple thorium recycling in FNS blanket for further generation of  $^{231}\text{Pa}$ .

Nuclide	Irradiation time, days <sup>1)</sup>				
	200	400	600	800	1000
$^{230}\text{Th}$	0.29	0.58	0.87	1.15	1.43
$^{232}\text{Th}$	997.	993.	989.	986.	982.
$^{231}\text{Pa}$	0.68	1.30	1.85	2.33	2.75
$^{233}\text{Pa}$ <sup>2)</sup>	0.45	0.46	0.46	0.47	0.47
$^{232}\text{U}$	0.03	0.13	0.29	0.51	0.78
$^{233}\text{U}$	1.77	3.94	6.09	8.23	10.3
$^{234}\text{U}$	0.0034	0.014	0.033	0.058	0.09
Fission products	0.51	4.54	6.87	9.27	11.64

1) Neutron load on the first wall - 1 MW/m<sup>2</sup>

2) Nuclide  $^{233}\text{Pa}$  transforms into  $^{233}\text{U}$  through  $\beta$ -decay with  $T_{1/2} = 27$  days

Table 2 - Nuclide composition of fuel generated in thorium FNS blanket, kg/ton Th

It can be also seen in Table 3 [9] that the content of  $^{232}\text{U}$  in uranium fraction reaches a rather significant value. Uranium fraction in irradiated thorium may be called as a "unique highly enriched uranium" because of the following reasons:

1. Uranium fraction contains above 90% of fissile nuclide  $^{233}\text{U}$ .
2. Uranium fraction contains unprecedented large content of other uranium nuclide  $^{232}\text{U}$  (at the level of several percents).
3. Uranium fraction contains negligibly small content of heavier uranium nuclides -  $^{234}\text{U}$  and  $^{235}\text{U}$ .

Nuclide	Irradiation time, days				
	200	400	600	800	1000
$^{232}\text{U}$	1.5	2.86	4.22	5.50	6.70
$^{233}\text{U}$	98.2	96.9	95.3	93.9	92.5
$^{234}\text{U}$	$1.5 \cdot 10^{-3}$	$3.1 \cdot 10^{-3}$	$4.8 \cdot 10^{-3}$	$6.3 \cdot 10^{-3}$	$7.7 \cdot 10^{-3}$
$^{235}\text{U}$	$0.2 \cdot 10^{-5}$	$0.9 \cdot 10^{-5}$	$2.0 \cdot 10^{-5}$	$3.6 \cdot 10^{-5}$	$5.6 \cdot 10^{-5}$

Table 3 - Nuclide composition of fuel generated in thorium FNS blanket, %

### 1.4. $^{231}\text{Pa}$ - $^{232}\text{U}$ - $^{233}\text{U}$ chain of nuclide transformations with gradual improvement of neutron-multiplying properties

In traditional (U-Pu) and (Th-U) fuel of nuclear reactors nuclides with neutron-multiplying ( $^{233}\text{U}$ ,  $^{235}\text{U}$ ,  $^{239}\text{Pu}$ ,  $^{241}\text{Pu}$ ) and neutron-absorbing ( $^{234}\text{U}$ ,  $^{236}\text{U}$ ,  $^{240}\text{Pu}$ ,  $^{242}\text{Pu}$ ) properties alternate. That is why neutron irradiation of traditional fuels in nuclear reactors decreases content of fissile nuclides and increases content of neutron-absorbing nuclides. As a result, reactivity and the value of fuel burn-up is decreased. On the contrary, if nuclide  $^{231}\text{Pa}$  generated in thorium FNS blanket is introduced into fuel composition, then the following chain of successive nuclide transformations with gradual improvement of neutron-multiplying properties can be initiated:  $^{231}\text{Pa}$  – the burnable neutron absorber,  $^{232}\text{U}$  – nuclide with moderate neutron-multiplying properties,  $^{233}\text{U}$  – nuclide with excellent neutron-multiplying properties. Unique feature of the chain consists in neutron coupling of two well-fissile nuclides  $^{232}\text{U}$ - $^{233}\text{U}$ .

Nuclide  $^{231}\text{Pa}$  can be used as a burnable neutron absorber. Micro cross-sections of radiative neutron capture are presented in Table 4 for  $^{231}\text{Pa}$  and, for comparison, for well-known burnable neutron absorber  $^{157}\text{Gd}$ , as well as for well-known fertile nuclides  $^{238}\text{U}$  и  $^{232}\text{Th}$  confirm ability of  $^{231}\text{Pa}$  to act as a burnable neutron absorber.

As is seen, radiative capture cross-sections of  $^{231}\text{Pa}$  in thermal and resonance energy

Nuclide	$\sigma_c$ (2200 m/s), barn	Resonance integral, barn
$^{157}\text{Gd}$	253 254.	784.
$^{231}\text{Pa}$	202.	540.
$^{238}\text{U}$	2.68	275.
$^{232}\text{Th}$	7.34	83.8

Table 4 - Micro cross-sections of thermal neutron capture and resonance integral

ranges are substantially larger than those of fertile nuclides  $^{238}\text{U}$  and  $^{232}\text{Th}$ , but remarkably lower than those of  $^{157}\text{Gd}$ . So, even small admixture (several percents) of nuclide  $^{231}\text{Pa}$ , being introduced into fresh fuel composition, can reduce initial reactivity margin thanks to large cross-sections of radiative neutron capture. However, radiative capture cross-sections of  $^{231}\text{Pa}$  are lower than those of  $^{157}\text{Gd}$ . As a result, content of  $^{231}\text{Pa}$  will be depleted slower than that of  $^{157}\text{Gd}$ . This can be regarded as a favorable factor because stabilization of neutron-multiplying properties can be prolonged up to the larger values of fuel burn-up.

Those neutrons which were captured by  $^{231}\text{Pa}$  will come back to the chain fission reaction via fission reactions of daughter nuclides. The first of them,  $^{232}\text{U}$  is a moderate fissile nuclide because its fission cross-sections are significantly lower than those of  $^{235}\text{U}$  and because fission cross-sections and radiative capture cross-sections are comparable each other in thermal and resonance ranges of neutron energy.

In the case of radiative neutron capture nucleus  $^{232}\text{U}$  can not be considered as a lost one because nucleus  $^{232}\text{U}$  converts into nucleus  $^{233}\text{U}$ , i.e. into well-known high-efficient fissile nuclide.

Thus, the nuclide transformations listed above will result in successive improvement of neutron-multiplying properties. Such the improvement, in competition with accumulation of fission products – neutron absorbers, can promote stabilizing neutron-multiplying properties of fuel during full reactor lifetime.

## 2. Physical parameters of LWR with ultra-long fuel lifetime

Numerical evaluations were carried out with application of the computer code package SCALE-4.3, widely used in the LWR licensing process. The governing module SAS2H was used to determine physical parameters of one-dimensional infinite lattice of fuel elements and to study evolution of nuclide fuel composition under irradiation. Neutron transport in an elementary cell was calculated in S8-approximation. The number of inner iterations was chosen to determine infinite neutron multiplication factor  $K_\infty$  with accuracy  $10^{-5}$ . Nuclide fuel composition was re-calculated with time interval of four years with accounting for 43 fission products having the most influence on reactivity. The 44-group library of micro cross-sections was generated from the evaluated nuclear data file ENDF/B-IV by the computer code AMPX. The number of secondary fission neutrons emitted by  $^{232}\text{U}$  was corrected according to the recommendations given in Ref. 10.

### 2.1. Neutron-physical grounds for reaching high values of fuel burn-up

Time evolutions of LWR reactivity are presented in Fig. 4 for VVER-type reactor loaded with traditional uranium dioxide fuel and with non-traditional nitride thorium fuel. As is seen, if traditional uranium dioxide fuel (4.4%  $^{235}\text{U}$ ) is used in LWR, then neutron multiplication factor monotonously drops down from  $K_\infty = 1.38$  to  $\sim 1$  at fuel burn-up of 4.2% HM (curve 1). Roughly the same result was obtained for LWR loaded with nitride  $^{232}\text{Th}$ - $^{233}\text{U}$  fuel containing 5.3%  $^{233}\text{U}$  (curve 2). Time evolution of LWR reactivity radically changes when  $^{231}\text{Pa}$ , the mother nuclide for linked pair of fissile nuclides  $^{232}\text{U}$ - $^{233}\text{U}$ , is introduced into fresh thorium-based fuel composition. Five options of fresh fuel compositions with different contents of  $^{231}\text{Pa}$  were considered. These options can be divided into the following two groups: the first group includes the options 3-6, the second group includes the option 7 (see Fig. 4).

In options 3-6 fraction of  $^{232}\text{Th}$  in fuel composition is a constant value, 69%. Nuclides  $^{231}\text{Pa}$  and  $^{233}\text{U}$  occupy the remaining 31%. As is seen in Fig. 4, high fuel burn-up (30% HM) can be reached without  $^{231}\text{Pa}$  (curve 3), but this requires extremely large content of main fissile isotope (31%  $^{233}\text{U}$ ) in fresh fuel composition. Evidently, this option is scarcely acceptable from the reactor safety point of view because of too large initial reactivity margin ( $K_\infty = 1.91$ ). Substitution of 5%  $^{231}\text{Pa}$  for 5%  $^{233}\text{U}$  (curve 4) reduces initial reactivity margin ( $K_\infty = 1.61$ ) for the same fuel burn-up (30% HM). Substitution of 10%  $^{231}\text{Pa}$  for 10%  $^{233}\text{U}$  (curve 5) reduces initial reactivity margin down to  $K_\infty = 1.37$ , roughly the standard value for  $\text{UO}_2$ -fuelled LWR. If fractions of  $^{233}\text{U}$  and  $^{231}\text{Pa}$  in nitride fuel are approximately the same (curve 6), then initial neutron multiplication factor is a rather moderate value ( $K_\infty = 1.1$ ), but sufficient to compensate neutron leakage and control the

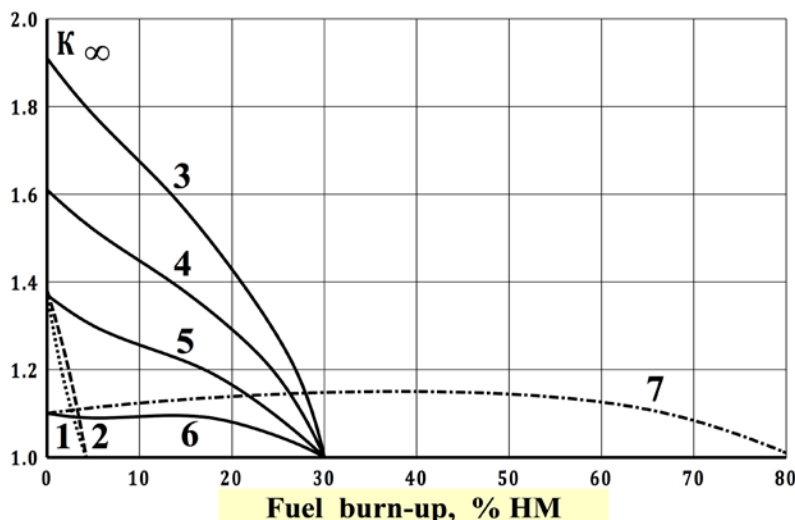


Fig. 4. Dependencies of neutron-multiplying properties on fuel burn-up for different fuel types

- 1 - (4.4% $^{235}\text{U}$ +95.6% $^{238}\text{U}$ ) $\text{O}_2$ ,
- 2 - (5.33% $^{233}\text{U}$ +94.67% $^{232}\text{Th}$ )N,
- 3 - (0% $^{231}\text{Pa}$ +31% $^{233}\text{U}$ +69% $^{232}\text{Th}$ )N,
- 4 - (5% $^{231}\text{Pa}$ +26% $^{233}\text{U}$ +69% $^{232}\text{Th}$ )N,
- 5 - (10% $^{231}\text{Pa}$ +21% $^{233}\text{U}$ +69% $^{232}\text{Th}$ )N,
- 6 - (15% $^{231}\text{Pa}$ +16% $^{233}\text{U}$ +69% $^{232}\text{Th}$ )N,
- 7 - (61% $^{231}\text{Pa}$ +39% $^{233}\text{U}$ +0% $^{232}\text{Th}$ )N.

reactor operation. Neutron-multiplying properties of this fuel do not practically change up to ~ 17% HM, then neutron multiplication factor smoothly drops down to  $K_{\infty} = 1.0$  at fuel burn-up of 30% HM. This fuel composition is a superior to other fuel compositions because of very smooth reactivity evolution with fuel burn-up. These options demonstrated the stabilization effect of neutron-multiplying properties in the process of fuel burn-up, and the stabilization effect is mainly caused by the growing role of  $^{231}\text{Pa}$ - $^{232}\text{U}$ - $^{233}\text{U}$  chain of nuclide transformations.

One else option (curve 7 in Fig. 4) describes, in opinion of authors, maximal achievable value of fuel burn-up, of course, under assumptions mentioned above, i.e. for the certain reactor type and fuel type [11]. In this option fraction of  $^{231}\text{Pa}$  in fresh fuel composition was chosen so to provide initial neutron multiplication factor  $K_{\infty} = 1.1$ . As nuclide  $^{231}\text{Pa}$  plays here the roles of burnable neutron absorber and, at the same time, neutron predecessor of two fissile nuclides ( $^{232}\text{U}$  and  $^{233}\text{U}$ ), it becomes possible to reach ultra-high value of fuel burn-up (~ 80% HM), when neutron multiplication factor drops down to  $K_{\infty} = 1.0$ . As is seen in Fig.4, time evolution of neutron multiplication factor in this option represents a very smooth curve that reaches maximal value ( $K_{\infty} = 1.15$ ) at fuel burn-up of 35% HM and comes back to  $K_{\infty} = 1.1$  at fuel burn-up of 67% HM.

## 2.2. Advantages of the higher fuel burn-up

The following benefits could be obtained from the use of nuclear fuels with stabilized neutron-multiplying properties up to high values of fuel burn-up. The first of all, the scope of technological operations related with fuel fabrication, fuel transportation and the reactor refueling may be radically shortened. For example, if traditional LWR fuel with typical values of fuel burn-up at the level of 4-6% HM is replaced by fuel with fuel burn-up about 30% HM, then the scope of technological operations listed above could be reduced by a factor of 5-7.

In addition to economical profits, the lower number of the reactor refuelings means that the number of operations, where fissile nuclides could be diverted from peaceful use to military purposes, decreases too. So, NFC protection against unauthorized proliferation of the weapon-usable materials could be enhanced.

One else factor, namely accumulation of  $^{232}\text{U}$  in uranium fraction, can significantly impede the use of such an uranium in nuclear weapons. Nuclide  $^{232}\text{U}$  is a powerful and long-lived source of alpha-radiation ( $T_{1/2} = 68.9$  years). Intensity of the radiation source increases with time because gradual build-up of radioactive daughter products of  $^{232}\text{U}$  decays. Intense alpha-radiation can impede application of the gas centrifuges for uranium isotope separation, i.e. for removal of  $^{232}\text{U}$  and for uranium enrichment with  $^{235}\text{U}$ . Besides,  $^{232}\text{U}$  is a powerful heat source (830 W/kg), that could overheat vital components of nuclear explosive devices (NED). High-energy gamma-radiation emitted by daughter products of  $^{232}\text{U}$  decays will require developing a dedicated distant technology for handling with nuclear charge made of uranium with relatively high content of  $^{232}\text{U}$ . Nuclide  $^{232}\text{U}$  is a powerful source of spontaneous fission neutrons (1300 n/s.kg). In addition, alpha-particles emitted by  $^{232}\text{U}$  are able to generate neutrons in ( $\alpha,n$ )-reactions with light chemical elements, impurities of fissile materials. As is known [12], energy yield of the NED charged with such uranium may be drastically decreased because spontaneous fission neutrons and neutrons from ( $\alpha,n$ )-reactions are able to provoke premature initiation of the chain fission reaction (pre-detonation of NED).

## 3. About our concept of the international closed NFC

The GNEP (Global Nuclear Energy Partnership) concept [13, 14] is based on the following organizational presumptions:

1. The international closed NFC.
2. Nuclear power units all over the world are fed by natural and regenerated uranium.
3. Excessive plutonium is completely eliminated in the dedicated plutonium incinerators.
4. The plutonium incinerators must be placed within the territory of the international centers in order to ensure the plutonium non-proliferation.

The GNEP concept is characterized by the following three unfavorable peculiarities:

1. Although the GNEP concept is oriented on wide use of cheap uranium resources, the concept implies future transition to artificial plutonium-based fuel. Two options arise: either full plutonium NFC must be embraced by the international centers or plutonium must be made proliferation-protected for its peaceful utilization outside of the international centers. Both alternatives are very difficult to implement.
2. As is known, incineration of one uranium ton in U-fuelled LWR can generate about 300 kg Pu. Energy utilization of the generated plutonium means that about 30% of global nuclear power must be concentrated within the international centers. This will be an unprecedented concentration of nuclear power plants even for the today NPI scale [15].
3. World-wide deployment of gas centrifuges for isotope separation of natural uranium could make (or already made) low-enriched uranium the most attractive material for its conversion into highly-enriched, weapon-grade uranium [16]. So, low-enriched uranium in fresh fuel assemblies of nuclear power plants must be reliably proliferation-protected.

Involvement of thorium-blanketed FNS into structure of the international centers can smooth these unfavorable peculiarities of the GNEP concept. Layout of the proposed international closed NFC is shown in Fig. 5. The NFC embraces the international centers for spent nuclear fuel repro-processing and full park of thermal nuclear reactors, main energy generators all over the world.

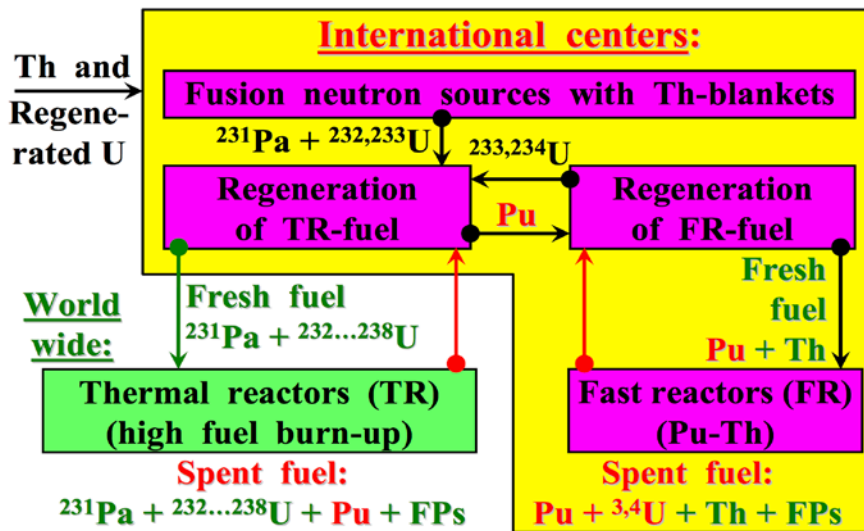


Fig. 5. Layout of closed NFC with joint utilization of thorium and regenerated uranium

It is assumed that, in the international centers fed with thorium and regenerated uranium, fast reactors will use (Pu-Th)-fuel and convert plutonium into  $^{233}\text{U}$ , thorium-blanketed FNS will generate mixture of nuclides  $^{231}\text{Pa}$ - $^{232}\text{U}$ - $^{233}\text{U}$ . Thermal reactors will use multi-nuclide U-based ( $^{232}\text{U}$ - $^{236}\text{U}$ - $^{238}\text{U}$ )+ $^{231}\text{Pa}$  fuel, which can be produced by blending of regenerated LWR uranium, i.e. nuclides  $^{234}\text{U}$ ,  $^{235}\text{U}$ ,  $^{236}\text{U}$  and  $^{238}\text{U}$ , with nuclides extracted from thorium FNS blankets plus  $^{233}\text{U}$  extracted from spent fuel of fast reactors. No isotope separation technologies are applied here.

Significant contents of  $^{231}\text{Pa}$  in fresh fuel compositions will stabilize their neutron-multiplying properties up to high values of fuel burn-up, improve neutron balance and shift neutron spectrum towards high-energy range. These effects will allow us to use stainless steel instead of Zr-based alloys as a cladding material for fuel rods and open new technical capabilities for the higher values of fuel burn-up.

The multi-nuclide fuel composition is a proliferation resistant fuel type because of the following reasons. Excellent fissile nuclides -  $^{233}\text{U}$  and  $^{235}\text{U}$  - are tightly encircled by the heavier and lighter uranium nuclides (neutron absorbers) and moderate fissile isotope  $^{232}\text{U}$  in significant quantity. Plutonium generation is substantially depressed because of low  $^{238}\text{U}$  fraction in fresh fuel composition. Nuclide  $^{236}\text{U}$  is the starting isotope for chain of nuclide transformations leading to generation of  $^{238}\text{Pu}$ . Sufficiently large  $^{238}\text{Pu}$  content makes plutonium absolutely unsuitable for NED. In a certain sense, nuclide  $^{238}\text{Pu}$  for plutonium is an analogue of nuclide  $^{232}\text{U}$  for uranium.

The proposed international closed NFC is able to utilize full energy potential of uranium and thorium, i.e. fuel resources of the global NPI become practically inexhaustible. By the way, share of FNS power in total NFC energy balance will be relatively small because of the following reason. The value of thermal energy accompanying excess neutron generation by thermonuclear reactions in FNS is substantially lower than the analogous value in accelerator-driven facilities and fast reactors. So, in principle, involvement of thorium-blanketed FNS into closed NFC can make structure of nuclear energy system [17]:

- more balanced with structure of energy utilization system;
- easier adapting to potential changes in requirements from the energy consumers;
- more flexible in respect of requirements on fuel utilization efficiency in nuclear power reactors;
- more oriented to potential changes in situation on the international markets (upgrading of NPI export potential).

## Conclusions

Numerical evaluations and their results presented above allowed to make the following conclusions.

1. Yields of nuclides, which define stabilization of neutron-multiplying properties and proliferation resistance of nuclear fuel, per one fusion neutron are larger in thorium FNS blanket than those in uranium FNS blanket.
2. Elementary LWR cell loaded with fuel extracted from thorium FNS blanket is characterized by high (30% HM) and ultra-high (80% HM) values of fuel burn-up. The presence of  $^{232}\text{U}$  in the fuel is a substantial factor in favor of its proliferation protection.
3. The proposed international closed NFC that involves thorium-blanketed FNS is able to utilize full energy potential of uranium and thorium, i.e. NFC resources become practically inexhaustible. Share of FNS power in total NFC energy balance will be relatively small. Such the global nuclear energy system would be flexible and easily

adaptable to requirements of the energy consumers with weak requirements to nuclear power plants on their fuel utilization efficiency.

## List of references

1. Kulikov E.G., Kulikov G.G., Kryuchkov E.F., Shmelev A.N. Increasing a fuel burn-up of light-water reactors at 231Pa adding into its content // Journal: Nuclear physics and engineering, 2013, Vol.4, №4, pp.291–299.
2. Shmelev A.N. On potential role of driven thermonuclear fusion in solving a problem of neutralization of RAW and in forming a protected fuel cycle with increased fuel burn-up // Journal: News of institutes of higher education. Nuclear energy, 1997, № 4. pp.53–59.
3. Shmelev A.N., Kulikov G.G., Kulikov E.G., Kryuchkov E.F., Apse V.A. Driven Thermo-nuclear Fusion: potential role of combined (Th-U-Pu) nuclear fuel cycle // Journal: Nuclear physics and engineering, 2011, Vol.2. №2, pp.101–111.
4. Shief H.E.J. et al. Measurements of the Reaction Rate Distributions Produced in a Large Thorium Cylinder by a Central Source of DT Neutrons. AWRE 20/77, United Kingdom Atomic Energy Authority, July 1977.
5. Krumbein A., Lemanska M., Segev M., Wagschal J.J., Yaari A. Reaction rate calculations in Uranium and Thorium blankets surrounding a central Deuterium-Tritium neutron source // Journal: Nuclear Technology, 1980, Vol.48. pp.110–116.
6. Weale J.W., Goodfellow H., McTaggart M.H., Mullender M.L. Measurements of reaction rate distribution produced by a source of 14-MeV neutrons at the center of a Uranium metal pile // Reactor Science and Technology (Journal of Nuclear Energy, Parts A and B), 1961, Vol.14, pp.91–99.
7. Haight R.C., Lee J.D., Maniscalco J.A. Reaction Rates in a Uranium Pile Surrounding a 14 MeV Neutron Source: Calculations of the Weale Experiment // Journal: Nuclear Science and Engineering, 1976, Vol.61, pp.53–59.
8. Schultz K.R. A Review of Hybrid Reactor Fuel Cycle Considerations // Papers of the II Soviet-American seminar "FUSION-FISSION", 14 March – 1 April 1977, Moscow, Atomizdat, 1978, pp.77–93.
9. Marin S.V., Shatalov G.E. Isotopic content of fuel in blanket of hybrid thermonuclear reactor with thorium cycle // Journal: Atomic energy, May 1984, Vol.56, №5. pp.289–291.
10. Shmelev A.N., Kulikov G.G. On neutron-physical features of modified (denatured) fuel cycles // Journal: News of institutes of higher education, series of Nuclear energy, 1997, №6, pp.42–48.
11. Shmelev A., Saito M., Artisyuk V. Multi-Component Self-Consistent Nuclear Energy System: On Proliferation Resistant Aspect // Proceedings of the Second Annual JNC International Forum on the Peaceful Use of Nuclear Energy, Tokyo, Japan, February 21-22, 2000, pp.87–95.
12. Mark J.C. Explosive Properties of Reactor-Grade Plutonium // Journal: Science & Global Security, 1993, Vol.4, pp.111–128.
13. Krakowski R.A., Davidson J.W., Bathke C.G., Arthur E.D., Wagner R.L., Jr. Nuclear Energy and Materials in the 21st Century // IAEA International Symposium on Nuclear Fuel Cycle and Reactor Strategies: Adjusting to New Realities, Vienna, June 1997, IAEA-SM-346/101.
14. Cunningham P.T., Arthur E.D., Wagner R.L., Jr., Hanson E.M. Strategies and Technologies for Nuclear Materials Stewardship // Proceedings of the International Conference on Future Nuclear Systems "GLOBAL'97", Yokohama, Japan, October 5-10, 1997, Vol.1, pp.720–725.
15. Shmelev A.N., Tikhomirov G.V., Kulikov G.G., et. al. On concept of international nuclear-technological centers for plutonium utilization // Journal: News of institutes of higher education, 1998, №4, pp.81–92.
16. Smirnov A.Yu., Apse V.A., Borisevich V.D., et. al. Adding regenerated uranium fuel into content of light-water reactors as a method of protection against proliferation // Journal: News of institutes of higher education, Series of Nuclear energy, 2011, №4. pp.3–13.
17. Shmelev A., Artisyuk V., Suzuki M., Saito M., Fujii-e Y. A Possible Contribution of Various Neutron Sources (Fission, Spallation, Fusion) in Excess Neutron Generation for SCNES // Proceedings of the Eighth International Conference ICENES'96, Obninsk, Russia, 24-28 June 1996, pp.110–120.

## 23 - First preliminary conceptual experimental set up towards a hybrid reactor blanket

**N. Cherubini<sup>a</sup>, M. Ciotti<sup>a</sup>, C. Innarella<sup>a</sup>, G. Innarella<sup>c</sup>, J.L. Manzano<sup>b</sup>**

<sup>a</sup> ENEA CR Casaccia, Via Anguillarese, 301, 00123 Roma, Italy

<sup>b</sup> ENEA CR Frascati, Via Enrico Fermi, 45, 00044 Frascati, Roma, Italy

<sup>c</sup> Stage at ENEA CR Casaccia, Via Anguillarese, 301, 00123 Roma, Italy

### Abstract

For the optimum design of a Fusion-Fission Hybrid Reactor (FFHR) plays a main role the availability of validated neutronic data in conditions as close as possible to the real ones. The 14 MeV neutron generator in operation at the ENEA Energy Center of Frascati, produces up to  $10^{11}$  neutrons per second and consists essentially of a deuterium-ion accelerator. The FNG offers a possible option to obtain a first set of such data.

We foresee, as a preliminary representative experimental set-up of the fission fuel breeder of a FFHR, an instrumented probe filled with Thorium and enclosed in a suitable envelope.

Neutron flux, spectra and evolution of the isotopes in the probe were calculated after several days of irradiation. The simulations have been performed with the MCNP6 code.

The instrumentation to be employed sees standard activation foils and a standard Radiochemical Techniques; the required performances of these sensors are analysed.

### 1. Introduction

Several hypothesis of a Fusion Fission Hybrid Reactor (FFHR) have been proposed, they differ in the solution adopted for the fusion driver, the type and layout of the fissile-breeder blanket. Many possible combinations are foreseeable but while the conceptual possibility has been assessed no much progress have been made towards the realization of a more detailed design.

As far as is known from the authors, until now very few experimental preliminary tests towards the advancement of the basic mechanisms knowledge or the technological feasibility assessment has been performed.

Due to the complexity of the task, we suggest that the most efficient approach would foresee the design, realization and characterization of each component, one by one, instead to start with a full reactor preliminary design. The most interesting component in this approach would be the fission blanket, where several new technological never tested solutions, have to be put together.

For this component the most urgent aspect to be evaluated is the neutronic behaviour with the dual objective to start to develop skill in experimental activities and to validate the calculation tools.

Our effort in this phase concentrates on the Frascati Neutron Generator (FNG), an existing facility at the Frascati ENEA Centre with a 14 MeV, mono-energetic,  $10^{11}$  neutron/s, where Thorium targets could be irradiated in a somewhat "mini-experiment".

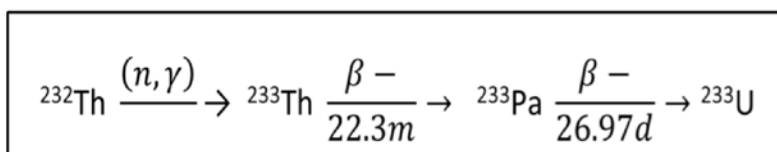
In order to prepare such experiment and its instrumentation a first measurement using a simple portable 14 MeV neutron generator is in progress at the Casaccia ENEA Centre, what we define a "micro-experiment".

This sequence of experiments will allow the planning and realization of tests in a more challenging conditions like those offered by the JET or others fusion large machines working in D-T reaction.

Aim of this study is to define both experimental set-up and to prepare their realization.

### 2. Foreseen results

In our measurements we are interested mainly in the U 333 generation chain:



In Fig. 1 the whole gamma spectrum to be expected after the irradiation of a Th sample with fast neutrons [1], is showed. According to [Anand et al.] [2], the most relevant expected emission peaks are placed at 441, 448, 459 keV from Th233 and 463 keV from Ac233 (fig 2), and they appear to be detectable over the background.

In order to understand the feasibility of the experimental measurements with our instrumentation we perform a first

rough calculation by means of the FISPACT code, not considering in a first approach the fission reactions. Results are shown in Table 1. We concluded that, considering that our instrumentation sensitivity threshold is around 10 c/s we are close to the instrumentation sensitivity limit. Therefore, the gamma emission from U233 chain would't be detectable after irradiation with the Casaccia generator. Radio chemical analysis only can provide data. As explained in the next chapter we are confident about the possibility to use radiochemical methods to investigate the reaction rates in this case.

	time	flux	Th 232	Th 233		Pa 231	Pa 233		U233
		n/cm**2/s	N. atm	N. atm	Bq	N. atm	N. atm	Bq	N. atm
<b>Casaccia</b>	1h (irrag)	5.00E+05	2.28E+21	2.14E+04	1.10E+01	5.90E+04	2.58E+04	7.67E-03	1.04E+01
	10min	0	idem	1.57E+04	8.12E+00		3.15E+04	9.37E-03	1.56E+01
	1h	0	idem	3.31E+03	1.13E-16		4.39E+04	1.30E-02	5.05E+01
	time	flux	Th 232	Th 233		Pa 231	Pa 233		U233
		n/cm**2/s	N. atm	N. atm	Bq	N. atm	N. atm	Bq	N. atm
<b>FNG</b>	20min (irrag)	1.00E+09	7.58E+20	7.79E+06	4.03E+03	4.39E+06	2.67E+06	7.93E-01	3.33E+02
	10 min	0	idem	5.71E+06	2.96E+03	8.76E+06	4.75E+06	1.41E+00	1.00E+03
	1h	0	idem	1.21E+06	6.25E+02				7.74E+03
	2h	0	idem	1.87E+05	9.68E+01		1.03E+07	3.05E+00	1.83E+04
	4h	0	idem	4.48E+03	1.53E-16		1.04E+07	3.09E+00	
	1.68 days	0		0			1.02E+07	3.02E+00	3.05E+05

Table 1 : FISPACT calculations (0.3 g Th 20 min), Thorium fission products were not calculated

While, after FNG irradiation, both analysis methods, radiochemical and gamma spectrometry, are applicable. Irradiation for time much longer than 22 min are not useful due to the Th 233 decay time. On the other hand longer time will cause a larger amount of nuclear reactions, increasing the compound formation and the consequent proliferation of decay elements. Materials as pure as possible are chosen in order to avoid such an effect and increase measurements cleanliness.

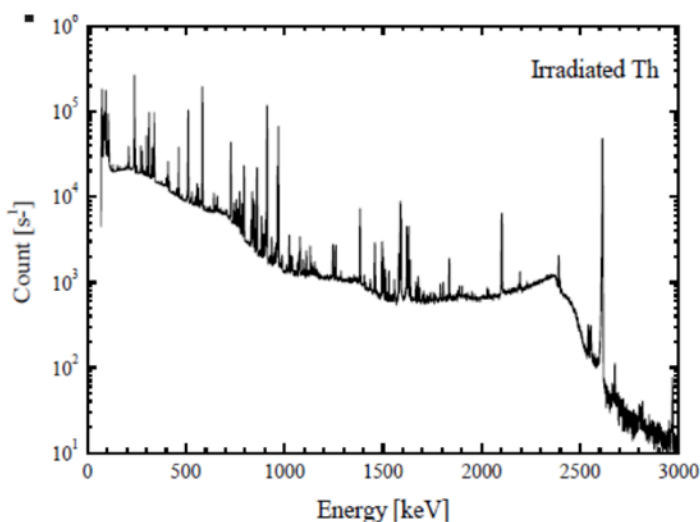


Fig. 1 - Measure  $\gamma$ -ray spectrum of irradiated  $^{232}\text{Th}$  plate (from [Pyeon et al])

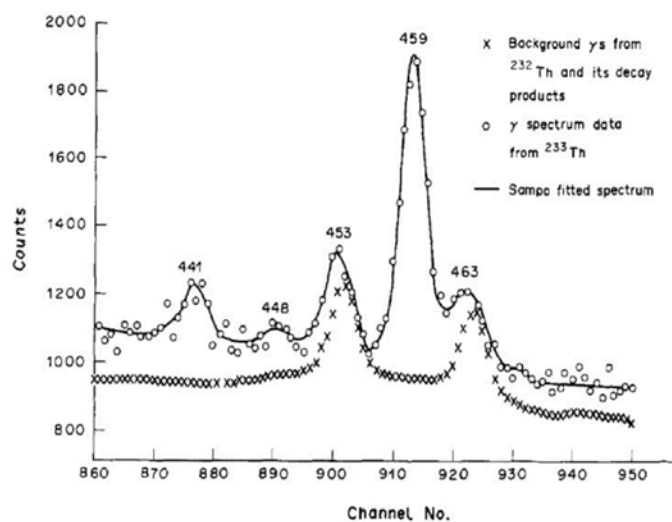


Figura 2 gamma spectrum from the Th233 decay around 459 keV

### 3. The Micro experiment

As just mentioned, for the first measurement set we intend to use a portable neutron generator. It consists of a compact linear accelerator that conveys deuterium (D) ions toward a target containing tritium (T); the D-T fusion reaction generates 14.1 MeV neutrons. As is known, the advantages of using as a source a neutron generator over a radioisotope one consist in its larger yields and its higher modulation flexibility.

The used reaction is



And its main characteristics are:

Maximum Neutron Yield,  $1.0 \cdot 10^8$  n/s ; 500 Hz to 20 kHz pulse rate, continuous mode of irradiation  
 Duty Factor, 5% to 100%  
 Minimum Pulse Width, 5  $\mu$ s  
 Maximum Accelerator Voltage, 80 kV  
 Beam Current, 60  $\mu$ A

The irradiation sample will consist of Thorium foils,

Chemical separations will be done on the Th sample to isolate or to concentrate the radioisotopes of interest.

Standard Radiochemical Techniques, are accurate and precise, but are more time consuming than the non-destructive ones. The type and activity of activation products will be determined using the following systems:

Absolutely calibrated High purity germanium and Liquid Scintillation Counting (LSC) detectors for quantitative gamma and beta spectrometry, respectively, on the irradiated samples.

And Alpha Spectrometry, to determine the activity per unit mass of  $\alpha$ -emitting radioisotopes.

Also elemental analysis by means of Atomic Emission Spectroscopy with Plasma Torch (ICP), both by Optical Detection (AES or OES) or Mass (MS) is mainly based on qualitative and quantitative determination of appropriate analyses through interaction light-matter, could be used.

#### 4. The mini experiment

As a second step we foresee the possibility to use a larger target on the Frascati Neutron Generator, this facility is a 14 MeV neutron generator based on the  $T(d,n)\alpha$  fusion reaction designed and built at ENEA Frascati; FNG produces up to  $10^{11}$  n/s in steady state or pulse mode. FNG can also produce 2.5-MeV neutron via the  $D(d,n)^3\text{He}$  fusion reaction. The overall facility layout is shown in Fig. 4. In Fig. 5 the neutron spectrum of FNG is shown.



Figure 4: The overall FNG facility layout

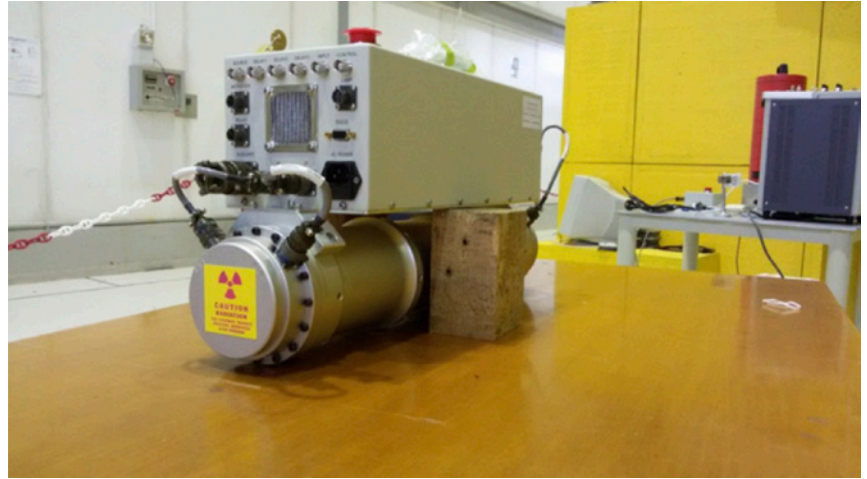


Figure 3: the portable neutron generator employed in the microexperiment performed at the ENEA Casaccia Center.

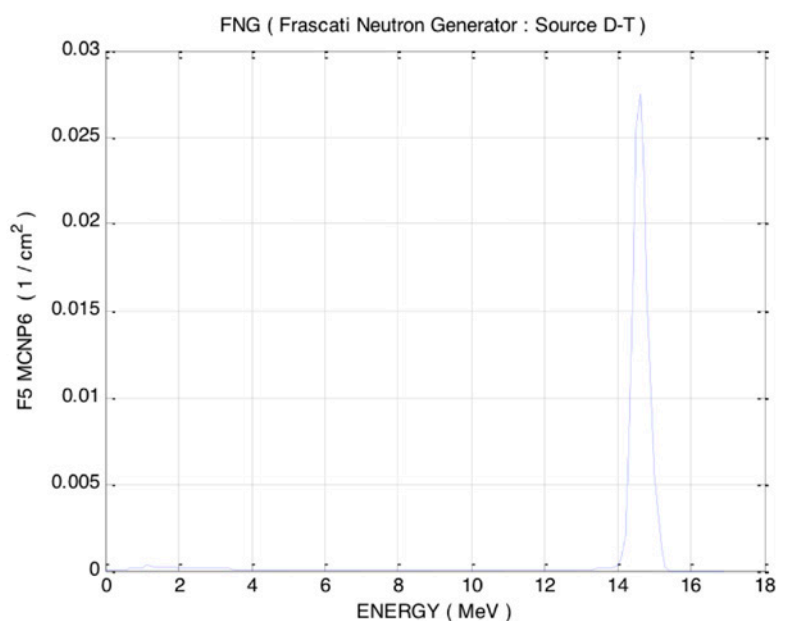


Figure 5: Neutron spectrum of FNG (Frascati Neutrons Generator) 14 MeV calculated at 0.5 cm from D-T source

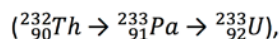
According to the FISPAC calculation shown in Fig 4 direct gamma spectrum measurement in this case would be possible, they will be made with thorium activation foils in a suitable sample which optimum dimensions will be determined with MNCP calculations as shown in the next section.

#### 4.1. MCNP Calculations

Aim of the calculations is the identification of the geometry for a test piece of Thorium to be irradiated with 14 MeV neutrons from ENEA FNG (Frascati Neutrons Generator) in order to obtain measurable emissions from the U 233 production by using simulation and analysis of the neutrons MCNP transport code.

##### 4.1.1 Neutron Analysis of a Thorium target without reflector

In order to analyze the behavior of a mass of Thorium irradiated with 14 MeV neutrons, which may constitute fertile material for a hybrid reactor, neutron transport simulations were carried out with the MCNP-6 /3/ of Thorium cylindrical targets with different masses and dimensions. MCNP computer model input of target is the neutron spectrum from a 14 MeV FNG (Frascati Neutrons Generator) source in Fig.5, measured at 0.5 cm from the D-T source. MCNP normalized parameters (neutrons for neutron source) of reactions (n,xn), fission, (n, γ) escapes, the parameter  $k_{eff}$  and neutron fluxes depending by Thorium mass were reported in the graphs in Fig.6, showing very interesting developments that deserve a comment. Capture (n, γ) and reactions (n,xn) are those of interest that we must maximize in the Thorium of a future hybrid reactor, being Thorium a fertile material. In fact the reactions (n,xn) increase the neutrons in the medium for the capture; neutron capture transforms thorium into Protactinium which decays ( $T_{1/2} = 28d$ ) into fissile Uranium-233



decreases the escapes and constitutes a γ rays distributed source together with the fission. Fission is linked to the  $k_{eff}$  value that highlights a collection of subcritical masses of Thorium. The neutron flux of the cell decreases with increasing the mass of Thorium. In order to find out an "optimum" solution a parametric dimensional analysis has been performed. In Fig. 6 the different possible processes have been evaluated as a function of the target mass

Three relevant regions have been highlighted:

- 1) M1 mass of 414.5 Kg at the beginning of saturation for fission reactions and for (n, xn) but with low values of the capture and elevated of the escapes;
- 2) M2 mass of 110524 Kg at the saturation of processes. It's experimentally unthinkable by high mass (purely conceptual reference);
- 3) Mi intermediate mass of 3315 Kg with (n,xn) and fission in saturation and capture values and escapes can be improved by adding a reflector.

##### 4.1.2 Neutron transport Analysis of a Thorium target with reflector and/or moderator

The Thorium target with mass of 3315 Kg seems to be the best candidate for useful irradiation. In the simulations this target was enveloped with reflector and/or moderator (interposed between source and target), made up of different materials. The objective is to increase the rate of reaction (n, xn) and capture to produce U-233. MCNP model based

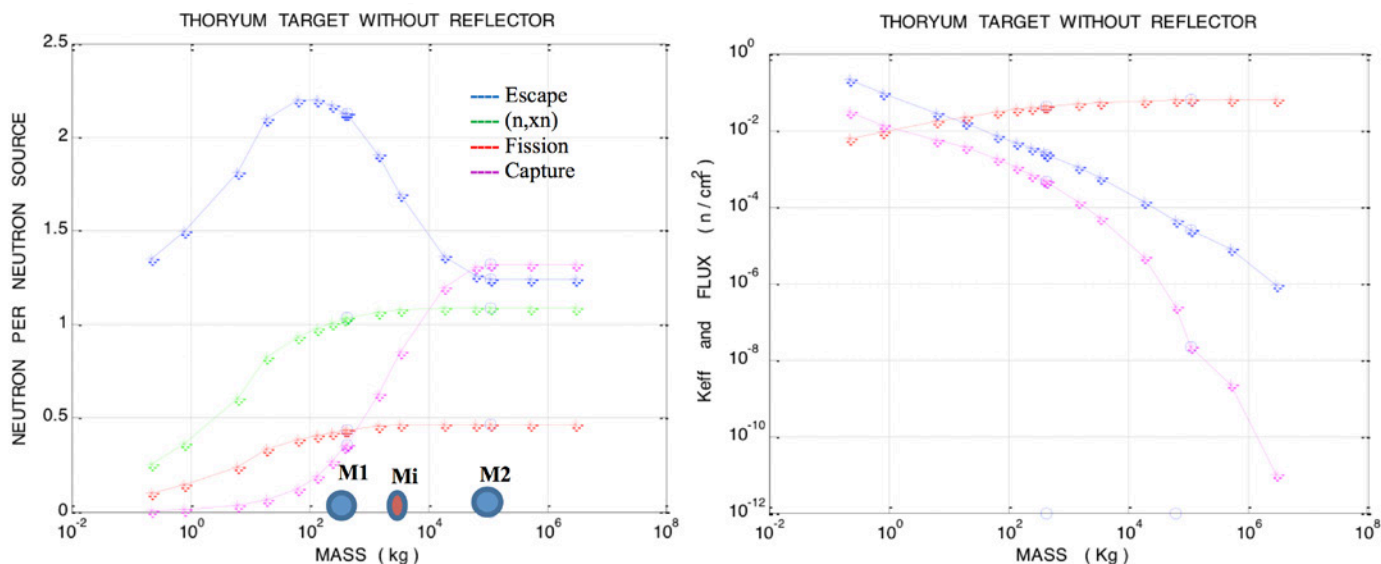


Figure 6 Neutron analysis of cylindrical thorium targets irradiated by FNG at 14 MeV

simulations have been carried out by selecting the materials /4/: Lithium (Li), Graphite (C), Beryllium (Be), Beryllium oxide (BeO), Copper (Cu) and Lead (Pb). It was also carried out a simulation with a target of Thorium dioxide ( $ThO_2$ ) without reflector. The MCNP simulations were grouped into three sets relating to Li, to C and to Be to have an overview of the processes. Results are shown in Table 2.

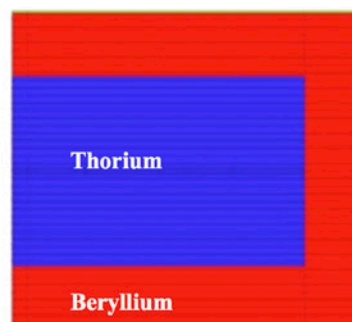
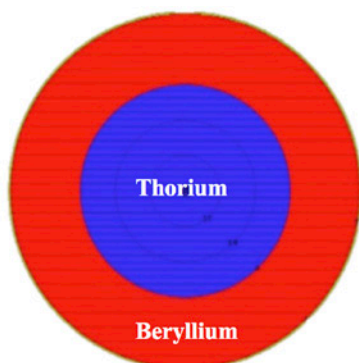
N-test		Moderator	Target	Reflector	(n,xn)	Fission	Capture	Escape
1	reference	-	Th	-	1.06000	0.45000	0.83000	1.70000
2		-	Th	Pb	1.06969	0.45217	0.99547	1.53200
3		-	Th	Cu	<b>1.05996</b>	<b>0.45202</b>	<b>1.11330</b>	<b>1.40470</b>
4	Lithium7	(*) Li	Th	Pb	0.27177	0.08470	0.33658	1.02210
5		(**) Li	Th	Pb	0.64908	0.26149	0.81684	1.09750
6		(*) Li	Th	Cu	0.27161	0.08480	0.31894	1.03830
7		(**) Li	Th	Cu	0.64911	0.26153	0.78112	1.13330
8		-	Th	Li	1.05659	0.45254	0.87334	1.64160
9		Graphite	(*) C	Th	Pb	0.01214	0.00618	0.34472
10	(**) C		Th	Pb	0.21202	0.09476	0.69607	0.61231
11	(*) C		Th	Cu	0.01214	0.00568	0.34204	0.67561
12	(**) C		Th	Cu	0.21201	0.09489	0.67633	0.63183
13	-		Th	C	1.05504	0.45218	1.12590	1.38700
14	Beryllium	(*) Be	Th	Pb	1.55610	0.00331	0.94690	1.61270
15		(**) Be	Th	Pb	1.39120	0.08560	1.23780	1.23990
16		(*) Be	Th	Cu	1.55600	0.00329	0.94484	1.61470
17		(**) Be	Th	Cu	1.39130	0.08550	1.21600	1.26180
18		(*) Be	Th	C	1.55620	0.00335	0.91297	1.64670
19		(**) Be	Th	C	1.39040	0.08604	1.17830	1.29960
20		-	Th	Be	<b>1.08583</b>	<b>0.45214</b>	<b>1.21800</b>	<b>1.32580</b>
21		(*) BeO	Th	C	0.65714	0.00067	0.55090	1.10730
22		(**) BeO	Th	C	0.65704	0.04165	0.79207	0.90724
23		-	Th	BeO	1.06986	0.45233	1.20420	1.32360
24		-	ThO <sub>2</sub>	Be	0.74390	0.30929	1.04620	1.01120
25		-	ThO <sub>2</sub>	BeO	0.73026	0.30925	1.03700	1.00710

(\*) Thickness = 50 cm moderator    (\*\*) Thickness = 20 cm moderator

Tab. 2 - Neutron Transport MCNP simulation

#### 4.1.3 The specimen of thorium with beryllium reflector

The Thorium target (mass = 3315 kg) with Beryllium reflector (1219 kg mass) without moderator showed the highest values of the MCNP parameters of (n-2n) and capture reactions compared to all the specimens examined with MCNP Code and achieves the aim to simulate the transport of neutrons by 14 MeV. The Fig.7 shows the sample MCNP computer model geometry. In Tab.3 are shown the parameters (weight) of the neutron reactions and average energies obtained with MCNP transport simulation. The reactions (n,xn) and (n,  $\gamma$ ) are fundamental to the production of fissile U-233. Gamma produced by capture and by fission interact with Thorium according to the Photoelectric effect, Compton scattering and Pair creation. MCNP's neutron spectrum results plotted for four energy groups: thermal ( $E < 10^{-7}$  MeV), epi-thermal ( $10^{-7} < E < 10^{-4}$  MeV), intermediate ( $10^{-4} < E < 10^{-1}$  MeV), fast ( $E < 20$  MeV).



In Fig.8 are given the radial distribution of fast and intermediate neutron spectrum.

Fig.7 The geometry of MCNP model of the Thorium-Beryllium target : internal diameter is 60 cm, reflector's thickness is 20 cm, total length is 120 cm

		NEUTRONS		
		Tracks	Weight	Energy (MeV)
Creation	Source	1000000	1.00000	14.0110
	(n,xn)	-	1.08626	2.5700
	Fission	-	0.45162	1.18620
Loss	Capture	-	<b>1.21630</b>	0.34816
	Escape	-	1.32790	1.10150

Tab.3 - Neutron Transport MCNP simulation in Thorium-Beryllium Target

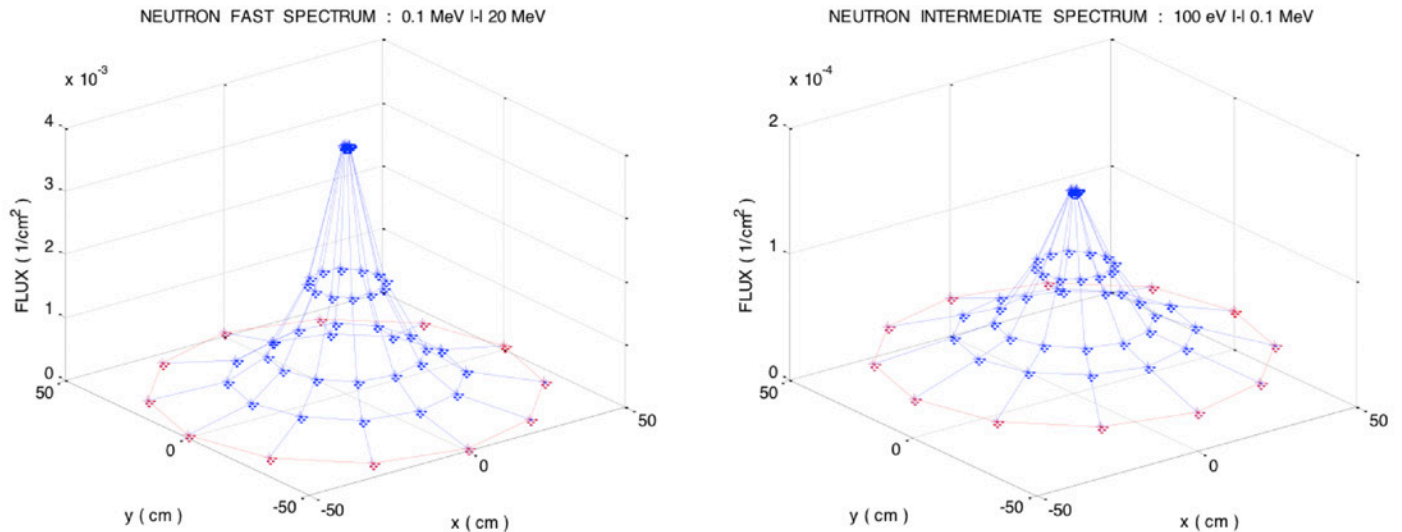


Figure 8 - Neutron fast and intermediate spectrum on Thorium Target with Beryllium Reflector

## 5. Summary

A roadmap toward the definition of sequential steps for the skill development of the competences to start a real design and testing activity for a first simple hybrid device has been carried on.

Two very small preliminary experiments have been outlined and the measurement procedures sketched together with code simulations.

To determine the expected generated particles/radiations we simulated the neutron transport inside the specimen to be irradiated by MCNP code, allowing to choose the materials, the geometry and the overall sample mass.

International cooperation on experimental activities on FFHR is strongly needed.

## 6. References

1. Pyeon et al. "Thorium-Loaded Accelerator-Driven System Experiments in Kyoto University Research, Reactor Institute", ThEC13, Geneva, 28th-31st Oct., 2013
2. Anand et al., " Neutron capture cross section measurement of  $^{232}\text{Th}$  in the energy range of 400-950 keV", Ann. Nucl. Energy, Vol. 16, No. 2, pp. 87-90, 1989.
3. MCNP6.1/MCNP5/MCNPX-EXE C00810 MNYCP 01, Los Alamos, Oak Ridge, USA
4. Neutronic calculation of a thorium-based fusion-fission hybrid reactor blanket, X.B.Ma \*, Y.X. Chen \*, Y. Wang \*, P.Z.Zhang \*, B. Cao\*, D.G. Lu\*, H.P. Cheng\*\*, \* North China Electric Power University, School of Nuclear Science and Engineering, Beijing 102206, China, \*\* China Nuclear Power Engineering Co., Ltd., Beijing 100037, China.

## 7. Thanks

The authors thank Salvatore Fiore for his useful contribution

## 24 - Neutronic Analysis of Spent Fuel Recycling Option in a Hybrid System with DUPIC Fuel

**S.H. Hong and M. H. Kim\***

*Department of Nuclear Engineering, Kyung Hee University, 17104, Rep. of Korea  
mhkim@khu.ac.kr*

### Abstract

As one of concepts of fusion-fission hybrid reactor (FFHR) system have been proposed for the incineration option of high level radioactive waste. Design optimization has been done for the large sized hybrid reactor with TRU loading at the blanket zone [1]. However, this concept showed a large reactivity swing resulting in high burden of plasma power variation. In this paper, reuse of PWR spent fuel which has process with DUPIC fuel is suggested [2]. Variation of reactivity swing has been reduced by using this fuel because of partial fissile breeding. In addition, production of high level radioactive waste is reduced in total.

In this paper, neutronics analysis was done for two models: model A with (U-TRU)Zr fuel and model B with addition of DUPIC fuel. All calculations were conducted with MCNPX 2.6.0.

Addition of DUPIC fuel makes reactivity swing and required  $P_{\text{fusion}}$  reduced. Furthermore, energy multiplication factor (EM) is increased. However, transmutation performance and reduction of radio-toxicity are degraded by Pu production from DUPIC fuel.

### 1. Introduction

One of the most problems is high level radioactive waste treatment in nuclear industry. Recently, Partitioning & Transmutation (P&T) is issued as a method of waste treatment. There are critical fast reactor, FFHR and Accelerator Driven Subcritical System (ADSR) for P&T. FFHR has some strengths compared with fast reactor and ADSR. Safety performance with FFHR is higher than with fast reactor because FFHR is subcritical system. FFHR has high neutron source efficiency compared with ADSR in producing the same energy, although FFHR and ADSR are subcritical system [3]. Therefore, FFHR for WT research has been promoted [4-7].

Design of Hyb-WT with large tokamak was completed [1]. In addition, transmutation performance comparison on fuel and coolant options was completed for design optimization [8-9]. Transmutation performance with Hyb-WT is significantly high, however it has a problem high reactivity swing. High reactivity swing means large reduction of keff level between Beginning of Cycle (BOC) and End of Cycle (EOC). As a result,  $P_{\text{fusion}}$  is increased to compensation of reducing  $k_{\text{eff}}$ . Reactor safety is declined because  $P_{\text{fusion}}$  is increased up to maximum design  $P_{\text{fusion}}$ . Also, integrity of structure material is more weaken. Therefore, in this study, reuse of PWR spent fuel which has process with DUPIC fuel is suggested in order to reduce the reactivity swing. As a proliferation-free option, DUPIC fuel was developed in the rep. of Korea in order to recycle PWR spent fuel in a CANDU (PHWR) reactor. DUPIC means direct use of PWR spent fuel into CANDU. R&D for fuel processing and fabrication have been accomplished for the real application [2].

When we load DUPIC fuel into FFHR, we can expect benefits in many aspects. First of all, PWR spent fuel can be reutilized at FFHR resulting in reduction of total high-level waste under the once-through cycle strategy. Reduction of amount of fissile makes more  $P_{\text{fusion}}$  to supply more external neutrons during cycle length. However, conversion of U-238 to Pu-239 leads to the reduction of required  $P_{\text{fusion}}$ . In this paper, characteristics of DUPIC fuel is compared with TRU fuel in the performance of waste transmutation and power production. Addition of DUPIC fuel was studied from the original fuel composition (U-TRU)Zr for the Hyb-WT [1].

### 2. Calculation Model Design

Neutronic analysis was conducted through MCNPX2.6.0 with ENDF/B-VII.0 neutron cross-section library. Design configuration and design parameters are shown in Fig. 1 and Table 1. Model A is designed (U-TRU)Zr fuel and LiPb coolant in Hyb-WT. It is not required extra Tritium Breeding Zone (TBZ). It is designed for WT purpose. Model B is designed by adding DUPIC fuel in Model A. (U-TRU)Zr zone of model A is divided 3 zones in model B. 1<sup>st</sup> zone is designed (U-TRU)Zr fuel and PbBi coolant for WT. PbBi is selected for neutron economy [9]. 2<sup>nd</sup> zone is designed DUPIC fuel and water coolant for fissile production. DUPIC fuel volume is minimized as a pebble type and it is surrounded graphite coating for moderation effect. In addition, water coolant is designed to improvement of DUPIC fuel availability thorough thermal system. In case of using water coolant in FFHR, it should be pressurized. Therefore, it is designed separated coolant channel in order to reduce the influence on other structure material. 3<sup>rd</sup> zone is TBZ, it is required since coolant contained Li is not used. TBZ is designed  $\text{Li}_4(\text{Li}6 \text{ 60\%})\text{SiO}_4$  which has high Li number density as a pebble type. Coolant is water coolant, it has same concept with DUPIC zone.

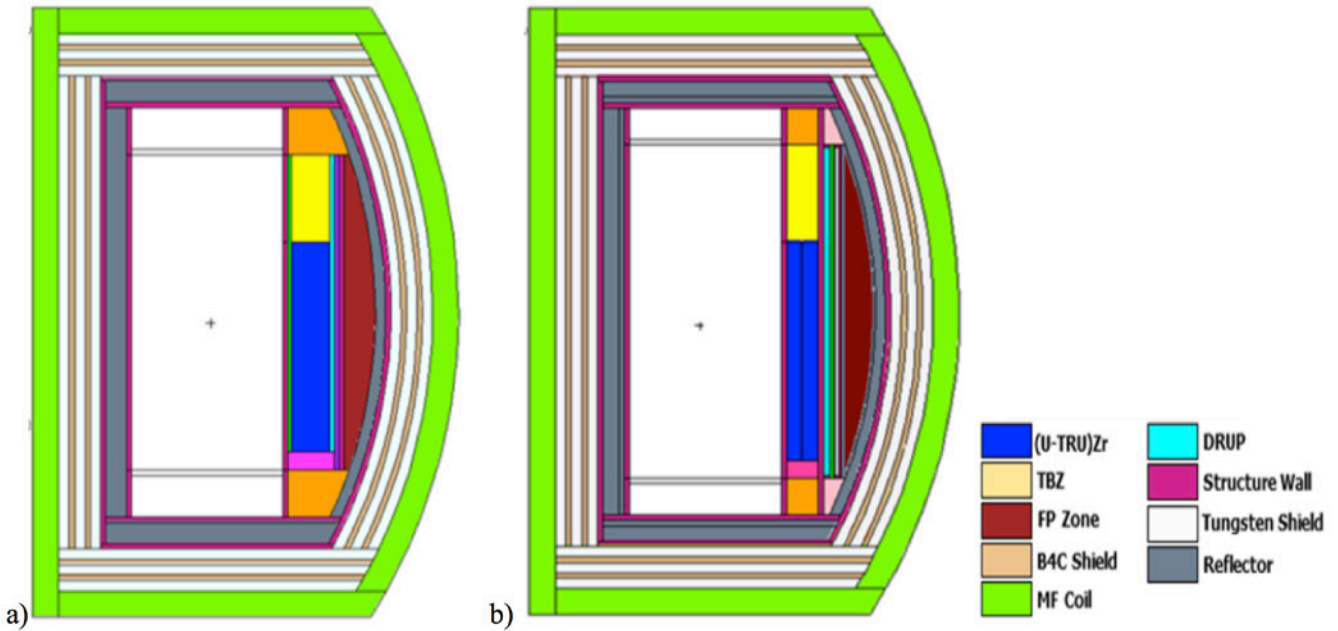


Figure 1. Calculation Model Design Configuration a) Model A, b) Model B.

Model A			Model B		
Region	Thickness (cm)	Volume Fraction (%)	Region	Thickness (cm)	Volume Fraction (%)
(U-TRU)Zr Fuel Zone	45	(U-30TRU)Zr; 23.84 LiPb: 38.98; SiC: 5.94; Clad: 3.54; Bonding: 17.7	(U-TRU)Zr Fuel Zone	21.8	(U-30TRU)Zr: 29.92; Pb-Bi 35.85; SiC: 6.11; Clad: 13.9; Bonding: 14.22
			DRUP Fuel Zone	6	DRUP: 27.34; C: 42.66, He: 30
			Tritium Breeding Zone	3.7	Li4SiO4 (Si: 3.4, Li6:8.69; Li7:4.97; O: 13.65); C: 29.28, He-gas:40
Structure Wall		5			ODS steel(MA957):70; He-gas:30
FP Zone		29			CsI (129I: 0.42; 135Cs: 1.76); 99Tc: 0.82; SiC: 2.5; C: 78; He-gas:16.5
Tungsten Shield		10			W
B4C Shield		5			B: 80; C: 20
Superconductor Toroidal MF Coil		20			Nb93:70; Sn:30; He
Reflector		20			C: 80; He-gas: 20

Table 1. Design Parameters.

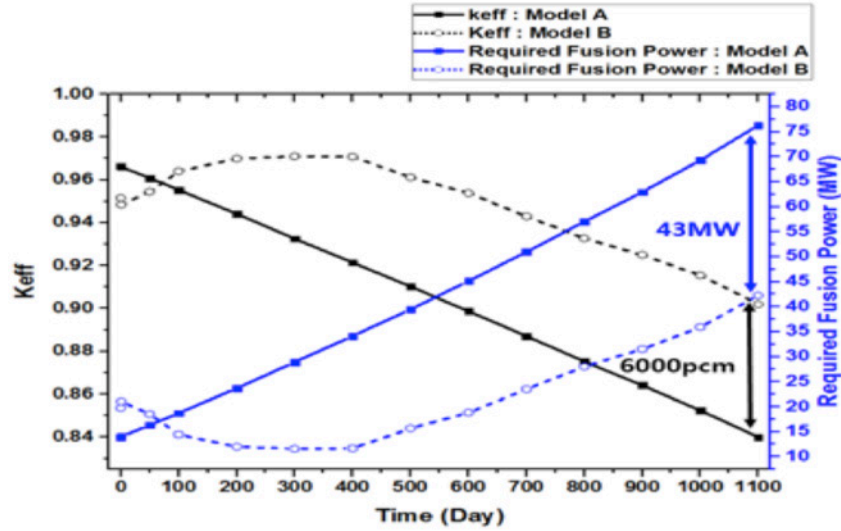
### 3. Performance Comparison Evaluation

#### 3.1 Neutronic Parameters

Neutronic parameters is listed in Table 2.  $K_{eff}$  level and required  $P_{fusion}$  during operation period.  $K_{eff}$  with model A is reduced continuously because of reduction of fissile material in (U-TRU)Zr fuel. Reactivity swing is 12641 pcm. As a result, required  $P_{fusion}$  is increased to 96 MW. On the other hand,  $k_{eff}$  with model B is increased to 400 days by fissile production from DUPIC fuel. Reactivity swing is 4948 pcm, it is significantly reduced compared with model A. As a result,  $P_{fusion}$  is increased to 53 MW. There is DUPIC fuel effect on EM factor. Because  $k_{eff}$  with model B is much lower than with model A at EOC, EM with model B is also increased. In other words, there is highly beneficial using DUPIC fuel within the framework of neutronic parameters.

Model	Model A	Model B
Cycle length	1100 days	
$K_{eff}$ [BOC / EOC]	0.96641/0.84	0.95151/0.90203
Required Fusion Power (MWth)	13.92 ~ 95.3	11.59 ~ 52.28
Average TBR	1.25	1.77
EM (Energy Multiplication factor)	26.19 ~ 143.51	47.24 ~ 172.28

Table 2. Neutronic Parameters.

Figure 2.  $K_{eff}$  level and Required Fusion Power.

### 3.2 Mass Variation

Mass variation with model A and B is listed in table 3. Fuel type is classified in order to check on fuel characteristic in model B. Fission to capture ratio with model A is lower than with model B. Because Li absorbs thermal neutrons strongly by designed LiPb coolant. Mass variation with model B is considerably high in only (U-TRU)Zr fuel with model A and B. This difference comes from coolant. In model A, most of thermal neutrons are absorbed by Li in LiPb coolant. On the other hand, most of thermal neutrons are absorbed by fuel in model B. Mass of U nuclides is fairly decreased by moderation effect of water coolant in DUPIC fuel. However, TRU is produced result from reduction of uranium mass. Especially, most of produced TRUs is Pu nuclides. In total mass variation with model B, TRU transmutation performance is thoroughly degraded compared with model A. Especially, fissile Pu is produced.

Model	Model A	Model B	
Fission to Capture Ratio	1.48	1.79	
Fuel Type	Total	Total	(U-TRU)Zr DUPIC
Mass Variation (kg)			
Initial Loading	56900	75600	51400 24200
Total Actinide	-2080 (-3.67%)	-9360 (-12.4%)	-5540 (-10.79%) -3820 (-15.82%)
Total U	-1050 (-2.63%)	-9220 (-15.4%)	-3390 (-9.42%) -5830 (-24.37%)
Total TRU	-1010 (-5.89%)	-358 (-2.31%)	-2330 (-15.23%) 1970
Fissile Pu	-920 (-10.1%)	472 (5.63%)	-979 (-11.85%) 1450
Total Pu	-926 (-6.36%)	-175 (-1.3%)	-2100 (-16%) 1930
Total MA	-117 (-8.05%)	-183 (-8.4%)	-229 (-10.59%) 46.6
Total FP	-190 (-7.6%)		-1040 (-37.4%)

Table 3. Mass Variation.

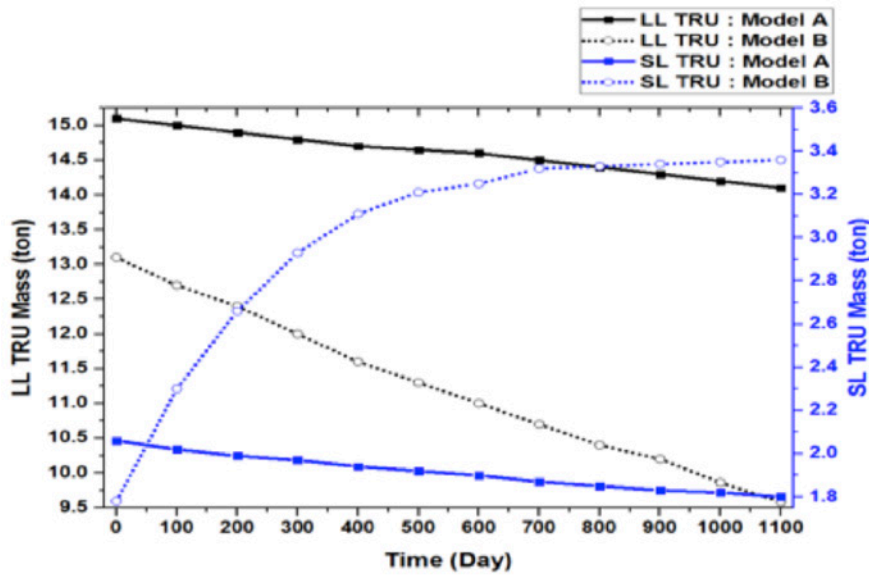


Figure 3. LL TRU and SL TRU Mass Variation.

Mass variation of TRU is shown in Fig. 3. TRU is classified 2 groups depending on half-life. LL (Long-Lived) TRU has half-life more than 100 years. SL (Short-Lived) TRU has half-life more than 10 years and less than 100 years. LL TRU and SL TRU with model A is reduced, although transmutation speed is slow. However, model B has different trend. LL TRU is significantly reduced, on the other hand SL TRU is increased.

The reason is shown in Fig. 4 and Fig. 5. In model A, all masses of  $U_{238}$  and Pu nuclides are reduced as shown in Fig. 4. However, there is difference between model A and B as shown in Fig. 5. Mass reduction of  $U_{238}$  and  $Pu_{239}$  is quite high in (U-TRU)Zr of model B. As a result, SL TRU ( $Pu_{238}$  and  $Pu_{241}$ ) is produced by capture reaction from  $U_{238}$  and  $Pu_{239}$ . Additionally, SL TRU with model B is produced by capture reaction from  $U_{238}$  and  $Pu_{239}$  of DUPIC fuel.

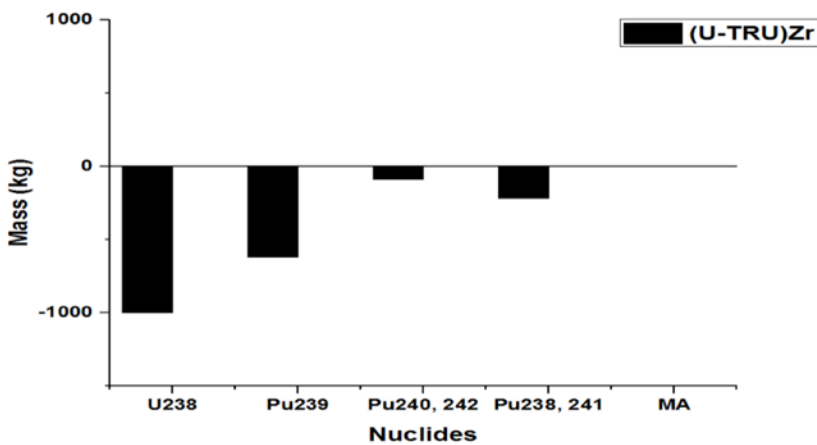


Figure 4. Main Actinides Mass Variation with Model A.

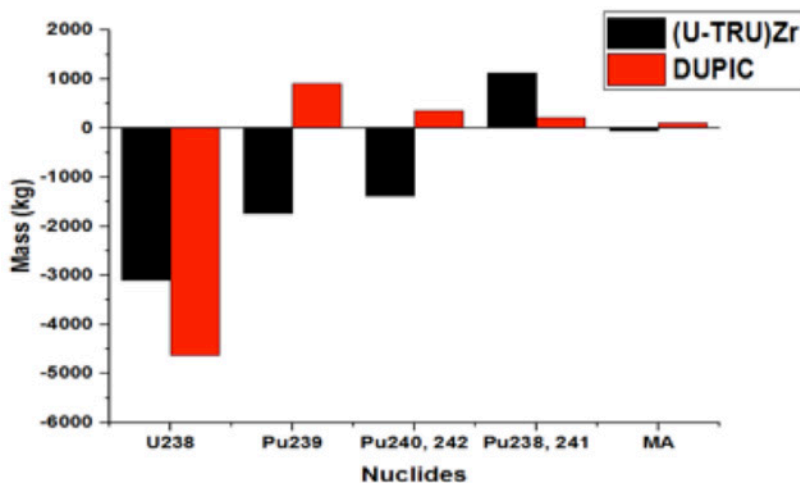


Figure 5. Main Actinides Mass variation with Model B.

### 3.3 Radio-Toxicity Reduction

Radio-toxicity reduction is evaluated on model A and B. Radio-toxicity is classified on ingestion and inhalation. It is obtained as calculated activity through MCNPX is divided by the limit value. Radio-toxicity with TRU is listed in Table 4. Ingestion and inhalation reduction with LL TRU is largely reduced in model B. In LL TRU, the highly radio-toxic nuclide is  $Am_{241}$  by low limit value. Reduction ratio of  $Am_{241}$  is about 1 % in model A, however  $Am_{241}$  is reduced about 19 % in model B. As a result, LL TRU radio-toxicity is largely decreased in model B. Radio-toxicity with SL TRU is increased. Increasing ratio with model B is higher than with model A. Most of SL TRU radio-toxicity is  $Pu_{238}$  and  $Pu_{241}$ . SL TRU especially  $Pu_{238}$  and  $Pu_{241}$  is produced, thus radio-toxicity is also increased.

Change of ingestion and inhalation radio-toxicity is shown in Fig. 6 and 7. Tendency of radio-toxicity change is same between model A and B. Just, inhalation value is shown highly, because limit values is relatively low. In model B, radio-toxicity change with ingestion and inhalation is steep up to 400 days. Since amount of produced fissile from DUPIC fuel is higher than amount of consumed TRU as  $k_{eff}$  is increased.

Model	Model A	Model B
<b>Ingestion</b>		
LL TRU	-2.05	-19.8
SL TRU	8.0	81.7
<b>Inhalation</b>		
LL TRU	-2.05	-19.8
SL TRU	10.7	78.1

Table 4. Radio-Toxicity Reduction.

#### 4. Conclusions

In this paper, adding DUPIC fuel in Hyb-WT is suggested in order to overcome high reactivity swing problem. As a result, reactivity swing is alleviated by fissile production from DUPIC fuel. Additionally, required  $P_{\text{fusion}}$  is reduced and EM factor is increased. On the other hand, transmutation performance is degraded. Since Pu nuclides are produced by  $U_{238}$  capture reaction from DUPIC fuel. Radio-toxicity with LL TRU is reduced, radio-toxicity with SL TRU is increased by production of Pu nuclides.

However, the use of DUPIC fuel is more efficient in terms of WT than the use of Th or depleted U for fissile production. Because PWR spent fuel is reused. Therefore, future research is required in order to improve transmutation performance.

#### References

- [1] M. T. Siddique and M. H. Kim, 'Conceptual design study of Hyb-WT as fusion-fission hybrid reactor for waste transmutation', *Annals of Nuclear Energy* 65 (2014) 299–306.
- [2] M.S. Yang, et al., 'The Status and Prospect of DUPIC Fuel Technology', *Nuclear Engineering and Technology* 38 (2006) 359–374.
- [3] W. M. Stacey, 'Capabilities of a DT tokamak fusion neutron source for driving a spent nuclear fuel transmutation', *Nucl. Fusion*, 4 (2001) 135–154.
- [4] W. Zheng, 'The neutronics studies of a fusion fission hybrid reactor using pressure tube blankets', *Fusion Engineering and Design* 87 (2012) 1589–1596.
- [5] W.M. Stacey, et al., A TRU-Zr Metal Fuel, Sodium Cooled, Fast Subcritical Advanced Burner Reactor, Report, Nuclear & Radiological Engineering Program, Georgia Institute of Technology, Atlanta, GA, 30332-0425, May, 2007.
- [6] Sümer Şahin, 'Utilization Potential of Thorium in Fusion-Fission (Hybrid) Reactors and Accelerator-Driven Systems', *Thorium Energy for the World* 05 (2016) 443–44.
- [7] Carlos E. Velasquez, et al., 'Fusion-Fission Hybrid Systems for Transmutation', *Journal of Fusion Energy* 35 (2016) 505–512.
- [8] M.T. Siddique, S.H. Hong, and M.H. Kim, 'Physical investigation for neutron consumption and multiplication in fusion-fission hybrid test blanket module', *Fusion Engineering and Design* 89 (2014) 2679–2684.
- [9] S. H. Hong, M. T. Siddique and M. H. Kim, 'Transmutation performance analysis on coolant options in a hybrid reactor system design for high level waste incineration', *Fusion Engineering and Design* 100 (2015) 550–559.

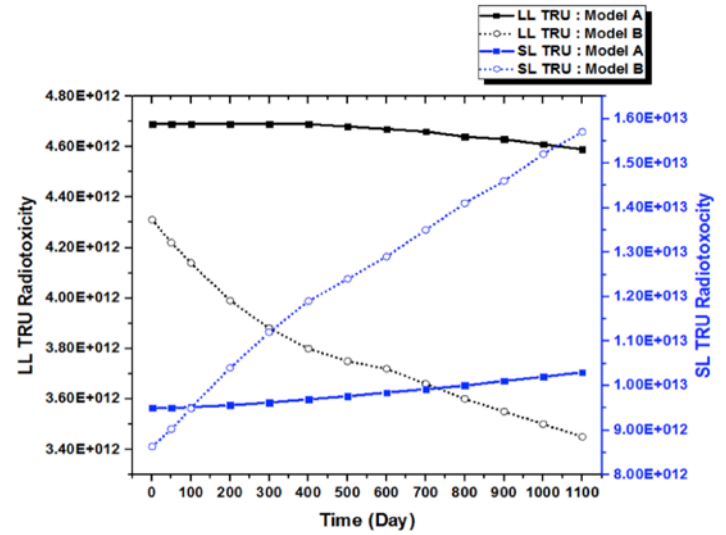


Figure 6. Ingestion Radio-Toxicity with TRU.

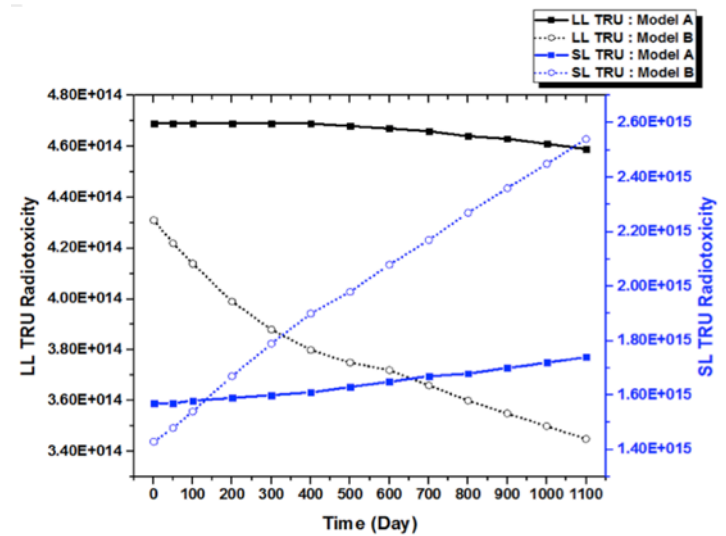


Figure 7. Inhalation Radio-Toxicity with TRU.

## 25 - Neutron Flux Map from Fusion to Fusion-Fission System

**Carlos E. Velasquez<sup>1,2,3</sup>, Graiciany de P. Barros<sup>4</sup>, Cláudia Pereira<sup>1,2,3</sup>, Maria Auxiliadora F. Veloso<sup>1,2,3</sup> and Antonella L. Costa<sup>1,2,3</sup>**

<sup>1</sup> Departamento de Engenharia Nuclear - Universidade Federal de Minas Gerais

Av. Antonio Carlos, 6627 campus UFMG -31.270-901, Belo Horizonte, MG - e-mail: claudia@nuclear.ufmg.br

<sup>2</sup> Instituto Nacional de Ciência e Tecnologia de Reatores Nucleares Inovadores/CNPq

<sup>3</sup> Rede Nacional de Fusão (FINEP/CNPq)

<sup>4</sup> Comissão Nacional de Energia Nuclear-CNEN - Rua Gal Severiano, 90 - Botafogo; 22290-901, Rio de Janeiro, Brasil

### Abstract

Fusion reactions such as the ones occurred in D-T plasmas produces neutrons with 14.1 MeV. This neutron due to its high energy propagates along the device. In spite of this, the neutrons produced are useful for the transmutation application. On the other hand, a nuclear reactor as known nowadays is based on fission reactions which produce about 2-3 neutrons per reaction with energies about 2-10 MeV. If both systems are coupled the materials will be exposed to two types of neutron irradiation the one coming from the fusion reaction and the other one from the fission. Therefore, neutron flux map of the fusion system helps to understand the neutron distribution of the fusion reactor with just fusion reactor and the distribution of fission reactor with the neutron produced by the fission chain on the transmutation layer inserted onto the fusion device. The simulations were performed on MCNP and the results allow mapping the neutron flux distribution axially and vertically on the device.

### 1. Introduction

The increment in the energy demand has been growing through the years, and it is expected to increase even more due to population and economic growth [1]. Currently, the most exploited energy source comes from non-renewable resources such as coal, oil, and natural gas [2]. The nuclear energy can respond to the demand without the greenhouse effect produced by the non-renewable resources. Inside of the nuclear energy exists two ways to produce energy by fusion and fission reactors.

Nevertheless, both of them have some issues to be solve, in the case of the fusion energy is a technology not available yet, the main problems are to reach the high temperatures for D-T plasmas and materials capable of withstanding these temperatures, as well as, tritium retention, neutron damage and plasma disruptions [3]. On the other hand, fission is a technology well known, but one of the major problems with this technology is the nuclear waste produced after burnup, which has high radiotoxicity and long half life.

In fact, both technologies are able to couple offering an important contribution to energy production. Either, the hybrid reactor could continue operating during pulses reset or plasma shutdown and still produce energy by the fission reactor or because the fast neutron flux produced by D-T reactions is able to transmute minor actinides (MA) by inducing fission reactions [4].

The main goal studied is the neutron transport through the different components of a Tokamak and a Fusion-Fission system (FFS). Therefore, it is to design a neutron flux map (NFM) axially and radially for the Tokamak and the FFS, to understand how the neutron transport works from the fusion device to a hybrid one. Therefore, three cases were created one just using the Tokamak (no-transmutation layer) and other two cases using a transmutation layer one at the beginning of cycle (BOC) and the other one at the end of cycle (EOC).

### 2. Methodology

The Tokamak design remains its main geometrical design from previous works but the materials were updated as presented in Table 1. On the other hand, a modification of the FFS from previous works [5,6] have been made also, the main purpose was to simplify the model enhancing simulation and neutron tracking. The transmutation layer has a 20 cm radially and 476.7 cm height, divided into 20 equally radially spaced zones, the first and the last of these zones contains the material HT-9 [7,8], and the other 18 intermediate zones were divided into four parts each, alternating between fuel and coolant, as an approximation of the transmutation layer, as shown in Fig.1. It is located inside the block shield and next to heat sink component.

The neutron transport obtained comes by tracking the particles in a mesh tool created on the MCNP [4], it allows plotting the neutron transport through both devices. Matlab [5] was used to process the data obtained from the MCNP's mesh. To analyze the neutrons neutron transport two meshes were created over the Tokamak and FFS, one in Cartesian coordinates (x-z axis) and the other one in cylindrical coordinates (r,θ, h), as shown schematically in Fig.2. The

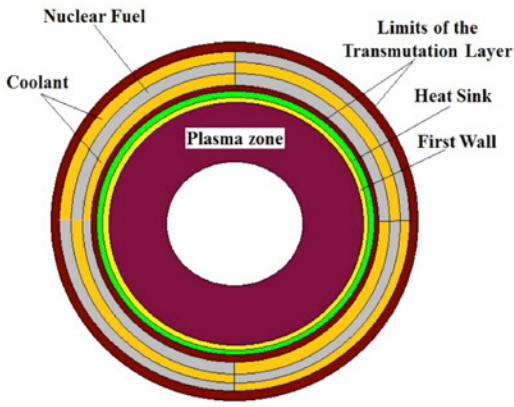


Figure 1. Schematically top view of the FFS

plasma chamber has a 402 and 853 cm of internal and external radius, respectively. The cylindrical mesh was divided into 36 angles of 10° each, 20 cm radially from 0 to 1000 cm and one division of 25 cm height. On the other hand, the rectangular mesh was divided in 50 x 50 grid from 250 to 1000 cm x -430 to 430 cm and a thickness of 5 cm. The fuel depletion and criticality calculation were performed with the MONTEBURNS code, which links the MCNP with the depletion code ORIGEN2.1, which was used to calculate the fuel depleted after the 10 years under irradiation.

Components	Material Composition	Temperature (K)
First wall inboard/outboard	Be-S65E/W1.1TiC	1013.15
Heat Sink	CuCrZr-IG	723.15
Blanket module block shield	SS316L(N)-IG (70%) + Water (30%)	613.15
Vacuum Vessel outer/inner shell	SS316L(N)-IG	533
Vacuum Vessel in wall shield	SS304B7 (55%) + Water (45%)	434.15
Thermal Shield	SS304L	100
TFC outer/inner shell	SS316LN	80
TFC	SS316LN (47.6%)+SS316L(1.5%)+He/liq-(12.9%)+Nb3Sn(6.3%)+r-epoxy(18%)+Cu (13.7%)	80
Cryostat	SS304L	95
Shield	Concrete	300
Central solenoid structure	SS316L(N)-IG	150
CS winding pack	Jk2SS (54.7%) + SS316L(1.2%) + Inconel(0.6%) + He/liq.(11.2%) + Cu(11%) + Nb3Sn(5.5%) + r-epoxy (15.8%)	4.7
CS fill	Nb3Sn	4.7
Coolant	Based on Lead	613.15
Clad	HT-9	900
Nuclear Fuel	UREX+/Th-(Th,TRU)	1200

Table 1. Materials and Temperatures for each Component [9-11]

### 2.1. Geometry of the Systems

The main differences between the Tokamak and FFS are the insertion of the transmutation layer, as can be seen in figures 3 and 4, show the fusion reactor with (left) and without (right) transmutation layer. The plasma has a major radius of 6.21 m and minor radius of 2 m. The neutron source strength is about  $\sim 1.44 \times 10^{21}$  n.s<sup>-1</sup>. The plasma chamber volume is about 837 m<sup>3</sup>.

### 3. Results

The NFP is represented by different colors for the two devices, Tokamak and FFS. The neutron transport through the medium allows to distinguish the neutron flux variation through the

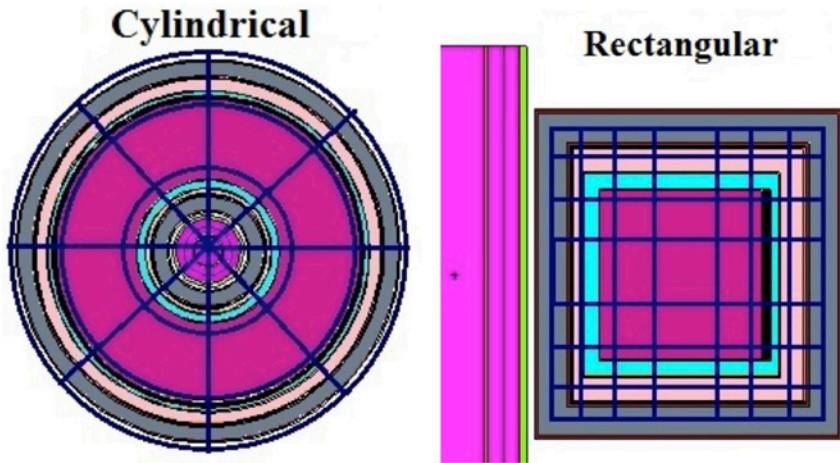


Figure 2. Left cylindrical coordinates and right rectangular coordinates

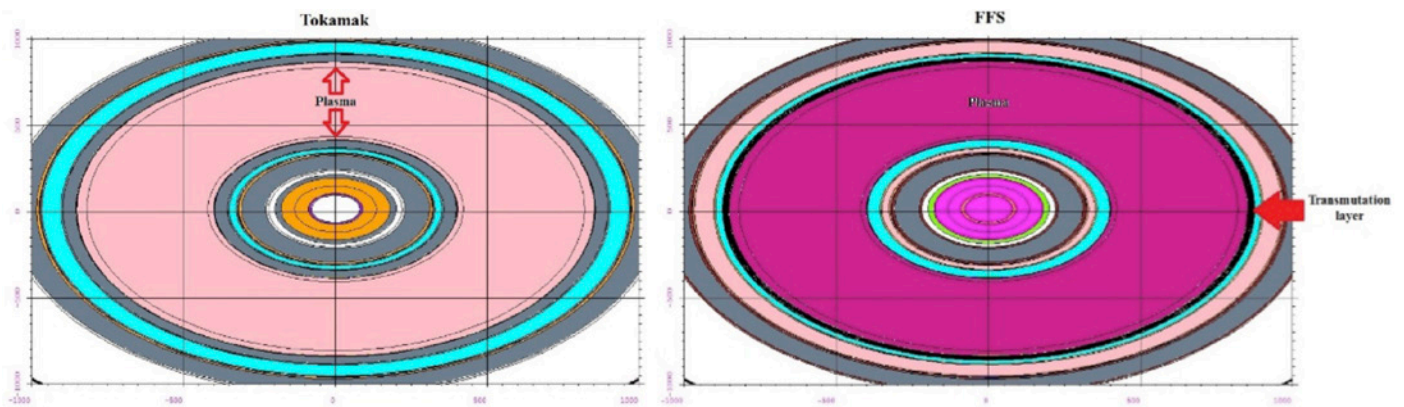
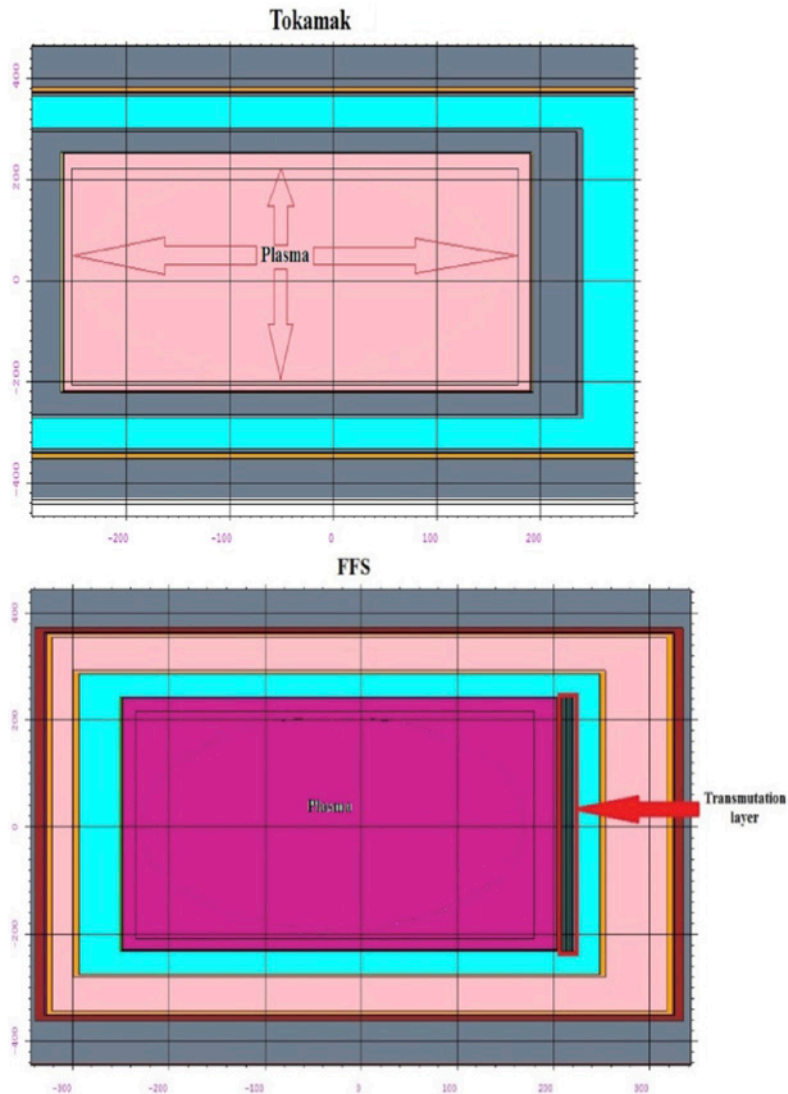


Figure 3. Radial top view of the Tokamak (left) and FFS (right)



system, which also corresponds to the hottest part of the devices.

### 3.1. Tokamak – NFP

Fig. 5 shows the modeled version of the Tokamak's top view (left) and its NFM by neutron flux zones (right), where can be seen that the red color in the line is the region where the plasma is created, in other words, the neutron zone production. Then follows a black surface which was not able to represent adequately the neutron transport through the device.

Nevertheless, to improve the resolution of the NFM, a contour tool was used to identify the neutron flux changes onto the system. Fig. 6 presents the old picture of the NFM (left) and the new one contouring the different neutron flux regions using a different color, where can be seen the neutrons attenuation through the different system components.

On the other hand, the NFM axially is presented in Fig.7, in this case, it was not necessary to utilize the contour option. The darkness yellow zone is the neutron source originated from the D-T reactions. The color degradation indicates the neutron attenuation through the system. It is uniformly distributed by regions, in which the fluxes decreases. The lines in black surrounded the reactor is noise originated by the code.

Figure 4. Axially view of the Tokamak (left) and FFS (right)

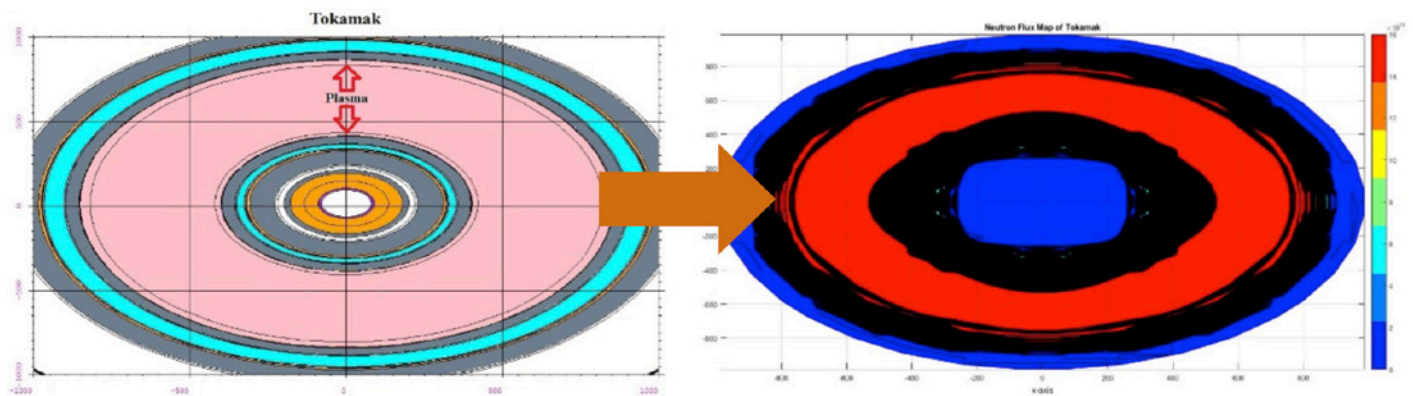


Figure 5. NFP from the Tokamak's radially top of view

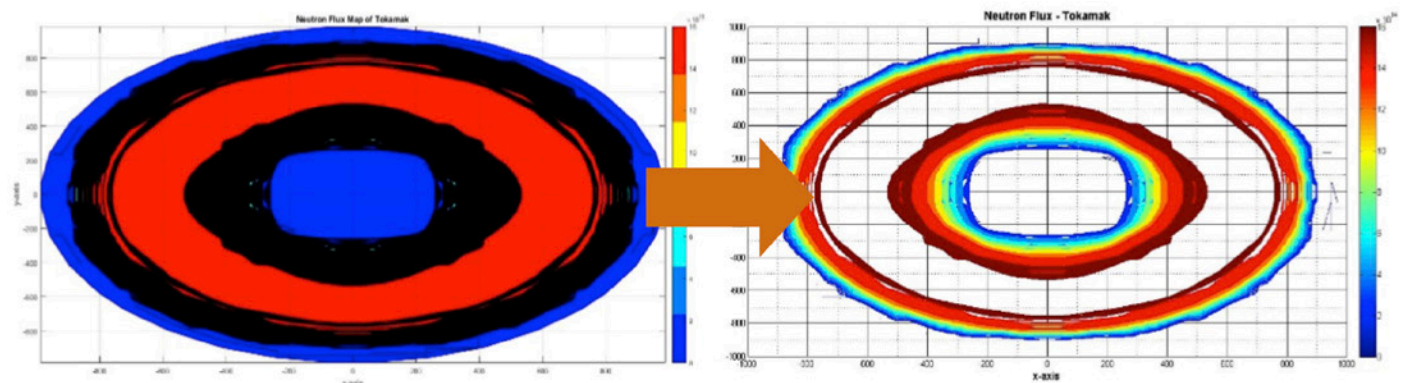


Figure 6. Radially NFP from the Tokamak by surfaces (left) and contours (right)

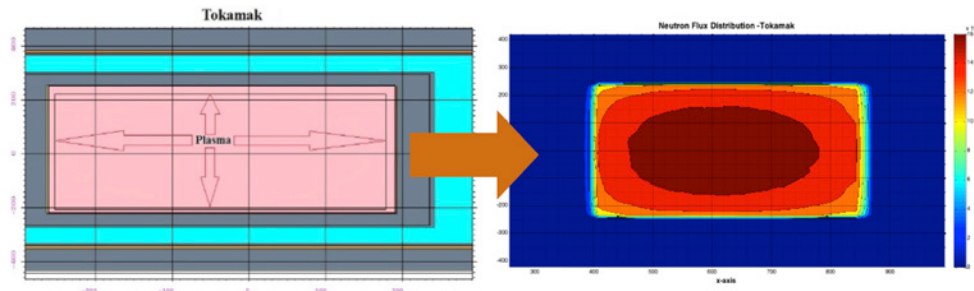


Figure 7. Axially NFP from the Tokamak by surfaces

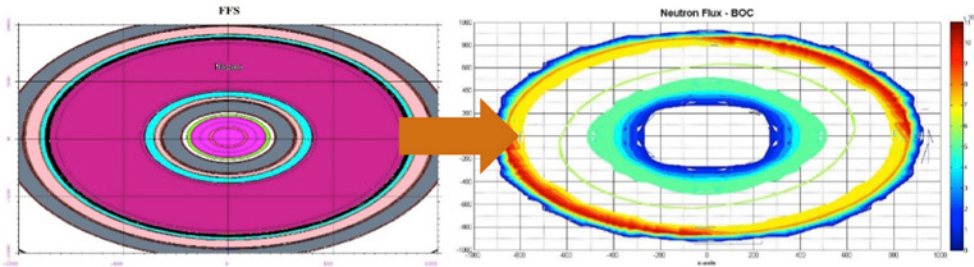


Figure 8. Fusion-fission system (left) radial design and its neutron flux map (right)

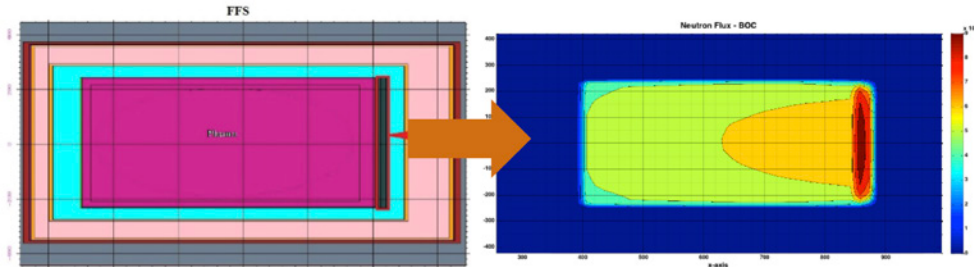


Figure 9. Axially Tokamak design (left) and the NFM at the BOC (right)

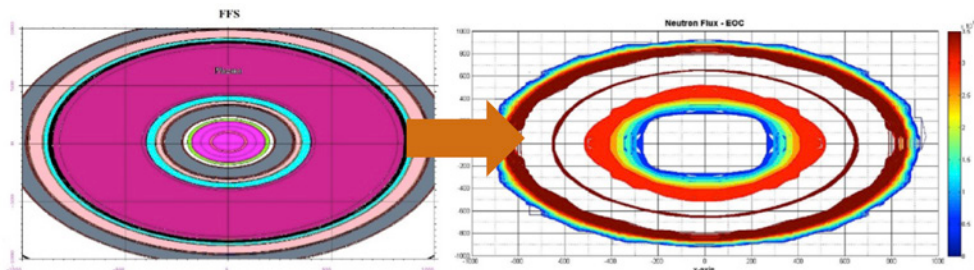


Figure 10. Radial design of the FFS (left) and NFM with the nuclear fuel at EOC (right).

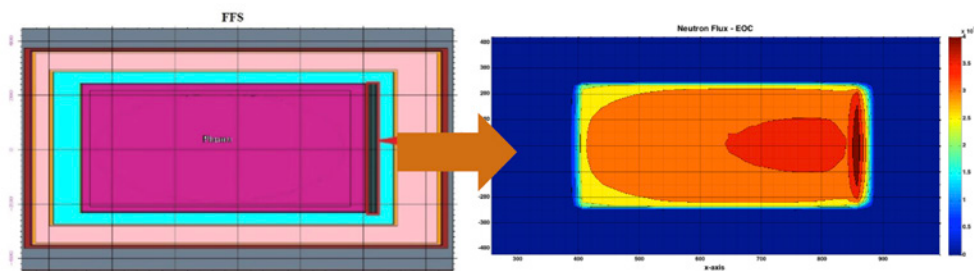


Figure 11. Axial design of the FFS (left) and NFM at the EOC

the neutron flux produced at EOC is weak and does not affect as much as BOC. On the other hand, Fig.11 shows the radial neutron flux distribution at the EOC. The highest neutron concentrations are located on the nuclear fuel region and inside the plasma chamber, which is not, as strong as, BOC changing the neutron flux distribution.

### 3.3. Neutron flux through the devices

Fig. 12 shows a comparison of the neutron flux through the different components for the Tokamak and the FFS, verifying the neutron flux variation between them. The FFS has higher neutron flux concentrations than the Tokamak due to the influence of the transmutation layer. These variations agree with the ones showed on the NFM calculations.

### 3.2. FFS – NFP

Fig. 8 shows the FFS design radially top view (left) and its NFM (right). The red zone on the NFM is the region where the nuclear fuel zone is placed before the coolant. The difference between the FFS and the Tokamak is that on the FFS the higher neutron concentration is found on the region with the nuclear fuel. This is easily explained due to the neutron flux produced by the fusion system and the ones produced by the fission chain are met together in this region, increasing the neutron concentration. Nevertheless, this can be decreased by placing the coolant in front of the nuclear fuel. In this case, the NFM was tracked at the BOC of the nuclear fuel.

Fig.9 presents the axially design of the FFS (left) and the NFM (right), as well as, the radial image the higher neutron flux concentration is located on the nuclear fuel region at the BOC. The NFM has a different shape than the neutron production by the plasma, it contains the neutron from both sides and even seems like both of them are mixing inside the plasma chamber.

Fig. 10 shows the axial design of the FFS (left) and the NFM (right) at the EOC, the zone with the highest neutron concentrations containing the nuclear fuel, as shown in Fig.8 is not anymore a high neutron concentration zone due to the fuel depletion decrease neutron flux generated. In conclusion,

## 4. Conclusions

The NFM variations show the variation from fusion to a fusion-fission system. The neutron concentrations will vary depending on the fuel depletion, becoming weaker at the EOC. The neutron fuel region had a higher neutron concentration due to the combination of the neutrons produced in D-T plasmas and the ones produced in the fission chain. As the transmutation layer is close to the plasma chamber it can be seen an influence on the neutron flux between the neutron production by fusion reactions and the one produced by fission chain.

## 5. Acknowledgments

The authors are grateful to the Brazilian research funding agencies, Coordenação de Aperfeiçoamento de Pessoal de Nível Superior - CAPES, Comissão Nacional de Energia Nuclear - CNEN, Conselho Nacional de Desenvolvimento Científico e Tecnológico -CNPq (Brazil), and Fundação de Amparo a Pesquisa do Estado de Minas Gerais -FAPEMIG (MG/Brazil)

## 6. References

- [1] U.S. Energy Information Administration (EIA), "International Energy Outlook 2016" Office of Energy Analysis, U.S. Department of Energy, Washington, <http://www.eia.gov/forecasts/ieo>, 2016.
- [2] International Energy Agency (IEA), "Key World Energy Statistics", OECD, IEA, [https://www.iea.org/publications/freepublications/publication/KeyWorld\\_Statistics\\_2015.pdf](https://www.iea.org/publications/freepublications/publication/KeyWorld_Statistics_2015.pdf), (2015).
- [3] Institute of Physics Report, "Fusion as an Energy Source: Challenges and Opportunities", IOP Institute of Physics, [https://www.iop.org/publications/iop/2008/file\\_38224.pdf](https://www.iop.org/publications/iop/2008/file_38224.pdf), (2008).
- [4] W.M.Stacey, Nuclear Reactor Physics, Wiley, Weinheim, (2007).
- [5] Carlos E. Velasquez, Graiciany P. Barros, Cláudia Pereira, Maria A. F. Veloso, Antonella L. Costa, "Fusion-Fission Hybrid Systems for Transmutation", Journal J. Fusion Energy 35 (3), 505-512 (2016)
- [6] C.E. Velasquez, C. Pereira, M.A.F. Veloso, A.L. Costa, "Layer thickness evaluation for transuranic transmutation in a fusion-fission system". Nuclear Engineering and Design, Vol. 286, pp. 94-103 (2006)
- [7] Mario D Carelli, Daniel T Ingersoll, "Handbook of Small Modular Nuclear Reactors", Woodhead publishing series in energy, (2014).
- [8] T.R. Allen, D.C. Crawford, "Lead-Cooled Fast Reactor Systems and the Fuels and Materials Challenges", Science and Technology of Nuclear Installations, Vol.2007, pp.1-11, (2007).
- [9] ITER, "Plant Description Document (PDD)- G A0 FDR 1 01-07-13 R1.0" [https://fusion.gat.com/iter/iter-fdr/final-report-sep-2001/Plant\\_Descptn\\_Docs\\_\(PDDs\)/](https://fusion.gat.com/iter/iter-fdr/final-report-sep-2001/Plant_Descptn_Docs_(PDDs)/)
- [10] H.HU, Y. Wu, M.Chen, Q.Zeng, A.Ding, S.Zheng, Y.Li, L.Lu, P.Long, FDS Team, "Benchmarking of SNAM with the ITER 3D model", Fusion Engineering and Design, Vol.82, pp.2867-2871, (2007)
- [11] Cardoso, F., Pereira, C., Veloso, M.A.F., Silva, C.A.M., Cunha, R., Costa, A.L.,. "A neutronic evaluation of reprocess fuel and depletion study of VHTR using MCNPXand WIMSD5 code". Fusion Science and Technology, Vol. 61, pp.338-342, (2012).

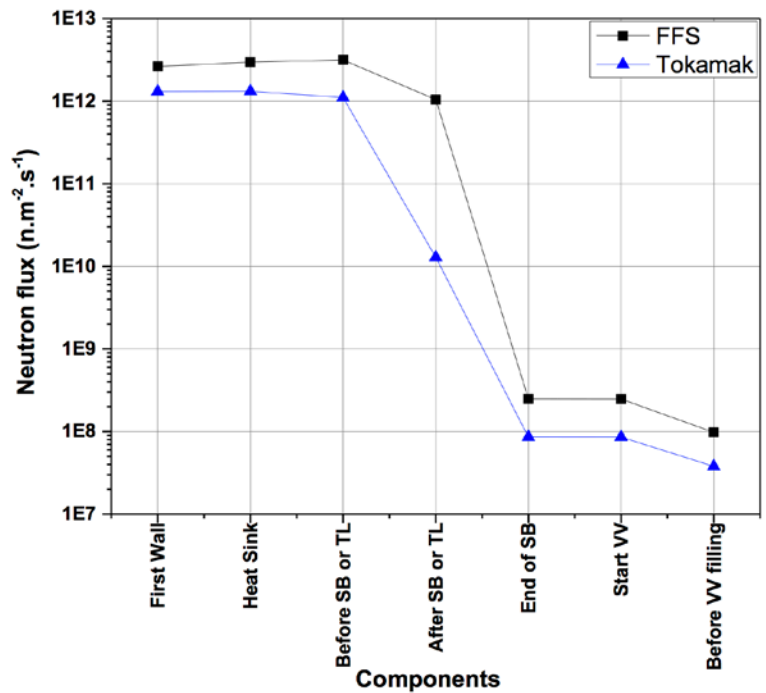


Figure 12. Neutron fluxes through the different components

## 26 - Neutron Production and Fast Particle Dynamics in Reversed-Field Pinch Plasmas in RFX-mod

**M. Zuin<sup>1\*</sup>, L. Stevanato<sup>2</sup>, E. Martines<sup>1</sup>, F. Auriemma<sup>1</sup>, B. Momo<sup>1</sup>, R. Cavazzana<sup>1</sup>, G. De Masi<sup>1</sup>, M. Gobbin<sup>1</sup>, W. Gonzalez<sup>1</sup>, R. Lorenzini<sup>1</sup>, M.E. Puiatti<sup>1</sup>, P. Scarin<sup>1</sup>, S. Spagnolo<sup>1</sup>, M. Spolaore<sup>1</sup>, M. Valisa<sup>1</sup>, N. Vianello<sup>1</sup>, W. Schneider<sup>5</sup>, D. Cester<sup>2</sup>, G. Nebbia<sup>3</sup>, L. Sajo-Bohus<sup>4</sup>, G. Viesti<sup>2</sup>**

<sup>1</sup> Consorzio RFX, C.so Stati Uniti 4, Padova, Italy - \*Corresponding author: [matteo.zuin@igi.cnr.it](mailto:matteo.zuin@igi.cnr.it)

<sup>2</sup> Dipartimento di Fisica ed Astronomia dell'Università di Padova, Padova, Italy

<sup>3</sup> INFN Sezione di Padova, Via Marzolo 8, Padova, Italy

<sup>4</sup> Universidad Simón Bolívar, Caracas 1080A, Venezuela

<sup>5</sup> Max-Planck –Institut für Plasmaphysik, EURATOM Association Greifswald, Germany

An experimental study of neutron production and particle dynamics in Deuterium plasmas is presented in the RFX-mod device operated in reversed-field pinch (RFP) configuration. In the RFP, the toroidal magnetic field is one order of magnitude smaller than in a tokamak, and is mainly generated by currents flowing in the plasma itself, thus reducing the need for superconducting coils. This feature underlies the main potential advantage as a reactor concept of the RFP, namely the capability of achieving fusion conditions with purely ohmic heating in a much simpler and compact device.

The present analysis is mainly based on data collected by means of a couple of neutron and gamma-ray detectors and of a neutral particle analyzer (NPA). The NPA resolves the energy distribution of the neutral atoms produced by charge-exchange processes, exiting the plasma on the low field side and on the equatorial plane of the machine. Energy and mass dispersion are produced by a combination of electrostatic and magnetic fields.

Neutron and gamma-ray fluxes are measured by means of 2 scintillators (EJ-301 liquid and NaI(Tl)) coupled to flat-panel photomultipliers, suitable for operation in a noisy magnetic environment.

The production of neutrons from D-D fusion reactions and gamma rays in RFP plasmas is found to be determined by the ohmic input power, with a threshold value of about 1.2MA in terms of plasma current. Above this threshold, neutron and gamma fluxes become strong function of the plasma current.

Neutron and gamma production dynamics is largely influenced by the MHD activity of the RFP plasmas. In particular, a bursty enhancement of neutron yields, correlated with the spontaneous magnetic reconnection processes, occurs almost cyclically in the RFP plasmas.

Magnetic reconnection, which is known to be associated to heating and particle acceleration, indeed is also found to modify the energy distribution of the collected neutral atoms having impact on both the Maxwellian component and on the observed higher energy tail.

The spontaneous generation of fast particles is of particular interest in RFP plasmas, as it has been proven by means of external beams that high energy ions exhibit good confinement properties, with a classical behavior and no enhanced radial transport. The possible role of such particles in the destabilization of the observed Alfvén eigenmodes is also discussed.

Data from RFP experiments are compared to those obtained in low-current tokamak campaigns also performed in RFX-mod.

## 27 - Development of liquid metal technologies for innovative nuclear systems

**A. Venturini<sup>a\*</sup>, M. Tarantino<sup>b</sup>, M. Utili<sup>b</sup>, A. Del Nevo<sup>b</sup>, I. Di Piazza<sup>b</sup>, D. Martelli<sup>a</sup>**

<sup>a</sup> University of Pisa, Dipartimento di Ingegneria Civile e Industriale, Largo L. Lazzarino 2, Pisa, Italy

<sup>b</sup> ENEA, Department for Fusion and Technologies for Nuclear Safety and Security, Experimental Engineering Division, C.R. ENEA Brasimone

Since 90's, ENEA is committed on the development of liquid metal technologies aiming at supporting the implementation of innovative nuclear systems, such as Gen-IV Lead-cooled Fast Reactor [1] and DEMO Reactor [2,3].

Great interest has been focused on the development and testing of new technologies related to HLM nuclear reactors, ever since Lead-cooled Fast Reactors (LFR) were conceptualized in the frame of GEN IV International Forum (GIF). In this frame, ENEA developed a large fleet of experimental facilities (e.g., CIRCE, NACIE-UP, HELENA, LIFUS5, LECOR, etc..) aiming at investigating HLM thermal-hydraulics, coolant chemistry control, corrosion behavior for structural materials and at developing components, instrumentations and innovative systems, supported by experiments and numerical tools.

On the other side, relating to fusion application, ENEA is involved on the breeder blanket (BB) design as well. Three out of four European breeder blankets concepts for DEMO use the eutectic PbLi enriched at 90% in <sup>6</sup>Li as breeder: Helium Cooled Lithium Lead (HCLL), Water Cooled Lithium Lead (WCLL) and Dual Coolant Lithium Lead (DCLL). The main functional requirements of the PbLi loop systems are: to provide adequate heating in order to maintain the coolant in the liquid state in all system locations; to circulate the liquid PbLi through the BB; to extract Tritium produced in the breeder modules from the coolant (this function is shared with the Tritium Extraction System); to control the coolant chemistry and to remove accumulated impurities; to ensure the operation of the loop in every condition.

Again, in this frame ENEA developed at Brasimone R.C. a relevant fleet of experimental facilities (e.g., TRIEX, IELLLO, EBBTF, LIFUS5, etc.), aiming at supporting the breeder blanket development in Europe.

The present work aims at highlighting the capabilities and competencies developed by ENEA so far in the frame of the liquid metal technologies, both for GEN-IV LFR and DEMO nuclear machines.

### 1. Introduction

A comprehensive R&D program related to the use of liquid metals is necessary on the associated technologies, properties, neutronic characteristics and compatibility with structural materials. Furthermore, innovations require qualification programs of new components and systems, together with the continuous program of code validation.

### 2. Activities related to GEN-IV LFR

Several experimental campaigns employing HLM loop and pool facilities (CIRCE, NACIE, HELENA, LIFUS5) were and are being carried out in order to support HLM technologies development. This chapter aims at providing a short overview of these activities.

#### 2.1. Activities on CIRCE

Suitable experiments were carried out on the CIRCE pool facility [4], which was equipped with the Integral Circulation Experiment (ICE) test section [5] in order to investigate the thermal hydraulics and the heat transfer in grid spaced fuel pin bundle cooled by liquid metal providing, among the other purposes, experimental data in support of codes validation for the European fast reactor development.

The study of thermal stratification in large pool reactor is relevant in the design of HLM nuclear reactor especially for safety issues. Thermal stratification can induce thermo-mechanical stresses on the structures and, in accidental scenarios, it could oppose to the establishment of natural circulation which is a fundamental aspect for the achievement of the GEN-IV safety goals. A Protected Loss of Heat Sink with Loss Of Flow (PLOHS+LOF) scenario was experimentally simulated and the mixed convection with thermal stratification phenomena was investigated during the transient. Two tests (C and D) of about 100 and 200 h were performed by achieving a steady state condition at full power (750 kW) and by simulating the transition in DHR conditions respectively in natural and forced circulation. After the transition to DHR conditions, the power supplied to the bundle is decreased to about 30 kW to simulate the decay heat.

The LBE mass flow rate through the ICE test section reaches a value of about 59.6 kg/s under forced circulation (argon flow rate of about 2.5 NI/s), while it is about 8.8 kg/s after the transition to natural circulation conditions.

In order to investigate the thermal stratification inside the large LBE pool all the 119 TCs installed in the pool region of the vessel are shown as a function of the axial depth in Figure 1 and Figure 2 at different times.

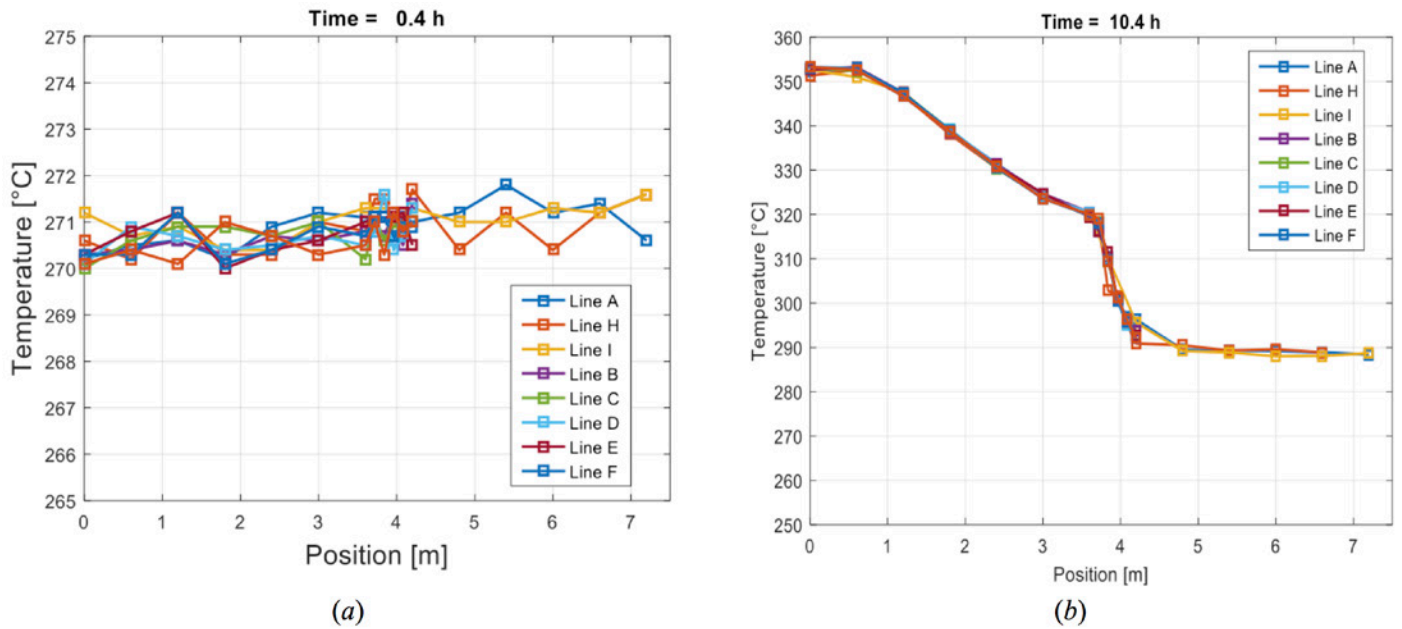


Figure 1: test C, pool thermal stratification.

At the beginning of the experimental test (Figure 1a), the LBE temperature is quite uniform inside the pool with an average value of about 270 °C. At the end of the full power phase (forced circulation conditions after about 10.4h) thermal stratification phenomena are evident inside the pool, with a thermal gradient of about 30°C in the first 3.5 m (up to the outlet section of the HX). Then, there is a region between the outlet sections of the HX and the DHR where the slope of the thermal gradient increase with a temperature difference of about 30°C in 0.5 m. In the lower part of the pool (from the inlet section of the ICE test section to the bottom of the vessel), the temperature is uniform with a value of about 290°C. After the transition to natural circulation conditions, the temperature field significantly changes becoming quite uniform in the entire LBE pool region.

Concerning the investigation of the heat transfer inside the fuel bundle, Nu number is calculated for test C from the experimental data in the central subchannel of the Fuel Pin Simulator (FPS) according to [6] and obtained results are compared with Nu values obtained from Ushakov and Mikityuk correlations [7,8]. To this end, high and low power run are subdivided into shorter intervals (no longer than 1 h) in order to maintain pins temperatures constant in the central subchannel of the FPS (for the low power run a time frame from 75 h to 99 h is considered).

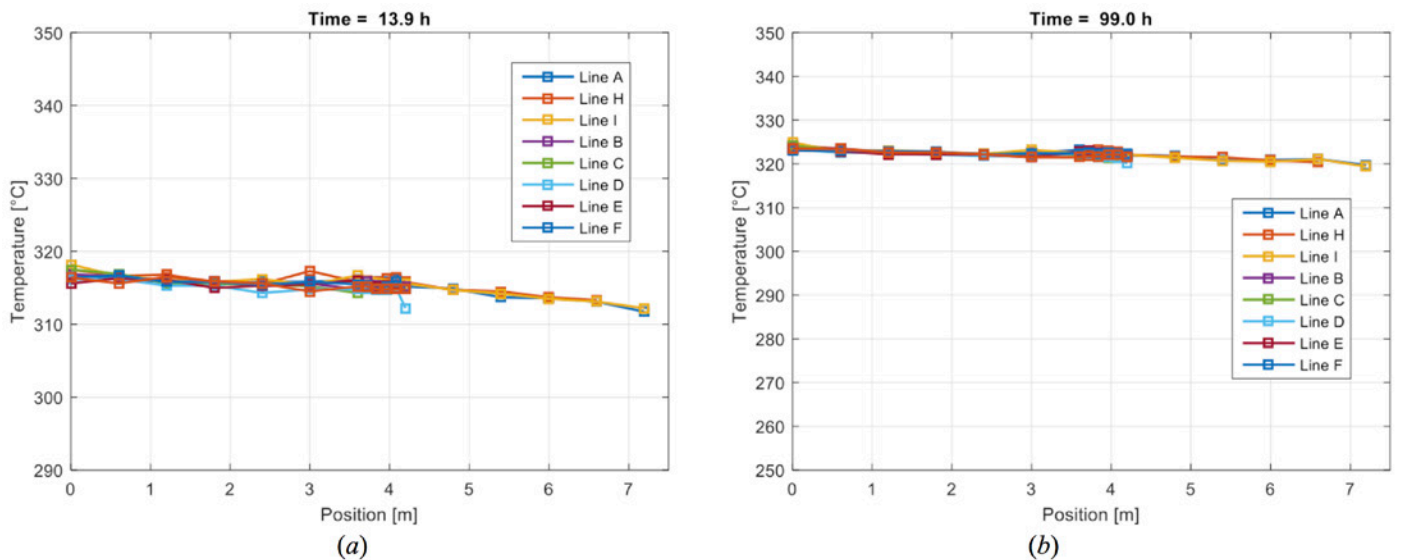


Figure 2: test C, pool thermal stratification.

A good agreement was found between the experimental data and the Mikityuk and Ushakov correlations with obtained data that show a general tendency to lie below Nu values given by the correlations.

## 2.2. Activities on NACIE-UP

A 19-pin fuel bundle was installed in the NACIE-UP facility [9] to study the heat transfer with a heavy liquid metal in a wire-spaced FPS. The FPS installed in the NACIE-UP facility was designed to be representative of the fuel assembly of the MYRRHA nuclear facility to be built at SCK-CEN [10]. In this framework, the NACIE-UP experiment is focused on the

low-intermediate mass flow rate and on the assessment of the coolability of the FA in these conditions. The availability of experimental data is also mandatory for the validation of codes. In particular, turbulence and heat transfer models need to be extensively qualified for the applications to liquid metals, which are characterized by low Prandtl number. The validation of CFD and SYS-TH general purpose codes for HLM is a very important issue not only for design but also for safety analysis.

The test section was instrumented with 67 thermocouples, placed at three axial positions, which monitor wall and sub-channel temperatures allowing to calculate local and section-averaged Nusselt numbers. The sub-channel Reynolds and Péclet numbers were respectively  $<12000$  and  $<400$ , in the laminar or early transitional range. Tests with natural circulation and gas-lift enhanced circulation flow regimes were performed.

Data acquisition started after that statistical steady state conditions were reached and data collection lasted about 15-20 minutes (900-1200 samples) in order to have a set of data statistically relevant. Collected data were post-processed by a Matlab routine which includes an error analysis numerical method consistent with the error propagation theory.

Measurements of wall thermocouples proved to be quite accurate. Some oscillations are presents in the signal, but the same oscillating trend is exhibited by all the TCs in the same sub-channel. Therefore, the wall-bulk temperature difference remains quite constant with a low error. Temperature differences  $T_w - T_b$  up to 2.5-3 °C are detected with good accuracy. For lower temperature differences the measure is affected by instruments errors leading to uncertainties in the calculation of derived quantities like the Nusselt number.

Two different analyses for heat transfer were performed: local analysis in single sub-channel and overall section analysis. Results on local analyses generally show consistency. Nusselt numbers in central channels are well represented by two of the correlation chosen. Nusselt in peripheral sub-channels are lower as the thermal field is affected by the heat transfer to the outer structures. Section-averaged analysis on heat transfer showed some differences which depend on the definition adopted for the average Nusselt. In this work, two definitions were chosen. The first one ( $Nu_1$ ) is based on section-averaged temperatures; while the second one ( $Nu_2$ ) on the weighted average among the local Nusselt numbers. The second method shows higher values of Nusselt than the first one at the same Péclet (30 % higher), proving that results depend on the adopted definitions (Figure 3). This is a key feature of the HLM cooled bundle thermal-hydraulics, where temperature difference in a section can be high, up to 50 °C in nominal conditions, and there is a substantial difference between central channel temperature and section-average bulk temperature.

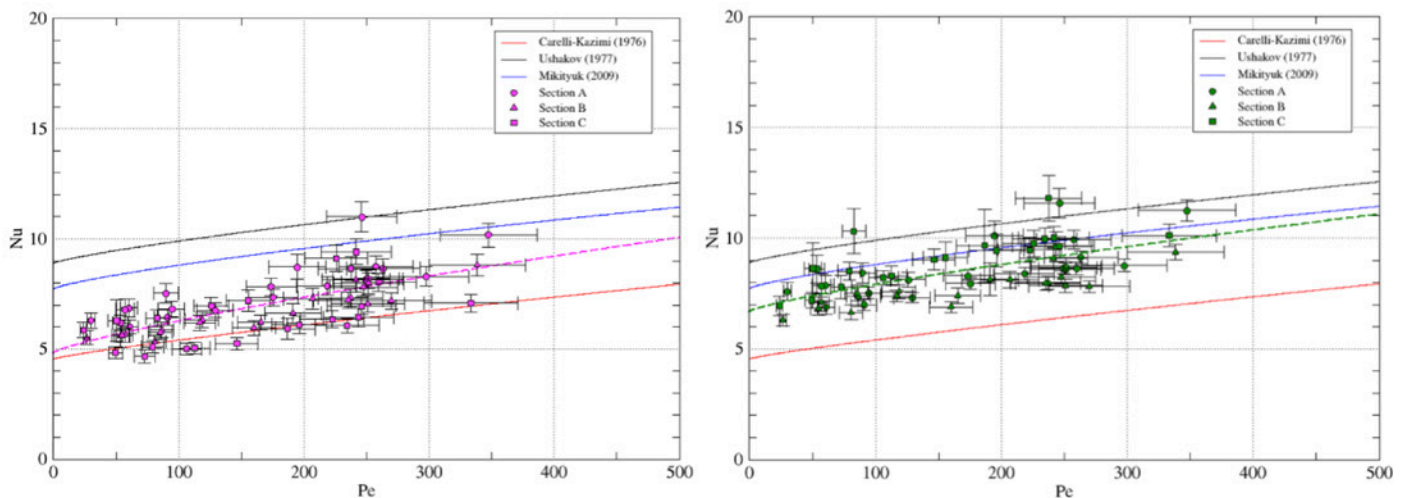


Figure 3: Section-averaged Nusselt number  $Nu_1$  (left) and  $Nu_2$  (right) at all the sections for all test cases.

The comparison of the experimental data with correlations is a good practice to investigate the global coherence of the data set, but the specific geometry in the specific flow rate range with heavy liquid metals probably was never investigated from experimental point of view in the past. Moreover, correlations for complex geometries are generally based on largely non-uniform experimental data sets. From this remark, probably the best practice is simply to describe accurately the experimental setup and the definitions adopted and to be very careful in comparison with correlations or other experimental data sets.

### 2.3. Activities on LIFUS5/Mod2

The study of the interaction between the secondary side coolant (water) and the HLM has an outstanding importance for the safety of LFR. This occurrence is known as Steam Generator Tube Rupture (SGTR) and it has to be considered a challenging safety issue in the design. In this framework, experimental activities were carried out at different scales and for different steam generators and reactor designs (i.e., MYRRHA and ELFR [11]).

LIFUS5/Mod2, small scale and high pressure facility, hosted a new test section having a geometry representative of the spiral tube bundle of ELFR steam generator [12]. Experiments were executed with boundary and initial conditions

relevant for the SGTR accident. The objective was to investigate the potential for tube-to-tube rupture propagation, as well as to demonstrate the reliability of computer codes in simulating the phenomena of interest. The implemented test section was composed by a vertical tube bundle of 188 tubes. The water supply system injected water in the central tube at 180 bar and about 270°C in a small vessel filled with LBE at 400°C with a cover gas of argon at about 2 bar. The experiments provided pressure, temperature and strain time trends at a frequency up to 10 kHz, suitable for the analysis of interaction phenomena and code validation.

Numerical codes were applied for supporting the experimental campaign, the design of experiments and for experimental data analysis. RELAP5/MOD3.3 supported the qualification of the facility water injection line. The post-test analysis was mainly based on the comparisons of the experimental and calculated pressure trends by SIMMER-III code. It provided for the first run an excellent simulation of the first pressure peak resulting from the rupture of the injector.

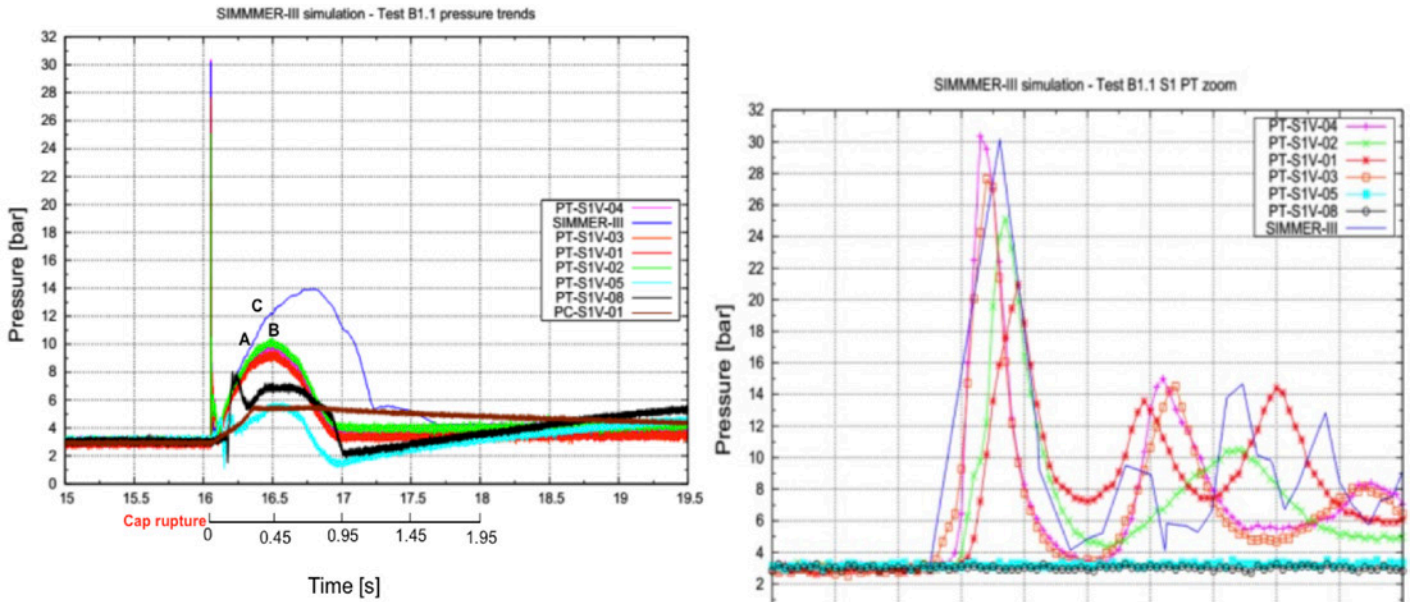


Figure 4: experimental and calculated pressure time trends in S1 (zoom of the first peaks on the right).

The experimental data of the first test (B1.1) showed that first pressure peaks were lower than 30 bar (Figure 4). The pressure wave propagation was largely damped by the “tubes tangle” and perforated plate of the test section. A preliminary post-test analysis was performed by SIMMER-III code. The nodalisation of LIFUS5/Mod2 facility in LEADER configuration was developed and set-up. The analysis demonstrated that the code is able to simulate the first pressure peak measured when the cap is broken. The code predicted the maximum pressure value (30 bar) and the timing of the phenomenon ( $10^{-3}$  s). The second pressure peak, due to the steam expansion in the reaction vessel, was also correctly simulated by the code, even though overestimated (4 bar higher). The deviation is probably correlated to a plug of LBE in the vertical section that connects the reaction tank to the dump tank due to geometrical approximations of the model. The final experimental and simulated values of pressure in tanks system were in agreement. This confirmed that the amount of water and steam injected in the simulation is consistent with the experimental one. The water injection at about 180 bar in the center of the tube bundle caused a pressurization measured at the reaction tank wall of about 30 bar for both B1.2 and B1.3 tests.

These experiments highlighted that no leakages occurred from the 12 pressurized tubes of the test section and a remarkable damping of wave propagation. This might imply a low probability of propagation of the tube rupture on surrounding tubes. Confirmation is expected at the end of the experimental campaign, when also the second and third series of tests, having higher injection orifice, will be carried out.

#### 2.4. Activities on corrosion in flowing LBE and lead

The corrosion behaviour of AISI 316L austenitic steel and T91 martensitic steel were investigated in flowing lead–bismuth eutectic (LBE) at 400 C. The tests were performed in the LECOR [13] and CHEOPE III loops [14] at low and high oxygen concentrations, respectively.

The results of corrosion tests performed revealed that oxygen concentration in LBE affects the corrosion mechanism of steels at present test temperature ( $T = 400$  C). At low oxygen concentration ( $C[O_2] = 10^8$ - $10^{10}$  wt.%) both steels exhibited the dissolution of alloy elements, and a weight loss was measured. For austenitic steel 316L, Ni depletion has been detected, with the formation of a ferrite layer in the corrosion area. This seems due to the high solubility of Ni in LBE. For martensitic steel T91 an uniform attack by LBE was observed, and the liquid metal penetration appears on the interface between steel and liquid metal. However, no preferential dissolution of alloy elements was detected

in the attack area. Comparing the corrosion rates of AISI 316L and T91, the corrosion rate found for the martensitic steel is higher than that for austenitic steel. The optical analysis on the corroded specimen showed a very limited attack after 1500 h for both steels, while the corrosion became evident on the whole surface of the T91 specimen after 4500 h. This behaviour could be explained assuming that a thin layer of natural oxide is present on the specimens at the beginning, and it acts as barrier against the liquid metal attack. Before that the corrosion can take place, this layer has to be removed. Under the test condition adopted in the LECOR loop, the natural oxide film on the martensitic steel is more easily removed by the LBE in comparison to the austenitic steel. This could be the reason for the higher corrosion rate obtained for the martensitic steel and could also explain the increase in the corrosion rate observed with increasing the time exposure.

At high oxygen concentration ( $C[O_2] = 10^5\text{-}10^6$  wt.%) a protective oxide layer on the specimens surface have been detected, and a weight gain was measured for both steels. The oxide layers can protect the steels from dissolution attack induced by LBE. Notwithstanding these layers are stable and compact for both steels, the one formed on the surface of austenitic steel is much more thin than that one formed on the surface of martensitic steel. From the data of weight gain and SEM analysis, the AISI 316L shows a higher resistance to oxidation, at the present test conditions. Concerning the oxide layer formed on the surface of martensitic steel, it consists of two sub-layers: the outer is magnetite while the inner is Fe/Cr spinel.

LECOR loop was recently updated and it will be used to perform an analysis of the corrosion behaviour of 15-15Ti(Si) and DS4 (15Cr-25Ni) austenitic steels, together with the  $Al_2O_3$  and TiN coatings laid on a layer of 15-15Ti(Si). The specimens were weighted and measured before being exposed in flowing lead. The specimens with the TiN coatings were also examined with the SEM microscope with the aim to evaluate the quality of the coating. At the end of the experiments the specimens will undergo metallographic analyses. The lead temperature is 550 °C, while its velocity can be varied in the range 0.3-1 m/s. The exposure times are 1000, 4000 and 8000 hours.

## 2.5. Activities on HELENA

The HELENA facility [15] is a loop working in pure lead for experiments in the field of corrosion for LFR structural materials, component testing, and thermal-hydraulic investigations.

A prototypical mechanical pump was designed and manufactured to properly work in pure lead at high temperatures. A long-run test on the component was performed in isothermal conditions at 400°C and with low oxygen content (<10<sup>-8</sup> wt.%). The oxygen content was continuously monitored. The pump was gradually driven to the reference mass flow rate of 35 kg/s and this mass flow rate was maintained for 1500 h, i.e. about 2 months. After this, the pump was stopped and the loop was drained. Then, the pump impeller was disassembled and it was analyzed for corrosion. A test on a ball valve was also carried out for a few months.

At the end of 2014, the facility was upgraded with the insertion of a FPS in the heating section and adding a secondary side. A 19-pin wire-spaced FPS was installed to measure the clad temperatures and the heat transfer coefficients in different conditions in the different ranks of sub-channels of the MYRRHA bundle. A test matrix on the forced convection condition in the wire-spaced bundle will be carried out. A shell and tube heat exchanger couples the primary lead loop with the secondary side filled with water at 100 bar. Lead flows in the 7 tubes, while water flows in the shell side. The gap is filled with a steel powder. Bubble tubes with flowing Ar are adopted to measure pressure losses in the different branches of the loop. An ancillary gas system ensures the cover gas for the loop.

## 3. Activities related to breeder blanket development

The development of a BB with PbLi as breeder require to overtake several technological issues, related to structural material compatibility (mainly corrosion and activation), Tritium handling, coolant chemistry and purification, magneto-hydro dynamics, pumping system, instrumentation and safety concerns. ENEA is giving a significant contribution to almost every topic by means of the experimental facilities installed at Brasimone R.C.

### 3.1. Activities on IELLLO

The Integrated European Lead Lithium LOop (IELLLO [16]) aims to carry out thermo-fluid dynamic tests on mock-up of HCLL blanket modules up to full scale, in ITER relevant conditions; characterization of instrumentations, auxiliary circuits and components relevant to lead lithium loops; LOCA simulations on HCLL TBM mock up (THALLIUM test section [17]). Thermo-hydraulic system codes are used in order to perform the thermodynamic design of PbLi loops and to analyse transient conditions during operation and safety analysis. Thus, code validation is another purpose of IELLLO facility. 77 circulation tests were carried out at different maximum temperatures (from 673 to 813 K) and pump speeds (from 100 to 700 rpm). The performances of the economizer and of the air cooler were assessed and compared with the results of RELAP5-3D simulations. The tests revealed performances of the economizer higher than those expected after the preliminary theoretical evaluations. In details, measured efficiencies are from 5% to 8% higher than the expected

ones. The air cooler can be operated in natural convection, simply opening its shutter, and in forced convection by switching on the blower. Similarly to the economizer, the performances of the air cooler in natural convection mode are higher for low mass flow rates. In spite of that, a  $\Delta T$  of about 70 K at the lowest pump rotational speed can be considered an interesting value, even in prevision of the ITER relevant tests, which will be performed at lower mass flow rates (0.2-1.0 kg/s). As far as the numerical simulations are concerned, RELAP5-3D tends to slightly overestimate the efficiency of the economizer at high flow rates, with an average error of 2.67 percentage points and a unique maximum error of 9.90 percentage points while underestimates the  $\Delta T$  produced by the air cooler with an average error of 2.95 K, with three exceptions at 1.28 kg/s where the error is about 20 K.

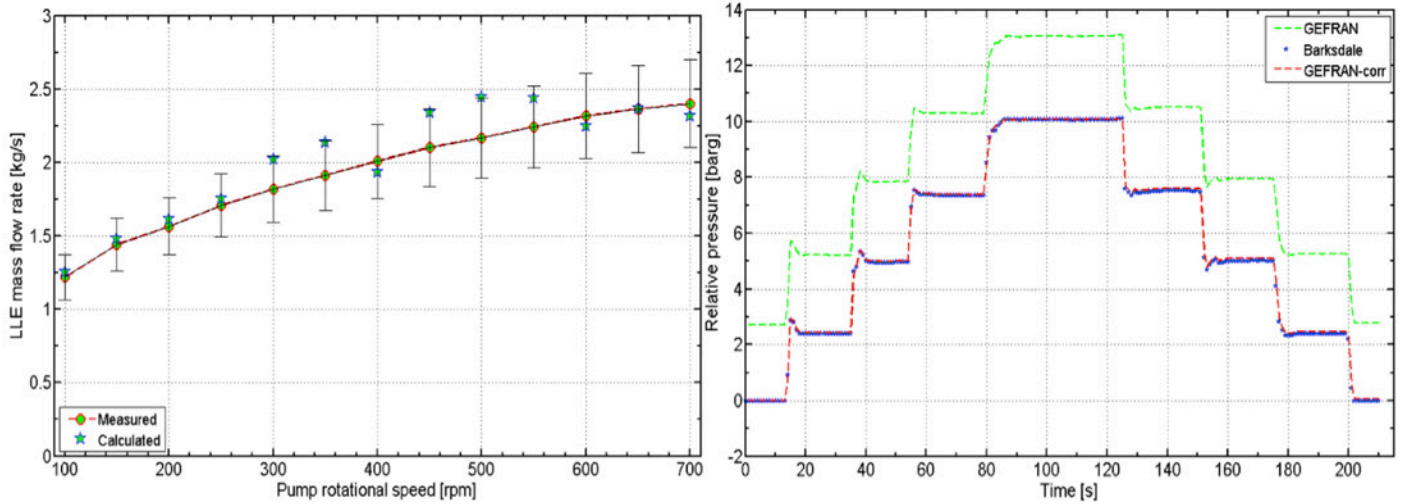


Figure 5: results of the flow meter qualification tests (left) and of the qualification of the pressure transducer (right).

This experimental campaign also evaluated the performances of a Vortex mass flow meter and of an absolute pressure transducer (Figure 5). The Vortex mass flow meter was firstly calibrated for water and, afterwards, adapted for lead lithium. To qualify the mass flow meter the real mass flow rate is calculated from a power balance across the electrical heater and compared with the measured one. The error bar is fixed at the 10 % mainly because of the uncertainties involved in the calculation of the power dissipated in the electrical heater. The pressure transducer was qualified with a special device and a corrective equation was found. After the implementation of the formula, the maximum error is around 100 mbar, while the standard deviation lies between 25 and 40 mbar. These values correspond to a maximum error of 0.5 % on the FSO for a 0-20 bar transducer. The pressure transducers revealed a good accuracy for temperatures between 523 K and 673 K.

The test section THALLIUM (Test HAMmer in Lead LITHIUM) is currently installed within IELLLO. It was designed to reproduce the geometry of the LLE loop of the HCLL TBM. The main objective of the ongoing experimental campaign is to study the release of high pressure He in the PbLi. The second objective is to validate the system code RELAP5-3D with the data produced. Furthermore, an additional task is to test new instrumentation and, in particular, pressure meters with acquisition frequency of 1 kHz and a guided-microwave level meter installed in the expansion tank. The experiments simulate the rupture of a pipe in a stiffening plate of the HCLL TBM and the consequent injection of He from the Helium Cooling System of ITER.

IELLLO can be coupled with the He facility HeFUS3 to constitute EBBTF (European Breeding Blanket Test Facility), a facility dedicated to the qualification of HCLL TBM before its installation in ITER and to test the main TBM auxiliary systems: tritium extraction system, coolant purification system, etc.

### 3.2. Design of the WCLL BB

Water-cooled lithium-lead breeding blanket is considered a candidate option for European DEMO nuclear fusion reactor. ENEA and the Linked Third Parties proposed and are developing a multi-module blanket segment concept based on DEMO 2015 specifications. The layout of the module is based on horizontal (i.e. radial-toroidal) water cooling tubes in the breeding zone, and on lithium lead flowing in radial-poloidal direction. This design choice is driven by the rationale to have a modular design, where a basic geometry is repeated along the poloidal direction. The modules are connected with a back supporting structure, designed to withstand thermal and mechanical loads due to normal operation and selected postulated accidents. Water and lithium lead manifolds are designed and integrated with a consistent primary heat transport system, based on a reliable pressurized water reactor operating experience, and the lithium lead system. Thermo-mechanics (TM), thermo-hydraulics (TH) and neutronics analyses were performed [18,19,20,21,22].

The Neutron Wall Load distribution (average 1 MW/m<sup>2</sup>) and radial nuclear power densities in materials are calculated by MCNP 5 code [23]. An average First Wall (FW) heat flux of 0.22 MW/m<sup>2</sup> is assumed for the evaluation of the thermal

balance and an HF of  $0.5 \text{ MW/m}^2$  is used for the design of the equatorial outer module. Irradiation limit of material during operation is assumed as 20 dpa. Tritium breeding ratio larger/equal to 1.1 is a requirement. Reference primary system thermodynamic cycle is based on coolant at inlet/outlet temperatures respectively equal to  $285 \text{ }^\circ\text{C}$  and  $325 \text{ }^\circ\text{C}$ , at 15.5 MPa. The design of the cooling system accounts for the maximum temperature limit of  $550^\circ\text{C}$ . The cooling system is designed for a nominal pressure of 15.5 MPa, the PbLi pipelines, manifolds and breeding blanket box are verified to withstand a pressure of 15.5 MPa + 10%, as Class IV condition.

Both inner and outer segments are divided into 7 boxes with straight surfaces, attached to a common back supporting structure. The breeding blanket boxes are constituted by the breeder zone and the FW. The FW is in the front part of the WCLL BB. It is an integrated part of BB module and it is cooled with an independent water system at the reference coolant thermodynamic conditions. The FW is an U-shape plate bended ( $150 \text{ mm}$ ) in radial direction. The thickness is of  $25 \text{ mm}$ , plus  $2 \text{ mm}$  of protective tungsten layer. The water flows in counter current direction in square channels with dimension of  $7 \times 7 \text{ mm}$  and pitch of  $13,5 \text{ mm}$ . The channels are  $3 \text{ mm}$  inside the steel along the radial-toroidal direction. Each module box has a "quasi" modular geometry. Basically, an "elementary cell" is repeated along the poloidal direction up to the lower and upper caps, which represent a discontinuity. The equatorial outer central module (EOCM) is considered as the reference for the geometrical description and the analyses. The EOCM is divided in 16 "elementary cells" in poloidal direction and 6 channels in toroidal direction. Each "elementary cell" has a baffle plate at the mid-plane: the PbLi enters in the bottom, flows in radial-poloidal direction and exits from the top. The breeder zone water cooling tubes are placed along a toroidal-radial direction. They are double walled and have the internal and external diameters equal to  $8 \text{ mm}$  and  $13,5 \text{ mm}$ , respectively. The layout and the number (21) of the tubes is repeated in each elementary cell.

3-D neutronics calculations were performed using MCNP5 and JEFF 3.2 nuclear data. Resulting maximum neutronics wall load is  $1.33 \text{ MW/m}^2$ , calculated in the outboard equatorial module. The global tritium breeding ratio is 1.127. The highest contribution is given by the EOM (i.e.  $\text{TBR}=0.142$ ) and the contributions of outboard and inboard blankets are 71% and 29% respectively. The overall nuclear power deposited on the breeder zone of DEMO 2015 is 1805 MW. The EOM is the largest contributor with 4.5MW. The shielding performance of the system BB/manifold/BSS is sufficient to ensure the safe operation of the vacuum vessel, i.e. damage is lower than  $0.03 \text{ dpa/FPY}$  (Figure 6), and to reduce the nuclear heating deposited in the toroidal field coils to acceptable level ( $<7 \times 10^{-6} \text{ W/cm}^3$ ).

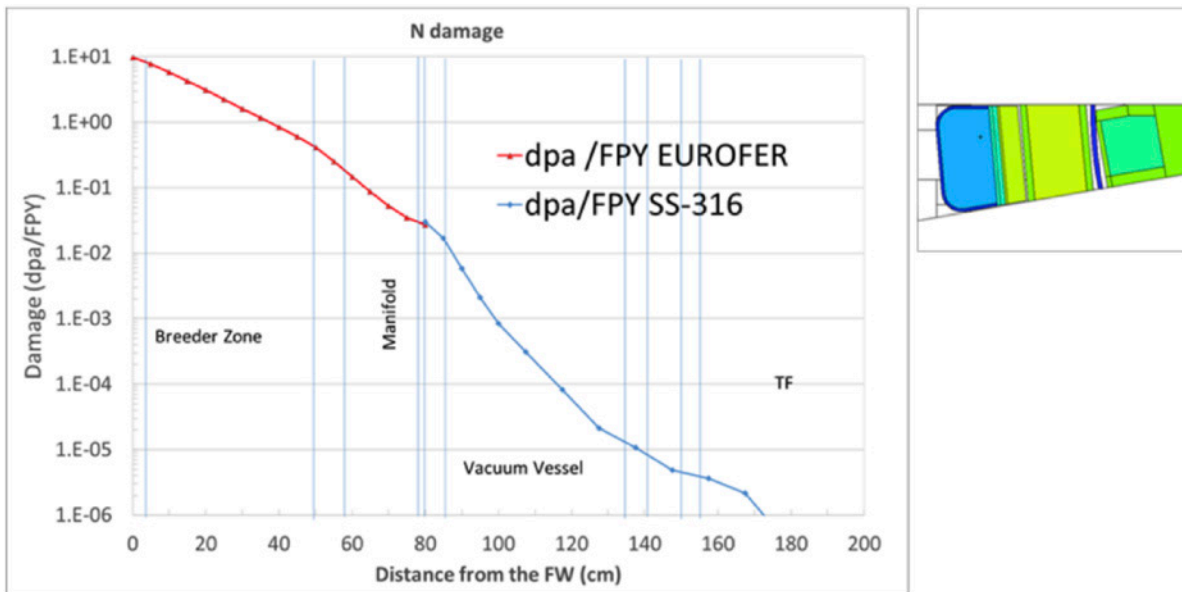


Figure 6: damage in EUROFER & SS316 (dpa /FPY) radial profile along inboard-midplane.

PbLi and water manifolds systems are in charge to connect the modules with the main pipelines. The PbLi inlet manifold is internal to the module box, between the Back Plate (BP) and the breeding zone. It ensures the PbLi distribution in the elementary cells through 6 orifices on the toroidal-poloidal plate. The system has been designed with the support of CFD [21]. MHD effects were neglected. The PbLi enters from 8 pipes exits through 32 pipes. Two manifolds (inlet and outlet) are placed on the back wall of the module box. They are connected with the breeder zone cooling system and with the main pipelines. Both manifolds are  $1750 \text{ mm}$  high and  $326 \text{ mm}$  width. The inlet and outlet pipes are placed in center and are DN 100. The FW cooling zone is fed by two manifolds (inlet and outlet). These are bended pipes DN40 and are joined to the FW cooling channels through tubes. The structure has been analyzed [22] considering the gravity, the thermal and the preliminary EM loads. Results have shown that EM loads make the BSS rotate clockwise in the poloidal-toroidal plane. Safety verifications, according to SDC-IC codes, are totally satisfied as far as each single load is concerned and also when the total load is taken into account, even if with a lower margin.

Six main pipes feed and collect the fluids of the module boxes. They are successfully integrated in the DEMO 2015 CAD

without interferences. FW and breeder zone cooling systems are separated, thus two pipes enter from the lower port to feed the modules and other two pipes exit from the upper port to deliver the hot coolant to the Primary Heat Transfer System. Dimensions of the pipelines are calculated according with the velocity limit of 7 m/s. The overall primary system coolant mass flow rate is 9035 kg/s. PbLi pipes (inlet and outlet) are routed from the upper port. The flow area of these pipes is the result of the total mass flow rate equal to 956.30 kg/s, calculated assuming 10 recirculations per day and the velocity limit considered in the main pipelines (50mm/s).

The back supporting structure is a poloidal-toroidal plate having maximum radial thickness of 200 mm attached to the modules by means of 4 ribs. It shares the space on the backside of the modules with the main pipelines and the manifolds.

The LIFUS5 facility is under upgrade to support the design of the WCLL providing new data on PbLi/water interaction and to validate a code that has the capability to simulate both thermodynamic and chemical processes (including the hydrogen production). Designing and execution of SET facility experiments in LIFUS5/Mod3 for code validation purposes are ongoing.

### 3.3. Activities on Tritium extraction

The first and main step of the HCLL blanket fuel cycle consists of Tritium extraction from the liquid breeder. In DEMO reactor a dedicated system, called TES (Tritium Extraction System), will be devoted to accomplish this task. Different technologies, belonging to the families of gas-liquid contactors, getters and tritium permeators have been studied in the last years. Gas-liquid contactors showed contradictory results. Plate, spray and bubble columns resulted in a very low-extraction efficiency. On the contrary, packed columns gave better results, although some doubt arise about the accuracy of the experiments performed in the past. For this reason, it was decided to further study them by means of a dedicated facility called TRIEX (TRItium EXtraction) [24]. The design was optimized to be compatible, in the future, with an installation in EBBTF.

In TRIEX the extraction efficiency of a packed column of variable height is tested in a systematic way, varying the flow rate of both gas and liquid metal as well as hydrogen content and partial pressure. Particular attention is paid to the hydrogen monitoring system in gas and liquid metal phases. The loop is operated in isothermal mode, at a maximum temperature of 770 K. The Saturator includes a PORAL diffuser to ensure small and dispersed argon and hydrogen bubbles. It is assumed that saturation should be achieved in one pass. The hydrogen concentration at the gas outlet of the extractor is measured by thermal conductivity sensors. Three permeation hydrogen sensors are foreseen to measure hydrogen content in lead lithium at the extractor inlet, outlet and at the saturator outlet.

The operating conditions are as follows:

- temperature range of lead lithium: 620–770 K;
- lead lithium flow rate: maximum 0.2 kg/s,
- gas stripping flow rate range (S3): 5–120 N l/h;
- Ar–H flow rate (gas injector): 10–100 N l/h;
- maximum hydrogen concentration in the Ar–H flow rate (gas injector): 5 vol.%.

TRIEX facility will be updated and used to qualify the Vacuum Sieve Tray and Permeation Against Vacuum methodologies in 2017-2019.

### 3.4. Activities on corrosion of RAFM steels and on hydrogen permeation

Corrosion tests of EUROFER bare and coated with PLD- $\text{Al}_2\text{O}_3$  in static Pb-Li will be carried out within cylindrical steel vessels, already used in the past for other corrosion tests. The heating is obtained by means of a heating resistance wrapped around the external surface of the cylinder. The thermal insulation has been obtained by wrapping mineral wool and an aluminum sheet around the hot part of the cylinder. The vessel is provided with an inlet and an outlet for the argon gas cover, opposite to one another in the cylinder body. The lid is equipped with valves for the insertion of the components required for the tests execution (e.g. sample-holders rods). Furthermore, a steel-made thermocouple is implanted in the lid for the continuous monitoring of the liquid metal temperature.

To perform the corrosion tests, the cylindrical vessel was equipped with different tools. First, an alumina crucible ( $\phi=125$  mm,  $h=220$  mm) was positioned inside and at the bottom of the vessel. The crucible acts as a container for the Pb-Li and prevents the contact between the liquid metal and the cylinder steel wall. In this way it is possible to avoid the contamination of Pb-Li with metallic elements which do not directly come from the corrosion of EUROFER samples. Secondly, the valves on the lids have been adapted to the insertion of other components required for the tests, in particular:

- sample-holders rods (3 per each vessel);
- connection to the melting furnace for the molten Pb-Li inlet in the vessel;
- connection to the vacuum system (pump).

Each sample-holder rod can hold two specimens. By inserting three rods per vessel, it will be exposed 6 samples

simultaneously for each fixed exposure time (3 bare and 3 coated EUROFER samples).

A filter placed in the outlet section of the melting furnace will allow to catch any oxide or slag during the melting process, preventing their entry into the vessel. During the loading, the outlet section of the melting furnace will be inserted directly into one of the valves of the vessel lid. The Pb-Li output from the melting furnace will be facilitated by creating the vacuum with a pump inside the vessel. The vacuum will also allow to purify the system from the oxygen, avoiding the formation of Li<sub>2</sub>O and thus the shift of the Pb-Li composition from the eutectic condition.

Once the Pb-Li loading and purification procedures are completed, the samples will be immersed in the liquid metal for the exposure test. Argon with a purity of 99,9999% will be fluxed into the system and kept inside with a slight overpressure in order to keep inert the atmosphere.

Exposure tests will be carried out at 1000, 2000, 4000 and 8000 hours of exposure for the corrosion investigation of the EUROFER and the Al<sub>2</sub>O<sub>3</sub> coating in static Pb-17Li. For the first tests, the pre-exposure analysis of PLD-Al<sub>2</sub>O<sub>3</sub> coated samples by SEM-EDS has already been performed (Figure 7). Regarding the bare EUROFER samples, the dimensional analysis has been carried out using a caliper and it will be used to determine the corrosion rate at the end of the exposure test. Finally, as regards the Pb-Li alloy to be used in the tests, a control analysis of the melting point has been performed by DTA (Differential Thermal Analysis). According to the results, the Pb-Li alloy melts at  $239,9 \pm 1,4$  °C (the nominal melting temperature of the Pb-17Li eutectic alloy is 235 °C).

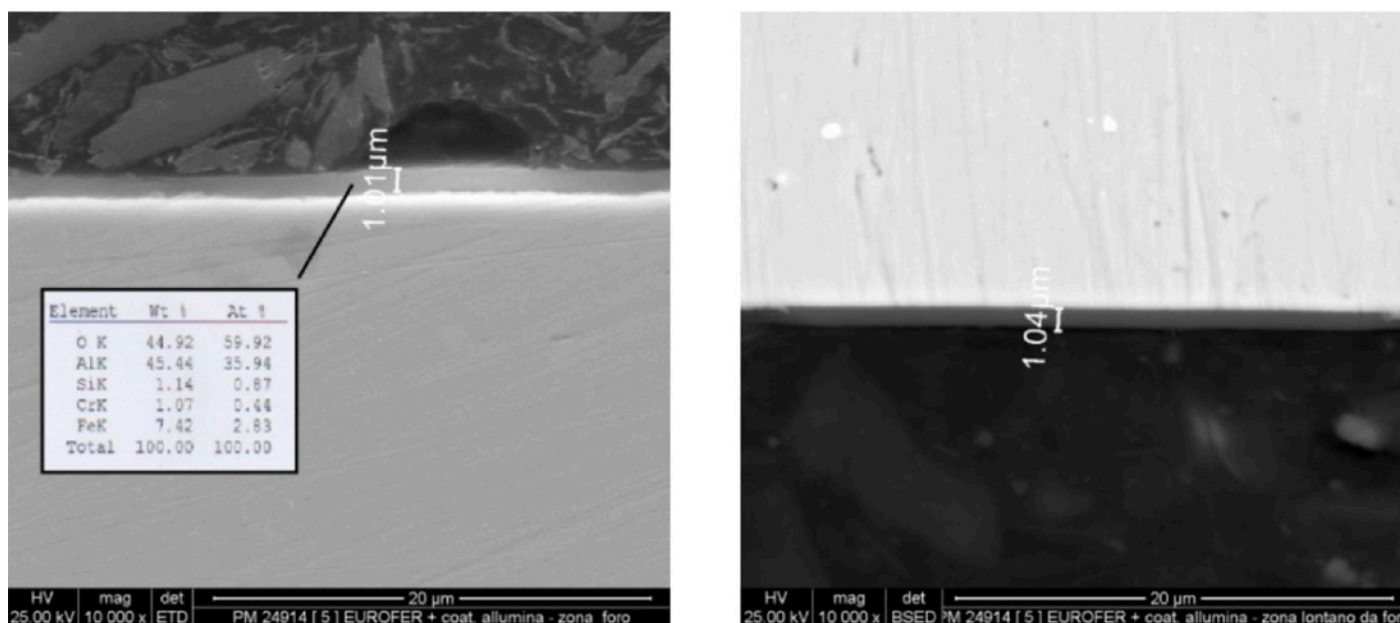


Figure 7: Cross-section at SEM of a PLD-Al<sub>2</sub>O<sub>3</sub> coated EUROFER plates, with indication of the thickness (about 1 μm) and the composition wt. % (obtained by EDX) of the coating.

For the investigation of the permeation behaviour, the activity will start with hydrogen permeation tests. The tests will be performed using the PERI II experimental facility of ENEA R.C. Brasimone. The test section of the facility is composed of two vacuum flanges separated by a sample-holder septum and heated at high temperature. The sample, which consists of a disk with a 2" diameter, is placed above the septum. The facility is prepared by heating the sample-holder septum and by creating a high vacuum in both flanges. Once the vacuum is creating into the system, hydrogen is flushed at a known partial pressure in the first flange ("high pressure" side). The gas permeates through the sample and is released into the second flange ("low pressure" side), generating a pressure increase. The equilibrium permeation flux exiting from the second flange is measured by a continuous flow quadrupole mass, in order to monitor over time the concentrations of the gaseous species.

The permeation tests will be performed by setting two hydrogen partial pressures in the "high pressure" side (10 and 100mbar). EUROFER samples will be coated with different thicknesses of Al<sub>2</sub>O<sub>3</sub> (0.5, 1, 5 and 10 μm). For each of the two hydrogen partial pressure chosen, tests will be performed for all the coating thickness and at different temperatures (from 250 to 600°C).

#### 4. Conclusions

Liquid metals technologies play a role of paramount importance towards the development of innovative fusion and fission nuclear systems. Indeed, some open points still preclude the advent of such systems. Structural materials and coolant chemistry are among the most relevant priorities, on which the lack of data and know-how is only partially covered in Europe (e.g. neutron irradiation behavior and synergic effects of corrosion/erosion).

ENEA is trying to address several of these issues, taking advantage of the large research infrastructure already installed

at Brasimone R.C. As this work tries to point out, the available experimental facilities are being used to produce new experimental data on safety-related phenomena, corrosion and material compatibility, tritium permeation, components reliability and instrumentation.

A large part of these new data will prove useful also to support the validation of thermo-hydraulic system codes and CFD programs, as well as to develop tools to couple the two of them.

Indeed, numerical tools can be important to support the design of systems, components and experiments. To this end, a comprehensive program of validation should be implemented and properly supported by the research institutions and stakeholders.

## References

- [1] L. Cinotti et al., "Lead-cooled Fast Reactor development Gaps", IAEA Technical Meeting on to Identify Innovative Fast Neutron Systems Development Gaps, IAEA Headquarters, 29 February – 02 March 2012, Vienna, Austria.
- [2] F. Romanelli et al., Fusion Electricity – A roadmap to the realization of fusion energy, EFDA (Nov., 2012), pp. 20–28 ISBN 978-3-00-0407.
- [3] L.V. Boccaccini et al., Objectives and status of EUROfusion DEMO blanket studies, Fusion Engineering and Design 109-111 (2016) 1199-1206.
- [4] Turroni, P., Cinotti, L., Corsini, G., Mansani, L., 2001. The CIRCE facility. In: AccApp'01 & ADTTA'01, Nuclear Application in the New Millennium, Reno, NV, USA, November 11–15, 2001.
- [5] M. Tarantino et al. "Mixed convection and stratification phenomena in a heavy liquid metal pool" Nucl. Eng. Des. 286, 261-277.
- [6] D. Martelli et al., "HLM fuel pin bundle experiments in the CIRCE pool facility", Nucl. Eng. Des. 292 (2015) 76-86.
- [7] K. Mikityuk, "Heat transfer to liquid metal: review of data and correlations for tube bundles", Nuclear Engineering and Design, Vol. 239, 680–687, 2009.
- [8] P.A. Ushakov et al., "Heat transfer to liquid metals in regular arrays of fuel elements", High Temperature, Vol. 15, pp. 868–873, 1977; translated from Teplofizika Vysokikh Temperatur 15 (5), pp. 1027–1033, 1977.
- [9] I. Di Piazza et al., "Heat transfer on HLM cooled wire-spaced fuel pin bundle simulator in the NACIE-UP facility", Nuclear Engineering and Design 300 (2016) 256-267.
- [10] Abderrahim et al., "MYRRHA: A multipurpose accelerator driven system for research & development", Nuclear Instruments and Methods in Physics Research A 463 (2001), pp. 487–494.
- [11] A. Alemberti et al., "European lead fast reactor-ELSY", Nuclear Engineering and Design 241 (2011) 3470-3480.
- [12] L. Cinotti., "Spiral-Tube steam generators for compact integrated reactors", Technical Meeting on Innovative Heat Exchanger and Steam Generator Designs for Fast Reactors, Vienna, 21-22 December, 2011.
- [13] C. Fazio et al., "Corrosion behaviour of steels and refractory metals and tensile features of steels exposed to flowing PbBi in the LECOR loop", Journal of Nuclear Materials 318 (2003) 325-332.
- [14] M. Azzati, A. Gessi, G. Benamati, ENEA report, HS-A-R-014, January 2003.
- [15] N. Forgiione et al., "Thermal-hydraulic analysis of HELENA facility", Report Rds/2011/48.
- [16] M. Utili et al., "The European Breeding Blanket Test Facility: An integrated design to test European helium cooled TBMs in view of ITER", Fusion Engineering and Design 84 (2009) 1881-1886.
- [17] M.Utili et al., "Validation of RELAP5-3D simulations of pressure wave propagation in the HCLL TBM", under review on Fusion Engineering and Design.
- [18] P. A. Di Maio, et. al., On the Thermo-Mechanical behaviour of DEMO WCLL equatorial outboard blanket module, Fusion Engineering and Design (2016).
- [19] A. Giovinazzi, et al., CFD analysis of WCLL BB module design, Fusion Engineering and Design (2016).
- [20] A. Tassone , et. al., CFD simulation of the magnetohydrodynamic flow inside the WCLL breeding blanket module, Fusion Engineering and Design (2016).
- [21] E. Martelli, et. al., Thermal-Hydraulics CFD analysis of WCLL BB PbLi manifold, Fusion Engineering and Design (2016).
- [22] P. A. Di Maio, et. al., Structural analysis of the back supporting structure of the DEMO WCLL outboard blanket, Fusion Engineering and Design (2016).
- [23] A. Del Nevo et. al., WCLL design report 2015, EUROfusion project WPBB-DEL- BB- 3.2.1-T002-D001 v1.0, 02 March 2016 (EFDA\_D\_2N6WLQ).
- [24] A. Aiello et al., "TRIEX facility: An experimental loop to test tritium extraction systems from lead lithium", Fusion Engineering and Design 82 (2007) 2294-2302.

# 28 - DEMO-like minimum set of Diagnostics and controls for a pilot FFH Reactor

Francesco Paolo Orsitto

CREATE Consortium and ENEA (Dipartimento Fusione e Sicurezza Nucleare) C R Frascati v E Fermi 45 00044 Frascati(Italy)

## Abstract

The Fusion-Fission Hybrid Reactor(FFH) can be considered an attractive actinide-burner or a fusion assisted transmutation for destruction of transuranic(TRU) nuclear waste. The hybrid reactor has two important subsystems: the tokamak neutron source and the blanket which includes a fuel zone where the TRU are placed and a tritium breeding zone. The reference tokamak models considered so far are equivalent from the Kadomtsev-Lackner similarity parameters, and the amplification factor  $Q_{FFH}$  is of the order of 5-7 times that possible on JET, of the order of half of  $Q_{ITER}$ . The availability and pulse length are that of a small DEMO, implying long pulses and high availability. These requirements are near to the limit of the presently available technology. The possibility of a pilot experiment is considered and the possible parameters are determined. The diagnostic system for a HR must be as simple and robust as possible to monitor and control the plasma scenario, guarantee the protection of the machine and monitor the transmutation.

**Keywords:** hybrid reactors, transuranic waste transmutation, diagnostics tokamak.

**PACS:** 28.52.Fa;29.30.-h;28.65.+a;28.52.-s;28.41.-i;28.41.Fr;28.41.Kw;28.41.My;25.85.Ec

## 1. Introduction

The Fusion-Fission hybrid reactor(FFH) can be considered an attractive actinide-burner or a fusion assisted transmutation for destruction of transuranic nuclear waste [1,2]. The FFH has two subsystems :i) a break-even class ( $Q\sim 3$ ) tokamak, as 14 MeV neutron source and ii) the transuranic burner. Two examples of hybrid load assembly [2,5] are taken as reference and analysed in the present study having a JET-like[9] device as neutron source. From the Lackner-Kadomtsev dimensionless parameter point of view the FFH models considered so far are equivalent. In general the parameters of the tokamak neutron source considered for FFH models are in the range: major radius  $R=3.75-4m$ , plasma current  $I_p=6-8MA$ ,  $B=5-6T$ , Aspect ratio  $R/a=3.4-4$ , 200MW fusion power. The motivations for building a Pilot experiment dedicated to explore solutions for the main issues of a FFH are related to the fact that the tokamak neutron source is a 'low power DEMO' with long pulses and high availability.

Diagnostic equipment of FFH must complement the tokamak measurements plus blanket diagnostics including Tritium regeneration and fission characterization. The diagnostics for tokamak are usually divided into the following categories:i) machine protection;ii) basic plasma control;iii) advanced control;iv)physics evaluation [3]. The tokamak of a FFH must have a simple equipment for basic plasma control, machine protection and some fundamental plasma measurement. In the present study the diagnostics systems related to machine protection and burn control are discussed, where some basic plasma measurements like electron temperature and alpha losses are included. The paper is organized as follows: in sec. 2 the FFH models considered having a tokamak as neutron source, are briefly discussed together devices characteristics, relation to ITER, relevance for DEMO[7,8]; in sec.3 the motivation and the parameters for a FFH Pilot experiment are presented; in sec 4 the criteria determining the diagnostics systems needed for a FFH, i.e. i)machine protection, ii) burn control, iii) fusion and fission blankets are introduced; in sec.5 the requirements on the measurements are presented; in sec.6 the diagnostics specific R&D needed for Hybrid reactors is discussed; in sec.7 the conclusions are presented.

## 2. Models for hybrid reactors

It is important having concrete models as reference, when diagnostics are considered. In this section two hybrid reactors models are briefly analyzed.

Devices characteristics and relation to ITER and relevance for DEMO[7,8] are briefly discussed.

Table 1 report the design of the China model FDS-I [5] with the machine parameters, compared to the ITER device. The other model taken as reference is the SABR[2,4] (Georgia (USA)) whose parameters are listed in table 2. The comparison between FDS-I and SABR (taking ITER as reference) is reported on Table 3. The main rationale of the comparison is to learn that the two models are similar with close parameters and concepts. The range of the plasma parameters are similar (i.e. electron density and temperature, neutron flux) for the two models and close to the ITER values. The only difference between FDS-I / SABR and ITER is the pulse length and the availability which is required as >70% for FDS-I /SABR while it is 4% for ITER.

The similarity between these devices can be quantitatively assessed using the Lackner-Kadomtsev dimensionless

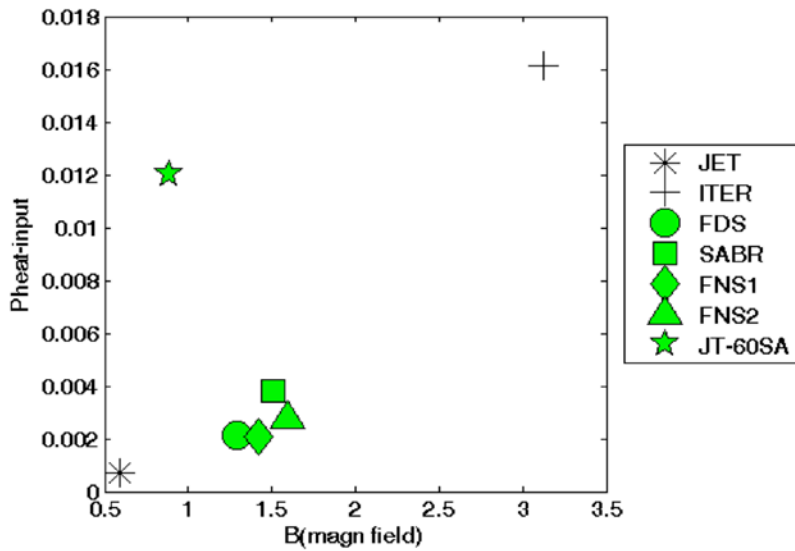


Fig.1 Kadomtsev-Lackner dimensionless parameter comparison between FFH tokamak neutron sources.

parameters	FDS-I	ITER
Fusion Power(MW)	150	500
Major Radius(m)	4	6.2
Minor Radius(m)	1	2
Aspect Ratio	4	3.1
Plasma Elongation	1.78	1.70
Triangularity	0.4	0.33
Plasma Current(MA)	6.3	15
Toroidal B on axis	6.1	5.3
Safety Factor(q95)	3.5	3
Auxiliary Power(MW)	50	73
Energy Multiplication(Q)	3	5-10
Average neutron wall load (MW/m <sup>2</sup> )	0.5	0.57
Average surface heat load(MW/m <sup>2</sup> )	0.1	0.2

Table 1 - Main core parameters of FDS-I

parameters	SABR(SABR extended)	ITER
Fusion Power(MW)	180(500)	500
Major Radius(m)	3.75	6.2
Minor Radius(m)	1.1	2
Aspect Ratio	3.4	3.1
Plasma Elongation	1.7	1.70
Triangularity	-	0.33
Plasma Current(MA)	8.3(10)	15
Toroidal B on axis	5.7	5.3
Safety Factor(q95)	3.0(4)	3
Auxiliary Power(MW)	60(100)	73
Energy Multiplication(Q)	3(5)	5-10
Average neutron wall load (MW/m <sup>2</sup> )	0.6(1.8)	0.57
Average surface heat load(MW/m <sup>2</sup> )	0.23(0.65)	0.2
Availability(%)	76	4

Table 2 - Parameters of SABR

parameters	Range	ITER
Major Radius(m)	3.75-4	6.2
Aspect Ratio	3.4-4	3.1
Toroidal B(T)	5-6	5.2
Plasma Current(MA)	6-8	13
Norm Beta(@N)	2-2.8	1.8
Confinement Factor HIPB98	1-1.1	1
Main Scenario	H mode/AT	H mode/AT
Energy Amplification(Q)	3	5-10
Pulse duration	>8hours or steady state	400s
Availability	>70%	4%

Table 3 - Comparison between SABR / FDS-I and ITER

parameter approach [17]: the figure 1 shows that in practice all the tokamak sources for FFH models considered so far are closely related. The models included in fig.1 are FDS [18], SABR, FNS1 and FNS2[19], JT-60SA[20], ITER and JET. The FFH tokamak neutron source is equipped with neutral beams and ECRH(Electron Cyclotron resonance heating) and/or LHCD (Lower Hybrid Current Drive) systems for heating and current drive(ECCD/LHCD). Also on this respect, building this facility is a strong extrapolation from the existing devices. The value of Q is of the order of 6 times that obtained in the JET campaign of Deuterium -Tritium experiments JET DT1[see ref.9, QDT =(Fusion Power from DT reactions) /(Input Power) = 0.4 -0.5 in JET-DT1]. The pulse length and the availability are an extrapolation also with respect to ITER values and typical of DEMO-like device. The blanket is also more complex than ITER /DEMO fusion blanket module(BM) since it includes two parts : the fusion BM devoted to the tritium generation and the fission BM devoted to the transmutation of the actinides. The pulse length and the availability are an extrapolation also with respect to ITER values and typical of DEMO-like device. The blanket is also more complex than ITER /DEMO fusion blanket module(BM) since it includes two parts : the fusion BM devoted to the tritium generation and the fission BM devoted to the transmutation of the actinides. The conclusion is that the tokamak neutron source for a hybrid reactor has the properties of a compact, low power Q=2-4 DEMO with a complex blanket having two parts: the fuel zone, where the long lived actinides are inserted, and the tritium regeneration zone where the lithium composites are placed.

### 3. Parameters of a pilot FFH experiment

The Pilot experiment can be designed to meet the minimal requirements for energy production which could be defined by the amplification factor

$$Q_{FFH\_P} = Q_{fusion} * Q_{fission} = 1. \quad (1)$$

Where  $Q_{FFH\_P}$  is the global amplification of the FFH Pilot system, and  $Q_{fusion}$  is the tokamak neutron source power amplification,  $Q_{fission}$  is the fission power blanket amplification. Since  $Q_{fission} \approx 10$ , we have that the required

$$Q_{fusion\_Pilot} \approx 1/10 \quad (2)$$

For the evaluation of the tokamak dimensions and plasma parameters of the Pilot FFH experiment with  $Q_{fusion} \approx 0.1$ , we take as

reference the JET DTE1 experiment[9] and we use the scaling laws described in [17] to get the major radius and plasma parameters.

We take JET DTE1 as reference, being QDT\_DTE1=0.6, and Pfusion=16MW. This means that the Pilot FFH will have (see (2)) a Qp= (QDT\_DTE1)/6.

Now we suppose that JET can obtain a Q\_JET\_DT=0.1 for some value of the (q, ρ\*(rho\*), β(beta), ν\*(nu\*)) and using the scaling laws given in [17] we can obtain the plasma parameters of the Pilot FFH tokamak, supposing that the aspect ratio(Ap) of the tokamak is Ap=AJET\*0.8.

Using the confinement scaling law IPBy2, and supposing that the tokamak of pilot FFH has the same q, ρ\*(rho\*), β(beta), ν\*(nu\*) ( see the usual definitions in ref.17) of the Q\_JET\_DT=0.1 discharge, we obtain that the Q scales as

$$Q = P_{fus} / P_{input} = P_{fus} / P_{heat} \approx (R^{-2}) * (A^4) \quad (3)$$

Where A=R/a=aspect ratio. Applying the scaling (3) implies that a Pilot tokamak neutron source has a major radius R=(R\_JET/(6<sup>1/2</sup>))\*((AJET/Ap)<sup>2</sup>)=1.77m, for Ap/AJET=0.82. The plasma current scales as Ip/IJET=(6<sup>1/8</sup>)\*(Ap/AJET)<sup>3/8</sup>=1.16 and the magnetic field as Bp/BJET=(6<sup>5/8</sup>)\*(Ap/AJET)<sup>35/8</sup>=1.28, the plasma current Ip=4.64MA and Bt=4.63T, Ap=2.52, The heating power scales as Ph\_IPBy2~R<sup>-1</sup> A<sup>3</sup>. ( if the IPBy2 scaling law for the confinement is used ), therefore the heating power needed for the Pilot FFH Tokamak is Pheatp=23.3MW.

RJET=2.92m	Rp=1.77m
AJET=R/a=3.07	Ap=2.52
BJET=3.6T	Bp=4.63T
IpJET=4MA	Ip=4.64
PheatJET=24.7MW	Pheatp=23.3MW

Table 4 - Parameters Pilot FFH Tokamak

### 3. Criteria determining diagnostic needs of hybrid reactors

The characteristics of a FFH device ( tokamak neutron source with two blankets, the fusion blanket regenerating the tritium and the fission blanket with transuranic elements) define the criteria determining the diagnostic systems needed. The diagnostics are divided in systems for measuring fundamental quantities and control of the tokamak neutron source and systems related to the measurements of characteristics of blanket modules.

#### 3.1. Diagnostics for tokamak neutron source

Since the plasma scenario is supposed to be assessed, no advanced diagnostic systems are needed for the scenario evaluation. The Table 5 shows a list of diagnostics needed for the neutron source. The diagnostics are devoted to machine protection and basic plasma measurements and control. The machine protection includes the divertor probes , thermocouples and monitors of divertor erosion and dust production, as well as lost fast particles( which could damage the vacuum vessel). The neutron flux monitors ( fission chambers) must be distributed in different parts of the machine. Disruption diagnostics are needed as well as halo currents and hard X-ray monitors to measure the high energy runaways electrons. The main plasma quantities are measured as the line integral of electron density by interferometry/polarimetry and electron density and temperature profiles by Thomson Scattering. The Zeff ( Z effective), i.e. the level of purity of plasma, is measured using the passive visible spectroscopy. The polarimetry can be used also for the real-time control of current profile whose main actuator is a neutral beam ( plus ECCD and or LHCD) which is used as main heating system.

Machine protection meas.	Basic Plasma measurements	Basic Plasma Diagnostics
Neutron monitors	Line average electron density	Interferometer/polarimeter
Neutron Activation Meas	Fusion power	Neutron monitors
Dα emission monitors	Zeff measurement	Visible spectroscopy spectroscopy
Divertor Langmuir probes	Impurity and D,T influx	Magnetic loops
Infrared TV Camera(Divertor)	Resistive wall mode	Magnetic loops
Runaways electrons	Halo Current	QuartzMicrobalances /Monitor Tiles
nT/nD in plasma core	Divertor Erosion Monitors	ECE/Thomson Scattering
Gas pressure(divertor & ducts)	Electron temperature	Bolometers
Surface temperature (divertor and first wall)	Plasma radiation	
Plasma shape and position		
Plasma current		
Lost Fast Particles		

Table 5 - Tokamak Measurements and Diagnostics

Table5 shows measurements need for machine protection and basic plasma control( first two columns, starting from left) , the last column on the right reports the diagnostics systems related to the measurements for the basic plasma control.

The ECE ( Electron Cyclotron Emission) diagnostic is used to monitor the electron temperature spatial profile also with the aim of providing a real-time sensor for the stabilization of the MHD modes through the ECRH/ECCD system. In practice the main sensors for the control of the plasma scenario are i) ECE fast detectors and ii) the polarimeter. The Table 7 shows the tokamak neutron source control plan . The main actuators for the control of neutron emission rate are the Neutral Beams and pellet injectors.

### 3.1.1. Minimum set of diagnostics for machine protection and burn control

The control of a FFH tokamak neutron source can be done also considering that a minimum set of diagnostics can be used for the two important functions of machine protection and burn control. Table 6 gives a list of diagnostics for machine protection.

Magnetics (Hall sensors)
IR Cameras ( W or Mo mirrors)
Polarimetry ( W or Mo mirrors )
Position reflectometry ( ITER project)
Fission chambers (ITER sensors)
X-ray spectroscopy
VUV and Visible spectroscopy

Table 6 - Minimum set of sensors for Machine protection

The minimum set covers most of the measurements given in Table 5 first left column.

The control matrix for machine protection is given in Table 7.

An important tool is the divertor control: keeping the control of the heat load on the divertor implies the use of impurity injections and the sensors can be The Table 7 shows the control matrix for machine protection. One important point of the matrix is the control of the divertor heat loads where the actuators are impurity gas injectors and/or pellets and sensors are bolometers and heavy impurity spectroscopy as well as IR cameras. The control of runaway electrons is another argument of interest in this context and this is carried out using massive gas injection valves and/or disruption mitigation systems and algorithms, the sensors are hard-X ray cameras as well as IR cameras .

control	actuator	sensor	physical quantity
disruption	ECRH, impurity gas injection, pellet, disruption mitigation system	Magnetics (Halo sensors in the blanket), reflectometry, ECE, visible bolometers	plasma current, temperature and density, heat load on divertor and wall, impurity influx
runaway electrons	gas injection valves, impurity gas injection, disruption mitigation system	hard X-ray monitors,	runaways density, divertor and wall heat load
Heat loads (divertor)	NBI, impurity gas injection, impurity pellet	IR cameras, spectroscopy, bolometers, divertor tiles thermocurrent and voltage	divertors and wall heat load
density control	gas injection valves, pellet, NBI	interferometry/polarimetry, reflectometry	electron density
plasma position	poloidal field coils	magnetics, reflectometry, ECE	plasma position equilibrium
fusion power	gas injection valves, pellet, impurity seeding	neutron cameras, microfission chambers, neutron spectroscopy, ECE	density, D/T ratio, temperature, dilution
core radiation	impurity seeding, impurity pellet	bolometers, X-ray spectrometers, IR cameras	X and IR radiation flux
Equilibria /MHD stability	poloidal field coils ECRH, NBI	magnetics, polarimetry/ interferometry	magnetic flux, current profile

Table 7 - Control Matrix for machine protection.

### 3.1.2. Burn Control

The fusion power and the burn control depends upon density, isotopic mix, dilution, radiation and geometry of the discharge ( see ref 18)

$$P_{fusion} \approx 5 * V * C_{\alpha} f_p f_{MIX} n^2 T_{eq}^2 = 5 * V * (1 - krad)^{1.6} f_p^{2.6} C_{\alpha}^{2.6} n^{2.14} f_{MIX}^{2.6}$$

where  $f_p$  is the pressure peaking factor,  $f_{MIX}$  the isotopic fraction,  $n$  is the electron density,  $C_{\alpha}$  the plasma dilution factor,  $krad$  is the ratio between the plasma radiation and the alpha power ( $krad=0.75$  is reasonable value).

Specifically the burn control is dedicated to the control of the equilibrium temperature which depends on the previous parameters ( and slowly from the plasma density):

$$T_{eq} \sim [(1-k_{rad}) * f_p * f_{MIX} * C_\alpha]^{0.8} n^{0.07} .$$

Temperature sensors like the ECE and/or the Thomson scattering are needed while the actuators are impurity injectors (to control the radiation fraction) and Neutral beams (to control the density and the isotopic mix). The Table 8 gives an overview on the Tokamak neutron source control plan.

### 3.2. Diagnostics for blankets

The principle scheme of the blanket for a FFH is given in fig.2 .

The figure shows the two parts of the blanket, whose diagnostics need to measure :

1. The content of isotopes ( measurement alpha lines of various radionuclides)
2. The neutron multiplication ( neutron flux / neutron spectroscopy)
3. The effective reactivity of the fission zone
4. Tritium breeding ( monitors of tritium)

Few notes on these measurements are given below.

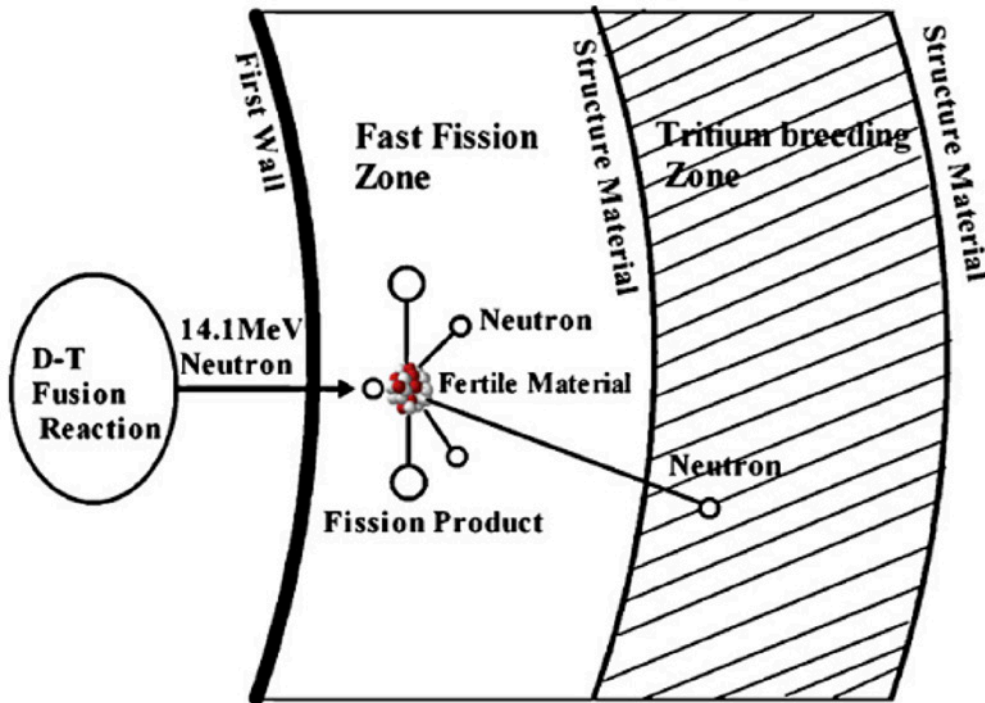


Figure 2 - scheme of a blanket for FFH

Quantity to be controlled	actuators	Sensors/diag systems
Electron density	Gas puff, pellet injector, divertor pumping	Interferometer/polarimeter
Neutron emission rate	P-NBI(ECRH, LHCD)	Neutron profile monitor
Plasma stored energy	P-NBI(ECRH, LHCD)	Diamagnetic loops
Density profile	P-NBI(ECRH)	Thomson Scattering
Current Profile	P-NBI(ECRH, LHCD)	Polarimeter
Radiation power	Impurity gas puff	Bolometer
Fusion power	P-NBI(ECRH, LHCD), gas puff, pellet	Neutron profile monitor
Temperature	P-NBI(ECRH, LHCD)	ECE /Thomson Scattering

Table 8 - Tokamak neutron source Control Plan

### 3.2.1. The content of isotopes

The measurement of isotopes can be carried out both :

1. Using alpha particle monitors inserted into the blanket very close to the containers of long life isotopes to monitor on line the 'transmutation' of long lived isotopes
2. Using off-line alpha particle spectroscopy.

The alpha particle and gamma ray spectroscopy can be a useful tool because the long lived actinides exhibit decays in alpha particles plus gamma rays , with energies in the range of  $E_{\alpha}$ 4-5 MeV and  $E_{\gamma}$ 27-86 keV ( Tab.9), Sensors for alpha particle detection and spectroscopy in the range of 4-5MeV (see Table 9) can be single-crystal diamond detectors[6] with technology and electronics well known and tested. These detectors have also a very good resistance to the high neutron flux, and they can be inserted inside the blanket in the fission zone. The off-line (high resolution) alpha particle spectroscopy measurements can be done using Germanium detectors.

Element(Mass Nr, half life)	Alpha decay(keV)	Gamma decay(keV)
Am(243,7370y)	5233.3	74.664
Pu(242,3.733 10 <sup>5</sup> y)	4856.2	44.915
Pu(239,24000y)	5105.5	-
Np(237,2.144 10 <sup>6</sup> y)	4788.0	29.37
Pa(231,32760y)	5013.8	27.36

Table 9 - Actinides decay in alpha particles and gamma rays

### 3.2.2. The neutron multiplication

The measurement of neutron multiplication implies the possibility of measuring the neutron flux in three positions: i) just outside the vacuum vessel, ii) in the fission blanket zone and iii) in the fusion blanket zone, and /or outside the fusion blanket zone.

A neutron profile monitor , providing also gamma ray spectroscopy channels , can be mounted outside the fusion zone at least in one equatorial port plug to ensure measurement of the spatial profile of the neutron and gamma ray emission.

The gamma ray spectroscopy channels must be equipped with neutron absorbers to make possible the gamma ray measurements with reasonable sensitivity.

The gamma ray emission is deriving from the following sources :

1. Gamma lines due to interaction inside the plasma between alpha particles produced by DT reactions (energy range of  $E_{DT\alpha} > 1\text{MeV}$ ) and possibly Be ions used as impurities to detect them.
2. Gamma lines produced by actinides in the energy range of  $E_{A\gamma} = 28-80\text{keV}$ .

The relative intensity of gamma<sub>DT</sub> and gamma<sub>A</sub> is a matter of careful evaluation to make the system working linearly in both ranges  $E_{DT\alpha} > 1\text{MeV}$  and  $E_{A\gamma} = 28-80\text{keV}$ .

In any case gamma ray channels can be dedicated separately to gamma ray derived from DT plasma.

## 4. Requirements on measurements

Following the classification of diagnostics given in sec.3 very simplified requirements on measurements can be outlined for the diagnostics related to the tokamak neutron source ( see Tables 7 ,8) and for the blanket fuel zone(Actinides) (Table 9).In practice three systems would provide profile measurements: Thomson Scattering (temperature and density) , ECE (Electron Cyclotron Emission) provides the temperature , and neutron profile monitor the spatial profile integrated along various lines of sight at different angles.The space resolution for the profile measurements of temperature and density is set to  $\Delta = a/10$  (a = tokamak minor radius) following ITER requirements, while the time resolution is set to  $\Delta\tau = 1\text{s}$ . Table 10 shows the requirements on measurements for tokamak neutron source.

The motivation for making the repetition rate of these measurements much slower than in ITER is that these measurements are intended only as monitors for long discharges, thus making simpler the system technology used.

For the laser diagnostics like interferometry/polarimetry and Thomson Scattering the problem of the plasma facing mirrors used is important due to the damage induced by the neutron flux on mirror materials and coatings. This problem has been studied for ITER mirrors, where Rhodium coated with copper substrate or monocrystalline molybdenum mirrors are used[3].

On the tokamak neutron source the measurement of the spatial q- profile could be also important , in particular to monitor and control the plasma scenario. In this case the Motional Stark Effect diagnostic could be used using the heating beams, as in ITER[13], to measure the q-profile interfaced to an equilibrium code. The measurement of lost

fast particles[10,11,12] can be a delicate point because the present knowledge on building such systems is limited to scintillator probes used on TFTR, JET and ASDEX devices which work at neutron fluxes definitely lower than a FFH neutron source.

Moving to the divertor diagnostics the divertor thermography and the tile erosion monitors are mentioned in the Table 11 thermography is carried out using IR viewing cameras, in various position of the divertor and main chamber.

Measurement(range)	Space Resolution, time res,accuracy	Diagnostic system
Temperature(0.01-30keV)	a/10,1Hz,10-20%	ECE/Thomson Scattering
Density(1-20 $10^{19}m^{-2}$ )	Line integral,1Hz,10-20%	Interferometer/polarimeter
Neutron flux emissivity( $10^{14}$ - $10^{20}n/s$ )	Integral,1Hz,10%	Diamond detectors
Neutron profile monitor ( $10^{14}$ - $10^{19}n/(m^2 s)$ )	a/10,1Hz,10%	Diamond detectors or scintillators
Zeff monitor	line integral,1Hz,10%	Visible spectroscopy
Escaping alpha(<2MW/m <sup>3</sup> )	a/10 along poloidal direction,100ms,10%	Scintillator probe

Table 10 - Requirements on Measurements for the Tokamak neutron source.

To measure the divertor erosion, diagnostic systems have not been fully tested. There are two techniques under consideration for ITER[14] : i) speckle interferometer and ii) laser radar erosion monitors.

Measurement(range)	Space resolution,time resolution	Accuracy
Divertor thermography(200-3000 C)	1-10mm,1Hz	10%
Erosion rate( $10^{-6}m/s$ )	10mm,1Hz	30%
Gas pressure( $10^{-4}$ -20Pa)	50ms	20%

Table 10 - Requirements on measurements for Divertor of the Tokamak neutron source

The diagnostics for the fission zone are mentioned in Table 11 the measurements and diagnostics are discussed in the sec.3.

Parameters(range)	Space resolution,time resolution,accuracy	detectors
Alpha particles(4-5MeV)	Integral,1Hz,10%	Diamond detectors(inside zone measurement)
Gamma ray(10-100MeV)	Integral,1Hz,10%	Ge detectors(off-line)

Table 11 - Requirements on measurements for blanket fuel zone

## 5. R&D needed for diagnostics

The HR features require measurements and control of important quantities like the current profile, the fusion Q, and for the safety of the device the lost fast particles flux on the wall, and divertor erosion on long discharges. The measurement of the neutron multiplication and the activity of the Actinides placed in the fuel zone are needed. In practice, the control of the neutron source is a matter to be carefully tested : this type of control, which means the scenario control, has been tested for short discharges on JET[15,16], using the neutron profile monitor as sensor and the heating beams( and LHCD ) as actuators. The novelty of the FFH is that it will use heating beams for long discharges, and the control of the scenario as well as the safety of the machine has been not tested on long discharges on the present devices. The lost fast particle monitor need a further evaluation. The neutron monitors inserted into the fuel zone need to be tested.

## 6. Conclusions

The FFH tokamak neutron source is a low-power ( low Q) device with some characteristics close to a DEMO having a quite complex blanket.

It will have long discharges, using heating and current drive systems to sustain the neutron production. There is no need for the scenario evaluation diagnostics and only systems aimed at the scenario control and machine safety on long discharges are considered as necessary. Monitoring the blanket in particular the fuel zone where the actinides are placed could be useful.

## References

1. M Kotschenreuther et al Fus Eng and Des 84(2009)83-88
2. W M Stacey J Fus Eng 28(2009)328-333
3. ITER Physics Basis, Nuclear Fusion 39 (1999), pag.2541, and 47(2007) pag.S337.
4. E A Hoffman and W M Stacey Fus Eng Des 63-64 (2002) 87-91
5. Wu-Yi Plasma Sci. and Tech. 3(2001) 1085
6. M Pillon et al. Nuc Inst Meth Phys Res A 640 (2011) 185-191
7. D Ward Plasma Phys Contr Fusion 52(2010) 124033,
8. H Zohm Fus Sci Tech 58(2010) 613
9. M Keilhacker et al. Nuclear Fusion 39 (1999) 209
10. M Garcia-Munoz et al. Phys Rev Lett 100(2008)055005
11. D.S. Darrow et al. Phys of Plasmas 3(1996)1875
12. S Baeumel et al Rev Sci Instr 75(2004) 3563
13. E L Foley et al. Rev Sci Instr 79(2008) 10F521
14. A Costley et al IAEA 2008 Cheng-du paper IT/P6.21
15. D Moreau et al. Nuclear Fusion 43(2003)870
16. E Joffrin et al. Plasma Phys Contr Fus 45(2003)A367
17. F P Orsitto et al 39th EPS/ICPP 2012 Stockholm paper 2.154 - Physics driven scaling laws for similarity experiments.
18. F P Orsitto et al, Diagnostics and control for the steady state and pulsed tokamak DEMO, Nuclear Fusion 56(2016)026009.

## 29 - Fusion Reactor Relevance of the ITER Diagnostics Developed in Russia

A.V.Zvonkov<sup>1</sup>, Yu.A.Kaschuk<sup>1,2</sup>, A.V.Krasilnikov<sup>1</sup>, E.E. Mukhin<sup>3</sup>, S.Ya.Petrov<sup>3</sup>, A.E.Shevelev<sup>3</sup>, S.N.Tugarinov<sup>1,2</sup>

<sup>1</sup> Institution "Project center ITER", Moscow, Russia

<sup>2</sup> SRC RF "Troitsk Institute for Innovations and Fusion Research", Moscow, Russia

<sup>3</sup> Ioffe Institute, Saint Petersburg, Russia

### Introduction

Focusing on plasma diagnostics relevant to future fusion reactor, we are discussing ITER diagnostics developed in Russia. Different methods of measurements like microwave (reflectometry and refractometry), optical and spectroscopic (charge exchange recombination spectroscopy (CXRS) and visible spectroscopy), ionizing radiation (neutrons and gammas) and neutral particles detection are under development for ITER project. There are two groups of diagnostics: some of them have high performance design and are relevant to the fusion reactor requirements, some others need extended R&D to meet reactor requirements.

Neutron diagnostics are the most relevant for fusion reactor, as well as microwave diagnostic. For neutron diagnostics, the main challenges concern the wide range of necessary measurements, calibration, lifetime of detectors, collimating for neutron camera and integration of diagnostics in the facility.

For reflectometry and refractometry the main issues are strong loads on waveguides and antennas inside vacuum vessel, integration of microwave path under the blanket, as well as first window, separating in-vessel part from air part of the microwave path.

The relevance of optical and spectroscopic diagnostics for fusion reactor is rather questionable. The main challenge here is the first mirror performance under the harsh environment of a reactor.

The use of neutral particles analyzers (NPA) diagnostic in a reactor seems most questionable because it creates a long vacuum extension through the shield, so the safety and contamination issues are serious. Besides, for good time resolution the NPA needs rather large aperture, thus creates problems with activation and radiation protection.

In the paper, the examples of the development of neutron, gamma, optical diagnostics as well as neutral particle analyzer are presented.

### Neutron diagnostic, DNFM

The divertor neutron flux monitor (DNFM) diagnostic is to provide ITER total neutron yield and fusion power measurements, which are necessary for the plant control during operation and overall data analysis and experiments planning. The major design-driving requirement for the DNFM is the ability to perform absolute calibration. To implement this requirement the diagnostics has to cover the seven decades dynamic range of measurable neutron flux. The neutron yield varies in the ranges  $10^{14}$ - $10^{17}$  n/s for pure deuterium plasma and  $10^{17}$ - $5 \times 10^{20}$  n/s for deuterium-tritium discharge. The corresponding fusion power varies in 100 kW – 1.5 GW. The measurements should provide temporal resolution 1 ms and uncertainties < 10%. To achieve the lower limit, the DNFM is arranged on the ITER divertor cassette body under the dome. Thus, the DNFM is to withstand hostile environment: magnetic field up to 6 T, nuclear heating in steel parts ~ 1 W/cm<sup>3</sup>, thermal load 20 kW/m<sup>2</sup>, and vacuum.

The 18 fission chambers (FC) with various amounts of <sup>235</sup>U and <sup>238</sup>U converters will be used as detectors of DNFM diagnostics. The combination of fission chambers is optimized to cover the desired dynamic range and to meet 1 ms temporal resolution requirement for both DD and DT operations. Besides, each FC signal is processed in three ways: pulse count rate, Campbell and current modes. For application at fusion reactor the count rate and Campbell modes look more preferably because EM noise and gamma-ray background is high. In the recent DNFM design the detectors are grouped in 3 pairs of detection units: one unit in a pair contains three commercial fission chamber KHT 30-5 (<sup>235</sup>U) and another - three FC KHT 30-8 (<sup>238</sup>U) (figure 1).

The FC <sup>238</sup>U is supposed to be used for high intensity neutron flux measurement, on low neutron source intensity the <sup>238</sup>U FC will be used for noise and gamma-ray subtraction. It is important to recall, that FC <sup>238</sup>U radiator operates as a threshold detector, only sensitive to neutron with energies above 1 MeV. According to our computations up to 60% of registered neutrons will be neutrons coming directly from plasma without scattering on surrounding materials. Therefore, the effect of uncertainty in the surrounding materials spatial distribution is minimized. This threshold is only possible if the radiator is made of high pure (99.999987%) <sup>238</sup>U.

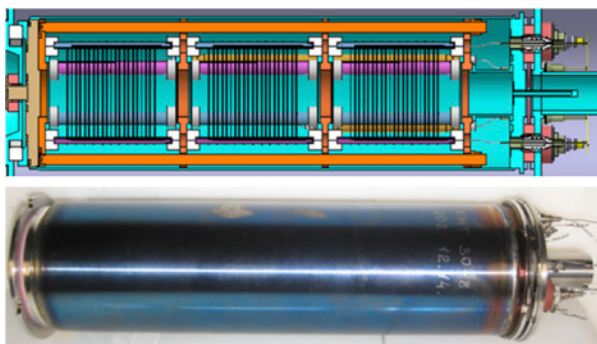


Figure 1. Commercial Fission Chamber KHT 30.

Moreover, the  $^{238}\text{U}$  is to be shielded with boron carbide layer to avoid  $^{239}\text{Pu}$  production, because  $^{239}\text{Pu}$  would cause the drastic change in spectral and absolute value of FC response during its lifetime. That is the reason to separate  $^{238}\text{U}$  FCs in a special, more complicated unit.

The DNFM calibration goal is to achieve 1% statistical error in count rate measurement for the most sensitive FC  $^{235}\text{U}$ . A compact high intensity neutron generator NG-24M has been developed to justify calibration methodology and to test neutron detectors. The most essential features of the NG-24M neutron generator [1] are:

- sealed replaceable tube (D+T mixture or pure D), lifetime  $\sim 300$  hours
- ion current 2.5 mA and accelerating voltage 250 kV
- neutron yield up to  $10^{11}$  n/s of 14 MeV neutrons
- dimensions  $\varnothing 0.43 \times 1.1$  m,
- weight 140 kg

Automatic feedback control of NG-24M operation demonstrates  $\pm 5\%$  stability of neutron yield during a tube lifetime. DT neutron generator NG-24M and 2D-positioning system are shown in Figure 2.



Figure 2 - DT neutron generator NG-24M (left) and 2D-positioning system for irradiation samples with tolerance less than 0.5 mm (right).

### Gamma spectrometer

Gamma ray spectrometer (GRS) as a part of ITER NPA system is intended for line integrated measurements of  $\gamma$  ray and hard X-ray emission from ITER plasma in equatorial plane [2]. Diagnostic can provide information on fast particles: fuel ratio in plasma core, alpha particle and other ions energy distribution, etc. GRS is unique in diagnosing runaway electrons (RE), particularly while they are in plasma (before hitting the wall) – RE maximum energy and other important parameters can be derived from the measurements.

Viewing the same plasma area in the equatorial plane as the rest component of the NPA system, GRS can significantly improve diagnostic abilities.

It is proposed to install gamma ray spectrometer in the port cell of the equatorial port EP#11 at the back of the NPA channel, embedded in the neutron dump. The arrangement of GRS units in the NPA neutron dump is shown in figure 3. Two types of  $\gamma$  ray detectors are proposed to be used in the system: a high purity germanium (HPGe) detector and a scintillation detector with large-size ( $\varnothing 76.2 \times 76.2$  mm) lanthanum bromide  $\text{LaBr}_3(\text{Ce})$  crystal. High-resolution semiconductor spectrometer basing on HPGe detector has been proposed for the diagnosis of the confined  $\alpha$  particles. This technique is based on the Doppler shape analysis (DSA) of the 4.44 MeV  $\gamma$  ray line related to the nuclear reaction  $^9\text{Be}(\alpha, n\gamma)^{12}\text{C}$  between  $\alpha$  particles and the beryllium impurity which will present in ITER plasmas. It is proposed to use in

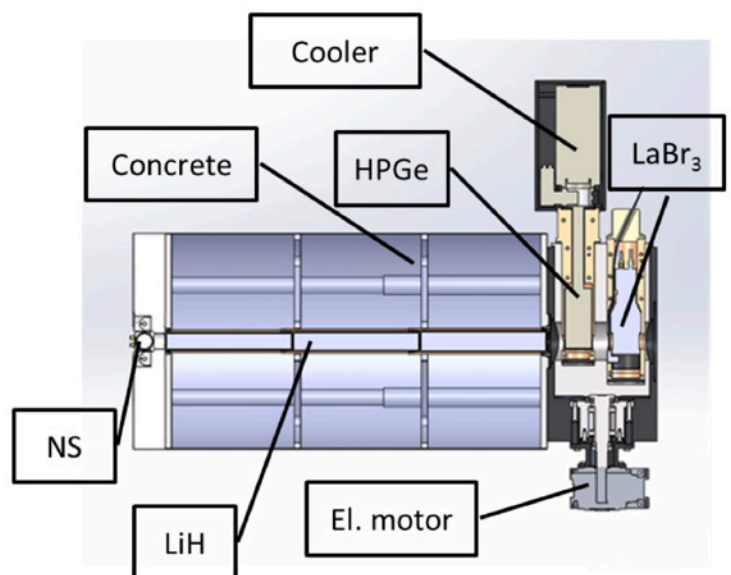


Figure 3 - Scheme of GRS and neutron spectrometer (NS) units arrangement in the Neutron Dump behind NPA in ITER equatorial port #11.

the GRS system a reverse electrode Ge detector (N-type detector) manufactured by CANBERRA and equipped with the electrically refrigerated cryostat Cryo-Pulse 5 Plus. N-type germanium detector can keep its working capacity at the total fluence up to  $\sim 10^{11} \text{ cm}^{-2}$  [3]. The second detector, serial LaBr<sub>3</sub>(Ce) detector manufactured by Saint-Gobain company, is based on the material with a fast scintillation decay time, which can provide high count rate spectrometry up to several MHz.

It is offered to arrange the detectors with their own axes perpendicularly to the axis of NPA beamline and to install them inside the revolving chamber, allowing interchanging the position of the detectors depending on experimental conditions and tasks. Revolving chamber is made of magnetic steel to protect the photomultiplier tube of LaBr<sub>3</sub>(Ce) detector from action of magnetic field. It will be supplied with electromotor to turn the chamber by 180° between ITER shots to swap the detectors.

To protect gamma ray detectors from neutron radiation and preserve the neutron dump properties it is proposed to install neutron attenuator modules in the collimator inside the neutron dump in front of the detectors. The attenuator is a hermetically welded metallic capsule containing lithium hydride (LiH) powder pressed into tablets. Three LiH attenuator units with 120 cm of total length will be used. Removable neutron detector module of neutron spectrometer (NS) is installed in front of LiH attenuators to provide neutron spectrum and flux measurements.

### Divertor Thomson scattering

The ITER divertor Thomson scattering (DTS) system is designed to measure the local  $T_e$  and  $n_e$  in the outer leg of the divertor providing the link between upstream and target electron parameter measurements with capabilities presented in table 1. The relative location of probing and viewing chords with magnetic field lines structure is shown in figure 4a. Figure 4b demonstrates relative locations of the described elements in the ITER buildings low level.

	Parameter	Range	Frequency	Accuracy
Divertor electron parameters	$n_e \text{ m}^{-3}$	$10^{19}-10^{22}$	50 Hz	20%
	$T_e \text{ eV}$	1-200	50 Hz	20%
		0.3-1		0.2eV

Table 1 - DTS measurement capabilities.

While the basic principles of Thomson scattering diagnostic will be similar to those operating in modern plasma devices [DIIIID, MAST, NSTX], the technique implementation in ITER divertor has to have advanced capabilities. The frontend optical components should be located in several meters from the vacuum

boundary and can be affected by possible mechanical deformations and/or displacements during cooling/heating and vibrations resulted from disruptions or abnormal events. Since the diagnostic equipment is working close to the source of impurities produced by physical and chemical sputtering at the divertor targets, the DTS optics require protection from deposition by sputtered first wall materials. Thus, the hardware solutions has to be developed addressing for practical usability and reliability under highly hostile environment, possible degradation of the collection optics transmission spectra and restricted access through the narrow gap between divertor cassettes. These limitations impose severe constraints on the diagnostic equipment design and force to develop new technical approaches.

a)

b)

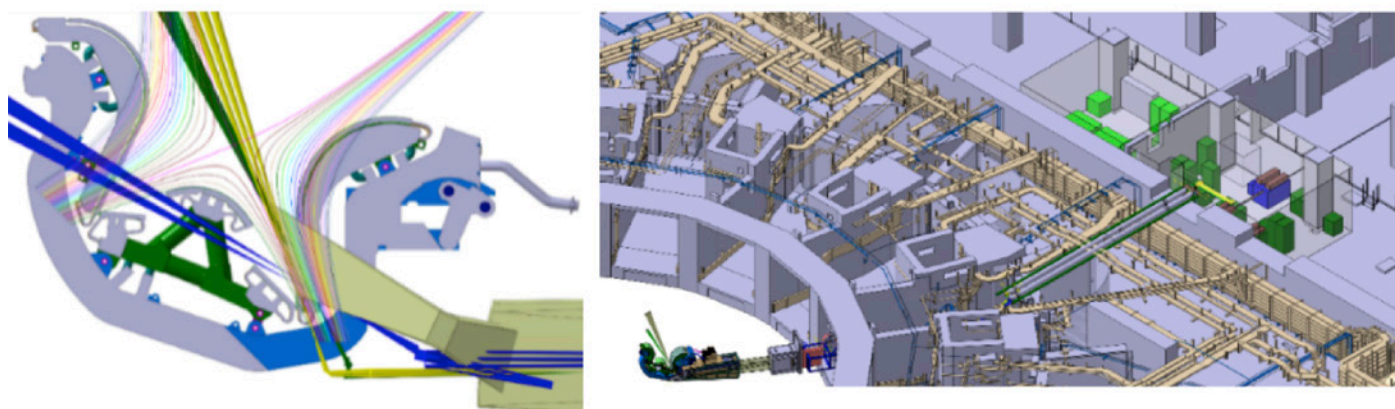


Figure 4 - DTS equipment on ITER low level. a) DTS probing chords and collection cones; b) overall hardware arrangement.

A number of innovative hardware products (lasers, polychromators [4]) and approaches (protection/cleaning techniques [5, 6, 7]) developed over last years for ITER DTS are applicable for other ITER diagnostics. Besides, they are able to extend diagnostics opportunities in already operating tokamaks.

## Neutral particle analyzer

The main purpose on the neutral particle analyzers (NPA) in ITER and future fusion reactor is to measure and control plasma fuel ratio in deuterium-tritium plasmas. The NPA system consists of two analyzers - LENPA (Low Energy Neutral Particle Analyzer) with 10 – 200 keV energy range of measured atoms and HENPA (High Energy Neutral Particle Analyzer) with 0.1 – 4.0 MeV energy range. Also, as shown in figure 5 it includes additional spectrometers: gamma-rays (HPGe and LaBr<sub>3</sub>(Ce)), fast charge exchange atoms (compact diamond) and neutrons (stylybene and compact diamond) spectrometers.

Gamma-ray spectrometer (GRS) will be used to measure signals related to fast D and <sup>4</sup>He ions, HXR, hence  $E_{\max}$  and runaway electron energy distribution, as well as to reconstruct alphas energy distribution from Doppler width.

Compact diamond spectrometer will be used to measure D, T charge exchange atom flux resolved in time and energy in low neutron rate experiments. It will provide the study of fast ions energy distribution dynamics under plasma instabilities, fusion products (alphas, protons, tritons) confinement and slowdown. Also, it will be used as a neutron spectrometer to measure plasma temperature and energy of fast ions during DT phase.

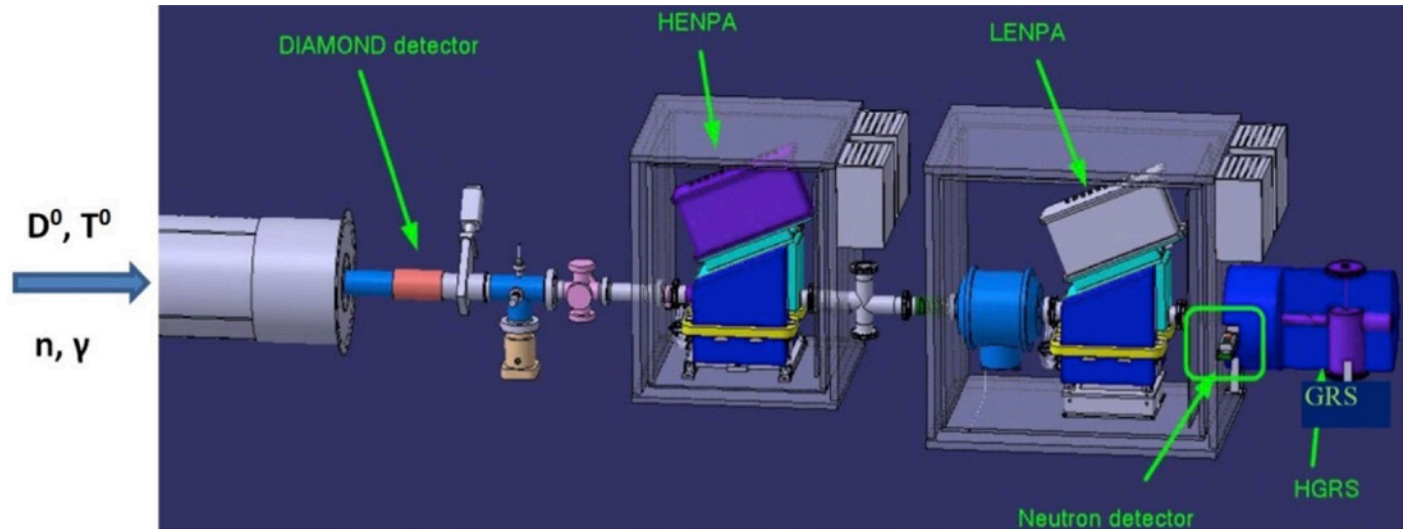


Figure 5 - NPA diagnostic system with additional spectrometers.

Neutron spectrometer (NS) will be used to measure DD and DT neutron energy distribution flux dynamics. It may be involved into the independent estimation of nT/nD ratio, which will provide NPA cross-calibration because it uses NPA line-of-sight. Also, it will be used as a neutron NPA background monitor to study the influence of neutrons on NPA performance. During the NPA system development, it was necessary to take into account a number of technical problems, which required new engineering solutions. Some of the problems are: high levels of neutron and gamma radiation; presence of the vacuum beamline, connecting the analyzers to ITER plasma vessel. These problems require development of the neutron shield to provide the acceptable neutron environment behind the equatorial port and a vacuum connector for quick connection/disconnection of the vacuum pipe.

One of the neutron shield components is a tungsten collimator shown in figure 6. It is located inside the port plug.



Figure 6 - Tungsten collimator mockup of ITER neutral particle analyzer system.

It is used to collimate the background neutron flux slightly decreasing the useful signal but significantly reduce neutron background. A special unit, vacuum connector, for quick connection/disconnection of the vacuum pipe is under development (figure 7). It is based on ITER vacuum requirements with using of the double silver sealing. The first tests show that conceptual design of the vacuum connector satisfies the ITER vacuum requirements.

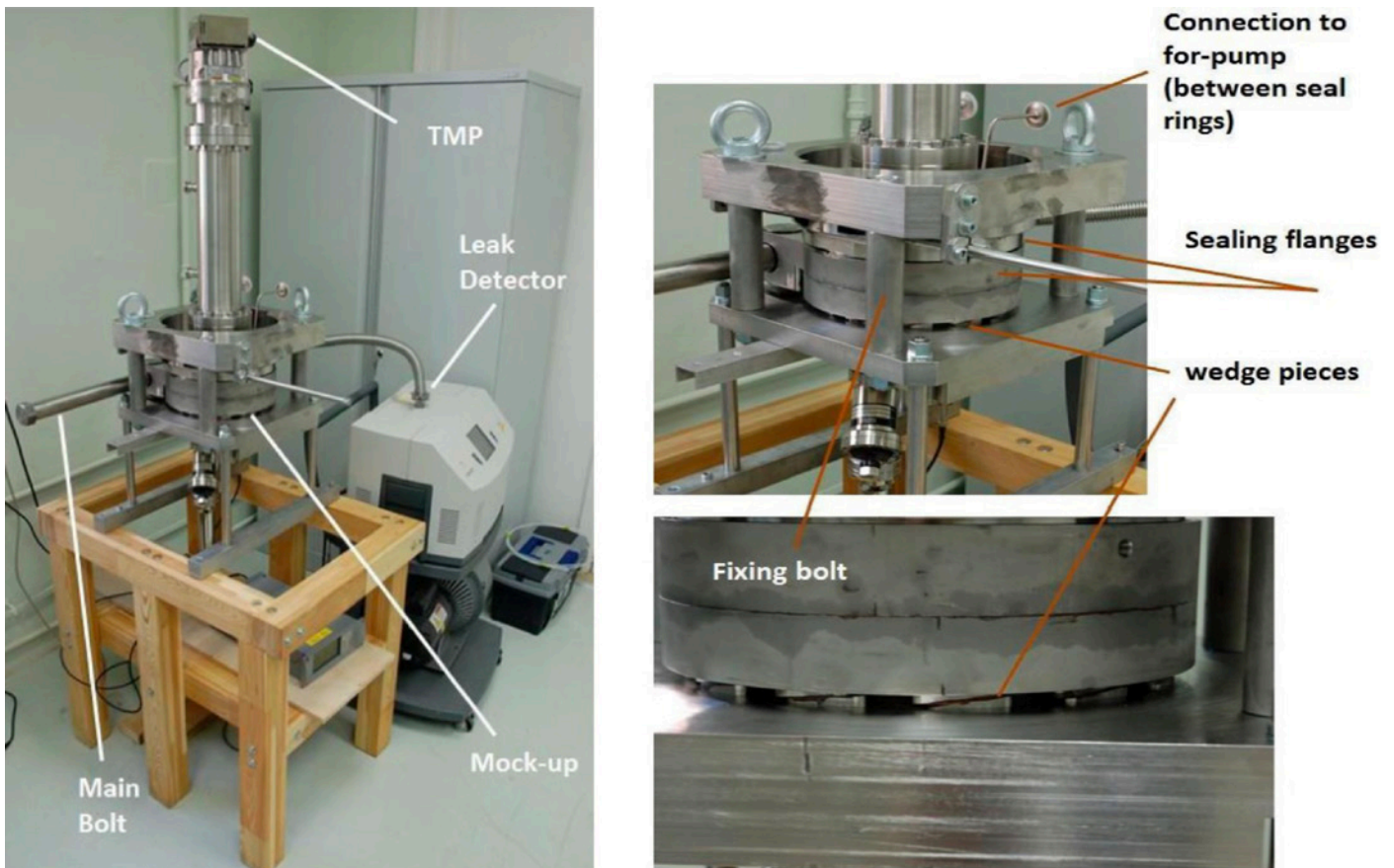


Figure 7 - Test facility for the vacuum connector mock-up.

The NPA system including gamma-ray spectrometer is developed by Ioffe Institute and Technoexan, LTD. The diamond detector and neutron spectrometers are developed by Institution "Project center ITER" and Technoexan, LTD.

### Charge Exchange Recombination Spectroscopy

Edge Charge Exchange Recombination Spectroscopy diagnostic (CXRS - edge) will provide the measurements of the basic ITER plasma parameters such as the ion temperature profile, light impurities density profile, toroidal and poloidal plasma rotation velocity minor radius distribution. CXRS diagnostics are based on measurement of radiation of excited ions produced due to charge exchange of plasma ions with neutral hydrogen provided by dedicated diagnostic neutral beam (DNB). The CXRS - edge diagnostic on ITER will have two optical cones of view (mainly toroidal, with small poloidal component) located in equatorial port plug EPP#3: one lower wide field of view (FOV) covering a spatial range along the DNB with  $r/a > 0.5$ , and a second upper narrow FOV covering a spatial range along the DNB with  $r/a > 0.85$ . The layout of the CXRS - edge side and top views in equatorial port #3 is shown in figure 8.

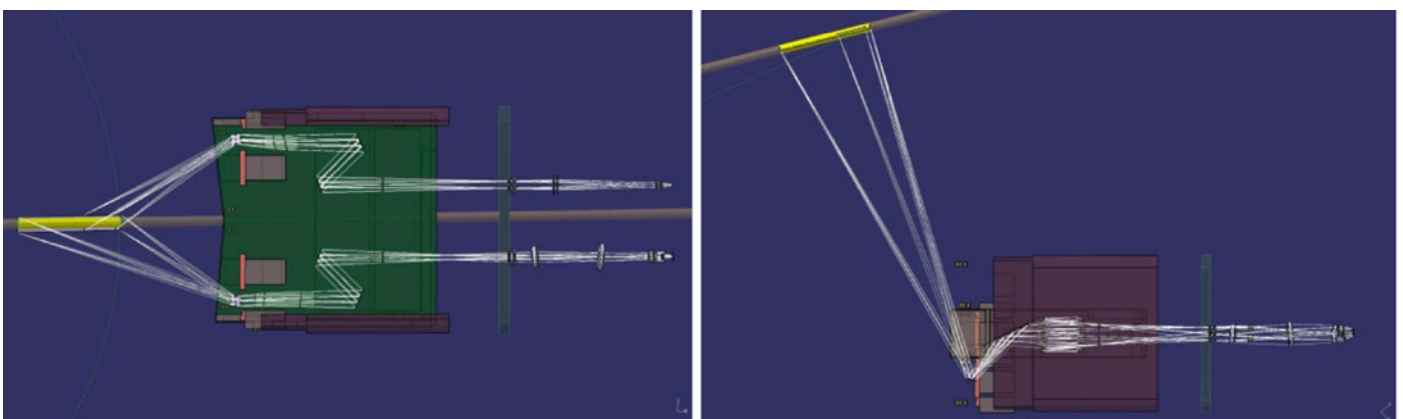


Figure 8 - Side and top views of the CXRS-edge layout in equatorial port #3.

The First Mirror (FM) of the optical collection system is the most critical element for the CXRS-edge diagnostic on ITER. The FM is closest to the plasma and gets to handle the highest heat and neutron loads. Single-crystalline molybdenum (SC Mo) is considered as the best candidate material for the FM. It maintains its acceptable optical properties under

erosion (or mirror cleaning that seems inevitable) and it can withstand the high thermal and neutron loads. Two samples of first mirror made of SC Mo plate connected by either hot isostatic pressing (HIP) or brazing to a poly-crystalline Mo substrate with cooling channels were manufactured (figure 9) and tested for image quality under pressure and temperature of cooling water adequate to ITER conditions.

Novel technique was developed allowing calibrating the impurity density measurements solely relying on a combination of the CXRS and beam emission spectroscopy (BES) measurement. This technique required the development of a three bands spectrometer. Moreover, this spectrometer needed to have a high etendue (to collect enough light) and a high spectral resolution (for accurate measurements of the radiation lines widths and shifts).

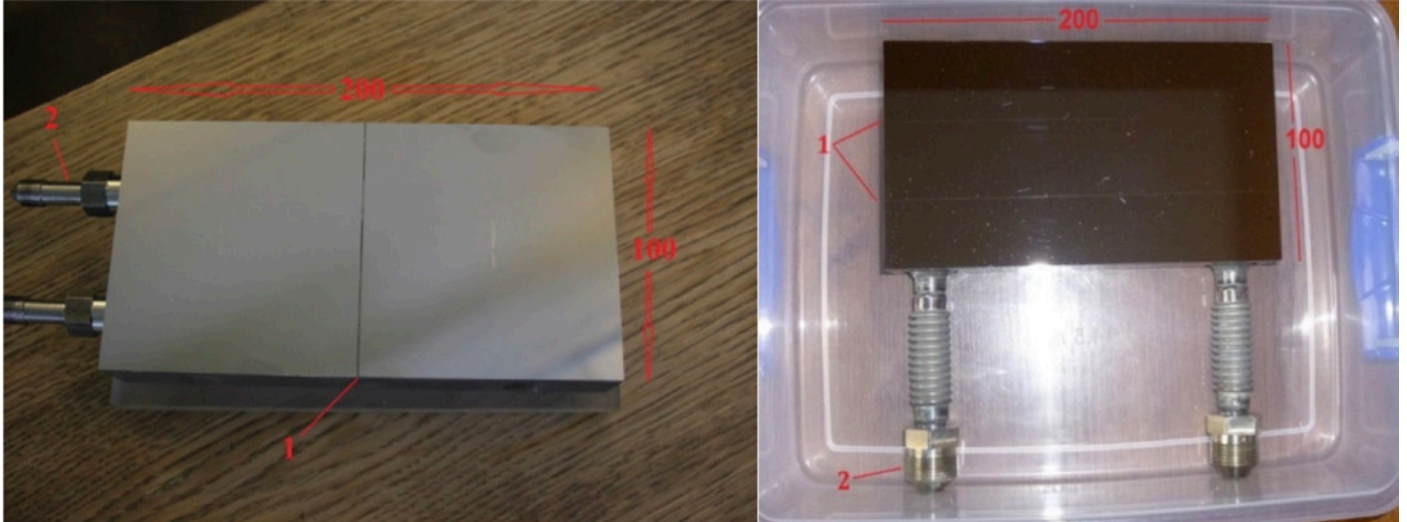


Figure 9. First mirror made of two square plates (left) and FM made of three stripes (right). 1 – gaps between single crystal Mo plates (4 mm thickness); 2 – water pipes.

The devices suitable for CXRS-edge diagnostic should combine features of both polychromator and high resolution spectrometer in three separate spectral ranges. Such kind of device based on transmission holographic gratings was developed. This spectral instrument has high etendue, excellent spectral resolution, and reasonable size. The design of the device ensures the same optical path for both CXRS and BES diagnostics that is favors the calibration. The scheme and the picture of high etendue spectrometer (HES) are shown on figure 10 and 11, respectively.

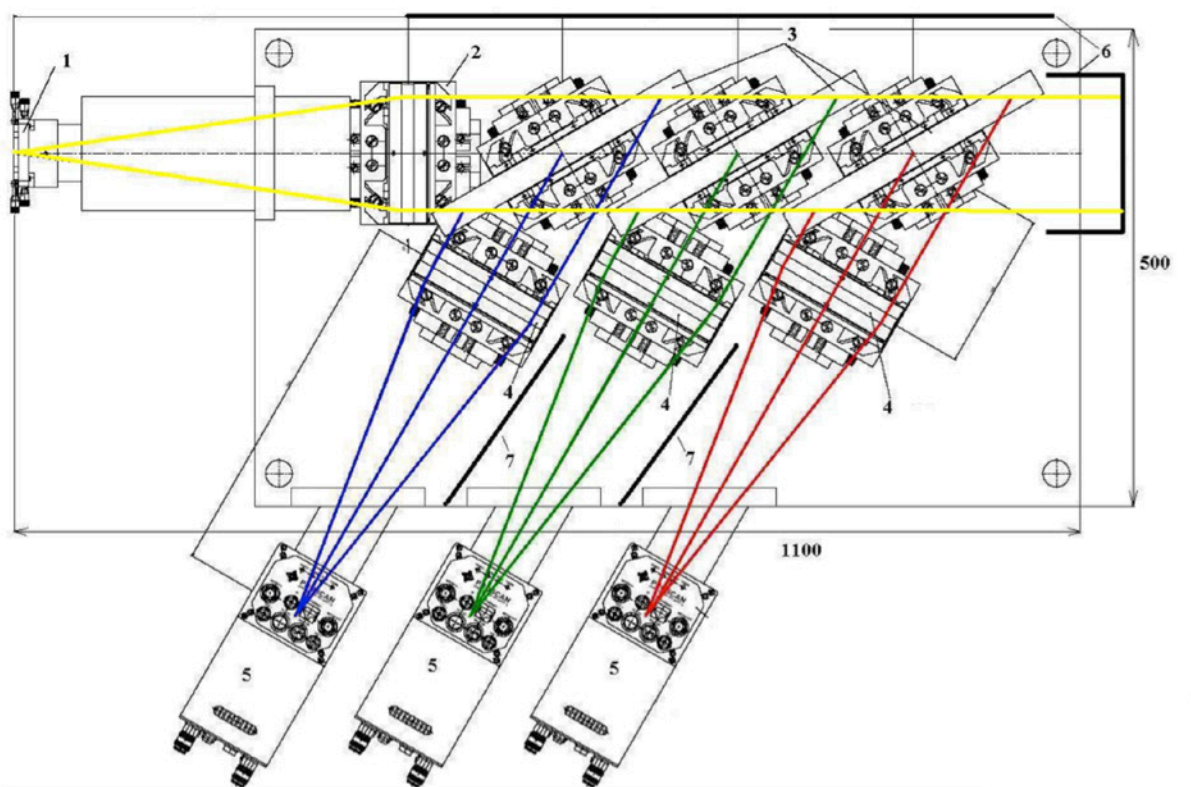


Figure 10. Principle scheme of the multi-channel HES spectrometer. 1 - entrance slit; 2 -collimator objective lens; 3 - holographic transmission gratings for  $468 \pm 5$  nm,  $529 \pm 5$  nm and  $656 \pm 6$  nm spectral ranges; 4 - camera objective lenses; 5 - CCD cameras; 6 - light traps/viewing dumps; 7 - light shields/baffles.

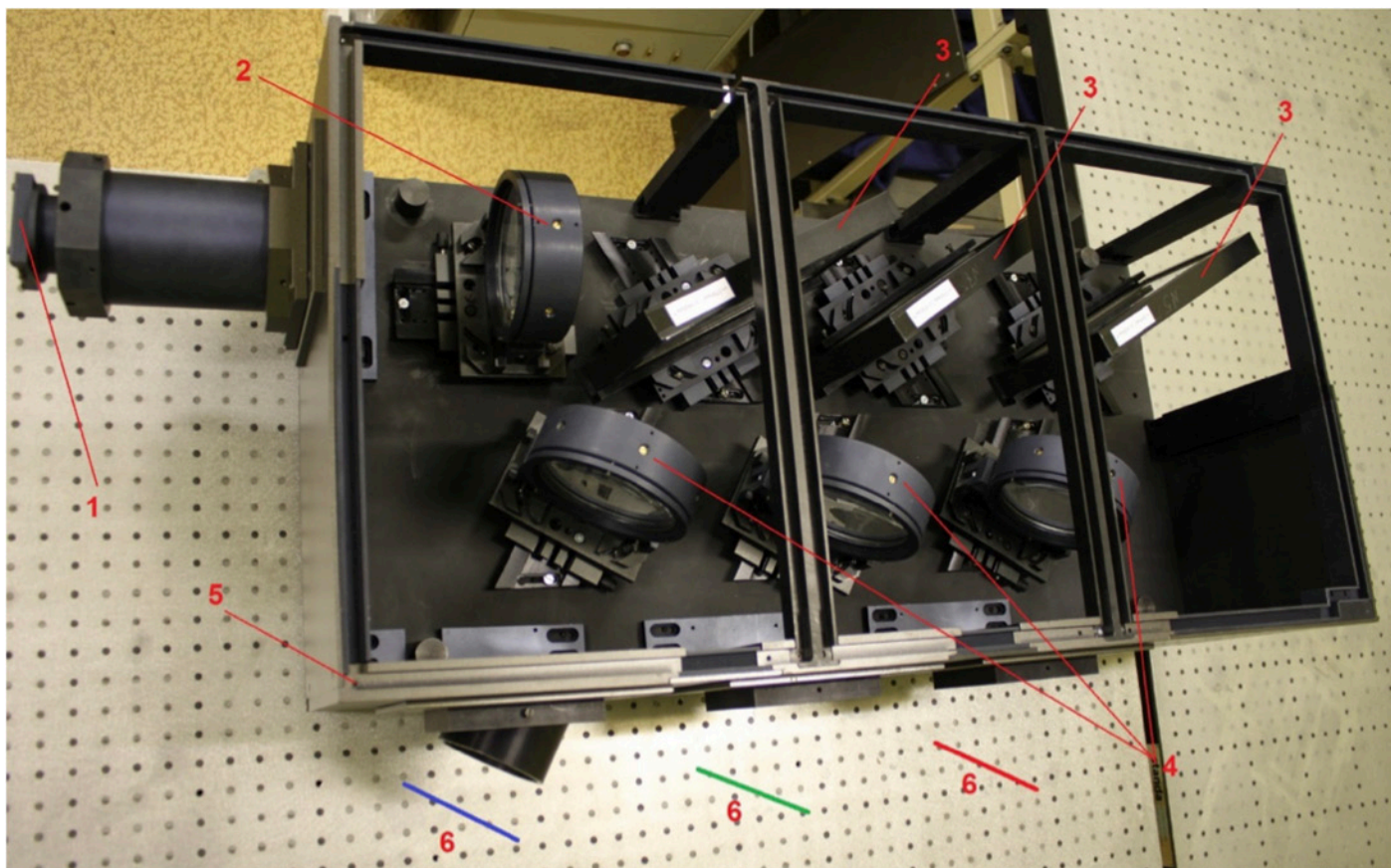


Figure 11 - Multi-channel HES spectrometer. 1 - entrance slit; 2 - collimator objective lens; 3 - holographic transmission gratings; 4 - camera objective lenses; 5 - enclosure; 6 - image planes.

Laboratory tests confirmed that the spectrometer meets the requirements [8]. The technical properties of HES spectrometer obtained during the laboratory tests are listed below.

- Working spectral ranges:  $468 \pm 5$  nm,  $529 \pm 5$  nm and  $656 \pm 6$  nm;
- 40 – 50% grating efficiency for the working spectral ranges;
- F-number = 3;
- Linear dispersion: 3.4 – 5 Å/mm;
- Stigmatic image (astigmatism value: 0.025 – 0.03 mm);
- Magnification (in horizontal and vertical direction) = 1;
- Entrance slit height: up to 25 mm;
- Image plane size: 25 x 25 mm;
- Maximal spectral resolution  $\sim 0.2 \text{ \AA}$  ;
- HES spectrometer contrast:  $K \gg 60\,000$ .

## Summary

The design of diagnostic systems for ITER creates a solid basis for development of diagnostics relevant for future fusion reactor. Substantial steps in this direction are made by RFDA: detectors for neutron diagnostics are developed as well as neutron generator for calibration, first mirrors for optical systems and methods of their cleaning tested, compact spectral devices designed, some engineering solutions proposed for work in harsh ITER environment.

## References

- [1] Sevast'yanov V. D., et al., "Formation of the Neutron Energy Spectrum Near the Target of a Portable NG-24M Neutron Generator", *Measurement Techniques*, Vol. 59, No. 9, December, 2016.
- [2] Gin D., et al., "Gamma ray spectrometer for ITER", *AIP Conference Proceedings* 1612 (2014) 149.
- [3] Pehl, R.H., et al., "Radiation Damage Resistance of Reverse Electrode GE Coaxial Detectors" *IEEE Transactions on Nuclear Science*, 1979, 26(1) p. 321-323.
- [4] Mukhin, E.E. et al, "Hardware solutions for ITER divertor Thomson scattering" *SOFT* 2016.
- [5] Mukhin, E.E. et al, "First mirrors in ITER: material choice and deposition prevention/cleaning techniques", *Nucl. Fusion* 52 (2012) 013017.

- [6] Razdobarin, A.G. et al, "RF discharge for in situ mirror surface recovery in ITER", Nucl. Fusion 55 (2015) 093022.
- [7] Razdobarin, A.G. et al, "Deposition mitigation and in-vessel optics recovery in ITER" FEC 2016.
- [8] Tugarinov S.N., et al., "The tri-band high-resolution spectrometer for the ITER CXRS diagnostic system", ISSN 0020-4412, Instruments and Experimental Techniques, vol. 59, No 1, 2016, pp.104–109.

## 30 - Neutron diagnostics for fusion-fission hybrid: lessons learned from integration of neutron diagnostics on JET and ITER

**M. Tardocchi<sup>1</sup>, J. Kallne<sup>2</sup>, M. Nocente<sup>3</sup>, G. Gorini<sup>3</sup>**

<sup>1</sup> *Istituto di Fisica del Plasma, Consiglio Nazionale delle Ricerche, Milano, Italy*

<sup>2</sup> *Department of Engineering Sciences, Uppsala University, Uppsala, Sweden*

<sup>3</sup> *Dipartimento di Fisica "G. Occhialini", Università di Milano-Bicocca, Milano, Italy*

The most promising fusion-fission hybrid reactor concept is based on the combination of a high power tokamak as fusion neutron source and a blanket of subcritical fission material. Neutron emission plays a key role in both processes: 14 MeV neutrons, produced from the fusion reactions  $D+T \rightarrow \alpha + n$ , escape the magnetic confinement and induce fission reactions in the blanket. Here more neutrons are produced from the fission reactions. The diagnosis of the neutron emission is therefore essential for both measuring the performance of the fusion neutron source as well as for the control of the criticality of the fission reaction chain.

The most advanced neutron diagnostics have so far been implemented on the JET tokamak and have been developed over a period of more than 30 years since its start in 1983. The experience, which relates to neutron yield, neutron spatial emissivity and high resolution spectroscopy measurements, includes plasma operation at neutron yields up to  $\sim 10^{16}$  n/s in D plasmas and a factor of hundred higher in DT ( $6 \cdot 10^{18}$  n/s corresponding to 16.7 MW fusion power). The next step ITER is planned for DT operation at up to 0.5 GW fusion power to be produced in long (103 s) discharges made possible by the use of superconducting coils.

The step from JET means that ITER must handle much higher neutron fluencies implying massive shielding. It is generally a fact that neutron diagnostics are affected by machine interface restriction which has been demonstrated at JET but was there compensated by the fact that the neutron yield was greatly increased compared to earlier tokamaks. On ITER it is difficult to exploit the increase fusion power for neutron diagnostics as the interface restriction will be much more severe. In this presentation we will review the state of the art of neutron diagnostics and address interface issues by examples from JET and ITER. Since gamma diagnostics is often sharing the collimated sight lines of neutron diagnostics its integration issues will also be addressed. Comments on the outlook for neutron diagnostic interface and possible changes of approach to increase feasibility will be discussed. In perspective neutron diagnostics can be envisioned to play a central role in future tokamaks for power production (e.g. DEMO) or in fusion-fission hybrid reactors.

## 31 - Gamma-ray diagnostics for fusion-fission hybrids

**M. Nocente<sup>1\*</sup>, G. Gorini<sup>1</sup>, M. Tardocchi<sup>2</sup>**

<sup>1</sup> Dipartimento di Fisica "G. Occhialini", Università di Milano-Bicocca, Milano, Italy,

<sup>2</sup> Istituto di Fisica del Plasma, Consiglio Nazionale delle Ricerche, Milano, Italy

\*Corresponding author: massimo.nocente@mib.infn.it

A fusion-fission hybrid (FFH) based on the tokamak concept as the neutron source will likely require a power gain ( $Q$  value) between 3 and 5 provided by the fusion reactions. In these conditions, the heating fraction  $f\alpha$  due to the alpha particles born from the fusion reactions between deuterium and tritium will be between 40 and 50% of the overall heating power, where the remaining half must be provided by the auxiliary systems. For comparison, the largest experimental tokamak currently under operation, the Joint European Torus in the UK, has achieved  $Q\approx 0.7$  in 1997, which corresponds to  $f\alpha\approx 12\%$ , while ITER, the largest magnetic fusion experiment presently under construction in the south of France, is designed to obtain  $Q=10$  and  $f\alpha\approx 67\%$ .

In FFH and tokamaks, intrinsic and extrinsic heating systems typically lead to the production of a minority population of supra-thermal ions in the plasma that needs to be well confined, monitored and controlled so to tailor the plasma performance towards the desired  $Q$ . This crucial task is aided by indirect measurements that make use of the spontaneous gamma-ray emission occurring from nuclear reactions between energetic ions and impurities in the plasma.

In this presentation, the principles behind gamma-ray emission in fusion plasmas will be summarized, where emphasis is put on the information that can be derived on the supra-thermal ions and, ultimately, on their role along the path towards  $Q\approx 3-5$  as needed for a FFH, with examples taken from experience at the Joint European Torus. We will in particular stress that a single, well calibrated spectrometer can be used to diagnose simultaneously both the intrinsic and the extrinsic supra-thermal ions through the detection of the different gamma-ray peaks born in their reactions with plasma impurities. By encompassing the most recent developments in nuclear detector technology, gamma-ray spectrometers that combine good energy resolution, neutron resilience, MHz counting rate capabilities and, for some applications, compact dimensions have recently been developed and their performance successfully tested at nuclear accelerators. In this sense, most of the technology that may be needed to characterize the supra-thermal ions of an FFH fusion source based on the tokamak concept seems to be available. A fundamental testbed of the readiness of gamma-ray measurements at high performance will be the forthcoming deuterium-tritium campaign at the Joint European Torus, where state of the art detectors will be for the first time under stringent test in conditions not far from those expected at ITER or in a future FFH.

## 32 - Comments on neutron measurements on fusion, fission and hybrid reactors

Jan Källne

Department of Engineering Sciences, Uppsala University, Uppsala, Sweden

### Abstract

This paper high-lights some features of neutron measurements in their present roles on fission and fusion (tokamak) reactors and projections forward, especially, for next step fusion power reactors and fusion-fission hybrids.

### 1. Introduction

Neutron emission is an intrinsic feature of energy releasing fission and fusion reactions such as  $n+^{235}\text{U}\rightarrow\text{F}_1+\text{F}_2+\nu n$  and  $d+\tau\rightarrow\alpha+n$  with the neutrons being, respectively, the sustainer of the fission chain reaction and the main energy carrier of the thermonuclear fusion reaction. Common for fission and fusion reactors is the use of neutron measurements (NM) to characterize/monitor the energy releasing process and the matter/condition states under which the processes can be sustained. Neutron detectors for fission reactors have been in use and development over more than 70 years and are, since the 1950's, used in the control and monitor (C&M) system of commercial power plants. R&D has been pursued for improved performance and for operation on next generation fast fission reactors. They are used to record the ambient flux at in- or ex-core positions. Fusion tokamak experiments started in the 1960's but it was not until late 1970 that thermonuclear fusion neutron emission DD plasma was evidenced (diagnosed) [1]. Dedicated instrumental development began in the 1980's to measure the neutron emission from selected plasma volumes in arrays of collimators (cameras) and the energy distribution (spectrum) of the flux from the plasma center. The first tests of NM diagnostics for DT plasmas took place in mid 1990's. The most advanced NM systems, for both D and DT, are now found on JET [2] which provides the platform for envisioning NM on next step tokamaks. The tokamak could also be the neutron source driver of subcritical fission in FuFi hybrids. Besides serving the C&M needs fusion and fission parts of hybrids, the NM system must also distinguish neutrons by their origin. Here, a plasma of simple (mirror) configuration is desirable for which only rudimentary NM experience exists. The focus of this paper is to envisage the potential use of NM on next generation fusion reactors for power production (DEMO and PROTO) and neutron production (hybrids) besides ignition studies in what can be called iDEMO. The starting point will be the NM systems developed and in use for D and DT plasmas at JET which is compared with what is planned for ITER (under construction). The aim is to illustrate principle NM capabilities, especially, spectrometers, but leaving out the difficult interface issues (sightline and detector accommodation) although these may very well be the final show stoppers.

### 2. Nuclear reactor concepts and development aims

Today's light water (thermal) fission reactors have poor (4 %) fission fuel burnout (FFB), which is wasteful and radiotoxic. The increased FFB should make improvements on both accounts as is the goal of future fast neutron reactors (Table 1). On the fusion side, the NM base is the JET tokamak with a power gain of  $Q=P_{ff}/P_{in}\approx 0.6$  in short pulses DT plasmas. However, an electricity producing reactor need to achieve  $Q>50$  for the same overall electric net efficiency ( $Q_E=20$ ) of a fission reactor (whose energy releasing chain reaction is self propelled, i.e.,  $P_{in}=0$  and  $Q=\infty$ ). Along the road, net electricity production would be shown in DEMO with tritium breeding (TB). A physics experiment could be aimed at the first ignition demonstration (iDEMO) such as the Ignitor project [3]. Another use of fusion is in FuFi hybrids for high fission fuel burnout and nuclear waste incineration. Electricity self-sufficiency ( $Q_E\geq 1$ ) could be attained already at  $Q\geq 1$  with TB excess capability. Mirror machines [4,5,6] would be attractive in this case where today's base is the GDT project [4].

Fission	Fusion		Hybrid
	Tokamaks	Mirror machines	
$Q=\infty, Q_E\geq 20$	Power reactor $Q=100, Q_E\geq 20$	Ignition exp. $Q=\infty$	$Q>1, Q_E>1$
Better FFB	$\uparrow$		High n flux source
	DEMO	iDEMO	Strong FBB+TB
$\uparrow$	$\hat{\uparrow}^{TB}$		$\hat{\uparrow}$
	ITER		
Low FFB	JET ( $Q=0.6$ )	$\rightarrow \square$	GDT ( $Q=0$ )

Table 1. Nuclear reactor development lines from today's base with indicated gross and effective power gain factors  $Q=P(\text{tot})_{\text{out}}/P_{\text{in}}$  and  $Q_E=P(\text{net})_{\text{out}}/P_{\text{in}}$ , besides fission fuel burnout (FFB). TB indicates tritium breeding.

### 3. Fuel burn rates and control

Fission reactors, typically, operate at constant power ( $P_{fi}$ ) which occurs when the fission reproduction constant is unity,  $k=1$ ; state self-sustained fission chain reaction is (critical reactivity). Higher/lower  $P_{fi}$  levels are reached by putting the reactor into a super/sub critical state ( $k=1\pm\epsilon$ ) under careful MN monitoring so that  $\epsilon < \beta$  (the fraction of delayed to prompt neutrons);  $\beta \approx 0.006$  for thermal neutron reactors operating with uranium fuel but decreases with the presence of transU nuclides (connected with high fuel burnout). For  $\epsilon=1-k$  approaching zero, the  $P_{fi}$  operating point is reached which is stably locked by the negative temperature feed back on  $k=1$ ; the operating state is monitored with NM and otherwise, and only long term condition drifts need normally to be adjusted for. Constant fission rate can also be maintained in the sub-critical state, such as  $k=1-\epsilon \approx 0.97$  in hybrids. Here, the sub-criticality level must be monitored with MN to stay within prescribed safe upper limit. Generally, MN is used to monitor the spatial power changes where the live flux detectors are complemented with activation measurements (in so called 'aeroball' systems). Finally, it is important that the neutron monitor system can reliably measure over a large dynamic range of some 15 orders of magnitude (from  $<1$  mW to GW).

Fusion reactors operate with plasma fuel at  $T \approx 10^5$  K° and  $p \approx 1-2$  atm. It is contained by a magnetic field genennerted with coils outside the vacuum vessel which are both protected by heat shield (plasma wall). The blanket absorbs and transports the fusion power ( $P_{fu}$ ) and the auxiliary plasma heating ( $P_{aux}$ , when applied) besides furnishes the n+Li tritium breeding. There is a limited domain of plasma parameters that constitute equilibrium (MHD) conditions (largely determined by the electrons) that allow the d and t fuel ions to do their thing, namely to burn. The aim is to achieve high (thermal) fusion power  $P_{fu}$  at high gain  $Q = P_{fu}/P_{aux}$  so as to achieve a large plasma self-heating fraction  $F_\alpha = P_\alpha / (P_\alpha + P_{aux}) = Q / (Q+5)$ . The purpose of the power reactor is to deliver electricity some of which is needed for  $P_{aux}$  heating at a finite conversion efficiency so it would take  $Q \approx 50$  for a electric power amplification factor of  $Q_E \approx 5$  in long pulses (practically continuous). Without the latter constraints, ignition experiments can be optimized for achieving self-burning plasma of short ( $\approx 10$  s) but sufficient to study the heating and other effects of alpha particles (which have a slowing down time on the scale 50 ms (Ignitor values [3]).

NM is not concerned with plasma MHD stability but only with the fuel ions and their burn. Clearly, NM provides essential diagnostics for burn control through the parameters that can be measured. Among the principal ones are the (absolute) total fusion power ( $P_{fu}$ ), ion temperature ( $T_i$ ) and d/t fuel ratio in addition to the radial profiles  $P_{fu}(r)$  and  $T_i(r)$ . Thermally stable equilibrium burn conditions, where plasma heating and loss are balanced by negative temperature feed back, have been discussed but remains unknown [7]. Active burn control requires NM as an essential part of the M&C system of fusion power reactors. Finally we can note that in ignited plasma studies, the alpha particle population would be a central topic to be addressed though NM.

### 4. Narrow detector base for neutron measurements

The elusive neutron was around for quite some time until the unknown radiation from the Po+Li source could be pinned down by Chadwick in 1932 using the proton recoil method. The discovery showed that neutron radiation is non-ionizing (=penetrating) and detectable only indirectly through nuclear interactions such as: Elastic scattering on light nuclei, np charge exchange, neutron capture including fission. There are only a handful potential NM processes available (Table 2) leading to charged particles (CP) generating detectable electric or light signals; of note are self-powered detectors based on  $n+^{51}\text{V}$  used in fission reactors, and the  $n+^{235/238}\text{U}$  fission reactions used in both fission and fusion reactors. Some lend themselves to measure ambient neutron fluxes. Others are suitable to record the collimated flux while the energy distribution is measured by spectrometers of adequate energy resolution. The latter one are most demanding but high in information output.

Elastic scattering recoils	Charge exchange	Neutron capture
$n+H \rightarrow n'+p$	$n+^3\text{He} \rightarrow p+t$	$n+^{16}\text{Li} \rightarrow \alpha+t$
$n+D \rightarrow n'+d$		$n+^{10}\text{B} \rightarrow ^7\text{Li} + \alpha$
$n+^3\text{He} \rightarrow n'+\tau$		$n+^{12}\text{C} \rightarrow ^9\text{Be} + \alpha$
$n+^4\text{He} \rightarrow n'+\alpha$		$n+^{51}\text{V} \rightarrow ^{52}\text{Cr} + \beta$
		$n+^{235/238}\text{U} \rightarrow F1+F2$

Table 2. Some principal nuclear processes and target nuclides for neutron measurements

NM on fission reactors have a long (70+ years) history and are now well tested parts in the C&M systems on today's reactors. Fission chambers of different kinds are used as neutron flux monitors of the fission reactivity, viz. the increase/decrease rate to reach the desired  $P_{fi}$  operating point including shut down state (zero reactivity). Some principle issues are signal availability, reliability, and relative and absolute (power) calibration. The latter is supported by reactor code calculations based on neutron cross section data and core state information from temperature and pressure gauges.

Existing NM development is aimed at enhanced performance and economy, and for use on the next generation (fast) neutron reactor. In the latter case the detectors must deal with other space and access constraints besides higher neutron flux densities and temperatures.

The experience from operating the neutron diagnostics of the fusion plasmas of JET constitutes now the platform for NM on the next step tokamaks such as ITER (under construction). ITER is first on the road map to a fusion power prototype reactor (PROTO, able to connect to the electric grid) with the envisioned intermediate step DEMO [8]. Alternatively, next NM generation could be tested on an ignition demonstration (iDEMO) tokamak (Table 3). Principal issues for fusion NM are signal availability, reliability, calibration and sensitivity just as for fission reactors.

Tokamak(Year)	T3(1967)	PLT (1980)	JET(1983-)	ITER (2020-)	DEMO (2035-?)	PROTO
NM type $\sphericalangle$					iDEMO	
Flux	→	✓		→		
Flux profile			→	→		
Spectrum		✓	→	~		

Table 3. Time line for NM involving flux, collimated flux (profile) and spectrum over period of 1967-2016

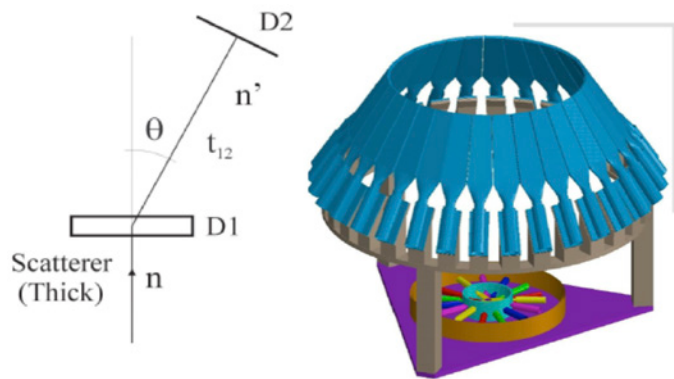


Fig. 1 The neutron TOF spectrometer principle and TOFOR design.

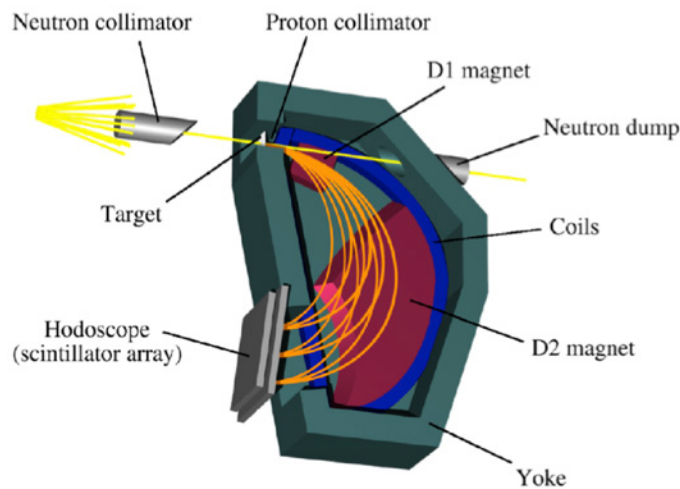
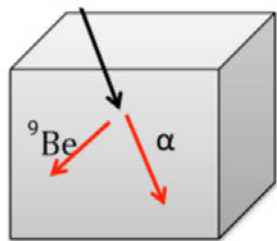


Fig. 2. magnetic MPR spectrometer with removed magnet yoke lid.



Diamond

Fig. 3 Compact

These are of the type that absorb the two energetic charged particles (CP) produced whose energies are obtained from detector signal, i.e.,  $E_n = C \cdot S_{CP}$  where the proportionality factor  $C$  requires calibration with a neutron source. One example is the (synthetic) semiconductor diamond (Fig. 3), which is under development [11]. Another is the

In addition, a high S/B signal-to-background ratio) is an important quality factor as is high (several MHz) event rate capability for collimated flux measurements (not normally used for fission NM); these are also heavy on the machine interface (not considered here). For next fusion reactors, dedicated instrumental developments can benefit from the rapid electronics progress digital signal recording, processing and storage.

The principal neutron instruments used at JET can be divided into three groups (Table 3): Ambient flux detectors:  $^{235}\text{U}/^{238}\text{U}$  fission and  $\text{BF}_3$  (ionization) chambers (also used on fission reactors) besides (liquid/plastic) scintillators. Some of the above and others are used as collimated flux detectors such as in collimator arrays (cameras). The cameras are used to determine neutron emission profile over the plasma poloidal plane. Here, one needs flux detectors with pulse height and shape discrimination to suppress the influence of low energy scattered neutrons (see Fig. 4) and gammas. Spectrometers are used to determine energy distribution of the collimated neutron emission from the plasma. Here it is appropriate to distinguish between large high performance instruments (TOFOR and MPR) and compact spectrometers (e.g., diamond semiconductors). High performance in the above cases was embodied in the design goals: high count rate for given neutron flux, just adequate energy resolution (set to match the 4-keV thermal spectral broadening), energy and flux calibration at quantifiable accuracy, stability and sensitivity including background suppression (high S/B ratio). The 2.5-MeV TOFOR (OR=optimised

rate) spectrometer is based on double neutron scattering time-of-flight (TOF) (Fig. 1). Here, the incoming neutrons scatter (at known angle  $\theta \neq 0$ ) in plastic scintillator 1 (detected as  $n + \text{H} \rightarrow \text{p} + n'$ ) followed by  $n' + \text{H} \rightarrow \text{p} + n''$  in detector 2. The neutron energy  $E_n$  is determined by the time difference  $t_2 - t_1$  (=TOF of  $n'$ ) [9]. Neutron scattered proton recoils,  $n + \text{H} \rightarrow \text{p} + n$  at forward angles  $\theta \approx 0$ , are used in the MPR (magnetic proton recoil) (Fig. 2) [10]. The protons are momentum analyzed and focused onto a focal plane giving a momentum dispersed x-distribution  $Pr(x) \propto \sqrt{E_n}$ . It is mostly used for DT plasmas to measure 14-MeV neutrons over the range  $\pm 3$  MeV, but can also be set for dd neutron (the range 1.5-3.5 MeV). The dimensions of TOFOR and MPR are  $\approx 1$  and  $\approx 1.8$  m by height (Figs. 1,2) [9,10]. Compact detectors attract interest for use as spectrometers as solution to solve interface problems.

historically important  $^3\text{He}$  (gas) ion chamber. Although the liquid NE213 scintillator is 'compact', it does not qualify as a spectrometer which should be obvious from the observation that it does not respond with a peaked SCP distribution to mono-energetic neutrons; i.e., there is no attributable FWHM (full-width-at-half-maximum) as measure of energy resolution. This elementary fact has not deterred continued efforts to demonstrate spectrometer functionality [12].

## 5. Fusion neutron diagnostic measurement and systems

Fission chamber detectors are used on JET as flux monitors with good ( $< 1$  ms) time resolution operating over a dynamic range of  $>10$  orders. They are calibrated so as to give the total neutron yield rate,  $Y_n(t)$ , from which fusion power,  $P_{fu}(t)$ , is derived. The critical calibration is based on using a standardized radioactive neutron source or generator tube in the plasma vessel with the assistance of neutron transport model simulations. It also involves a neutron activation system with samples sent and retrieved from measuring points near the plasma. The modeling that links the monitor response to the in situ source emission is problematic when it comes to ascribing (absolute) uncertainties quantitatively. This invasive method would be undertaken once on power reactors as on ITER. Otherwise, flux measurements have worked satisfactorily on JET can be expected to be the case on ITER with the developments made to meet performance and interface conditions.

JET is equipped with two collimator arrays (cameras). The 2.5-MeV neutron fluxes are measured with liquid scintillator (counter) detectors to allow discrimination against  $\gamma$ 's and low energy (down-scattered, cf. Fig 4) neutrons and plastic scintillator detector for 14-MeV neutrons from DT plasmas. Camera measurements are difficult for many reasons, one is the calibration that is important for the main task, namely to measure the plasma neutron emission profile (sight line distribution). Here, the focus must be on the relative channel calibration for which the absolute calibration is not needed and may even be detrimental for the relative one if tried. High neutron fluence conditions will present a challenge to in-flux detectors. ITER will present a first mild test for power reactor conditions.

Many types and designs of spectrometers have been used and developed at JET, first for 2.5-MeV dd neutron emission from D plasmas and since 1996 for 14-MeV dt neutrons from DT plasmas [2,10]. Today, the large TOFOR and MPR instruments [9,10] remain in routine use with some development tests of compact diamonds. The MPR spectrometer is of most interest in the forward perspective of DT plasmas whose capabilities are illustrated below.

Ion temperature is determined from the measured spectral 14-MeV peak width ( $W=177/\sqrt{T}$  in keV) for thermal (th) ion reactions which can be distinguished from supra-thermal (st) ion contributions from the Paux heating and, hence the power ratio  $P_{fu-st}/P_{fu-th}$  (Fig. 4). A special st contribution is AKN (alpha particle knock-on neutrons) [14] which is also a sensitivity demonstration. The AKN appears as a weak (10<sup>-5</sup>) feature on the high energy tail of the principal main neutron distribution (Fig. 5). The total neutron flux, i.e.,  $P_{fu}$  and the ratio  $P_{fu-st}/P_{fu-th}$ , can be determined with low ( $\leq 15\%$ ) uncertainty mostly based on factors with known absolute errors [15]. With profile information from cameras, the results can be improved further. A dedicated test of this calibration method of the flux monitors could be done at JET during the next period of tritium operation (2019?). Confirmation would have profound forward impact. While not tested on JET, a potential simultaneous measurement of the dd and dt spectral components ( $S_{dd}$  and  $S_{dt}$  at 2.5 and 14 MeV) with the MPR (Fig. 5) would give information on the density ratio  $n_d/n_t = \rho S_{dd}/S_{dt}$ , i.e., the isotopic fuel ratio RD/T, where  $\rho$  is determined from known reactivities at T (measured) but an estimated  $\rho_{st}$  when supra-thermal contributions are involved [16]. The isotopic fuel composition is an essential parameter for fusion reactor operation. TOFOR and MPR are the first built based on these concepts and hence prototypes possessing potential for further development based on experience gained. This has been demonstrated in TOFOR2 of dedicated designed for full digital signal processing to enhance performance in general and sensitivity in particular [13]. Further potential lies in dedicated designs for next

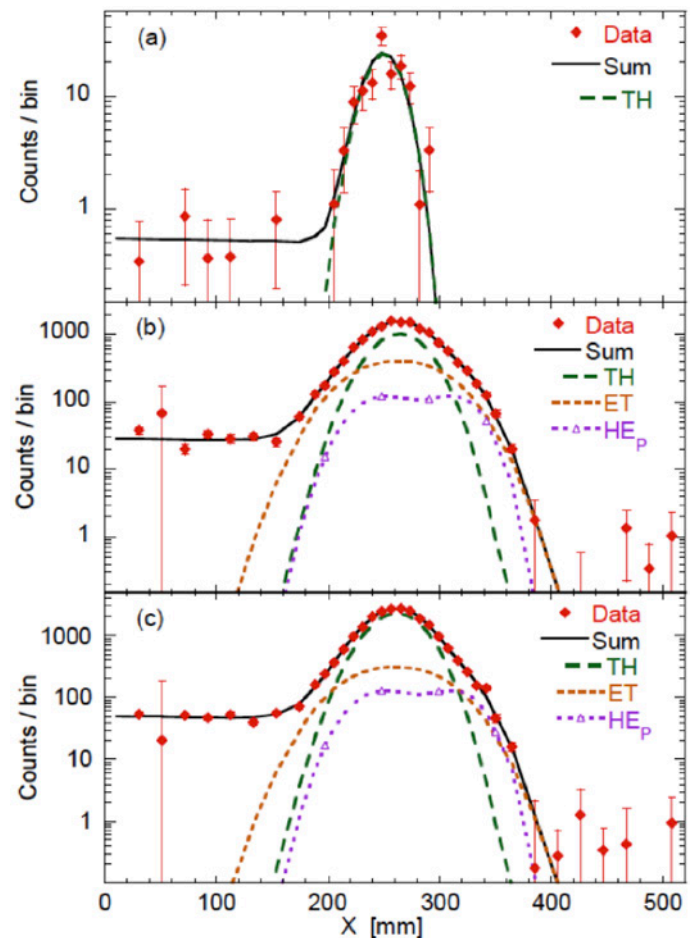


Fig. 4. Example of MPR data for JET from DT campaign of 1996 for plasma periods into the plasma from top: 10-12 s ( $P\Omega$  only  $\rightarrow$  thermal plasma); 13-13.7 ( $P\Omega+PNBI$ ); 14-15 s (after giant plasma saw tooth [13]). Proton momentum and  $\sqrt{En}$  increases with position coordinate  $x$

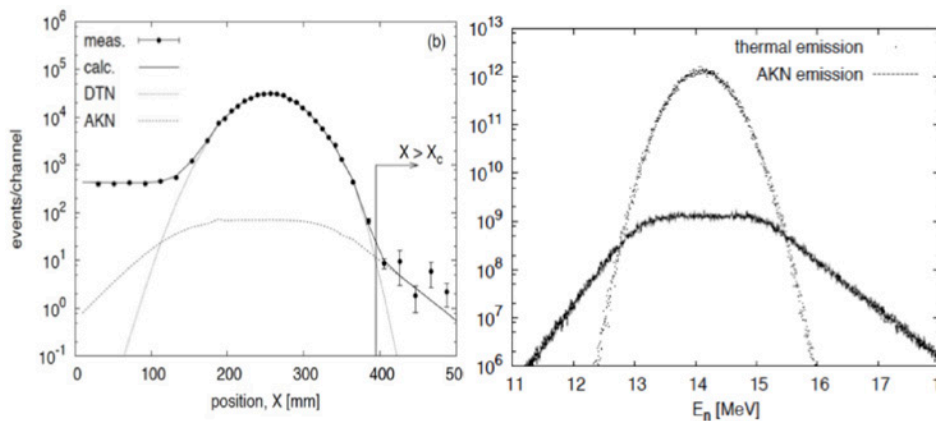


Fig. 5. Left: MPR data from JET plasma (@  $T_e = 10$  and  $T_i = 20$  keV) showing the contribution from AKN to the right of  $X_c$ . Right: Calculated  $E_n$  spectrum for DT (50:50) plasma with  $T_e = T_i = 20$  keV showing thermal and AKN contributions [15].

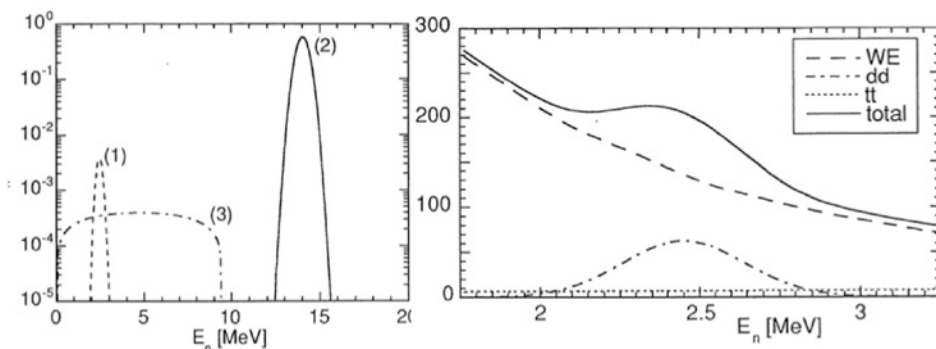


Fig. 6. Calculated spectrum of neutron emission from (50:50) DT plasma for  $T_i = 20$  keV showing dd (1), dt (2) and tt (3) peaks and detail of 2.5-MeV region on scattered neutron background [16].

addressed to find active compensation methods and passive shielding. The MPR spectrometer is of most interest in the forward perspective of NM on DT plasmas and

## 6. Prospects for neutron measurements on future nuclear reactors

Foretelling the future is difficult but to be a bit right is not so bad. From Jarvis 1993 [2]: 'little scope for development for 2.5MeV (but) considerable scope for innovative designs of spectrometers for use with 14-MeV neutrons'. Let us consider the situation of NM systems on reactors that lie in front of the present (JET) illustrated by ITER, DEMO and iDEMO (exemplified by Ignitor [3] (Fig. 6) . As indicated earlier ITER has weaker NM capabilities than JET reflecting the difficulty to accommodate these instruments as add-ons after the machine design has been frozen. It is now realized that the planning of DEMO diagnostics must be an integral design part of the reactor [18]. There is a big step to take as it is only the ambient flux monitors that come with experience beyond that of JET. What concerns cameras and spectrometers, ITER will offer scant experience on the former (because of limited viewing of the plasma) and none on the use of high performance spectrometers. A general question is what is the minimum number of NM diagnostics and types needed on DEMO and, in the extension, for the C&M system on commercial electric fusion reactors. ITER will tell if its reduced NM capacity was sufficient or not. If not, then experience on interfacing/using them would remain wanted.

NM on an iDEMO machine, such as Ignitor, would, in addition to the C&M function, have burning plasma studies as an objective. Cameras and spectrometers would be essential and such measurements would be simplified by the lower fluence levels and the high neutron emissivity of the plasmas (some 10x higher than for JET). Moreover, a plasma fully  $\alpha$ -heated (ignited) would be thermal and the supra-thermal fuel ions would be generated the MeV burn products are  $\alpha$  and t. We have already shown how the slowing down  $\alpha$ 's manifest themselves in the neutron spectrum and the one in (Fig. 5) illustrates what could be expected at Ignitor (but for the low energy scattered neutron tail). The count rates would be much higher on Ignitor than on JET but this will be needed main time resolving power relative to time scale of phenomena to observe (e.g., the 100 time shorter alpha slowing down time). Neutron spectrometry is a given tool for ignited plasma studies [19] besides giving experience for next step applications

The NM diagnostics of a fusion reactor in a hybrid present extra challenges, even if one assumes a 'simple' mirror plasma (Fig. 7) [20]. Aside from the daunting interface problems, the NM system must provide the fusion neutron yield rate (and Pfu) to the C&M system of the hybrid which controls the fusion power  $P_{fis} \approx [4.4k/(1-k)]P_{fus}$ . This will definitely

generation applications for plasmas of  $T_i \geq 10$  keV and corresponding relaxed energy resolution. This would have significant impact on scintillator geometry choice and dimensions. TOFOR would be used for D plasma operation that would precede high power DT operation. Next generation MPR for DT plasmas, for instance, could be equipped with new (curved) detector (to follow the focal plane) to improve the S/B ratio and energy resolution that can be traded for increased efficiency and sensitivity. In particular, the magnet beam optics could be optimized with modern computer codes implying shrunk dimensions and/or improve performance such as higher flux efficiency and better control of neutron beam halo effects. An MPR of dedicated design for 2.5-MeV neutron is of interest to explore the potential to measure dd neutron emission from DT plasmas, possibly a combined dd and dt instrument. The magnetic field interference between instrument and machine is a general issue that need to be

need a high performance spectrometer to single out the 14-MeV fusion neutrons in the total flux. Also monitoring the neutron flux near the fission fuel will be a challenge beyond the situation for a stand alone fast neutron reactors. Moreover, measurement of neutrons that can be ascribed to the fusion and fission origins is needed in order check that the k-value does not drift off from the operating point ( $k \approx 0.97$ ) into an unsafe region and with correct start-up k. Some of the interface issues were illustrated in Ref. [20].

## 7. Concluding remarks

In this comment we have stated that JET has a full complement of neutron measurement diagnostics including flux detectors, cameras and spectrometers and there has been room for development, over time, with input from experience gained. This has been used in planning and implementation on ITER but only partially for cameras and very little for spectrometers, because these have been interfaced to the machine as add-ons. Only time will tell if the reduced neutron diagnostic capacity of ITER was sufficient. Or if it was not, what is the experience base for developing the needed ones for the next step (DEMO) on the road map for fusion. Perhaps one could go off road and gain that experience on an ignition demonstration machine (iDEMO) coming earlier in time. From the JET platform, the forward spectrometer R&D has had been unilaterally steered towards so called compacts (even in lieu spectrometers) so as to fit the ITER interface constraints. This means that the developments potential of high performance spectrometers remains unexplored and innovative R&D in new directions have been hampered. Such a forward thrust for next step fusion neutron measurements is needed as it seems commonly accepted that neutron diagnostics are needed to operate fusion power reactors, and one could even dare the statement that no reactor would run without high performance spectrometers. This comment paper has lead me to the opinion that fusion-fission hybrids would not be able to do without them.

## References

1. JD Strachan et al, Nature 179(1979)626 and Nucl. Fusion 21(1981)67.
2. ON Jarvis, 'Neutron measurement techniques for tokamak plasmas', Plasma Phys. Control. Fusion 36(1994)204, and A Murarai, et al, 'New developments in the diagnostics for the fusion products on JET in preparation for ITER', Rev Sci Instr. 81(2010)#2.
3. WEB 2016: <http://ignitorproject.com/index.html>.
4. AA Ivanov, 'Fusion neutron research at Novosibirsk incl. experiments' in AIP Conference Proceedings 1442(2012)139.
5. O Agren, 'The hybrid reactor project based on the straight field line mirror concept' in AIP Conference Proceedings 1442(2012)p. 173
6. TC Simmonen, 'Summary of results from the tandem mirror experiment'. LLNL report UCRL 53120 (26/2 1981).
7. JP Freidberg, 'Plasma physics and fusion energy', Cambridge University Press ( 2007).
8. F Romanelli, 'Fusion electricity: A roadmap to the realisation of fusion energy' <https://www.euro-fusion.org/wpcms/wp-content/uploads/2013/01/JG12.356-web.pdf>.
9. M Gatu Johnson, et al 'The 2.5-MeV neutron time-of-flight spectrometer TOFOR for experiments at JET'. Nucl. Instr. Meth. A. 591(2008)417.
10. J Källne, 'MPR neutron spectrometry at JET and its ITER implications.', In Proc. of the workshop on diagnostics for ITER, Varenna, Sept. 1997, Plenum Press 1998.
11. C. Cazzaniga, et al, 'A diamond based neutron spectrometer for diagnostics of deuterium-tritium fusion plasmas', Rev Sci Instr 85,(2014)11E101
12. L. Giacomelli, A. Zimbal1, K. Tittelmeier, H. Schuhmacher, G. Tardini, R. Neu. 'The compact neutron spectrometer at ASDEX Upgrade'. Rev. Sci. Instrum. 82, 123504 (2011)
13. H Henriksson et al, 'Systematic spectral features in the neutron emission from NB heated JET DT plasmas', Uppsala Univ Neutron Physics report, UUNF2003#2.
14. L Ballabio, 'Calculation and measurement of the neutron emission spectrum due to thermonuclear and higher-order reactions in tokamak plasmas, Thesis Uppsala Univ. (2003), and J.Källne, et al "Observation of the alpha particle "knock-on" neutron emission from magnetically confined DT fusion plasmas", Phys Rev Lett 85(2000)1246.
15. G.Gorini, et al 'Relationship between neutron yield rate of tokamak plasmas and spectrometer measured flux for different sight lines',. Rev Sci Instr 82(2011) 033507.
16. J Källne, L Ballabio and G Gorini,'Feasibility of neutron spectrometry diagnostic for the fuel ion density in DT tokamak plasmas'. Rev. Sci. Inst. 68(1997)581.
17. X. Zhang, J. Källne, et al 'Second generation fusion neutron time-of-flight spectrometer at optimized rate for fully digital data acquisition', RevSci Instr 85(2014)043503.
18. W Biel et al, 'Fusion Engineering and Design', Fusion Eng Design 96.97(2015)8-15.
19. R.V. Budny, 'Fusion alpha parameters in tokamaks with high DT fusion rates', Nucl. Fusion 42 (2002)1382.
20. J Källne et al, 'Neutron diagnostics for mirror hybrids' in AIP Conf. Proceedings 1442(2012) 291.

# 33 - Nuclear Detectors for Hybrid reactors : Lesson learned from the EU Tritium Breeding Modules of ITER

**M. Angelone<sup>1</sup>, R. Pilotti<sup>2</sup>, F. Stacchi<sup>3</sup>**

<sup>1</sup> – ENEA Centro ricerche Frascati, via e. Fermi, 45 – 00044 Frascati (Italy)

<sup>2</sup> - Università degli Studi "Tor Vergata" Dipartimento Ingegneria Industriale, via del Politecnico, 1 00100 Roma (Italy)

<sup>3</sup> – Università degli Studi "La Sapienza" 00100 Roma

## Abstract

Hybrid fusion-fission reactors (HFFR) are characterized by a very harsh environment with intense neutron and gamma fluxes and high temperature. This environment results very hostile for hosting the nuclear detectors to be used for monitoring the nuclear parameters (e.g. neutron flux, tritium production). Presently, no detectors are available for being hosted in such a harsh environment. However, some important lessons can be learned from the activities presently ongoing in the EU for studying and realizing nuclear detector prototypes to be located inside the European Tritium Breeding Module (TBM) for ITER. ITER-TBMs experience high neutron and gamma fluxes and working temperature up to 600°C or higher. The goal is to develop and test prototype detectors able to measure relevant nuclear quantities (e.g. nuclear flux and spectrum, tritium production, gamma flux, etc.) to be compared with those predicted by the calculation tools which need to be qualified by comparison with experimental data in view of their application for designing the breeding blanket of DEMO.

Despite the difference, the ITER-TBMs and the breeding blanket of HFFR experience a number of similarities in terms of radiation level, use of liquid metals and high working temperature, so the lesson learned so far in the development of nuclear detectors for the ITER-TBMs can be very helpful to study and develop nuclear detectors to be used in hybrid reactors.

In this paper the activities and results ongoing at ENEA Frascati for developing nuclear detectors for ITER-TBMs are highlighted and the possible follow out to hybrid reactors discussed.

## 1. Introduction

Long term availability of abundant and safe energy represents a goal and is among the main issues to be faced and solved by humanity. The capability to fulfil such a goal will affect the life of next generations. Many ideas and proposals have so far been considered but no definitive projects and technological solutions have been proposed nor are available. Among the possible candidate of future energy production systems, hybrid fusion-fission reactors (HFFR) play a primary role as they promise to produce energy by solving the safety and proliferation problems still affecting the nuclear fission reactors while overcoming the request, not yet achieved, of operating the fusion reactors in steady-state mode.

HFFR principle is very simple as it consists of a coupled fusion-fission system [1,2]. A plasma produces (14 MeV) neutrons via the  $D+T \rightarrow \alpha+n$  reactions. The neutrons move inside a "blanket" region mainly constituted by sub-critical fissile material (made by not otherwise burnable fissile materials) so producing nuclear fission. The neutrons produced in the blanket are used not only to sustain the fission chain but also to produce the Tritium (e.g. via  $n+Li$  reactions) needed as fuel for the tokamak. Owing to the high power density, liquid metals (e.g. Pb) are proposed as coolant for the HFFR systems, this in turn, requires high operational temperature .

From the schematic description above, it is clear that HFFRs are characterized by a very harsh environment with intense neutron and gamma fluxes and high working temperature. On the other hands, it is known as any nuclear system requires a dedicated nuclear instrumentation to be located "in-core" to monitor a number of fundamental nuclear parameters (e.g. neutron and gamma fluxes, fission rates, on-line tritium production, reactor power, etc.). Presently, no detectors are available for being hosted in the HFFR harsh environment. However, some important lessons can be learned from the activities presently ongoing in the EU under F4E specific grants (e.g. F4E-FPA-395) for studying and realizing nuclear detector prototypes to be located and used inside the European Tritium Breeding Modules (TBM) of ITER. EU is proposing two different concepts for the ITER TBM, the so called Helium Cooled Liquid Lead (HCLL) and Helium Cooled Pebble Bed (HCPB) TBM [3,4].

ITER-TBMs experience high neutron and gamma fluxes and working temperature up to 600°C or higher. The goal is to develop and test prototype detectors able to measure relevant nuclear quantities (e.g. nuclear flux and spectrum, tritium production, gamma flux, etc.) to be compared with those predicted by the calculation tools. This is a fundamental task since the TBM performances are studied and predicted only by calculation tools which need to be qualified by comparison with experimental data in view of their application for designing the breeding blanket of DEMO.

Despite the difference, the ITER-TBMs and the breeding blanket of a HFFR experience a number of similarities in terms of radiation level, use of liquid metals and high working temperature, so the experience gained and the lesson learned

so far in developing nuclear detectors for the ITER-TBMs can be very helpful to study and develop nuclear detectors for hybrid reactors and can represent a starting point. A synergy between the two activities (at least at the level of methodology) can be envisaged.

In this paper, the used methodology and the activities ongoing at ENEA Frascati for developing nuclear detectors for ITER-TBMs are highlighted as well as some results and the possible follow out to hybrid reactors are discussed.

## 2. Functional Requirements and Specifications of Candidate Sensors for TBM

As already stated, EU is proposing two different concepts for the ITER TBM, the so called Helium Cooled Liquid Lead (HCLL) and Helium Cooled Pebble Bed (HCPB) TBM. Despite the many intrinsic differences in the two proposals (e.g. in the HCLL there is liquid Pb while in HCPB lead is solid), since both TBMs must withstand very similar working conditions (Table-1) they share common issues, problems and, some time, similar solutions too and their design is going to be homogenized. This is also the case of nuclear sensors/detectors to be located inside both HCLL and HCPB TBMs to monitor and measure fundamental nuclear parameters (e.g. neutron flux and tritium production). Due to the many constraints (e.g. high neutron and gamma flux intensity, high temperature, scarce accessibility, limited room to host the detectors inside TBMs, integration issues, etc.), the neutron detectors/sensors to be used in the EU-TBMs must fulfil and meet very challenging working conditions and parameters and their development must face many technological challenges. To select the most appropriate sensors a list of functional requirements and specifications is mandatory and represent the first step. This list of requirements/constraints/parameters must be fulfilled by each one of the proposed sensors. It is thus necessary to prepare a dedicated R&D program where these requirements & specifications will represent the input data for the design of each nuclear detector. Furthermore, a step-by-step approach to develop the detectors seems the more appropriate so to have a selection procedure which is based on feed-back from the lesson learned at each step of the development program.

### 2.1. Definition of Measurable Quantities and Uncertainty Margin

A fundamental aspect to design any measuring system is to define the quantities of interest and the accuracy required for each parameter to be measured. The main nuclear parameters to be measured in a TBM, but also in a hybrid fission-fusion reactor, are:

- Neutron flux (and energy spectrum) at several positions
- Gamma-rays flux (and energy spectrum) at several positions
- On-line tritium production

Parameter	HCLL		HCPB	
	Max.	Required Uncertainty	Max.	Required Uncertainty
<b>Neutron flux (<math>n\text{ cm}^{-2}\text{ s}^{-1}</math>)</b>	$2.0 \times 10^{14}$	$\pm 10\%$	$2.0 \times 10^{14}$	$\pm 10\%$
<b>Neutron Energy Spectrum</b>	20 MeV	$\pm 10\%$	20 MeV	$\pm 10\%$
<b>Gamma Flux (<math>\gamma\text{ cm}^{-2}\text{ s}^{-1}</math>)</b>	$4.5 \times 10^{13}$	$\pm 10\%$	$4.5 \times 10^{13}$	$\pm 10\%$
<b>Gamma-Ray spectrum</b>	30 MeV	$\pm 10\%$	30 MeV	$\pm 10\%$
<b>Temperature (<math>^{\circ}\text{C}</math>)</b>	500	$\pm 1.0$	650	$\pm 1.0$
<b>Nuclear Heating (<math>\text{W}/\text{cm}^3</math>)</b>	5.0	$\pm 10\%$	8.0	$\pm 10\%$
<b>Tritium Production (<math>T\text{ cm}^{-3}\text{ s}^{-1}</math>)</b>	$10^{12}$	$\pm 5\% - \pm 10\%$	$10^{11} - 10^{12}$	$\pm 5\% - \pm 10\%$

Table 1: Summary of the nuclear working conditions in HCLL & HCPB TBM for DT phase (data refer to ITER at 500 MW fusion power)

All these quantities must be measured as a function of time. Another important point to be addressed is that to gain in reliability and also to reduce the uncertainty margin an effort is to be made to develop and use at least two or more different detectors for measuring each parameter so to rely, at least, upon two independent measurements. One proposal is to use both passive and active detectors. Owing to the present technology the former (e.g. activation foils) seems more feasible. One draw-back of passive systems is that they need insertion/extraction systems (e.g. rabbit system) with the related need for integration in the system. Furthermore passive detectors present very low time resolution. On the other hands, active detectors require for cabling (and perhaps for dedicated cooled channels) so the integration with the system is not easier than for passive detectors.

Once fixed the type of nuclear parameters of interest (this does not mean that all the listed parameters will be actually measured) the second step is to propose a reliable range of uncertainty margin that can be accepted (not necessarily the same for the various quantities). This is a very challenging task since the uncertainty range is to be fixed "a priori"

considering the present lack of the needed instrumentation. A satisfactory uncertainty for all the quantities to be measured should be in the range  $\pm 5\%$  -  $10\%$  for TBM. However, in a blanket of a HFFR reactor this uncertainty margin could be too large (e.g. reactor power).

### 3. Requirements and Selection of Nuclear Detectors

A first list of detectors has been written for TBM considering both passive and active detectors. To mention that the list is not frozen because new entries/deletion can be foreseen according to the development of new technologies or the demonstration of limits and difficulties with some of the proposed technologies. The active and passive nuclear sensors that presently are considered for TBM are :

ACTIVE Detectors :

- (micro) Fission chambers
- Self-powered neutron detectors SPND (for total neutron flux measurement)
- Diamond detectors (covered with  $^6\text{LiF}$  for tritium measurement)
- (micro) Ionization Chambers (I.C)

PASSIVE Detectors :

- Nuclear Activation System or NAS

The use of active detectors is necessary for on-line monitoring (e.g. neutron flux and dose rate level) since can provide time-dependent response thanks to their time resolution responses, while passive detectors usually provide time-integrated responses. However, the duration of the integration time is arbitrary, to this end passive detectors can be seen as low time-resolution instruments.

Owing to the specific need of HFFR a different, more dedicated, detectors list can be considered. Among these detectors there are advanced detectors based e.g. on glasses, fiber optics, flow of micro/nano-sphere for activation, and of course micro-fission and ionization chambers.

#### 3.1. Common Requirements and Specifications for Nuclear Detectors

As it was pointed out above, the nuclear detectors to be proposed for the TBM (and HFFR) must fulfil a number of constraints and technical restrictions that are reported here after. The list is not complete but can be seen as a starting point :

a) *Invasiveness* : The small dimensions are crucial for any active or passive detector to be located in-situ especially if a certain number of them are foreseen to monitor the whole system. Indeed, state-of-the-art SPND and micro fission chambers can be manufactured with very small dimensions. Similar conclusion can be drawn for the other proposed detectors.

b) *Cabling* : cables are needed to connect the active detectors to their electronics. These cables will go from the inside of the TBM (HFFR) till the laboratory where signals are collected so extending for several (tens) meters. Owing to the intense radiation fields and the high temperature the cables are necessarily of the mineral type (Ref. 5). Mineral cables are used since many years in nuclear plants and mainly for in-core instrumentation such as fission chambers and SPND so from this respect there are not concerns about their use in the TBM and in HFFR. Mineral cables can withstand temperatures as high as  $800\text{ }^\circ\text{C}$  and neutron fluence  $> 1020\text{ n/cm}^2$ . Mineral cables have also been tested under harder neutron flux spectra such as those available in the ADS systems [5].

c) *Electrical Signals* : The transport and pick-up of the electrical signals is directly connected to the cabling. The proposed detectors can, in principle, work either in pulse or current mode. Due to the intense neutron flux the current mode will be most suitable and in some case it is the preferential operational mode (e.g. SPND, ionization chamber). The detector's signal must be well resolved respect to the noise and/or background signal. As far as methods for measuring/subtracting/suppressing the noise and/or background are concerned, the most used in harsh environment is to locate back-to-back two detectors one of the two being incomplete (dummy detector, e.g. fission chamber without fissile deposit) and to subtract the signal from the dummy detector from the real one. "Ad hoc" calibration methods are to be studied. The experimental uncertainty will depend largely on the capability to subtract the noise and/or background. Work is to be done for each sensor to address these effects.

d) *Radiation Hardness* : This is the main point of concern for the nuclear instrumentation. The radiation hardness of any nuclear detector will characterize its working life and the degree of accuracy for the measured quantities because degradation of the performances will occur during the operational life. As far as SPND (and fission chambers) are concerned, the information regarding their capability to withstand intense nuclear fields relate to their use in nuclear reactors. These information were extrapolated to TBM (and HFFR) but are not fully reliable

since radiation (e.g. neutron) effects depend upon the neutron spectrum. Another approach could be the one based on simulation.

e) *Burn-up* : To be considered for detectors such as fission chambers, the LiF deposit of diamond detectors and SPND. This is a well-known problem for fission chambers and SPND operated in high neutron flux reactors. The fissile deposit is burnt by the nuclear reactions they undergo. When the amount of the deposit and thus the number of reacting atoms is small compared to the numbers of atoms involved in the reaction rate (as for micro-fission chambers), the continuous reduction of the material alters the response of the detector. The time dependent decrease in the detector response cannot be neglected and must be accounted for and corrected, it can be of several percent per year. The burn-up affects also the accuracy of the measurements.

f) *Capability to withstand EM fields* : It is difficult to foresee the EM fields in the detectors location and to overall to prevent their effects. However, in tokamaks there is a long experience in facing and correcting these effects, so in principle it should be possible to deal with EM noise both in TBM and HFFR.

g) *Neutron-Gamma discrimination* : this represents an essential issue for the proper and reliable operation of any detector located in a mixed neutron-gamma field. The discrimination between the two signals is often very difficult and can have a not negligible impact on the results and their accuracy. This problem is also common to passive detectors whose response can be affected by gammas especially if their energy spectrum is extending up to tens of MeV. There are several methods that can be employed to control and solve the problem, however they depend upon the used detector, the requested accuracy, the used electronics etc. When operating in current mode the techniques of using a "double detector" configuration can be proposed. For SPND the sensitivity to gammas can be measured in a pure gamma field.

h) *Calibration* : All active neutron flux sensors will most likely be restricted to producing a signal proportional to the integral over the product of a interaction cross section and the local neutron spectrum, i.e., they map a multidimensional parameter onto a single dimension. Since the interaction cross section will be larger than zero for a range of neutron energies and not constant too over this energy range, the proportionality factor mentioned above will depend on the neutron spectrum. The error on the calibration largely affects the quoted experimental uncertainty (and thus the validation of the calculation tools). To get valuable and sound experimental results we must trust on the detectors calibration. The calibration of nuclear sensors needs both neutron and gamma fields. Calibration will results more accurate and reliable the more the used calibration field reproduces the "real" neutron field. The lack of experimental facilities TBM (HFFR)-like for performing calibration is one of the main issue to be considered and faced (solved) for the nuclear measurements.

i) *Safety & Integration* : All the proposed detectors and detection systems must ensure the safety levels according to the prescription for the other part/components of the TBM (HFFR). This is to be considered since the early design phase of these systems.

#### 4. Development of SPND for TBM

We report an application of the approach presented above by presenting the activities carried out at ENEA to design and to realize one prototype of a SPND devoted to measure neutron fluxes in the HCLL-TBM. Self-powered neutron detectors are rugged miniature devices which are used for fixed in-core reactor monitoring both for safety purposes and neutron and gamma flux mapping. As their name implies, they operate without any applied voltage and this fact contributes to their extra reliability and their ability to withstand the radiation damage suffered in the reactor core. The detectors are usually constructed in a coaxial configuration in which the central conductor is called the emitter and is usually the material that determines the characteristics of the device. The other electrode or metallic sheath is called the collector and the two are separated by a coaxial insulator (see Fig. 1a).

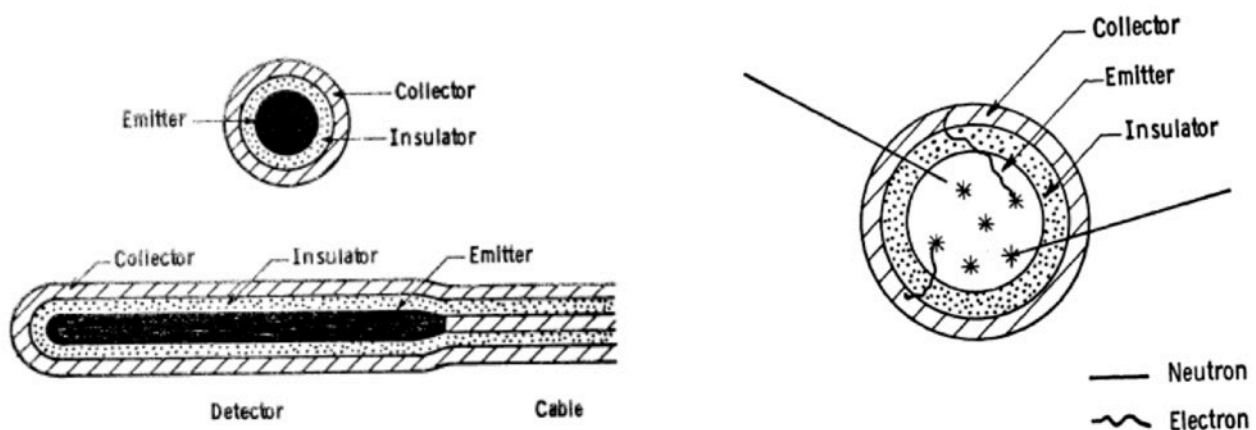


Fig. 1 : a) Typical configuration of SPND; b) Mechanism of current production in SPND

SPND are devices in which the emitter material is selected to have at least a moderate neutron capture cross-section and where the activation product decays by means of beta emission. The means by which current is produced is illustrated in Fig. 1b. The figure shows that those neutrons which interact in the emitter produce an unstable reaction product which, in turn, will beta decay giving rise to a fast electron. This electron will then travel through the emitter material and eventually come to the rest in it or will escape from it. Those betas which originate in the emitter and stop there do not contribute to the detector current while the bulk of the detector current results from betas which are passing the insulator and are reaching the collector or escaping from it. Some current is also produced indirectly by electrons stopping in the insulator [Ref....]. The SPND presently available on the market have been developed and are used in nuclear reactors, so we can expect that these SPND are not suitable for a reliable operation in the ITER-TBM since the neutron spectrum in TBM is much "hard" than in a nuclear reactor. Indeed, the used emitter materials (e.g. V, Co, Rh etc.) present high activation cross-sections at thermal neutron energy but these cross sections are very small at the neutron energy typical of a TBM. Furthermore, the gamma flux is about ten times higher than the neutron flux thus the effect of gammas cannot, in principle, be neglected. The intense neutron flux poses also the problem of the burn-up of the emitter material as well as the radiation hardness of the materials to be used for the constructions. This means that it is not necessary, perhaps, to use emitters with a very high cross-section. Indeed, usually at high neutron energy the cross-sections are lower (up to some order of magnitude) in their absolute values than for thermal or epithermal neutrons. This may compensate or at least reduce the burn-up effect due to the high neutron flux. The energy spectrum of prompt gammas due to fast neutrons is, on the average, higher than that of prompt gammas due to thermal neutrons, so perhaps the Compton and photoelectric effects inside the insulator could be slightly reduced (the probabilities of both effects decrease quickly with the gamma-ray energy). Last, but not least, the operation at temperatures of the order of 400-600 °C is another point of concern. Commercial SPND are usually designed to operate at 200-300 °C and thus tests at high temperature must be performed too. The few points discussed above clearly indicate that the use of SPND with fast (14 MeV) neutrons requires a deep analysis of all the aspects related to the physics, construction and operation of a SPND detector. This was done at ENEA, the first step was to calculate and compare the activation induced in a number of metals using different neutron spectra including the one in the TBM. The output of this study was a list of a few metals which can produce enough activation to be used as emitters in SPND designed for TBM [6]. Among these metals Cr and Be resulted the more interesting and a prototype of SPND with Cr emitter was realised. The prototype SPND with the Cr emitter (SPND\_Cr) is basically similar to the commercial ones so to reduce technological problems. It uses a mineral cable 10 m long, the insulator is made of Alumina (as for the commercial detectors). The sheath is in stainless steel. The Cr emitter is a rod of 100 mm length and 2 mm diameter (Fig. 2a) for a total Cr mass of about 5.5 gr.

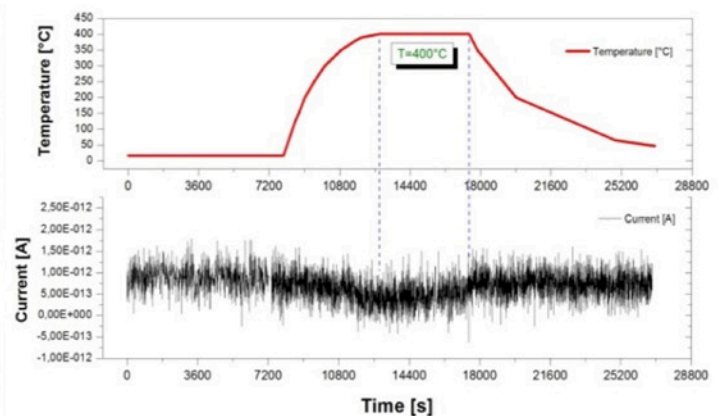


Fig. 2 : a) Picture of the prototype SPND with Cr emitter; b) Measured "dark" current of the SPND\_Cr detector at 400 °C

The prototype SPND\_Cr was thus tested studying its behaviour at high temperature. The first goal of the test was the measurement of the background current versus temperature (in the range 300-450 °C of interest for HCLL) so to get insight about the magnitude of the "dark" current induced by the temperature. For the measurements a cylindrical heater was used which uses a double solenoid to heat the detector. In this way the current simultaneously flows in two opposite directions and the magnetic field produced by the current is null. A Keithley 6487 picoammeter was used and directly connected to the detector. For measuring the temperature inside the heater a Fluke thermocouple was used. The heating procedure was the same for each temperature. The wanted temperature was kept constant ( $\pm 2^\circ\text{C}$ ) for at least one hour. The heater was thus switched off and the measurement continued till the temperature inside the heater cooled down to room temperature. An example of the measured response of the SPND\_Cr detector at 400 °C is shown in Fig. 2b. It is shown that the dark current is almost stable with the temperature. Similar results were obtained at other temperatures, however the magnitude of the dark current resulted to increase slightly with the working temperature. The sensitivity to gammas was thus investigated by irradiating the SPND\_Cr detector with an intense Co-60 gamma ray source available at ENEA (CALLIOPE facility). The measurement were performed at room temperature while those at

high temperature will be performed in the next. The results are in Fig. 3a, which shows that the detectors is somewhat sensitive to gammas. Good linearity of the produced current versus the dose rate was observed (Fig.3b).

Further tests are scheduled to better study the performances of the SPND\_Cr prototype under different working conditions. Therefore a problem to be faced is with the lack of neutron sources which for intensity and energy spectrum can reproduce those expected in TBMs. This is limiting the study and putting some concern for a proper and detailed study of the prototype. This problem is common to all the detector to be developed for TBM as well as for fusion tokamaks and HFFR.

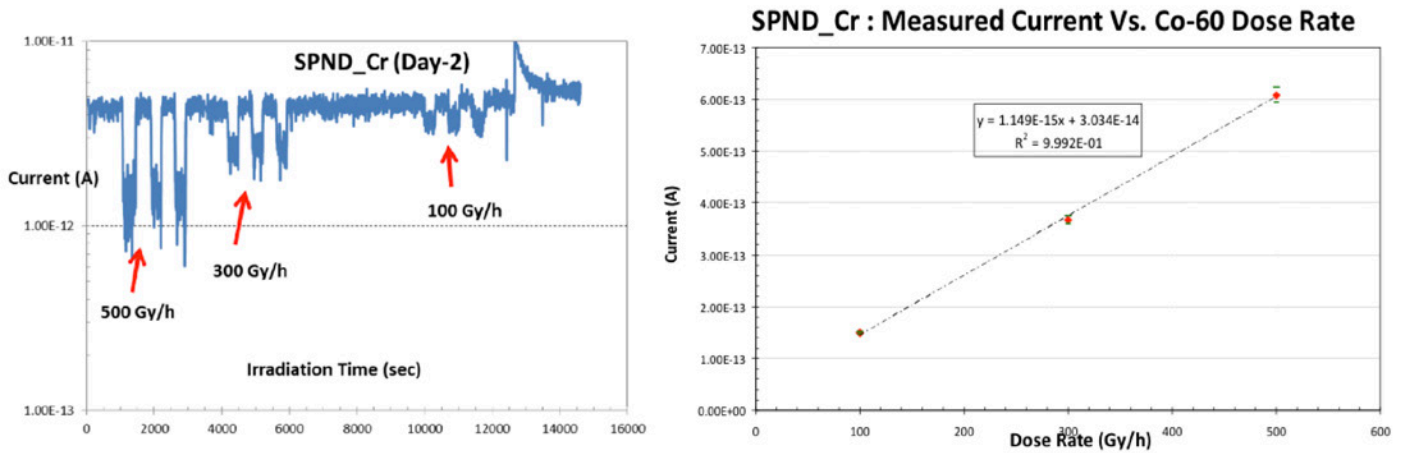


Fig. 3 : a) Measured response to Co-60 source;

b) Measured current vs. Co-60 dose rate

## 5. Discussion and Conclusion

The analysis of the various requirements listed above points out that a big effort is necessary to develop nuclear detectors suitable to withstand and properly operate in the TBM and HFFR radiation fields. As a matter of fact, presently no detectors are available, even the most "ready" among them (e.g. fission chambers, ionization chambers, SPND) require "ad hoc" study/prototyping, optimization and test under reliable neutron/gamma fields and working conditions. Considering the proposed active detectors (SPND and FC operated in current mode), with proper technological development the time dependent measurement of the neutron/gamma flux/dose seems feasible. More challenging seems the measurement of the on-line tritium production and, over all, of the neutron energy spectra. Furthermore, if the goal of the measurements in TBMs and HFFR is that to provide useful information not only for the functioning of the machine but also for qualifying the calculation tools, the experimental data should have enough accuracy to get reliable comparison with calculation.

The main conclusion of the present paper is that, owing to the status of available technologies, "ad hoc" R&D activity is mandatory to study, develop, prototype and test candidate detectors for HFFR. To this end it ought to be stressed that a further issue is represented by the lack of proper radiation fields in terms of neutron/gamma fluxes and spectra where to test and calibrate the prototype detectors. The development of nuclear detectors for HFFR can borrow the approach already used for ITER-TBM as the working environment and the requests for the data to be measured are very similar. An example of almost immediate application of the results already got for ITER-TBM is represented by the SPND, probably owing to the similarity of the neutron energy spectra the same detectors already developed for TBM can be considered at least as a starting point. This is putting in evidence the need for synergy between researches than are studying similar problems.

## References

1. B.R. Leonard Jr., A review of Fusion-fission (Hybrid) concepts, Nuclear Technology vol. 20 (1973) 161
2. R.J. Barret, R.W. Hardie, The fusion-fission hybrids as an alternative to the fast breeder reactor, Los Alamos Report LA-8503-MS September 1980
3. G. Rampal et. al, HCLL TBM for ITER-design studies, Fus. Eng. Des. Vol. 75-79 (2005) 917
4. F. Cismondi et. al., Design update, thermal and fluid dynamic analyses of the EU-HCPB TBM in vertical arrangement, Fus. Eng. Des. Vol. 84 (2009) 607
5. <http://www.thermocoax.com/>
6. M. Angelone et. al., Development of self-powered neutron detectors for neutron flux monitoring in HCLL and HCPB ITER-TBM, Fus. Eng. Des. Vol. 89 (2014) 2194

## 34 - Level of readiness of technologies used in Fusion devices proposed for Fusion-Fission hybrid (FFH) reactors

Francesco Paolo Orsitto<sup>1</sup>, Thomas N Todd<sup>2</sup>

<sup>1</sup> CREATE Consortium and ENEA Dipartimento Fusione e Sicurezza Nucleare,  
C R Frascati V E Fermi 45 00044 Frascati (Italy)

<sup>2</sup> Culham Centre for Fusion Energy, UKAEA, Abingdon OX14 3DB, UK

### Abstract

The starting point is the definition of Technology Readiness Level (TRL) for fusion technologies adopted in ref.1 (see Table A1). The TRL 4/5 (Technology basic validation in laboratory /a relevant environment) was referred to technologies demonstrated in JET experiments so far (including DTE1[2]). The TRL2 (Technology concept and/or application formulated) and TRL7 (Technology prototype demonstration in an operational environment) can be taken as reference points as the farthest and nearest point (respectively) to the maturity of a technology for a FFH system based on a tokamak neutron source. There are two important technologies with label TRL2: i) the demonstration of a discharge many hours long (at least three hrs) at relevant plasma parameters, and tokamak continuous operation for many months; ii) study of divertor geometry and control in a high radiation environment. A TRL4 can be proposed for the heating systems, in particular the demonstration of operation of 100keV NBI sources is needed for *long pulses (ideally CW sources) and extensive machine operation times (one full power year)*. TRL5 can be defined for most of the plasma diagnostics needed for FFH (basic diagnostics are: neutron, gamma, X rays; Microwave systems (ECE and reflectometer); magnetics (Hall probes outside and FOCS (Faraday rotation effect fiber optic current sensors) to be considered). The main point here, for diagnostics, is the demonstration of plasma control with minimum possible set of diagnostics[1]. A TRL7 classification can be given to the mechanical structures and vacuum vessel: the material selection and system design is well demonstrated in existing machines (*for low power neutron flux*). It is apparent that even for the low-gain compact devices intended for FFH systems, most of the required technologies are presently quite far from the high TRL needed to move into a detailed design stage.

### References

1. F P Orsitto et al, Diagnostics and control for the steady state and pulsed tokamak DEMO, Nuclear Fusion 56(2016) 020009
2. M Keilhacker et al., High Fusion performance from deuterium-tritium plasmas in JET, Nuclear Fusion 39(1999)209

**2017 ENEA** - National Agency for New Technologies, Energy and Sustainable Economic Development

ISBN: 978-88-8286-357-9

**Copy editing, graphic design scheme and cover design:**

Flavio Miglietta

**Printing:**

Laboratorio Tecnografico ENEA - Frascati

**ENEA**

Promotion and Communication Service

[www.enea.it](http://www.enea.it)

October 2017

